TÜBINGER
GEOWISSENSCHAFTLICHE
ARBEITEN (TGA)

Reihe C:
Hydro-, Ingenieur- und Umweltgeologie

Schriftleitung:
G. Teutsch, G. Einsele

Martin Sauter

Quantification and Forecasting of Regional Groundwater Flow and Transport in a Karst Aquifer (Gallusquelle, Malm, SW. Germany)

TGA, C13, 1992

Herausgeber: Institut und Museum für Geologie und Paläontologie
der Universität Tübingen
Sigwartstr. 10
D-72076 TÜBINGEN

Schriftleitung für die Reihe C:

Lehrstuhl für Allgemeine und Angewandte Geologie
Prof. Dr. G. Teutsch, Prof. Dr. G. Einsele

ISSN 0935-4948

Vorwort

Im Anschluß an frühere Tübinger hydrogeologische Untersuchungen im Malm-Karst der Schwäbischen Alb (zuletzt durch die Dissertationen von J. Behringer und G. Teutsch) hat Herr Sauter ein Projekt übernommen, bei dem der Einsatz zahlreicher, teils neuer Untersuchungsmethoden zu einem besseren Verständnis der Vorgänge in der wasser-ungesättigen und gesättigten Zone eines wichtigen Grundwasserleiters im Karst führen sollte. Dazu wurde das Einzugsgebiet der großen, für die Trinkwasserversorgung genutzten Gallusquelle im Laucherttal zwischen Gammertingen und Sigmaringen ausgewählt. Dieses Gebiet bot die seltene Möglichkeit, sowohl langjährige Quellschüttungs-Messungen und regelmäßig durchgeführte Wasseranalysen zu nutzen, als auch Grundwasserstandsbeobachtungen in Aufschlußbohrungen im Quelleinzugsgebiet für Tracerversuche, Bohrlochmessungen und hydraulische Auswertungen heranzuziehen. Die Bohrungen waren vor ca. 30 Jahren in Verbindung mit dem Rohrleitungsstollenbau der Bodensee-Wasserversorung niedergebracht worden. Weiterhin lieferten Bohrungen und Tracerversuche im Zusammenhang mit einer Abfalldeponie bei Bitz wichtige Informationen über die Verhältnisse in einem weit von der Quelle entfernten Teil des Quelleinzugsgebiets.

Die vorliegende Arbeit war sehr breit angelegt mit einem Meßprogramm, das sich über mehrere Jahre erstreckte. Es umfaßte neben geologischen und bodenkundlichen Aufnahmen und Landnutzungserhebungen vor allem Klimadaten, Schüttungsganglinien, wasserchemische und isotopenchemische Bestimmungen, Grundwasserstands-Ganglinien, Tracertests, Pump- und Injektionsversuche sowie Temperaturmessungen in Bohrlöchern.

Besondere Sorgfalt wurde u.a. auf die Ermittlung der Grundwasserneubildung gelegt, bei der viele Einflußfaktoren einschließlich der Interzeption in den Waldbeständen berücksichtigt wurden. Die verschiedenen Verfahren zur Auswertung von Aquifertests werden mit ihren Vor- und Nachteilen bei ihrer Anwendung auf ein Karst-Aquifersystem ausführlich besprochen. Dieses wird in Anlehnung an moderne Arbeiten im Ausland und an die Dissertation Teutsch als Doppel-Porositätssystem aufgefaßt, das aus einem Leitersystem mit geringem Hohlraumanteil (0,01 bis 0,03 %, "rasches" Karstwasser) und einem Speichersystem mit bedeutendem Hohlraumanteil (1 bis 2 %, "langsames" Karstwasser) besteht. Es wird gezeigt, daß die Aquifer-Kennwerte, besonders die hydraulische Leitfähigkeit, jeweils entscheidend von der Dimension des betrachteten Aquiferkörpers abhängen, d.h. mit abnehmender Dimension ebenfalls kleiner werden.

Numerische Modelle werden u.a. dazu eingesetzt, um nachzuweisen, welche Parameter für die Interpretation der Geländemeßdaten von ausschlaggebender Bedeutung sind. So bringt z.B. die Nachmodellierung der stark schwankenden Quellschüttung und der Grundwasserstände im Aquifer die Erkenntnis, daß das Feinkluftsystem ganz überwiegend die Speicherung und den Durchfluß von Karstwasser reguliert, nicht das Grobkluft-Leitersystem. Auch die zeitliche Spreizung von Tracerdurchgängen geht im wesentlichen auf das Feinkluftsystem mit seiner relativ hohen Dispersivität (hier 70 m gegenüber 10 m im Leiter-System) zurück. Schließlich belegen die Sensitivitätsanalysen, daß der flächenhafte Eintrag von Umweltisotopen (hier Sauerstoff-18) sich im rasch ansprechenden Leitersystem nur wenig bemerkbar macht, im Gegensatz zu punktförmig eingebrachten Markierungsstoffen. Nur 4 bis 10 % der gesamten Quellschüttung beruhen auf rasch zirkulierendem Wasser im Kluft-Karst-Leitersystem.

Neu bei Karstuntersuchungen im süddeutschen Raum ist die Betrachtung der auch im Ausland noch wenig beachteten "subkutanen Zone", die als Zwischenspeicher für neugebildetes Grundwasser dient, bevor es die tiefer liegende gesättigte Zone erreicht. Diese oberflächennahe Zone steuert nicht nur zu einem großen Teil den Spitzenabfluß von Quellen, sondern bewirkt auch deutliche Veränderungen in der Beschaffenheit des Quellwassers.

Herr Sauter hat seine Arbeit in englischer Sprache geschrieben, um sie einem breiteren internationalen Interessentenkreis zugänglich zu machen.

Tübingen, im September 1993 G. Einsele

Tüb. Geowiss. Arb.	Reihe C	Nr. 13	150 S., 82 Abb., 19 Tab.	Tübingen, Dezember 1992

Quantification and Forecasting of Regional Groundwater Flow and Transport in a Karst Aquifer (Gallusquelle, Malm, SW. Germany)

MARTIN SAUTER[1]

ABSTRACT: Karstaquifers represent an important groundwater resource and they are highly vulnerable with respect to contamination due to fast transport through the karst system and due to the limited attenuation of contaminants in karst terraines. In order to understand such a complex system, consisting of the compartments epikarst, vadose zone and the phreatic saturated zone, and to predict the variations in concentrations of point and non-point source contaminants, numerical groundwater modelling techniques are frequently employed.

This study considers two main aspects: firstly, the selection of an appropriate modelling tool for the simulation and prediction of groundwater flow and transport in a karst aquifer system, the adaptation of the model to the specific problem, the construction, testing as well as validation of the model. Secondly, the provision of data input, required for the modelling of such a complex flow system.

A Double-Continuum Porous Equivalent Model was found to be the most appropriate for the study area. Each of the two flow systems of the aquifer, the fast flow, i.e. conduit system, and the slow, i.e. fissured system, is simulated with a separate continuum, and both are coupled by an exchange term. The model applies to flow from a catchment, that discharges at a spring, or where the flow into a river via alluvial deposits can be quantified.

A large number of borehole logs together with information from water level fluctuations and fluvial history enabled the identification of aquifer base and zones of higher and lower hydraulic conductivities.

A soil moisture balance approach together with a water balance for the canopy (accounting for interception loss) produced sufficiently accurate values for groundwater recharge. Important parameters in the recharge calculation are the field capacity the interception capacity and the rapid recharge threshold. Although the rapid recharge component as a total percentage of the annual recharge is of only minor importance, it provides recharge for periods, where otherwise no recharge would have been calculated, although observed in the field. The importance of the influence of the epikarstic zone on the temporal distribution of recharge input and the relative distribution of recharge between fast and slow system needs to be stressed. The analysis of time series of hydraulic and physico-chemical parameters yielded storage and recession constants for the drainage from the subcutaneous zone, which could be devided into a fast and a slow recharge component.

The analysis of spring flow, temporal and spatial variation of groundwater levels, borehole hydraulic tests and also the time series of physico-chemical parameters of spring water allowed the quantification of storage and hydraulic conductivity for both, the slow (fissured) and the fast (conduit) system, for flood as well as drought conditions. The importance of the dependance of the above parameters on the measurement scale due to the heterogeneous distribution of fast and slow flow paths was recognized. The relationship between hydraulic conductivity and the sampled volume could be determined by evaluating the parameters at the catchment, several different borehole and laboratory scales. This procedure allowed the allocation of hydraulic conductivity at the modelling scale. The analysis of the various time series provided an insight into the different processes affecting the recharge and groundwater circulation. The chronology of the different parameter variations helped to understand the sequence of events.

The dominant hydraulic parameters in the flow simulation are the storage coefficient and the hydraulic conductivity of the fissured system, that control the storage and release of groundwater over time. The transport model is applicable to point-source and non-point source input, which also allows the modelling of complex recharge events, where a number of events of different intensity are superimposed. The determining hydraulic parameters in the transport simulation have been identified as the hydraulic conductivity of the fissured system and the transmissivity of the conduit system. The model has been validated and can be employed for predictive purposes, i.e. without any further corrections and calibration, the model could reproduce time variant fluctuations of $\delta^{18}O$, a nonpoint-source tracer as well as the breakthrough of a point source tracer.

---

[1]Dissertation at the Geowissenschaftliche Fakultät, Universität Tübingen

Author's address: Geologisch-Paläntologisches Institut, Sigwartstr. 10, 7400 Tübingen, FRG.

Acknowledgements

I would like to thank my advisor Prof. Dr. G. Einsele for his guidance and his valuable scientific, financial and administrative support. Particularly his faith in my work and the freedom to operate, provided a fertile ground for scientific and individual development. Despite some initial scepticism, he supported the purchase of essential computing and field measuring equipment at a time, when the outcome of the project was still uncertain.

Prof. Dr. D. Ford, McMaster University, Canada, and Prof. Dr. K.-D. Balke, Tübingen, volunteered to evaluate my thesis and to act as referees. Next to their busy schedule it was certainly a major effort to read through the whole report. It is very much appreciated.

I am also indebted to my colleague and friend Prof. Dr. G. Teutsch for constructive and critical discussions and for reading the manuscript. Many an idea developed out of stimulating discussions on the topic. I am further grateful to my colleague and friend Dipl.-Geol. Johannes Körner for helpful discussions, concerning the interpretation of oxygen isotope data and to my colleagues Dipl.-Geol. Helmut Schlöser and Dr. Peter Grathwohl for bearing with my need for communication. Furthermore many thanks to my Diplom-students Dipl.-Geol. P. Merkel and Dipl.-Geol. S. Renner for their interest in my work and many helpful discussions. P. Merkel and S. Renner also supported me with the digitisation of some of the thematic maps. I would also like to thank all my other colleagues not mentioned above, working in Room U11 and in the laboratory, who, with their great sense of humour, helped me to get over some despairing moment at the computer.

The project was supported financially by the Federal State of Baden-Württemberg within the context of the research project "Geowissenschaftliche Umweltforschung" and direct funding by Prof. Einsele. The Deutsche Forschungsgemeinschaft (DFG) supported the analysis of oxygen isotopes with a lumpsum of DM 8000.

Valuable data were provided by the Zweckverband Bodenseewasserversorgung. I would like to thank Dr.-Ing. Naber and Dipl.-Ing. Pflüger. Without hesitation, they let me make use of all their geological and hydrological data of the Albstollen-project. Further geological and tracer test data were provided by the Geologisches Landesamt Baden-Württemberg, Freiburg. Particularly Dr. E. Villinger and Dr. W. Käss were very helpful with their experience and assistance. A large proportion of the daily spring flow, river discharge and groundwater hydrograph data were provided by the Landesanstalt für Umweltschutz. Grateful thanks are due to Messrs. Lisiecki and Schmiedl. From the same institution, I could obtain the data for the time series on chlorinated hydrocarbons. Thanks are due to Mr. Straßburger and Mr. T. Ertel, Umweltwirtschaft, Stuttgart. Precipitation and climatological data were provided by the Deutscher Wetterdienst, Offenbach/Main and by the Wetteramt Stuttgart. I would like to thank Mr. Bläsing for his assistance in helping me to find my way through the numerous types of different data. Numerous data of double-packer tests were provided by the Deutsche Bundesbahn. Furthermore, Dr. B. Hanauer also sent me some information on evaluation procedures and test results. All this help is gratefully acknowledged.

I am very much indebted to Mr. Beilharz from the Zweckverband Zollernalb for the permission to install measuring and sampling equipment at the Gallusquelle spring, as well as the provision of historical water quality data.

Without the assistance of the Institut für Hydrologie, Gsf, Neuherberg, it would have been impossible to analyse the 1200 groundwater and rainfall samples for oxygen isotopes, from a technical and financial point of view. Grateful thanks are due to Prof. Dr. P. Fritz and Dipl.-Phys. Trimborn and also to Prof. Dr. K.-P. Seiler for helpful discussions concerning the interpretation of the isotope data.

The project implied a large component of field work. Without the voluntary help of many local individuals, it would have been impossible to obtain continuous measuring and sampling records with only minor gaps. I would like to thank Mr. Leuze from the Gemeindeverwaltung Neufra, Messrs. Gaiser and Endris from the sewage works Veringendorf, Mr. Bairer from the sewage works Burladingen, Mr. Schick from Realschule Winterlingen and Mr. Schiereg from the Bauhof Bitz for their help as well as my brother Otmar for letting me use his tank and tractor for the water injection tests. All this help is very much appreciated. I am particularly grateful to Messrs. Paul and Peter Knaus and their families for their help and the care they took of the instrumentation at the Gallusquelle, as well as their hospitality. I felt always welcome.

Finally I would like to thank my parents, who this thesis is dedicated to for their continuing support, which I could always rely upon.

Table of Contents

List of Figures

List of Tables

List of Appendices

1 Introduction

Prediction is an integral part of the management of karst water resources as well as of protection strategies against potential contamination, which karst aquifers are particularly subjected to.

However, for a long time, karst hydraulics has been considered as somewhat mysterious and unpredictable. Unexpected flooding in cave passages, sudden formation of sinkholes and also extreme contrasts between floods and drying up of springs contributed to this impression.

Early this century (Cvijic, 1918), the approach in karst hydrology changed from the description of single phenomena to an attempt to quantitatively understand the development and functioning of the whole karst system, including the unsaturated zone, and to predict flow and transport processes. With the theoretical background provided by Darcy (1856), Hagen (1839) and Poiseuille (1846), general groundwater hydraulic principles were applied to karst as well as channel flow theories, which however either failed to explain the observed high transport velocities or the slow recession after major recharge events.

As a tool for the simulation of flow and transport processes in karst areas, models have been frequently employed. They range from black box models, such as recession analysis and transfer functions to distributed parameter models, such as equipotential maps, equivalent porous medium and discrete fracture models. Black box models are used if there is only information on input and/or output and distributed parameter models can be employed if data on hydraulic characteristics, flow path geometries, head distribution and their respective variability are available. Problems, associated with the black box models are that they are not based on the physics of flow and transport and therefore lack predictive power. On the other hand, for discrete fracture models, the input data are difficult and frequently impossible to obtain. Equivalent porous medium models suffer the drawback of either only representing parts of the total system (fast/conduit - slow/diffuse) or only simulating either flow or transport processes. Teutsch (1988) for example managed to model flow and head distribution of a karst aquifer with an equivalent porous medium approach. The model proved useful for water resources problems, however the high velocities of tracer breakthrough curves could not be reproduced with the above approach.

Teutsch (1988) first introduced a numerical double continuum model, capable of simulating high groundwater velocities in conduits as well as sustained flow from the slow (diffuse) flow system. Unfortunately, due to the sparse information on aquifer geometry, hydraulic parameters and data on the dynamic response of the system, it was impossible to perform a detailed calibration and to properly validate the model.

The theory of modelling flow and transport in fractured and karstified rocks as well as the corresponding numerical models are in most cases ahead of the methods used for calibration and validation of the models. The delineation of aquifer boundaries, determined by the postdepositional erosional history, rather than by the primary lithology, is extremely difficult to perform, because of the highly heterogeneous nature of the flow paths. Recharge input is highly variable in space and time. It can be subdivided into fast and slow input, the relative distribution of which varies with the characteristics of the particular event. This fact complicates the evaluation of daily recharge input, essential for calibration of the model parameters. Frequently fitting parameters, such as the fracture-matrix-exchange term, which cannot be measured in the field, are used to describe the hydraulic characteristics of the rock for flow between the slow and the fast flow system. Finally, because of the dependancy of the flow parameters on the measuring scale (extreme heterogeneity in the flow parameters), i.e. the hydraulic characteristics vary between a tight rock and rapid turbulent flow, the measured field parameters cannot be used directly as model input parameters.

The large discrepancy between the processes that can be modelled and those, that can actually be quantitatively measured in the field is open to wide interpretation and ambiguities.

1.1 Objectives of the Investigations

The research efforts, presented in this thesis started at the described level of information and attempted to fill the gap between the model requirements and the field data provision.

The objectives of the presented investigations were primarily:

- The development of a reliable predictive tool for the simulation of the behaviour of karst aquifers, that firstly incorporates flow and transport processes and is capable of modelling the whole range of field observations, described in the introduction and in Teutsch and Sauter (1991). Those are for example high flow variability and at the same time prolonged recession characteristics, while the aquifer geometry, measured hydrographs and the field equipotentials match the modelled ones. Further, the simultaneous occurence of the observed high and low transport velocities should be integrated into the model.

- The assessment of general input parameters, such as the definition of aquifer geometry and boundaries, groundwater recharge including its temporal variation, and the hydraulic and transport parameters applicable to slow and fast flow system.

- The quantitative evaluation of the observed scale dependancies of the hydraulic parameters and the assessment of their implications for the modelling work.

- The incorporation of areal source transport phenomena into the model, development of appropriate methods to determine specific input parameters and calibration procedures.

- The evaluation of the determining factors in regional flow and transport.

The main emphasis of the investigations was put on the provision of the field data, that can be used as model input in order to provide the basis for a physically sound and unambiguous groundwater flow and transport model.

1.2 Methodology

The investigations were performed in the karstified limestone spring catchment of the Gallusquelle (Chap. 2), where, as a result of a large scale tunneling project (27 km water supply pipeline of the Bodenseewasserversorgung, Albstollen) detailed geological borehole information and longterm (since 1965) hydrological and hydraulic records were available (Fig. 1-1). The network was extended to include further automatically recording raingauges and digitally recording dataloggers, measuring water level fluctuations and physico-chemical parameters, in order to allow a thorough examination of single flood events.

After the customizing and the development of the required modelling tools, the initial work concentrated on the determination of the aquifer geometry, derived from borehole logs and the analysis of water level fluctuations. A detailed calculation of groundwater recharge, attempting to take into account all important variables, provided the model input. Due to the large proportion of forested land, interception losses could not be neglected. Particular emphasis was put on the evaluation of the temporal variation of groundwater recharge and the fractional allocation of the water to the slow and fast system. The quantitative analysis of hydraulic and chemical spring water time series proved to be extremely useful within this context.

A major portion of the investigations concentrated on the evaluation of hydraulic parameters using various methods, applicable at catchment, borehole and laboratory (from literature) scale. A main objective of the hydraulic parameter evaluation was the determination of the parameters at the modelling scale.

The examination of the time series served several purposes. Firstly it allowed the quantification of a differentiated recharge input into the fast and slow flow system, secondly the determination of storage within conduits and epikarst, and it provided the time variant recharge input for the unsteady state model calibration. With the above input, flow and transport models were built and calibrated for the complete spectrum of flow conditions, point source and areal source tracer input. Model runs with varying parameters demonstrated the sensitivity of the models to different hydraulic parameters.

1.3 Format of the Report

Chapter 2 presents a general overview of the area of investigation and demonstrates how insight can be gained into the flow system, using geological, hydrological and geomorphological information.

Chapter 3 describes various attempts in classifying karst flow systems and introduces the different approaches used in the modelling of flow and transport. Some examples from the literature demonstrate their applicability to different aquifer situations.

The major part of this thesis is devoted to the topic of model input data provision, outlined

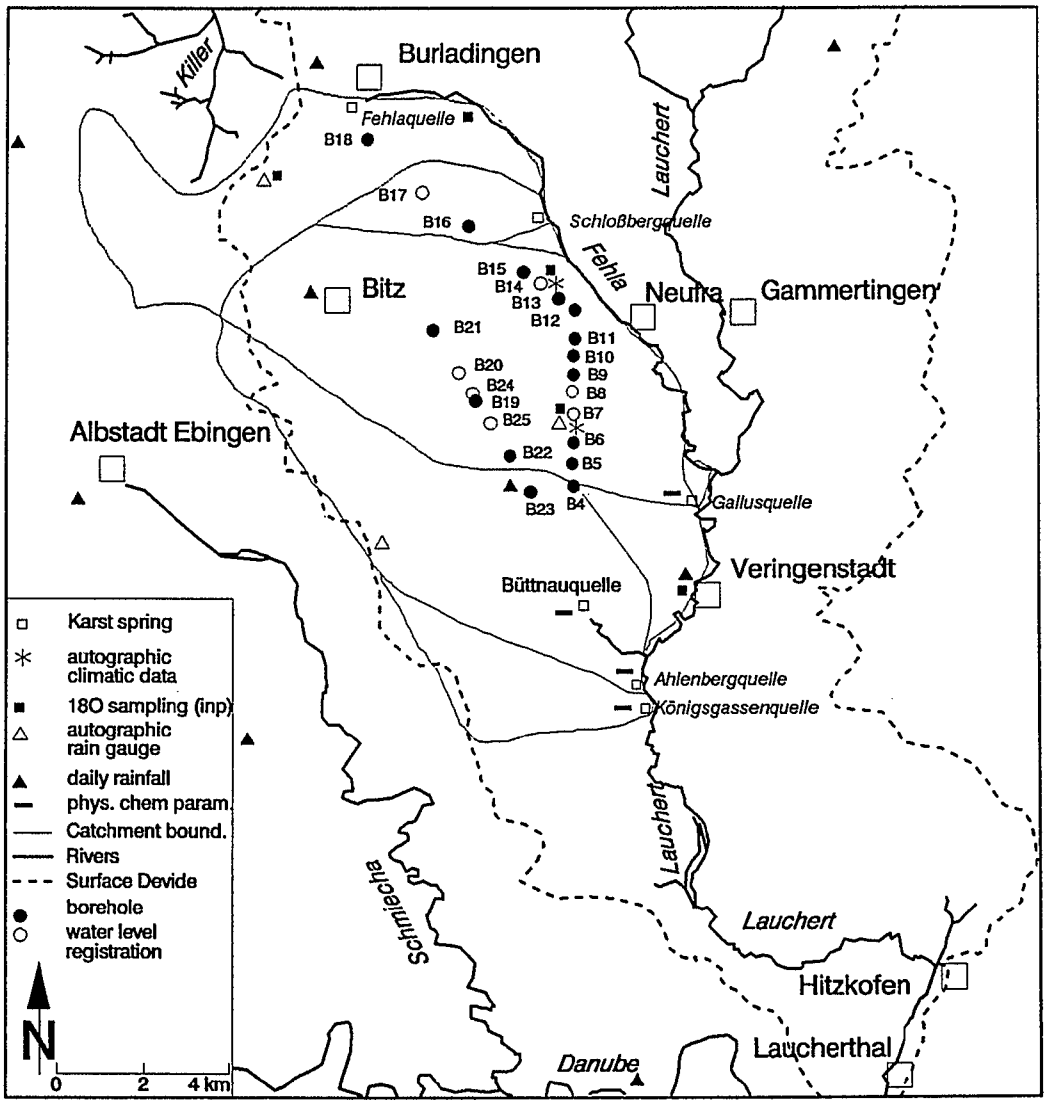

Fig. 1-1 Measuring Network in the Gallusquelle Spring Catchment

in chapter 4. It is subdivided into a recharge evaluation, the determination of hydraulic parameters and the analysis of the flow dynamics.

Chapters 5 and 6 deal with the actual modelling of flow and transport and include sensitivity analyses.

The reader and the author frequently face the problem of extracting the conceptual and most important information from a comprehensive and detailed text. Therefore this kind of information and conceptualisation is presented in italic typescript.

2 Project Area

The spring catchment of the Gallusquelle was selected for the investigations. It is situated in south-west Germany on the Swabian Alb, a small mountain range that stretches in approximate south-west north-east direction for circa 200 km (Fig. 2-1).

2.1 Topography, Geomorphology and Pedology

The Swabian Alb can be described as a tilted plateau, a part of a cuesta landscape, with topographical heights varying approximately between 700 and 900 m a.s.l. (Fig. 2-2). Commencing with a steep escarpment in the north-west the plateau gently dips south-east down to the valley of the river Danube. Geomorphologically, the major part of the area of investigation belongs to the "Kuppenalb", a rugged area, which was not levelled off by the transgression of the Miocene sea, which existed from the Oligocene until the Upper Miocene. The area to the south of the "cliff", the coast line of the Miocene sea (Fig. 2-2), is known as the "Flächenalb", a term which expresses the genetic history of this area as the abrasional plane of the Tertiary sea.

The landscape has been developing since the end of the Upper Jurassic, when the carbonate plateau emerged from the sea. Evidence suggests that only during the Middle and Upper Miocene, the southern parts of the Swabian Alb were temporarily inundated. However, during the more recent fluvial history since the Pliocene, steepening of the relief has occurred and the young erosional processes, mainly dominated by tributaries of the Rhine, could form terraces and steep escarpments in the north of the Swabian Alb (Fig. 2-3, from Gwinner, 1976, Fig. 3). Under these conditions a more rugged terrain could develop, even in the "Flächenalb". The geomorphological forms of the "Kuppenalb" can be attributed to the differential weathering and denudation between the domeshaped Jurassic spongial reefs (bioherms) and the basin fills (Cement Marls, tiZ).

Characteristic of the landscape are the dry valleys (Fig. 2-4). The valleys are interpreted as the result of formerly active water courses. They are assumed to have been reactivated

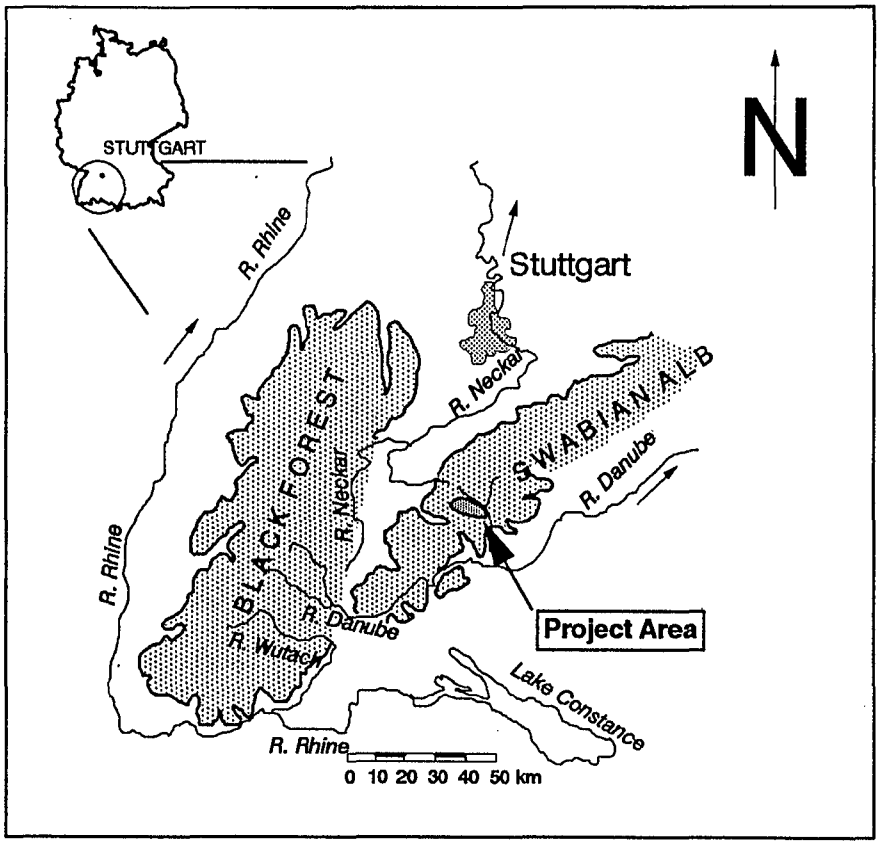

Fig. 2-1 Project Area

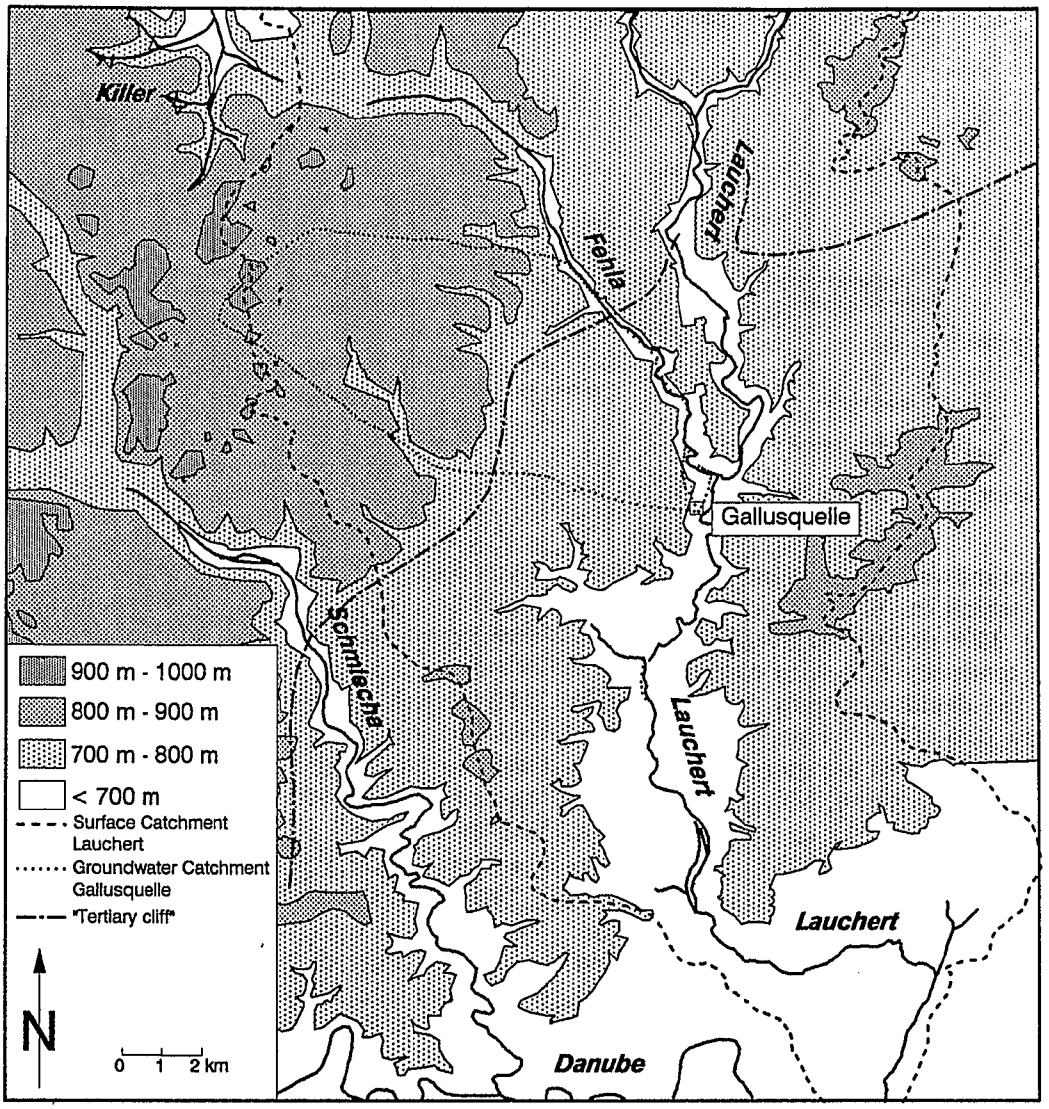

Fig. 2-2 Topography of the Project Area

during the glacial periods, when, due to permafrost, runoff occurred mainly at the surface. Strayle (1970) could show that the directions of the dry valleys were largely determined by the structural elements of the Hohenzollern graben and the Lauchert graben (see Chap. 2.3.3).

The two main river courses in the area are the river Lauchert and the river Fehla. Both valleys exhibit narrow cross-sections through the massive limestones and a low gradient with expressed meandering.

The limestone soils on the Alb plateau generally exhibit a regressive soil development, i.e. their characteristics are determined by different degrees of erosion. The soils range from predominantly orthic luvisols (terra fusca), various types of rendzina to syrosems (Müller, 1963, Agsten, 1977, Werner, 1978) with thicknesses between 20 cm and 80 cm. Acid brown soils, alvisols and colluvial soils prevail in surface depressions and dry valleys (Hemme, 1970) with thicknesses of up to several meters. The flint nodules, sometimes found in the soil profile, are interpreted in the literature as being the residual weathering products of the bioherm massive limestones, that originally stem from the silicious sponges.

2.2 Vegetation

The vegetation in the project area is determined mainly by the somewhat colder climate in the topographically elevated position and by the type and the thickness of the soils. Approximately 60% of the total area of the Gal-

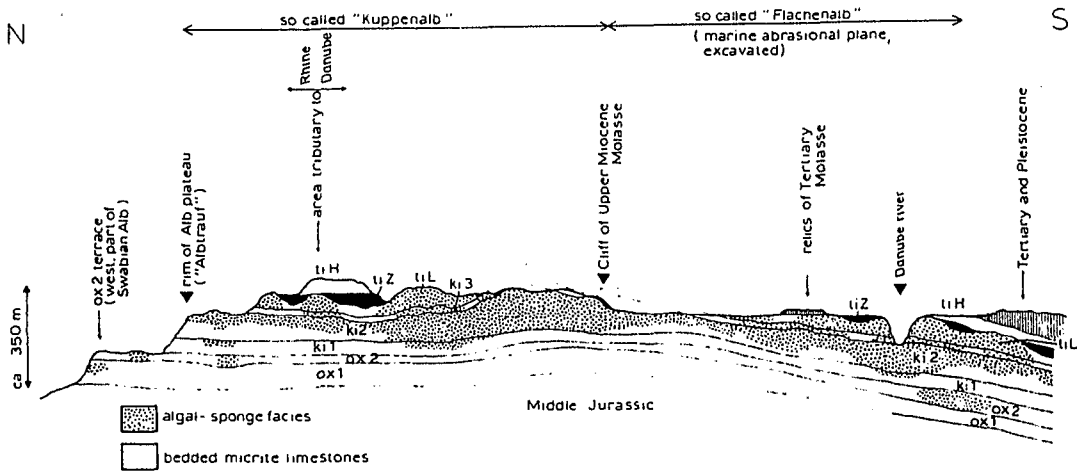

Fig. 2-3 Schematic Cross Section of the Swabian Alb (Gwinner, 1976)

lusquelle groundwater catchment is covered by forests, of which ca. 70% comprise coniferous stands and 30% deciduous species. There is however a tendency that with older stands (> 60 years), the deciduous trees dominate. Approximately 70% of the whole forested area is covered by trees which are more than 40 years old (pers. communication, Mr. Röther, Forstamt Gammertingen). The remaining 40% of the total catchment area is used agriculturally. The areal distribution of forest/agriculture is shown in Fig. 2-5; grassland covers approx. 65% of the total agriculturally used area and of the remaining arable land, approximately 80% is used for wheat growing. Because of the climate and soil conditions, potatoes and fodder beet are cultivated relatively infrequently (pers. communication, Mr. Thierjung, Landwirtschaftsamt Sigmaringen).

2.3 Geology

Apart from the relatively less important younger glacial and alluvial deposits, the project area is composed exclusively of the carbonate rocks of the Upper Jurassic, bedded, massive and marly limestones (Fig. 2-3, from Gwinner, 1976, Fig.3); the whole sequence can reach thicknesses of between 200 m and 500 m. In the project area, they probably range between ca. 250 m and 300 m (Gwinner, 1973).

2.3.1 Stratigraphy

The Upper Jurassic is characterized by two different kinds of facies, a "normal" bedded limestone facies and an algal sponge bioherm facies. The stratigraphy, petrography and the extent of the bioherm facies is presented in App. 2-1. The relationship between the lithostratigraphy and the karst aquifer development is shown in Fig. 2-6.

The lowest unit within the Upper Jurassic, the Oxford Marls, consists of a series of marls with intercalated limestone beds. They reach thicknesses of between 90 m and 100 m (Etzold et al., 1975) and can be considered as the base of the karst aquifer system.

The Oxford Marls (ox1) are overlain by a well bedded micritic limestone sequence, the Oxford Limestones (ox2), which form the aquifer in the Fehla catchment (Fig. 2-17 and Fig. 2-21). They have thicknesses of around 50 m (Etzold et al., 1975) and are only karstified in the north-west of the project area.

With the commencement of the Kimmeridgian, the marly limestones of the ki1 set in, with thicknesses of between 50 m and 80 m (Etzold et al., 1975), which in many parts of the Swabian Alb form the base of the main karst aquifer. The development of bioherms was somewhat reduced.

With the onset of the ki2, the algal sponge bioherms dominate the petrography for the remaining time of the Kimmeridgian. The thicknesses of the Kimmeridgian are determined by the former submarine relief and range between 80 m and 170 m for the complete series. The ki 2/3 constitute the main aquifer formation, the development of the aquifer porosity is enhanced by the high percentage of coarsely crystallized dolomite. The dolomite is considered as the product of a diagenetic recrystallisation. It can be hypothesized that the "Lochfels" facies, a cavernous limestone with large vugs and 'sucrosic' dolomite within the ki 2/3, is the result of dolomi-

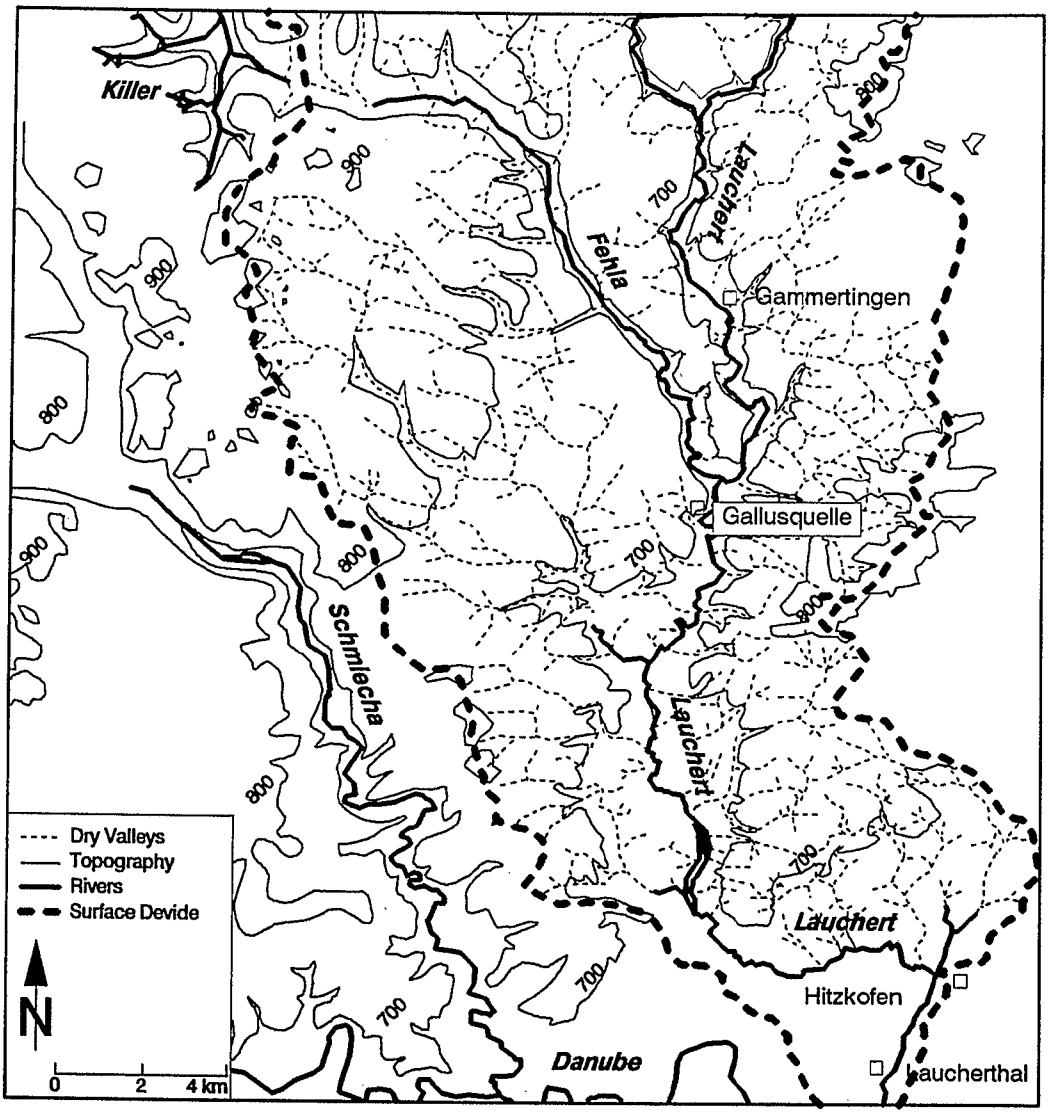

Fig. 2-4 Surface Hydrological Network

tisation of the higher permeable bioherms within the mixing zone (Hanshaw and Back, 1979; Morrow, 1982) of fresh water and sea water. Dedolomitisation might possibly occur when the dolomite comes into contact with solutions that are supersaturated with respect to calcite and undersaturated with respect to $MgCO_3$. This theory however requires further detailed examination, which is outside the scope of the present study.

The Tithonian is only found in depressions and is of relatively minor importance for the karst aquifer. The petrographic description is shown in App. 2-1.

South of the Gallusquelle catchment area, some of the deposits of the transgression of the Tertiary sea are still preserved. They consist of red nodular limestones and carbonate duri crusts (Krustenkalke) of Middle Miocene age and the Juranagelfluh, cemented gravels of Upper Miocene age. As opposed to the nodular limestones, the Juranagelfluh is a terrestrial deposit, with gravels of Jurassic origin. Relics of Old Tertiary deposits, such as quartzitic sands and iron ore concretions (Bohnerz), can sometimes be found in crevaces, cavities, dolines and other vertical solution structures.

The late Pleistocene deposits, found mainly in the Lauchert valley, commence with the early Riß period with sands and gravels of several meters (max. 10 m) thickness, deposited during the advancement of the glaciers (rise of erosional base due to the blocking of valleys by the glaciers, Göttlich and Werner, 1968). They are followed by clays and varve deposits of the former Riß Lauchert lake (see also Chap. 2.4), reaching thicknesses of up to

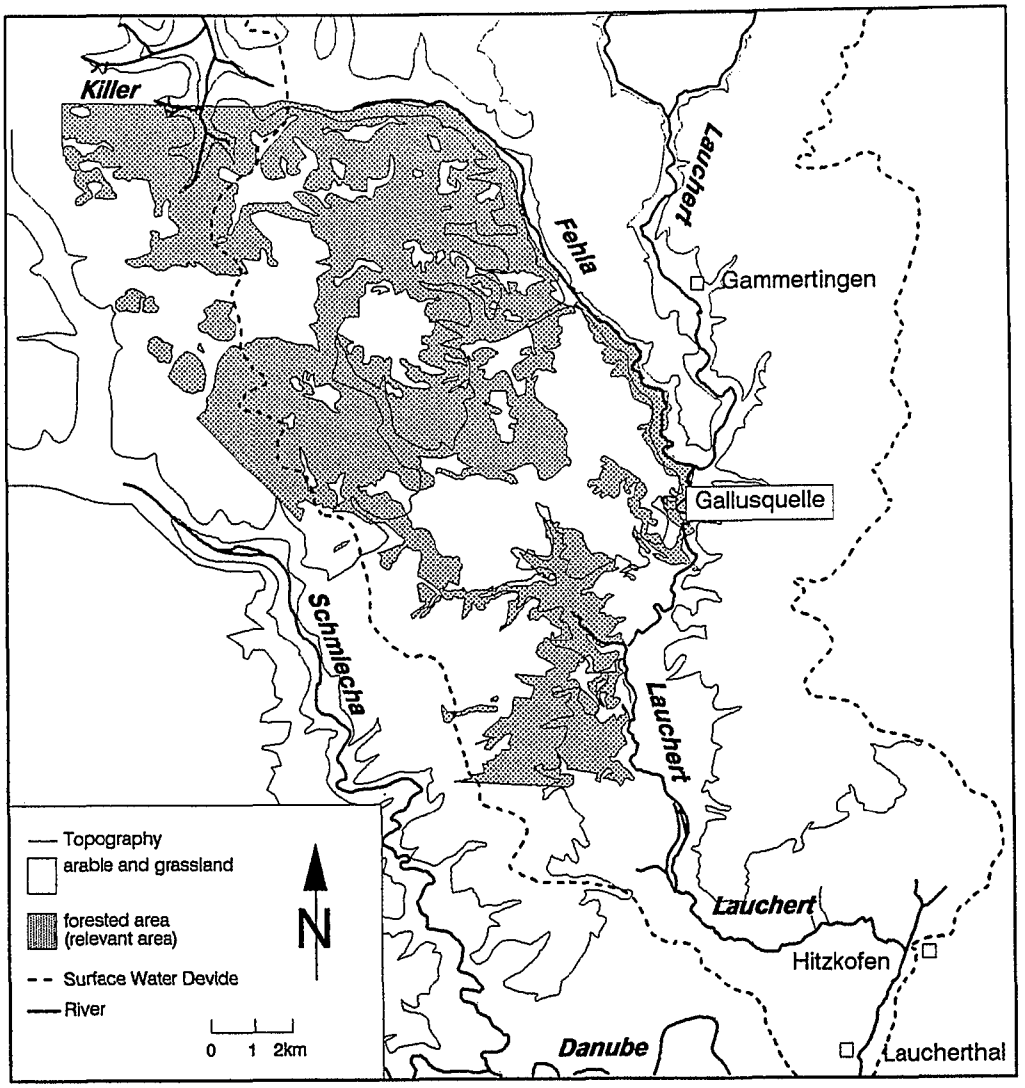

Fig. 2-5 Distribution of Vegetational Cover

15 m. The Würm (Wisconsin) cold period further filled up the valley with sands and gravels, loam and debris, which reach a total thickness of between a few and ca. 10 m.

Holocene deposits, consisting of clayey - silty sediments, with varying proportions of organic components, travertine and travertine sands and peat, range between thicknesses of 4 m and 15 m.

2.3.2 Geological Map

The regional outcrop area of the various geological units, including the distribution of normal and bioherm facies, is displayed in Fig. 2-7. Fig. 2-8 shows the geology of the project area. Due to the south-east dip of the whole series, the oldest units were mapped in the north-west. As a result of the rapid advancing erosion near the escarpment one finds the stratigraphical sequence from the ox1 up to the ki2/3 within a relatively small area. The plateau is predominantly formed by the massive ki2/3 limestones and the Tithonian was protected from erosion only in former submarine depressions and in structurally lowered areas of the graben zones.

In the south, remnants of the transgressions of the Tertiary sea, mainly of Miocene age, have been mapped.

The alluvial deposits can be found in the valleys of the rivers Lauchert, Fehla and Schmiecha.

2.3.3 Geological Structure

Within the project area, the whole limestone sequence gently dips south-east at an angle of

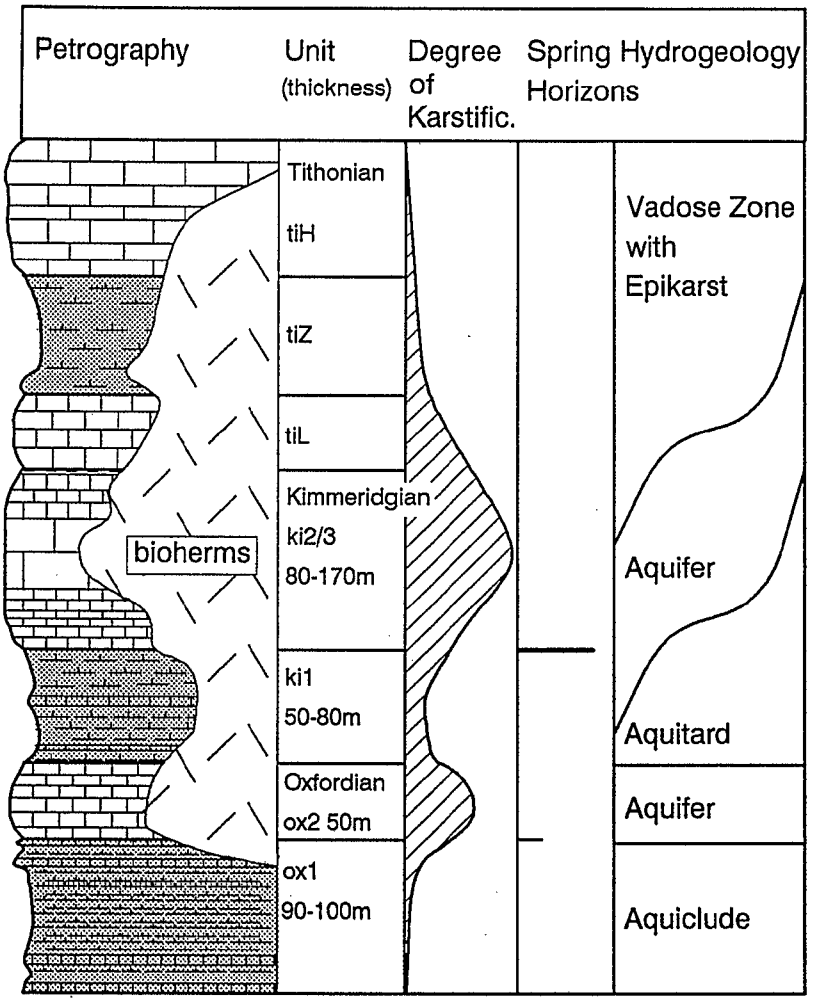

Fig. 2-6 Relationship between Lithostratigraphic Features and Aquifer Development

about 1.2 degrees (Fig. 2-9). A flexure can be assumed to occur at approximately 6 km north-west of the spring, which can also be explained by faulting. However, there is no surface expression of such a fault. On the other hand, borehole information indicates intensive faulting (B8, B10, B11, B15), but no definite directions and throws could be derived from the logs. The structure of the area can be taken from Fig. 2-10, which displays the topographic heights of the reference horizon ki1-ki2.

Two major fault zones have been mapped: one in the north-west, the Hohenzollern graben, which is tectonically still active, and the second, the Lauchert graben in the south-east. The throws of the main Hohenzollern graben range between ca. 100 m in the north-west and 70 m in the south-east, and those of the Lauchert graben were estimated at approximately 50m. The structural features of these two fault zones also become apparent in the main directions of the small scale fracturing, which could be measured by Golwer (1978), Merkel (1991) and Kriele (1969). The fractures are largely the result of structural/tectonic processes and to a lesser degree due to tension relief. The dominant direction is 0-30°, parallel to the Rhine graben and the Lauchert graben. Fractures were measured by Villinger and Koerner (in Golwer, 1978) in several tunnels, which were excavated for water supply pipelines by the Bodenseewasserversorgung. The majority of them were associated with the massive lime-stone facies. Whereas fractures with a strike of 0-30° are more or less restricted to a number of intensively fractured zones, joints with a strike of 100-140° (direction of the Hohenzollern graben) are more evenly distributed.

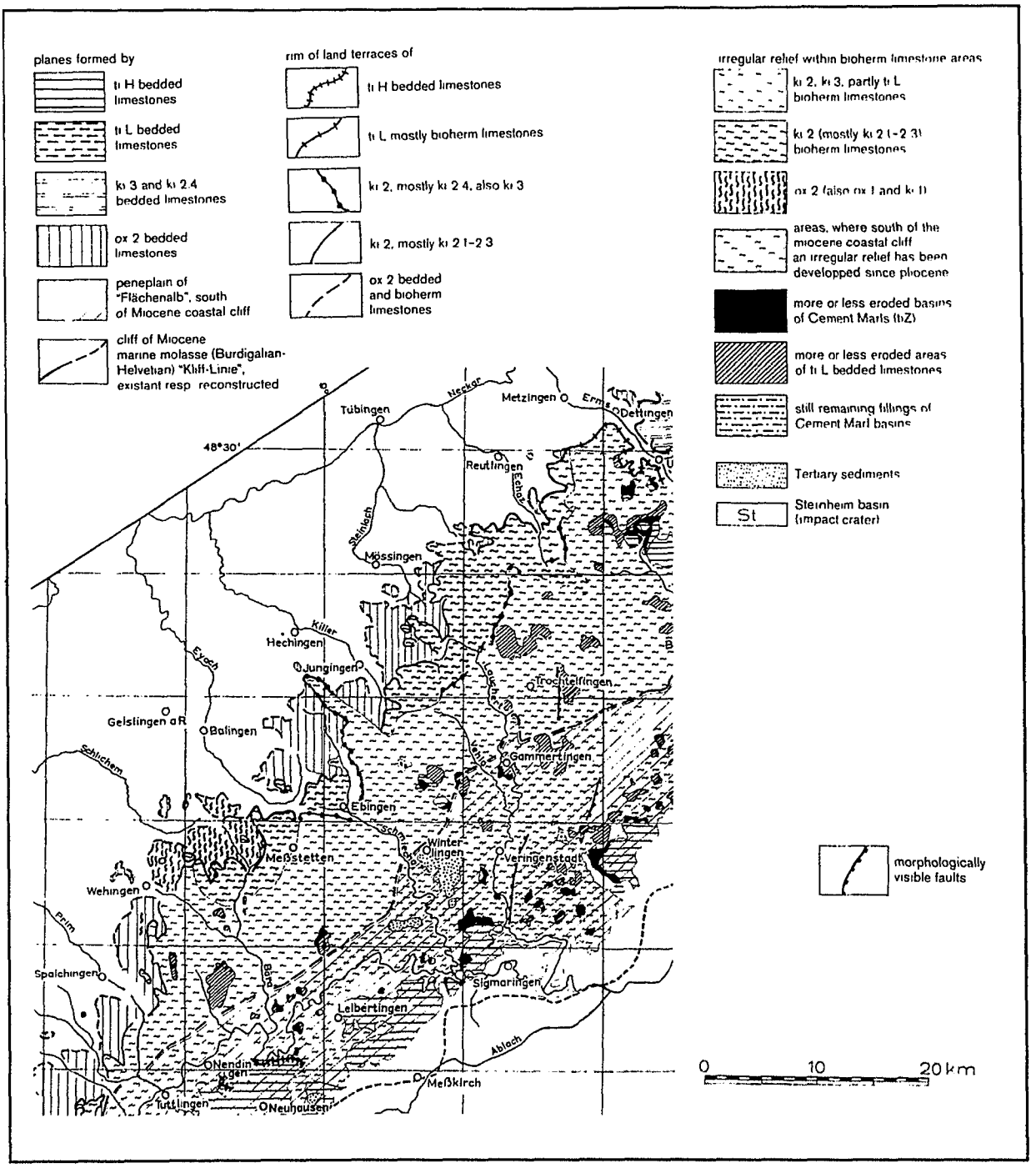

Fig. 2-7 Geological and Morphological Map of the Swabian Alb (Gwinner, 1976)

The structure in the area of highest density of information (south-east), is the most difficult to put into some meaningful context. There is strong indication for substantial faulting within the area of the boreholes (Villinger, 1973, in Gwinner, 1973). Within the lower part of the borehole B15 and B4, the whole sequence is tilted by 20° or 10-40° respectively, without any indication of primary bedding. The cores from B8, B10, B11, B14 display strong fracturing, and it was assumed by Koerner (1965) that the ki1/2 boundary was lowered in some areas, possibly along 3 antithetic fault zones.

2.4 Development of the Karst Aquifer and Evolution of the Fluvial System

The development of a karst aquifer is deter-

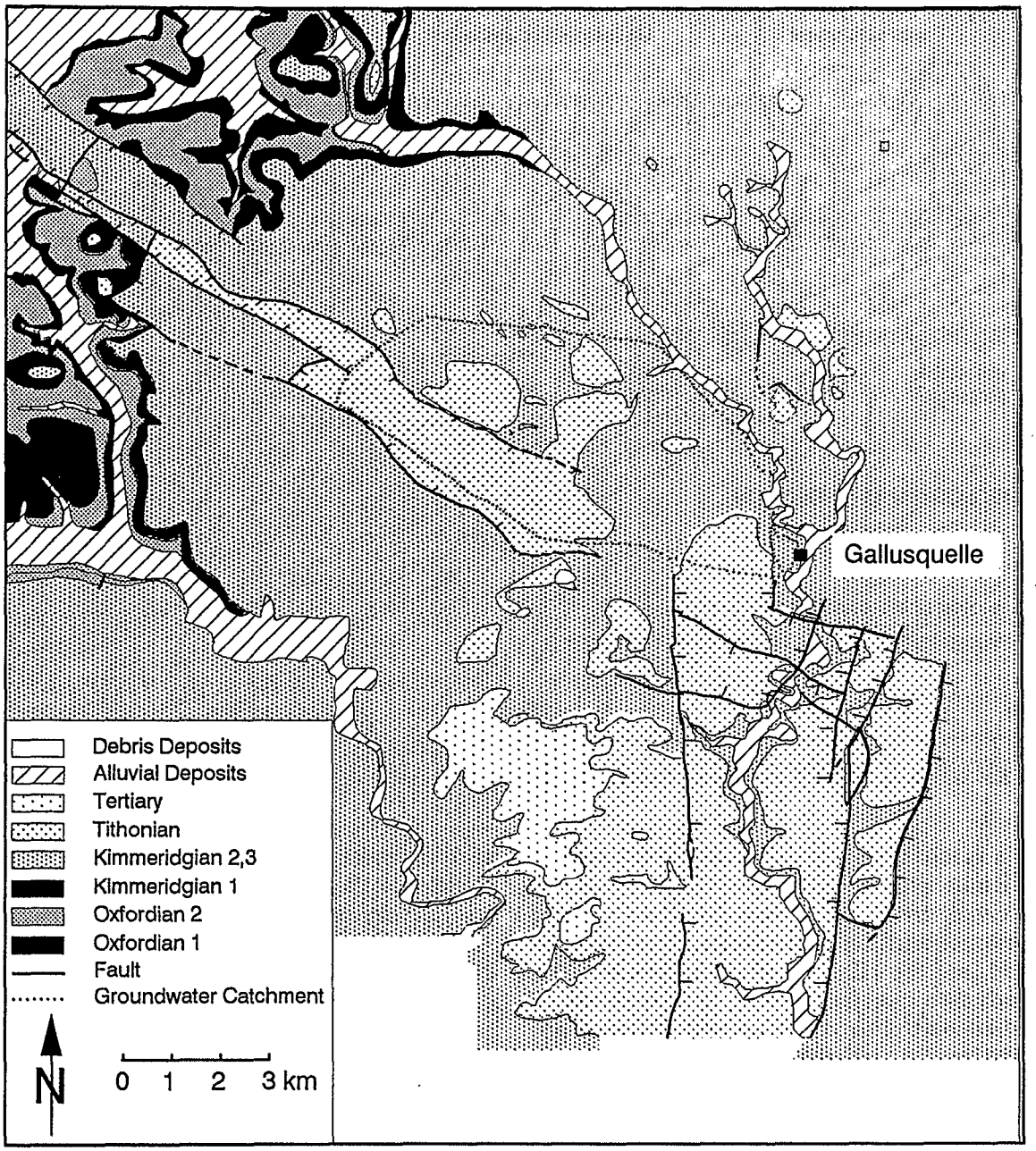

Fig. 2-8 Geological Map of the Project Area

mined by both intrinsic (carbonate content, mineral composition, distribution of massive/-bedded facies, geological structure, degree of fracturing, primary permeability) and extrinsic factors (erosional base, level of discharge point, uplift, climate, time span, vegetation) (James and Choquette, 1984, 1988). The relative importance of each of these controls is however difficult to assess.

A detailed model depicting a feasible genetic history of the karst development in Southern Germany was proposed by Villinger (1986). According to the model, the carbonate plateau of the Upper Jurassic emerged from the sea at the end of the Jurassic. Due to the resistance of the marly and bedded limestones of the Tithonian to karstification and the low elevation of the carbonate plateau above sea level, karstification was hindered in its progress. It can be assumed that the massive limestones formed the outcrop since the Upper Oligocene after the Tithonian rocks were eroded. The transgression from the Oligocene to the Upper Miocene however, which even flooded parts of the Alb plateau, prevented karstification at these relatively high sea water levels.

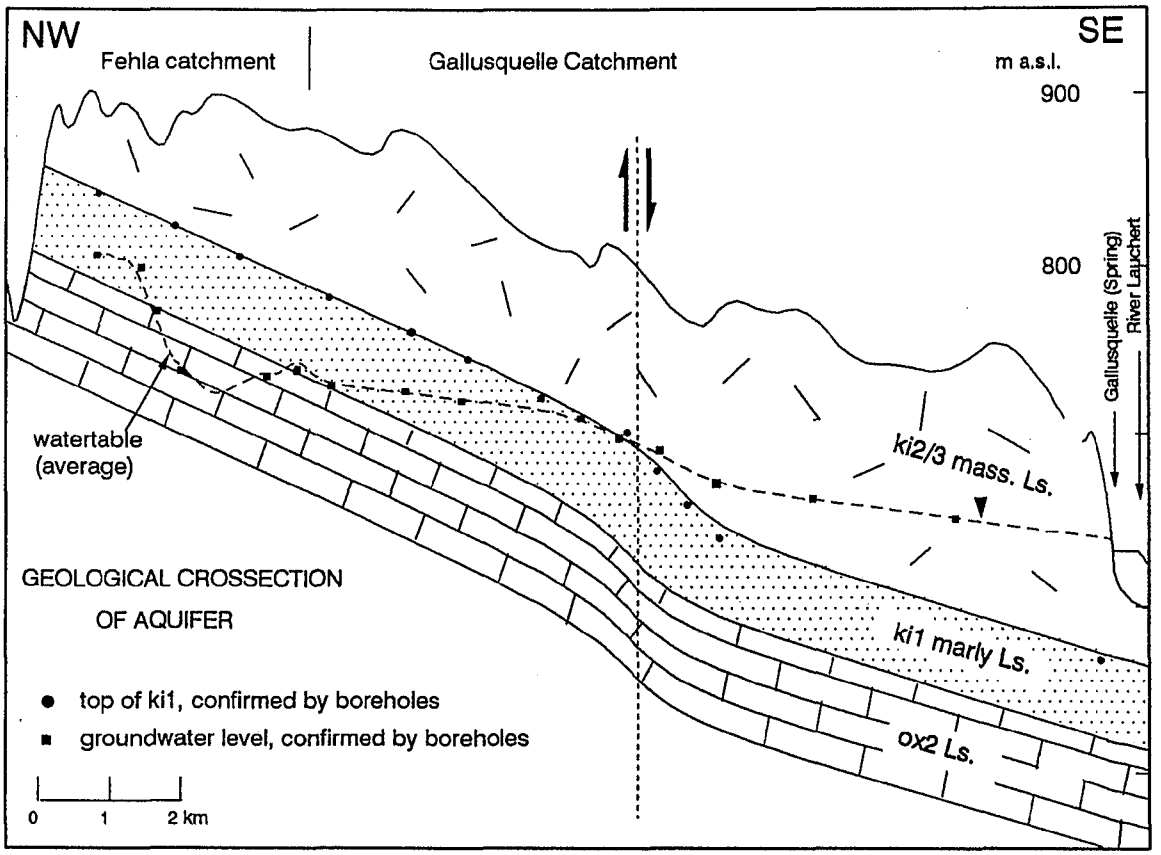

Fig. 2-9 Geological Cross Section of the Gallusquelle Karstified Limestone Catchment

As a result of uplift and rifting in the area of the Rhine graben during the Upper Miocene, the rivers could cut deeply into the massive limestones and the groundwater level was lowered into the ki2/3 massive limestones. With the advance in karstification, the tributaries of the Lauchert river dried up and drainage occurred mainly via the subsurface. Carbonate dissolution could then proceed not only at the surface (epikarstic zone), but predominantly within the range of the water level fluctuations. Denudation rates within the subsurface can be expected to be of the same order as those within the surface zone (Gascoyne et al., 1983).

Recent investigations into the theoretical basis of karst solution processes by Dreybrodt (1988) indicate that significant karst systems can develop from initially fractured rock with fracture apertures of around 100 µm, within several thousand years. From the time when solution kinetics changes from 4th to 1st order, i.e. when turbulent flow prevails, the apertures are widened at a rate of ca. 100 µm/a. Important variables are the solution rate, the hydraulic gradient and the initial apertures of the fractures. White (1988) could also demonstrate that mature karst systems could develop, given the right conditions, within very short periods (10 000 years)

During the glacial periods, drainage occurred chiefly at the surface via the dry valleys because of the sealing effect of the permafrost zone. Ford and Williams (1989) devoted a large part of their book on karst to the role of climate, particularly cold climate and they came to the conclusion that the 'development of karst systems does not appear to be significantly restricted in the sporadic permafrost zone'. By interpreting gypsum subrosion structures, Hebestreit (1990) could show that apart from approximately 17 000 years, the hydrology during the Würm glacial period (100 000 years duration) can be characterized by drainage that occurred to a major degree via the subsurface. Although the advance of the glaciers extended further north during the Riß glacial, similar conditions can probably be assumed throughout the Pleistocene.

It can even be assumed that karst development in the subsurface is even enhanced during the glacial periods as opposed to the interglacials. During the warmer interglacials, when the soil zone is dethawed, carbonate

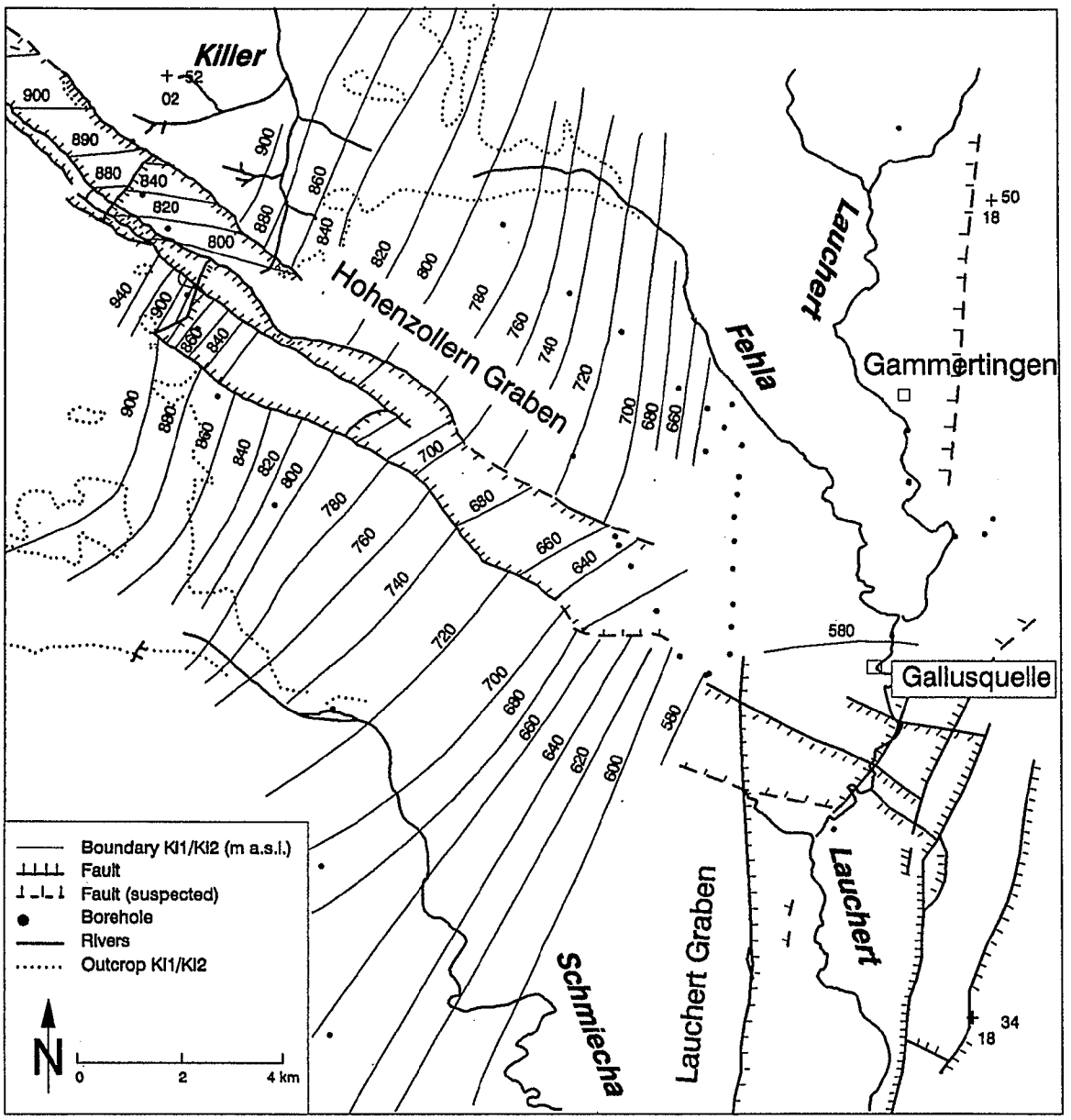

Fig. 2-10 Geological Structure of the Project Area (relative to the ki1/ki2 boundary)

dissolution occurs predominantly within the upper part of the unsaturated zone (subcutaneous zone) and by the time the water reaches the groundwater table, the recharge water is almost saturated with respect to calcite. Whereas during glacial times, melt water collected in surface depressions, initiated by the development of dolines, dethaws, due to its heat content the permafrost cover, and relatively aggressive undersaturated recharge water is conducted directly to the water table. Due to this mechanism, recharge water could be very effective in promoting karst development within the zone of water table fluctuations, even with low CO^2 partial pressure.

The former levels of the river Lauchert constitute a major influence on the karstification process. The lowest erosional river level can be assumed to have existed during the early Riß glaciation. The advance of the glacier caused the blockage of the old Danube valley, of which the Lauchert is a tributary, and the Lauchert valley was filled with sediment of the Middle Riß period. During the time of the most northern position of the icefront, lakes could form in the Danube and the Lauchert valleys with varve sediments of more than 10 m thickness in some areas. Delta deposits (Göttlich and Werner, 1968) can be used to ascertain the level of the Danube lake at a topographic height of 665 m a.s.l., whereas there remains some uncertainty regarding the level

of the Lauchert lake. The maximum level can probably be assumed at 684 m a.s.l., which most likely only existed for a short period (Villinger, 1973, 1985, Werner,1978); for most of their existence, the levels of both lakes can be assumed the same at 665 m a.s.l.. Since the Holocene, the level of the Lauchert river near the Gallusquelle spring remains at about 10 m to 15 m above the early Riß level.

2.5 Hydrology of the Lauchert Catchment

Together with other information, the surface catchment of the Lauchert river is displayed in Fig. 2-11, with the boundaries indicated as the dotted lines. The northern boundary extends for approximately 4 km further north than displayed in the drawing and continues into the catchments of the Reutlinger Alb. Discharge was measured up to the year 1980 in Hitzkofen and thereafter at gauging station Laucherthal. The surface catchment area was only increased by approximately 1% from 448 km^2 to 452 km^2. Tributaries of the Lauchert are the rivers Seckach in the north-east and the river Fehla in the north-west. Further gauging stations are located in Mägerkingen (Lauchert), Trochtelfingen (Seckach) and Gammertingen (Lauchert). Unfortunately, no weirs exist at the mouth of the Fehla river and south of the Gallusquelle spring.

There are a number of rain gauges distributed fairly regularly throughout the catchment. The rain gauge, Bitz, is however the only station within the catchment of the Gallusquelle, and for this reason, the network was extended to include the stations Winterlingen, Herrmannsdorf, B14 and B7.

A similar problem exists concerning weather stations, recording climatic data. Records are available from Albstadt-Onstmettingen and Sigmaringen. For the karst project, digitally recording systems were installed at B14 and B7, measuring air temperature and air humidity, in order to be able to transform the longterm records of Sigmaringen station, applying the necessary corrections, to values applicable to the Gallusquelle catchment.

Although longterm records exist, data were collected from 1965 until 1990, because since 1965, groundwater hydrographs have been available. The reason for such a lengthy observation period was to enable the calibration of the recharge calculation (Chap. 4.1) and the flow model parameters (Chap. 5). It could be assumed that a sufficient number of extreme years (wet, dry) were covered by this 26 year time span in order to be able to calibrate the important parameters also for extreme conditions.

One of the main objectives of performing a water balance for a particular catchment is to obtain a representative areal rainfall. The usual procedure is the application of weighting factors by constructing either Thiessen polygons or to use interpolation methods like bicubic splines or multiple hyperboloid surfaces. However, due to the areal distribution of the rain gauges, the influence of the escarpment and the fairly extreme change in topographical height from more than 900 m (NW) to approximately 600 m (S), the above methods are somewhat tentative, especially in a low density network. Therefore, 7 stations, for which longterm records existed (Albstadt-Burgfelden, Meßstetten, Burladingen, Trochtelfingen, Stetten, Sigmaringen, Veringenstadt) were lumped together and the arthmetic average was taken, without applying any individual weighting. For the recharge calculation (Chap. 4.1), rain gauges within the Lauchert catchment received higher weights, in order to improve the simulations. Unfortunately however, the desired improvement of the fit between modelled and measured recharge could not be obtained. On the contrary, a general deterioration of the fit between the measured and calculated data was observed. Fig. 2-12 shows the variation of the annual rainfall, relative to the mean annual rainfall (1965-1989) of 913 mm. This figure clearly shows relatively dry years (1971, 1972, 1976, 1985, 1989) and wet years (1965, 1986, 1988). Monthly rainfall varies from less than 10 mm to more than 180 mm per month (Fig. 2-13).

Evaluating the longterm averages of all rain gauges by completing their records using regression analysis for respective years between long series and fractional records and integrating the topographical information into the interpretation, allows an isohyetal map to be constructed (Fig. 2-11). From the figure it is apparent that the annual average longterm rainfall depth decreases from more than 1000 mm/a in the north-west to less than 800 mm/a in the south-east. The low rainfall in Albstadt-Lautlingen (900 mm) and Albstadt-Ebingen (910 mm) provides indication for the existence of a rain shadow effect within the Schmiecha valley.

Climatic data, required for the evaluation of the potential evapotranspiration (E_{pot}) were

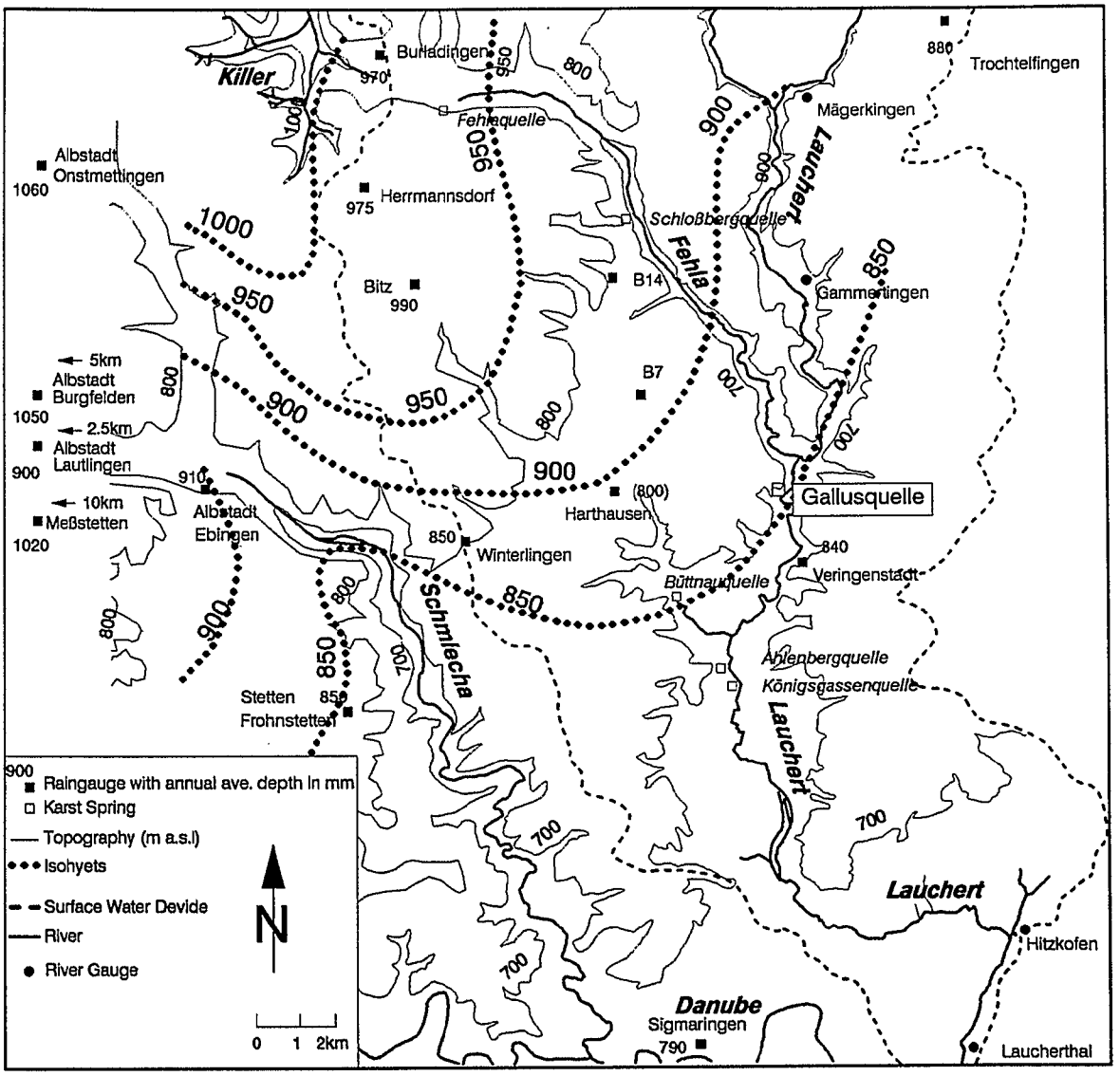

Fig. 2-11 Isohyetal Map of the Project Area

derived from Sigmaringen weather station and converted to values applicable to the catchment investigated, by using a regression analysis for the period 1988-1990, for which parallel records existed (B7, B14 - Sigmaringen). Fortunately, a linear relationship exists between the longterm Sigmaringen records and the B7 and B14 data. The decrease in temperature with increasing topographical height (≈ 0.9°C/100m) lies well within the range indicated by Linsley et al. (1982) of 0.5°C to 1.0°C/100 m.

Annual totals for potential evapotranspiration (see Chap. 4.1, $E_{Haude, grass}$) vary between 420 mm and 580 mm for the hydrological year (1.11.-31.10) about an average of 480 mm/a. Daily values (averaged over one month) of relative air humidity and air temperature are displayed in Fig. 2-14 showing the variation and extreme years. The average air temperature varies around 7.2°C and the relative air humidity around 80%.

Fig. 2-15 shows the monthly variation of the potential evapotranspiration, calculated with the Haude (1955) method (E_{Haude}) for three selected years (see also Chap. 4.1). Because the E_{pot} calculated with this method only applies to grassland, Sokollek (1983) extended this method to different crops and forested stands. It is apparent that $E_{pot, grass}$ is dominant during spring, but during summer and autumn months, forested areas are capable of evaporating considerably more than grassland. Interception, which leads to a further increase in evapotranspiration, is not accounted for in the evapotranspiration calculated for spruce and

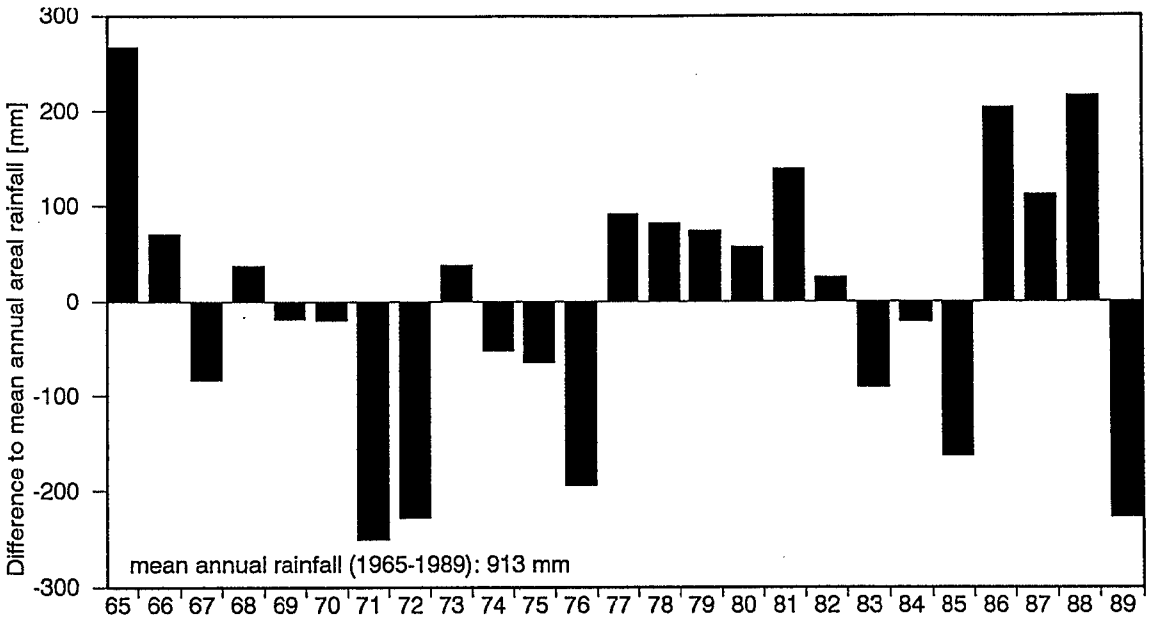

Fig. 2-12 Variation of the Mean Annual Rainfall Relative to a Longterm Average

beech. The difference in E_{pot} between spruce and beech becomes obvious during the spring, when evapotranspiration is lower in beech stands because of the not yet fully developed foliage. The difference between $E^{pot,\ beech}$ and $E^{pot,\ spruce}$ are very low, due to the fact that interception is not accounted for.

The discharge of the Lauchert is displayed in Fig. 2-16 for the period 1981-1987, and for the remaining years 1965-1980 in app. 2-2. The surface water discharge was measured in Hitzkofen up to 1980 and thereafter in Laucherthal. Although the catchment became larger with the change in gauging station, the discharge was less by approximately 1 m^3/s. This difference is a result of abstraction by an industrial plant and the loss was corrected for (pers. communication, Mr. Heinzelmann, Wasserwirtschaftsamt Sigmaringen). The Lauchert discharge was compared with the spring discharge of the Gallusquelle (multiplied by 10 to take account of the smaller Gallusquelle catchment). Both hydrographs agree fairly well, except for some extremely high discharges, when the flow from the spring exceeds that of the river. During low discharge conditions,

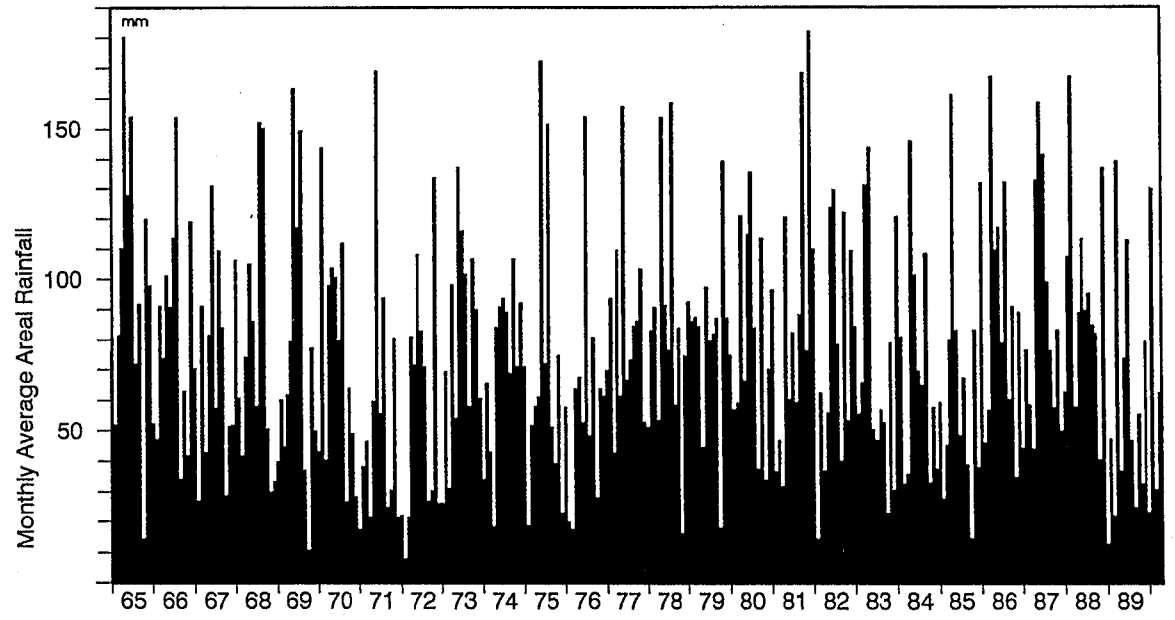

Fig. 2-13 Monthly Average Areal Rainfall

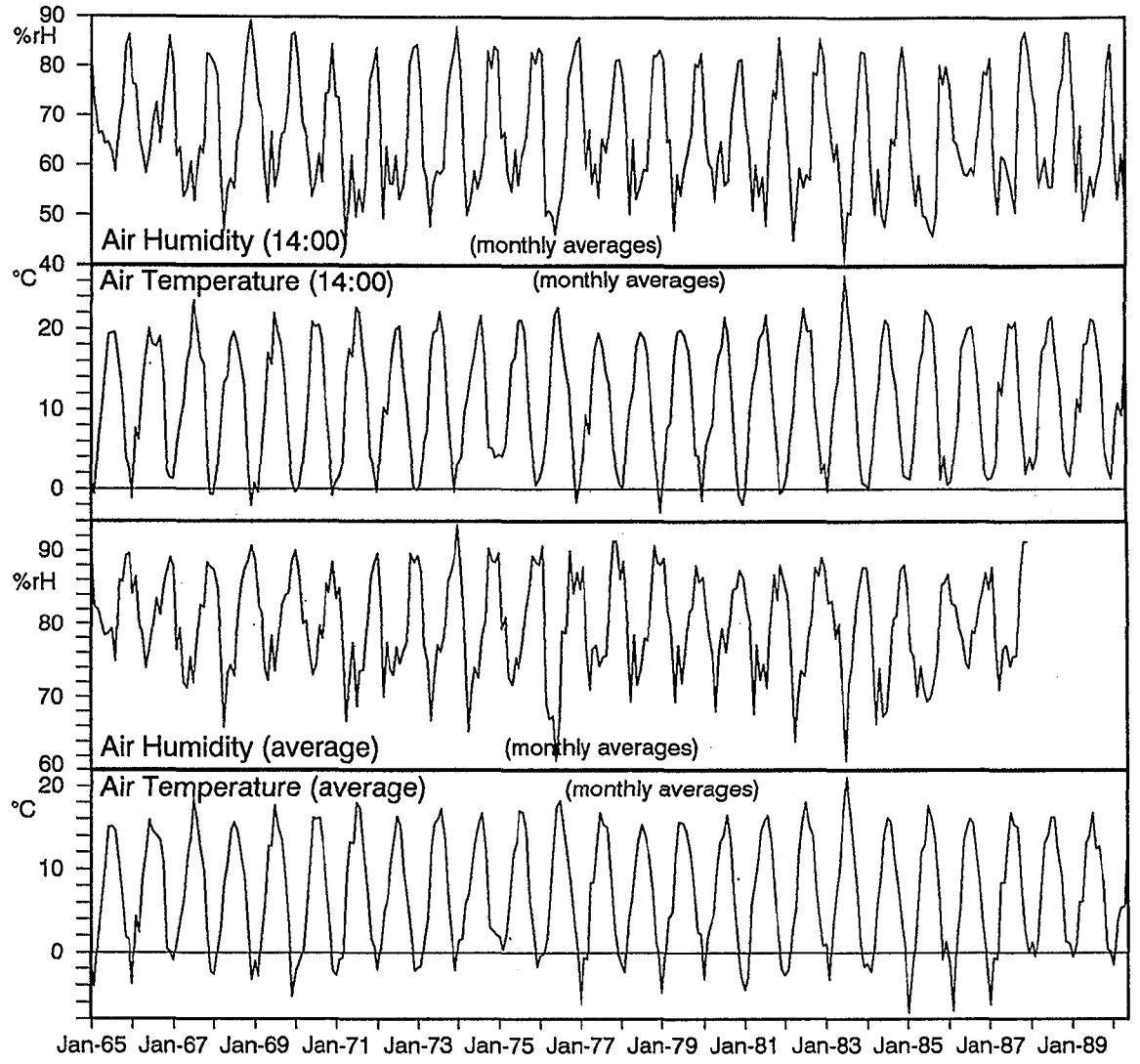

Fig. 2-14 Variation of Air Humidity and Air Temperature

especially during dry years, spring discharge drops much more rapidly than the Lauchert discharge. This feature becomes especially obvious, when the average daily discharges of Lauchert and Gallusquelle are compared in form of their flow duration curves. The deviation at low flow conditions between surface water (mainly composed of karst groundwater) and spring discharge, which becomes apparant at flows below 2 m^3/s (0.2 m^3/s Gallusquelle), might be indicative of the flow underneath the spring weir. It can be argued that the Gallusquelle does not represent average conditions of the Lauchert catchment. Due to the geographical situation of the spring catchment within the high rainfall area (Fig. 2-11), recharge can be expected to be somewhat higher.

The groundwater hydrology and the response of the subsurface water is discussed in detail in Chap. 2.6.3.

2.6 Hydrogeology of the Gallusquelle Groundwater Basin

The Gallusquelle groundwater catchment belongs to the "Deep Karst" (Katzer, 1909, Gradmann, 1931, Villinger, 1977), a term, which refers to a type of aquifer, where the piezometric surface is always situated well above the aquifer bottom. In a deep karst, the head gradients are controlled by the topographical level of the regional outlet. In the Gallusquelle catchment, karstification is moderately developed and groundwater flow is believed to occur in a network of conduits/fractures and small scale solution channels.

In the "Shallow Karst", the waterlevels within

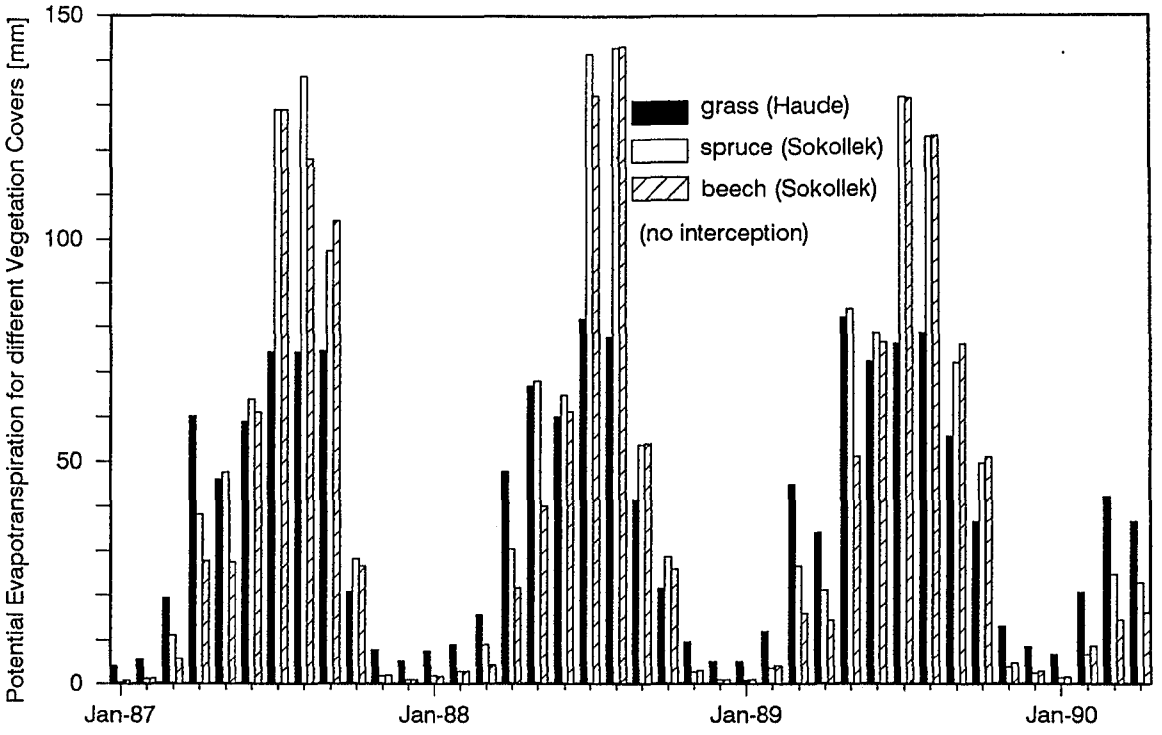

Fig. 2-15 Monthly Variation of Potential Evapotranspiration for different Vegetation Covers (Interception not accounted)

the aquifer are determined by the topographic level of the sealing aquifer bottom, e.g. the oxl marly limestone in the Fehla catchment. The shallow karst in the Fehla catchment is characterized by steep head gradients, intensive karstification and flow is usually turbulent and non-Darcian.

2.6.1 Karst Aquifer Geometry

Due to the very nature of the genesis of a karst aquifer and the often complex geological

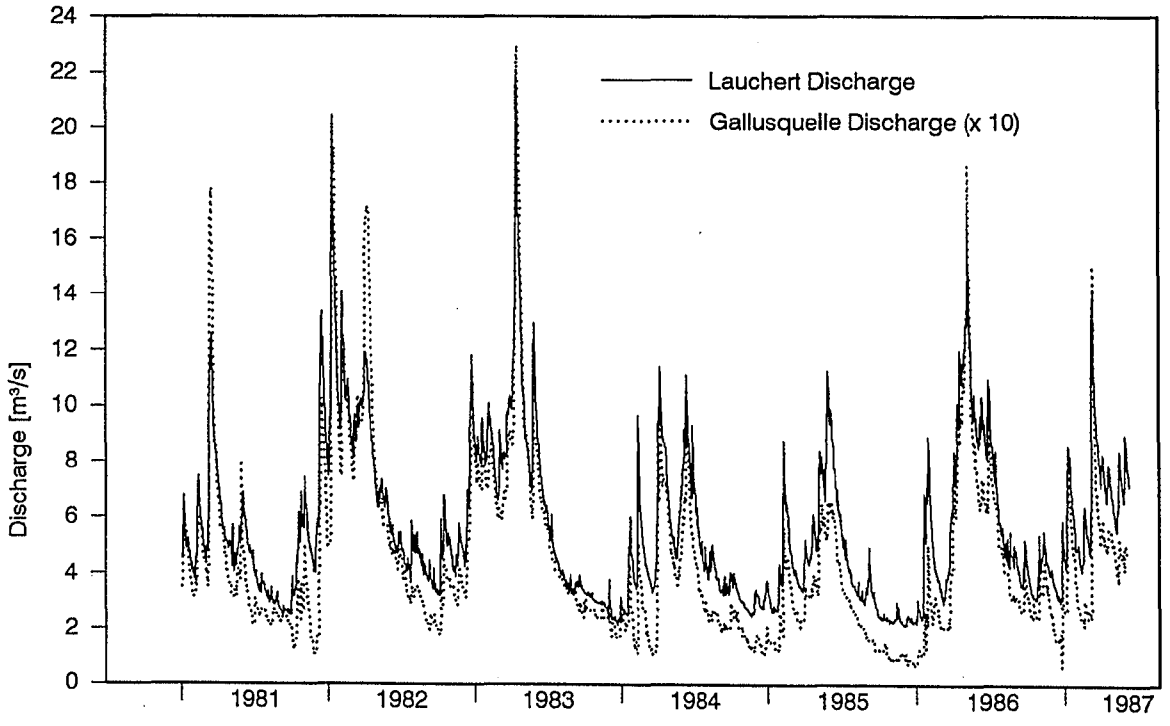

Fig. 2-16 Comparison Between Lauchert and Gallusquelle Discharge

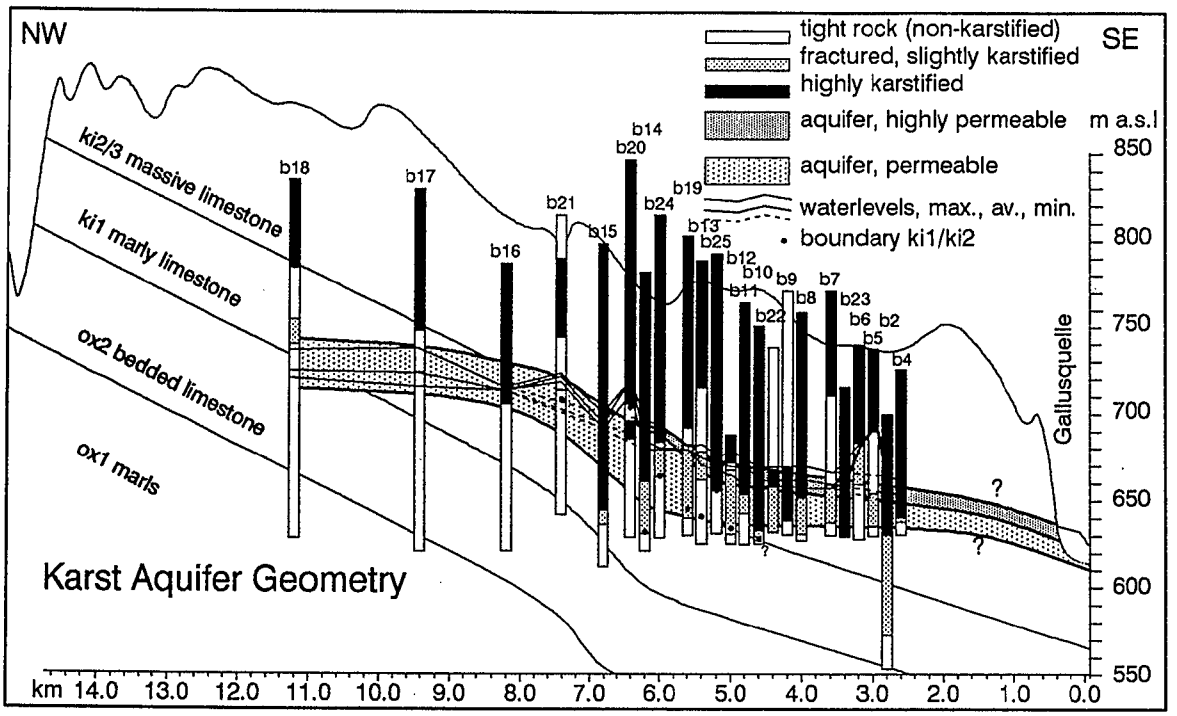

Fig. 2-17 Geometry of the Gallusquelle Karst Aquifer

history together with the resulting paleohydrology, it is very difficult to accurately delineate the boundaries of the aquifer. Structural elements, such as large and small scale fracturing and the level of the discharge point are likely to have a dominant influence on the development of the aquifer base and the development of higher permeable horizons. Further important factors include the petrography (Fig. 2-6) and the quantity of groundwater recharge.

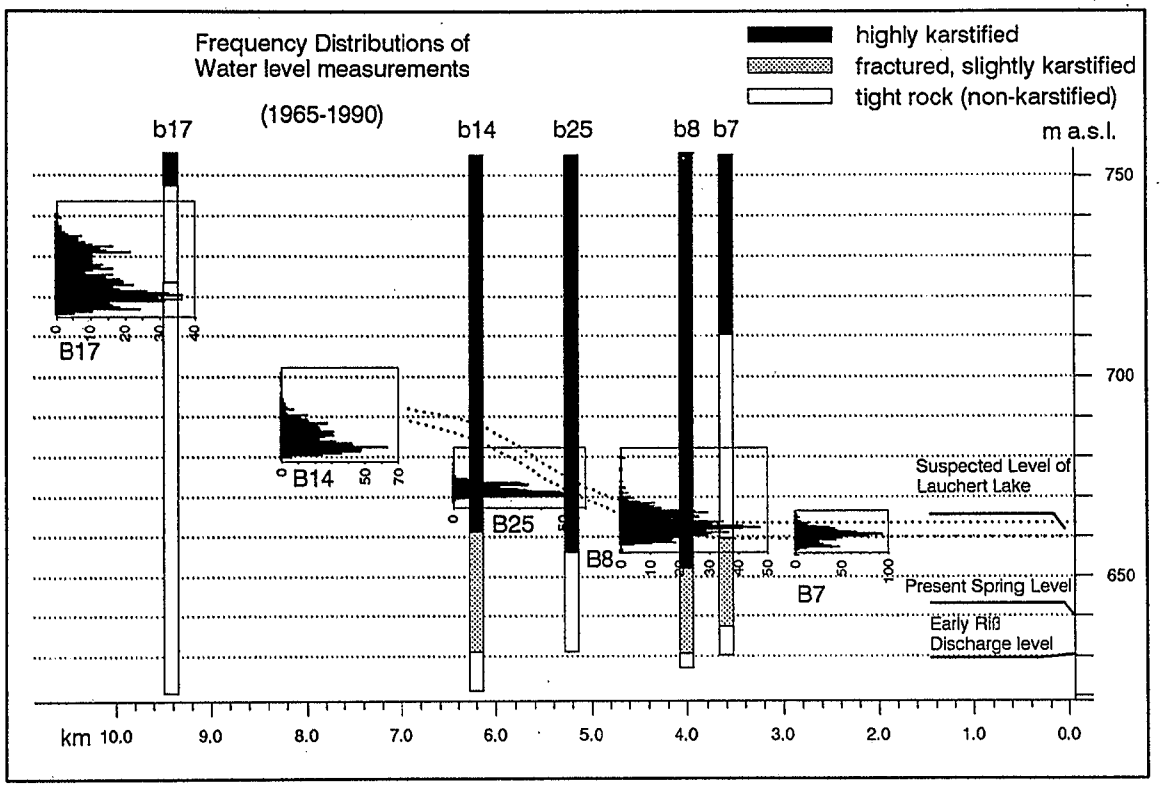

Fig. 2-18 Range of Water Level Fluctuations

Considering the above, it could not be assumed that the base of the aquifer runs parallel to a less permeable geological unit. Fortunately, some information from borehole cores existed, which provided evidence of the existence of karstified horizons and although the boreholes were not evenly distributed throughout the catchment, they still allow some estimate of aquifer boundaries.

As shown in Fig. 2-17, the aquifer is formed by three geological units, the massive limestones (ki2/3) in the south-east, the marly limestones (ki1) in the centre and the well bedded limestones (ox2) in the north-west. The aquifer base does not follow any stratigraphical boundary. Fig. 2-17 shows highly transmissive and permeable zones of the Gallusquelle groundwater catchment. The boreholes were all projected onto a profile line, assuming no variations vertical to the profile, and the borehole logs were interpreted in terms of tight rock, fractured and slightly karstified and highly karstified. Where faulting has been reported, boreholes were given lower weights in the determination of the aquifer base. As discontinuities, they could not be expected to be representative of continuous aquifer boundaries. This procedure, however, did not take into account the geological situation within the Hohenzollern graben itself. Boreholes B19, B22, B23 and B25 were drilled within the graben. The karstified zone in borehole B25 and B19 does not appear to differ from areas not affected by the graben zone. This finding is not surprising, in view of the fact that the graben structure dates back to the Oldest Tertiary, i.e. before the beginning of the main karstification. On the other hand, in wells B23 and B22, the base of the karstified horizon was not reached. It can be assumed that the graben forms an important groundwater storage area, due to the lowering of the more highly karstified massive ki2/3 limestones. Nonetheless information from B25 and B19 regarding the degree of karstification indicates that this effect might be reduced further upgradient, which would necessarily be expected further away from the discharge point. The highly karstified zones in boreholes B23 and B22 suggest that the Hohenzollern graben has a stronger influence on the groundwater hydraulics closer to the regional outlet, although the throw decreases from 100 m in the north-west to only several tens of meters in the south-east. In boreholes B4, B5 and B6, no evidence was found to suggest any difference to boreholes outside the graben zone. *The aquifer base was drawn at the level, where fractured limestone changed into tight rock and the highly permeable zone was marked, where the majority of cores indicated high degrees of karstification. Information, derived from the groundwater hydrographs supported the geological information. Due to the fact that it cannot be assumed that the water levels of the geological past ran parallel to the presently measured levels, the presence of other higher transmissive zones, especially in the range of the unsaturated zone cannot be excluded, especially at higher topographic levels. Judging by the recent drainage system, they can probably assumed to be of minor importance and only activated at extremely high groundwater potentials.*

Geological information on the former position of the "cliff" (Chap. 2.1) indicates that the highly karstified area south-east of the steep increase in water level (km 7 in Fig. 2-17), was situated at various times during the Tertiary within the range of the salt/fresh water mixing zone, encouraging karstification processes.

Other valuable information can be derived from groundwater hydrographs, which were, excluding the years 1974 and 1975, regularly measured once a week for the last 25 years. They express the dynamics of the groundwater flow within the aquifer, whereas the logs are only an indirect measure. Fig. 2-19 shows the hydrographs of the piezometers B7 and B14. Maximum waterlevel fluctuations in B7 (7m) are usually half of those in B14 (14m), which might be considered as a qualitative estimate of the hydraulic parameters T and S, i.e. that the area surrounding B14 is lower in T or S or both. During the extreme recharge event in March/April 1988 however, the fluctuations were approx. 20 m in both piezometers, which might indicate that the higher permeable zone does not extend far beyond the observed range of average water level fluctuations and that the transmitting capacity of this zone is exceeded. The observation that the level in B7 drops back quicker to pre-event levels is another clue for a higher transmissivity in the region of B7, a feature, which can be expected in the area of flow concentration near the spring.

The form of the individual hydrographs reveals some further information about the aquifer properties and internal aquifer structure and heterogeneity. If the aquifer could be as-

sumed to be homogeneous, the rate of change in water level would be continuous and gradually decreasing with decreasing potential difference. Plotting a frequency distribution of water level measurements, taken at the same time intervals, should then produce a skewed distribution, with the maximum shifted towards lower water levels because of the lower rate of level change during low flow conditions. The boreholes in Fig. 2-18 however usually displays bimodal frequency distributions, which means that there is an increased probability to measure a water level at higher elevation, other than at low water level conditions. The hydrographs of B14 and B7 in Fig. 2-19 also reveal a decrease of the rate of level drop above the level of 660 m a.s.l. in B7 and above 685 m a.s.l. in well B14. This kink in the hydrographs, which can be repeatedly observed, year after year, is particularly marked in May 1989, when there is no interference by rainfall events. *This range of the second maximum in the distributions is interpreted as a zone of high transmissivity or storage or both, limited to only a few meters (B14: 685.5-689 m, B7: 660-663 m a.s.l.) and the boreholes are tentatively connected. Its origin can be probably related to the presence of the Lauchert lake, which existed during the Riß glacial (see Chap. 2.4), when the water level at the discharge point was kept constant for a substantial length of time (in the order of 10 000 years) at ≈ 665 m and the groundwater table fluctuated within a small range, encouraging solution processes.*

The top of the aquifer is formed by the watertable, i.e. the aquifer is unconfined.

Lateral boundaries are the Hohenzollern graben in the south-west and the River Fehla in the north-east. Effluent conditions prevail in the upper river course of the Fehla, whereas there is some uncertainty about the degree of connection of the aquifer with the surface water in the lower course, as described in Chap. 2.6.3. It is possible that the river Lauchert forms the discharge point, i.e. there is possibly no interaction of the Fehla river with the groundwater, that might have a marked influence on groundwater flow in that particular area. Several decades ago, the river Fehla dried up completely during some years, but since suspended matter increased with industrial sewage discharge, the river bed became more or less sealed. A tracer test in the year 1963, with the input south of the village of Neufra, showed a connection between the Fehla and the Gallusquelle spring. However, only traces of the dye were found in the spring water. As far as the water balance and the recharge area is concerned, the uncertainty about the Gallusquelle and the Fehla does not have a marked effect. Villinger (1973, in Gwinner, 1973) estimated this unknown quantity in the order of between 10 and 20 l/s.

The hydraulic characteristics of the fault zones of the Hohenzollern graben are not very well known. There is evidence (Tunneling work Albstollen, Zweckverband Bodenseewasserversorgung, Gwinner, 1973), for the assumption that the southern fault zone acts as a sealing fault. The discharge during the tunneling work, which started near the Bütt-nauquelle, following the line of boreholes from B22 to B24 up to the town of Burladingen, had a very low discharge up to borehole B25 of maximum 35 l/s.

In the north-west, the groundwater devide between the catchments of the Fehla spring and the Gallusquelle catchment forms the boundary. Its position can be derived reasonably well from the groundwater heads and tracer test data. The groundwater mound in the north-west (Fehla catchment) can be attributed to the tectonic lowering of the ki2/3 massive limestones within the Hohenzollern graben (Villinger, 1977).

In total, the catchment area is estimated at approximately 45 km^2. Villinger (1977) estimated the area to range between 40 km^2 and 45 km^2.

As far as it can be derived from water level information, the catchment boundaries do not change markedly throughout the year (Villinger, 1977).

2.6.2 Recharge and Discharge

Recharge to the Gallusquelle groundwater basin occurs via precipitation, apart from the minor quantities added within the lower course of the river Fehla. The mode of entry can be termed autogenic (Williams, 1983), which implies that recharge occurs as diffuse recharge over the whole catchment area and not as recharge via stream sinks. Except for very short periods of snow melt, when the soil is still frozen, surface runoff is not observed, so that the total discharge of the spring is equal to groundwater recharge. Because of the unknown quantity of flow below the Gallusquelle weir, the Lauchert discharge was used for an initial estimate of groundwater

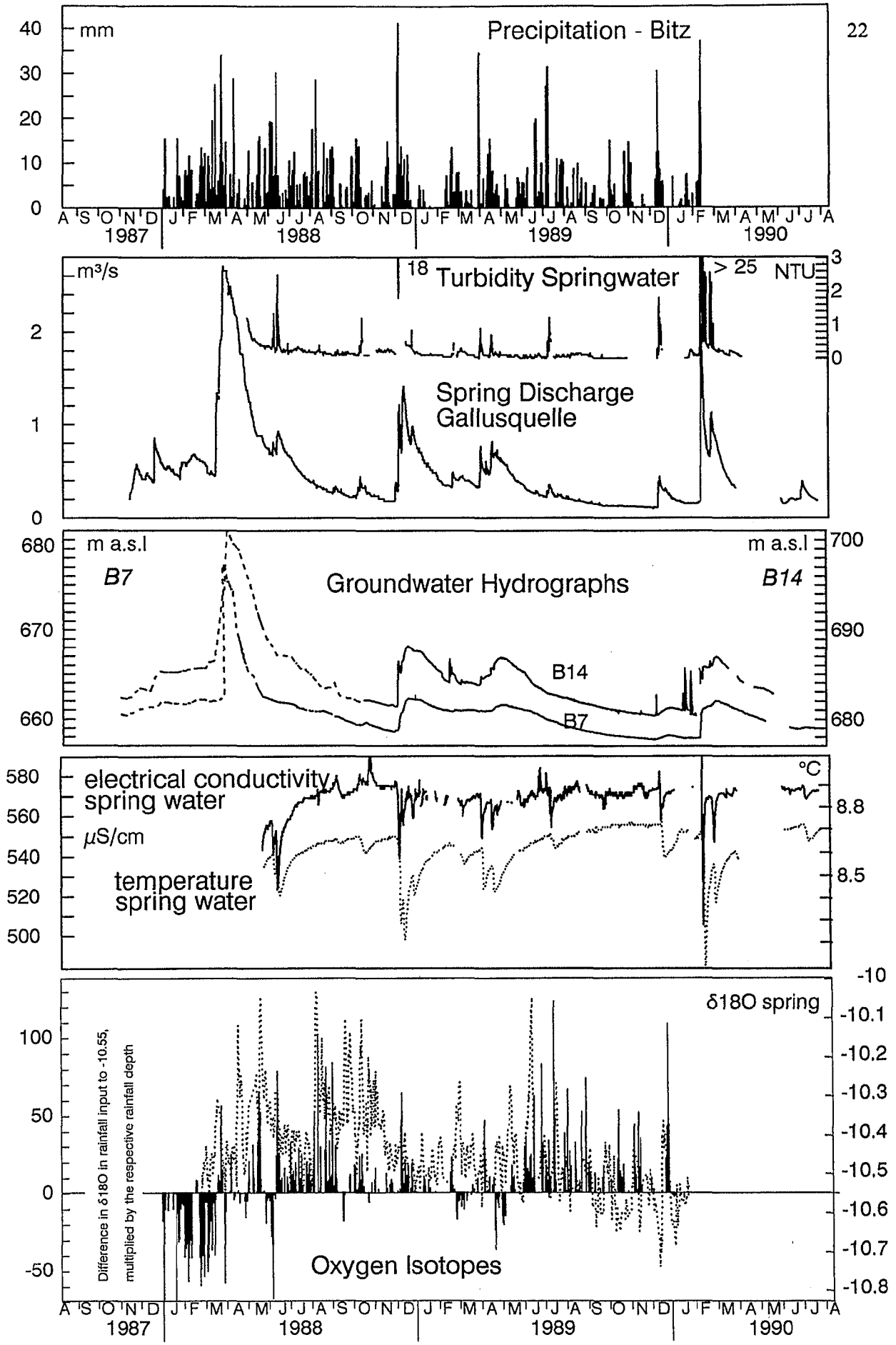

Fig. 2-19 Time Series of Hydraulic and Physico-Chemical Parameters of Spring Water

recharge, which amounts to ca. 360 mm/a for the years 1965-1989, taking into account storage changes. This quantity represents approximately 40% of the average areal rainfall of 900 mm/a. Due to the fact that the Gallusquelle catchment is situated in the northwest of the Lauchert catchment, i.e. near the high rainfall area (Chap. 2.5), groundwater recharge can be estimated to range between 380 and 390 mm/a, which corresponds to an area normalized recharge rate of approximately 12.2 l/s km^2. An average annual recharge for the Gallusquelle catchment was calculated with a recharge model (Chap. 4.1) at 390 mm/a, which included several years, where the estimated areal rainfall was probably above the actual rainfall. In the model calculations, groundwater recharge ranged between 150 mm/a (1972) and more than 500 mm/a (1988). Villinger (1977) calculated an average rate of 13.5 l/s km^2 (1967-1968) for the catchments of the springs Gallusquelle, Ahlenbergquelle, Fehlaquelle, Schloßbergquelle and some other low discharge springs. The calculated recharge was expected to be higher than the value of Villinger (1977), because, according to the authors definition, short term discharge, i.e. fast karst water is not included in the recharge. On the other hand, in the respective table of Villinger (1977, p. 78), the average discharge (MQ) is taken for the estimation of recharge, i.e. the fast component was included. The main source of difference probably lies in the estimation of the catchment area, because the years considered in Villinger (1977) are average years, compared with the period 1965-1989. If the Gallusquelle catchment was estimated at 40 km^2 instead of 45 km^2, similar values could be obtained.

The regional outlet for the groundwater is at the Gallusquelle spring, although some flow can be assumed to occur below the weir. Merkel (1991) attempted to quantify this unknown flow (see also Chap. 4.1.1.5) and estimated it at 200 l/s, which is probably too high. The comparison of area normalized flow duration curves between the Gallusquelle and the Lauchert catchments shows that both curves behave similarly throughout most of the time. At low flows, i.e. the discharge is less than 200 l/s of the Gallusquelle, the discharge of the spring deviates markedly from that of the river. This can be explained by the increased importance of the flow below the gauge, as compared to the total discharge. This unknown rate however is assumed not to be far above 50 l/s.

Fig. 2-19 exhibits time series of the discharge rate, groundwater hydrographs and physicochemical characteristics of the spring water. Although the discharge hydrograph can be described as flashy, the flow out of the groundwater system is considerably delayed (relative to the time of the storm event, based on groundwater hydrograph readings) by approximately two to three months, compared to only a few days in very maturely karstified groundwater basins. The magnitude varies from 2.5 m^3/s to 0.08 m^3/s with an average flow of approximately 0.5 m^3/s.

2.6.3 Analysis of Water Level and Hydrograph Data

Water level data were recorded at weekly intervals, with some interruption, since 1965 for some of the wells (B7, B8, B14, B20, B21, B24, B25). For the other boreholes, readings are only available from 1965-1973. For the wells situated in the west, only single readings exist.

In a number of wells, perched water levels have to be assumed. In the case of B20, the waterlevel is measured about 40 m above the regional groundwater level. Records of the Bodenseewasserversorgung show that immediately after borehole completion, the waterlevel measured corresponded to what could be expected at this particular location, i.e. the waterlevel was lower and the fluctuations displayed were typically high. Similar conditions apply to boreholes B5 and B6. During sampling for chlorinated hydrocarbons it was discovered that Fluorescein dye from 25 years ago was still left in the borehole (B24), which shows also that the connection is not well developed. It has to be mentioned however that the boreholes are completed as piezometers and only the bottom 6 m are screened, so that there is no real exchange between the hole and the aquifer. The hydrograph of B21 responds very rapidly to recharge events but drops also rapidly to a water level which hardly fluctuates at all throughout the year. This could be explained by the lack of proper connection of the piezometer to the aquifer or by the fact that the boundary kil/2, which approximately corresponds to the average water level, forms the basis of the aquifer in this area. There is a tendency that water level fluctuation increases slightly upgradient (B17,B18, Fig. 2-20).

This information allows the construction of a piezometric map as given in Fig. 2-21. An

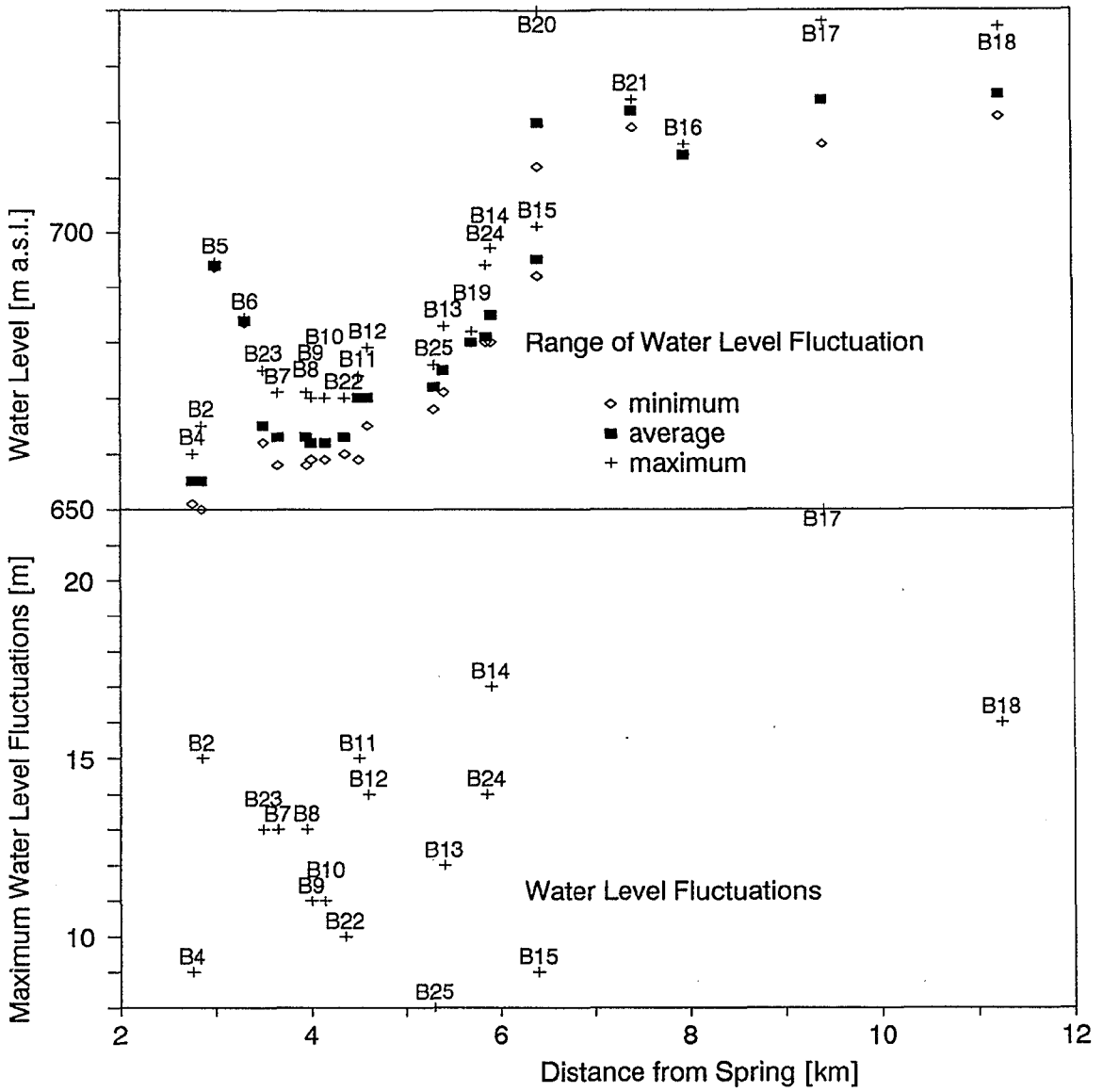

Fig. 2-20 Analysis of Water Level Fluctuations

increased gradient of the piezometric surface can be observed in the centre of the catchment (Fig. 2-21, 2-17)), where the water table cuts across the less permeable marly limestones. Further upgradient and close to the spring, lower gradients were measured. Higher degrees of karstification due to flow concentration near the spring and a reduced throughput upgradient in the north-west are plausible explanations for the lower gradients in the other areas. As already indicated in Chap 2.6.1, the hydrological situation is not very clear in the lower course of the river Fehla, which is indicated by the dotted equipotentials. In this case, discharge is directly to the river Lauchert and the Fehla is perched above the water table. It was attempted to delineate the depth of the water table next to the Fehla river with resistivity soundings, but because of highly conductive alluvial sediments and the low contrast between saturated and unsaturated limestone (low porosity), no clear answer could be obtained.

In order to be able to use all the available data, average water levels were used, instead of measurements on a specific day. As already mentioned above, Villinger (1977) compared the equipotentials during high and low discharge conditions and came to the conclusion that the shape of the water table did not change markedly.

Fig. 2-22 shows selected hydrographs of piezometers that could be expected to be representative of the aquifer. They are arranged

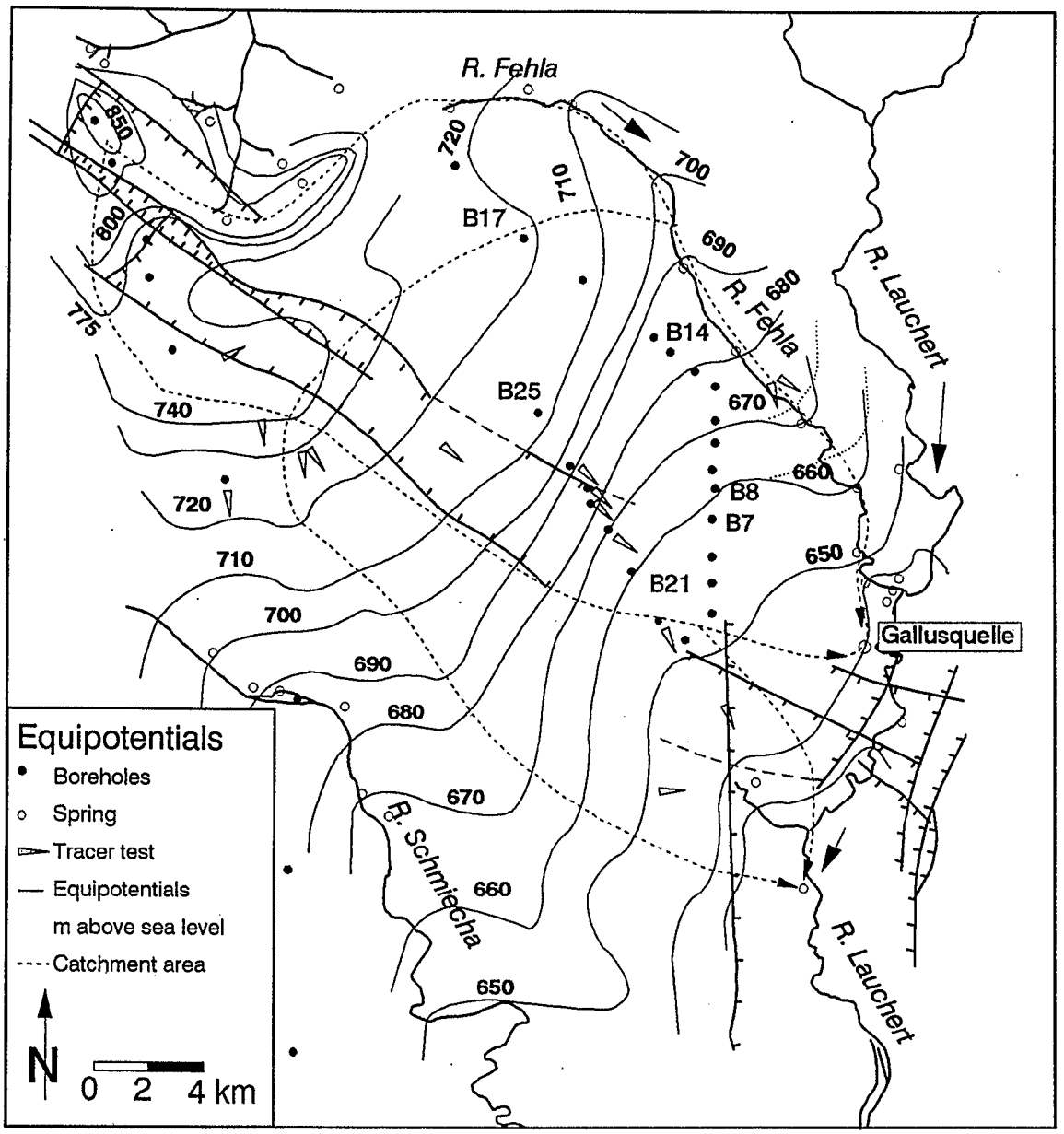

Fig. 2-21 Equipotential Map of the Project Area

with the water level fluctuations increasing downwards. The degree of karstification decreases from B25 over B8, and B14 to B17, except for B7, which is moderately karstified, indicated by the geological logs (Fig. 2-17). As could be expected, the average water level fluctuations increase from approximately 6 m in B7, B8 (8 m), B14 (10 m) to more than 20 m in B17. *The hydrographs also allow the delineation of the active part of the aquifer. During the dry years 1971-1973, water levels appear to tend towards an asymptotic value (for B25, B14 and B17 derived from manuscripts), which can be interpreted as the base of the active aquifer, because the discharge during that time is less than 0.070 m^3/s (average 0.5m^3/s, flow below the gauge not taken into account), i.e. the contribution of the remaining saturated zone is minimal, it merely keeps up the gradient. No satisfactory answer could be found for the sudden drop of the water table in 1973 (B7) and 1971 (B8). The top of the aquifer can also be taken from the hydrographs as the topographic level, where the hydrographs become very peaky. Analyzing the extreme recharge event of spring 1988 more carefully reveals that, except for B25, all the fluctuations in all the wells are approximately the same. This can be explained by assuming that the transmissive capacity of the main aquifer horizon is exceeded, and that the aquifer properties above this horizon are those, applicable to the*

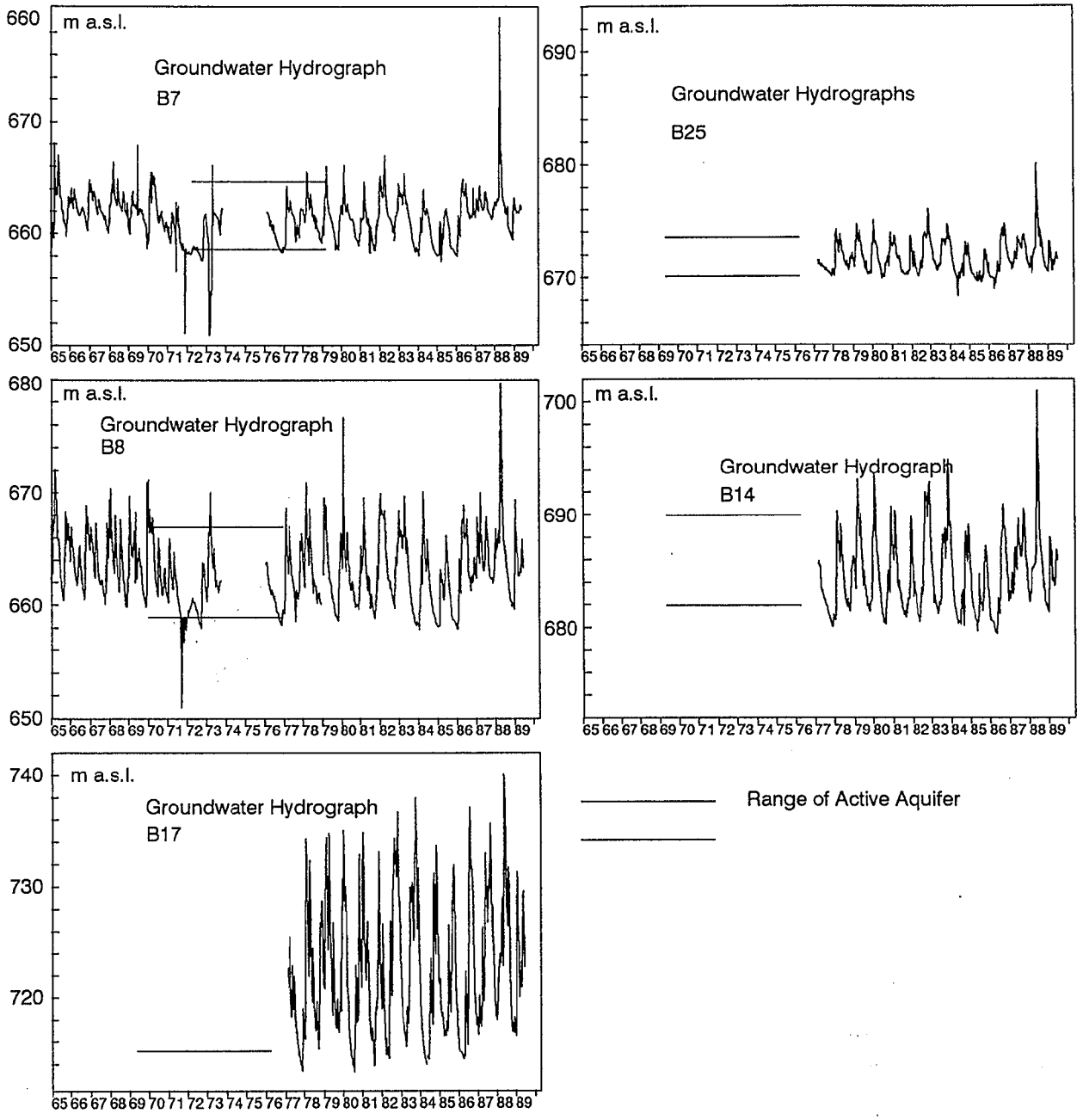

Fig. 2-22 Determination of Active Zone of Aquifer by Groundwater Hydrographs

surroundings of B17. The borehole B25 shows a lower peak level which is explained by its particular position close to the northern fault zone of the Hohenzollern graben (high karstification). Hydraulic test results give corresponding high permeability values (see also Chap. 2.6.1).

2.6.4 Hydraulic Parameters and Dynamic Response of the Aquifer System

Depending on the scale, the respective parameter is measured at, the hydraulic parameters vary substantially (Chap 4.2, 4.3). On a regional, i.e. catchment scale, the hydraulic conductivity of the slow aquifer flow system ("regional matrix/fissured system") varies from $2*10^{-5}$ m/s to $2*10^{-4}$ m/s, depending on the area considered, and that of the conduit, fast system ranges between 2 m/s and 10 m/s, depending on the assumptions used (see Chap. 4.3.1.1.). The final combined hydraulic conductivity depends on the relative fractions of the respective flow system per unit volume

permeable rock.

The storage of the conduits could be determined to range between 0.01% and 0.03%, using several different methods (see Chap. 4.2.2.). The actual value depends more on the method chosen than on other variables, such as discharge or groundwater levels. For the slow (Darcy flow) system, storage could be evaluated at 1% to 2%.

The response to rainfall events is fast, i.e. approximately 1.5-2 days after the highest intensity in rainfall, maximum discharge is measured. Another 1.5-2 days later, the actual fresh water begins to appear at the spring, indicated by temperature and electrical conductivity variations of spring water. Further details to the flow mechanism are discussed in Chap. 4.5.

Maximum groundwater levels are not measured synchroneously with maximum discharge, but after a lag time of between 1 to 5 weeks. The electrical conductivity, indicative of the fast water component, recovers quickly to pre-event levels within a few days, whereas the temperature reveals a considerable memory effect of the aquifer for the recharge event, because it also shows the effect of the slow, delayed recharge component. Memory effects of previous storms are registered up to three months, counting from the time of the recharge event. It can be frequently observed that higher turbidity levels (measure for the quantity of suspended solids) occur before the arrival of the fresh water, which indicates high flow velocities within the aquifer and not only the arrival of the actual recharge water. Therefore this parameter can be also an indication for the time period when the fast water component is dominant.

The relative abundance of ^{18}O in spring water does not show any longterm response to summer and winter recharge events. The high frequency and at the same time dampened fluctuations reflect rather more the short-term reaction to rain storms. In order to get a quick impression of the longterm response of the aquifer to recharge events, the difference of the input $\delta^{18}O$ to a baseline value of -10.55‰ (Chap. 4.5.3) has been multiplied with the respective rainfall depth in Fig. 2-19. The spring water $\delta^{18}O$ were weighted according to the discharge and then smoothed, using moving averages with a window of three days.

3 Modelling Approaches in Fractured and Karstified Rocks

3.1 Classification of Karst Aquifers

The modelling of an extremely heterogeneous aquifer such as a karst groundwater basin with numerical methods, requires a careful analysis of the various model assumptions (mainly Darcy flow). It has to be examined whether the flow system complies with the assumptions or whether only parts of the aquifer system can be represented by a given model. It has also to be decided how to deal with the non-compatible part or whether its influence can be neglected.

The first step in any case is a classification of the complex aquifer systems and each category can then be treated individually, depending on the problem investigated.

A very important attempt to build a conceptual model of karst aquifers was presented by Smart and Friederich (1986). In this model, three fundamental attributes, governing the response of a limestone aquifer are identified, i.e. recharge, storage and transmission (ground water flow). Recharge ranges between concentrated and dispersed end members (Burdon and Papakis, 1963), storage between high and low and/or saturated and unsaturated (includes subcutaneous storage). It can be argued that "saturated" and "unsaturated" cannot be regarded as a continuous variable because of the multiphase rock-water-air "unsaturated" system. In the light of the recent recognition of the importance of the unsaturated zone in the recharge process, it is essential to include both categories as discrete variables. Finally, the ground water flow is categorized on a scale that ranges from diffuse flow to conduit flow. As Smart and Hobbs (1986) pointed out, the three attributes are independent of each other and can therefore be decompartmentalised. Recharge and unsaturated storage are treated separately and are accounted for by a recharge calculation and its respective distribution over time (Chap. 4.5). Only saturated storage and the flow modes have to be integrated into a numerical groundwater flow model.

It is very useful to arrange different karst aquifers on a scale from "diffuse" over "mixed" to "conduit" flow (White, 1969) as illustrated in Fig. 3-1 (Quinlan and Ewers, 1985). The diagram describes the increasing importance of pipe flow and increased maturity of the karstification.

In an effort to represent this trichotomous variable by a continuous one, Mangin (1975) defined a parameter k as the ratio between the maximum cumulative baseflow volume (over a year), and the average event volume extended to a year. The value of k varies between 1 and 0, with the porous aquifers having values close to 1, and the smaller k, the faster the transit of water through the aquifer. Mangin (1975) uses another parameter i to describe the flood recession curve (2 days after the beginning of the recession, Mangin, 1975, p.103). Bakalowicz and Mangin (1980) suggest that if k is greater than 0.5, the approach used for porous media can be applied, between 0.2 and 0.4, those methods may be questionable and below k=0.1, they deliver erroneous results.

In a later analysis using spectral analysis, Mangin (1984) suggests to use memory effect (days) and spectral bands to classify karst aquifers, which is also supported by Obarti et al. (1988).

The above systematics however only indirectly take into account the underlying physics of the system, the understanding of which is essential, if modelling for prediction purposes is intended.

3.2 Lumped Parameter Approach

Two fundamental approaches to modelling karst water resource systems have been taken: the black box model and distributed parameter model.

As a result of the scarcity of spatial data, the heterogeneity of the aquifer parameters and because of its relative simplicity, a black box approach has been frequently preferred in the simulation of karst aquifers. Despite its global approach, encouraging results have been obtained by recession analysis (Atkinson, 1977), the identification of transfer/kernel functions (Dreiss, 1989a, Aiguang et al., 1988, Avias and Joseph, 1984), mixing cell models (Simpson, 1988) and also through simple regression analysis (Zaltsberg, 1984).

The parameters obtained through recession analysis were also frequently used for volume estimation of groundwater resources (Pfaff, 1988) and even for regional hydraulic parameter estimation (Atkinson, 1977). Frequently, different flow regimes can be identified by different recession coefficients, although there is sometimes a misconception in the literature of an expected kink that is supposed to indicate a sudden change in aquifer properties.

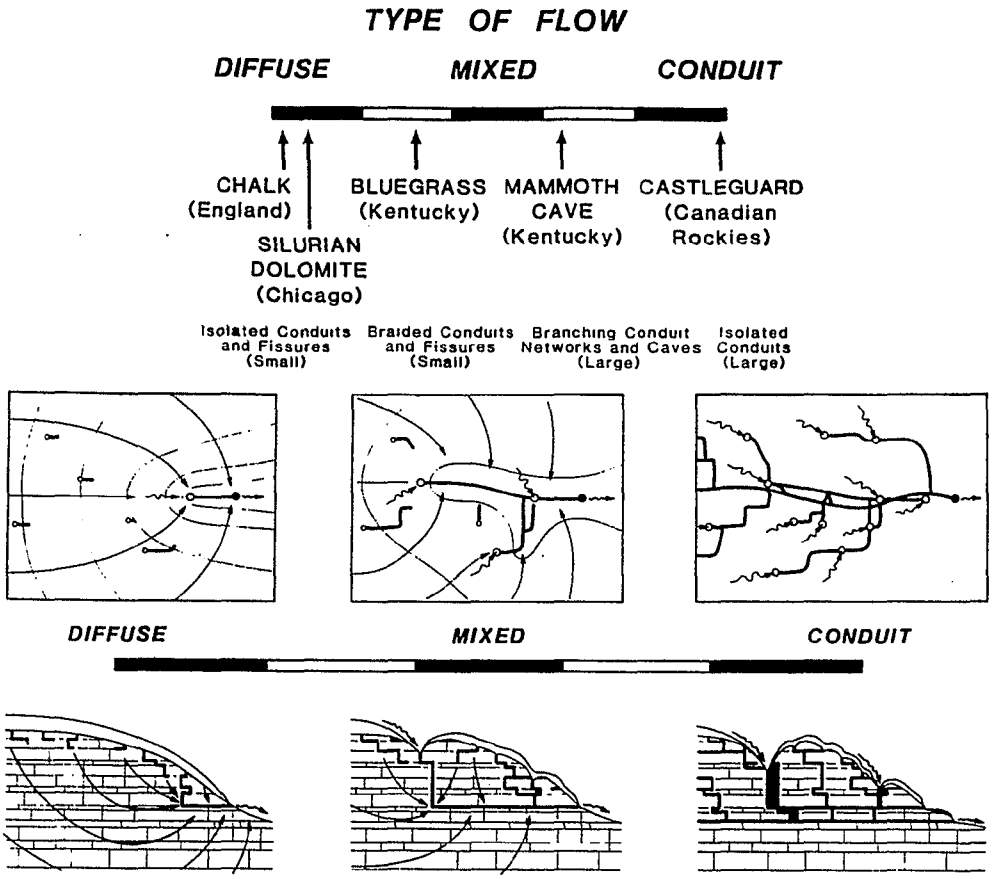

Fig. 3-1 Flow Systems and Classification of Different Karst Aquifers (Quinlan, 1985)

Frequently, the slow and the fast flow system are also unrealistically considered as isolated from each other. In any case, such a change has to be a gradual one and will in most cases result in a smooth curve.

Linear systems analysis has been employed for years in the area of hydrology to describe the relationship between rainfall and surface water runoff, and was successfully applied to regional solute transport in fractured aquifers by Duffy and Harrison (1987) and Rinaldo and Gambolati (1987). Duffy and Harrison (1987) identified kernel functions to interpret changes in tritium concentrations in a karst aquifer of the Swiss Alps. Dreiss (1989b) uses discrete deconvolution techniques and time moment analysis for the identification of kernel functions to simulate regional transport (storm response). By comparing the first and the second moment of a physically based dual porosity model with its kernel, Dreiss (1989b) managed to evaluate regional effective dispersion coefficients. New kernels have to be however evaluated if, instead of storm responses, tracer tests have to be modelled. Pulido-Bosch (1988) also applied deconvolution methods to simulate spring discharge of a karst aquifer in eastern Spain. The results were compared with a single porosity finite difference model. Judging by the spring hydrograph, which reveals characteristics of a fairly moderately karstified aquifer, such an approach appears to be applicable.

Although they do not give direct information on the response of a karst aquifer with time, flow duration curves can also be put into the category of lumped parameter models. They reveal some information on how the system responds at a certain discharge level (syphoning, overflow into another catchment, polje discharge) with a change in slope (Bonacci, 1987, Soulios, 1985).

Hydrological models, such as the Stanford Watershed Model (SWM) (Bonacci, 1987) and the CREG model (Drogue and Guilbot, 1977) have also been applied to simulate karst groundwater discharge. The CREG model makes allowances for the two flow regimes inherent in karst and develops transfer functions for the fast and the slow system and also

integrates a coupling term for the two reservoirs. The input function for these models is usually effective rainfall. Analytical models (e.g. Maloszewski and Zuber, 1985) were used to simulate tracer experiments through fractured rock.

It can be concluded that because of their non-physical nature, lumped parameter models generally lack predictive power.

3.3 Distributed Parameter Models

The inadequacies of the black box models become apparent when one attempts to model spatially variable output phenomena, such as characteristic water level fluctuations, that have a definite physical basis. Frequently, geological information that could explain observed differences, which in many cases is of a spatial nature has to be ignored in such models. Moreover, they fail to consider the different processes that determine flow and transport in a karst aquifer, i.e. the mechanism of groundwater recharge, the influence of the unsaturated zone and the phenomena in the aquifer itself. Furthermore, each of these factors in turn has a different influence on fast and slow flow components.

A viable alternative is the distributed parameter modelling approach. Three major methods have been used to describe the flow and transport through fractured porous media, (1) the equivalent porous medium, (2) the discrete fracture and (3) the double porosity or double continuum approach.

Equivalent Porous Medium

When the fractures are narrow, evenly distributed, and if there is a high degree of connectivity, an equivalent porous medium model (EPM) can be applied (Pankow et al., 1986). A recent development for this kind of model has been described by Neuman (1987). The author simulates the flow in the fractured porous rocks with an equivalent porous medium model, integrating the permeability as a stochastic variable. Aquifers termed "Deep Continuum - Flow Carbonate Aquifers" by Thrailkill (1986), seem to fall into this category. Most of the karst aquifer models built, have been based on the assumptions of the EPM.

Discrete Fracture Models

The second approach, the discrete fracture model usually implies that the effect of the matrix is neglected. In its simplest form, flow is simulated by considering it as flow between two parallel plates and it requires some detailed information on fracture apertures, fracture length, density, orientation and connectivity (Snow, 1965; Irmay, 1964; Romm, 1966). Especially as it is very difficult, if not often impossible to obtain the required information at the relevant scale, the fracture networks are statistically simulated (Long et al., 1985; Smith et al. 1987).

Kraemer and Haitjema (1989) theoretically studied the effects of large fracture zones and statistically generated fracture networks for regional aquifer flow.

Although the theory for joint controlled flow is outlined in many textbooks and publications (White, 1988, Ford and Williams, 1989, Cullen and LaFleur, 1984) and although the laws and parameters governing turbulent open channel flow and pipe-flow were described in detail, to the author's knowledge, these principles have not been applied to real aquifer situations, except by Atkinson (1977) and Thrailkill (1991).

Double Porosity/Continuum Models

The modelling of flow and transport in fractured rocks could benefit greatly from studies carried out by petroleum engineers in the field of reservoir engineering and from the research efforts in the search for safe repositories for radioactive wastes. The preferred approach in these areas of research has been the double porosity approach (Barenblatt et al., 1960; Warren and Root, 1963; Duguid and Lee, 1977). The fractured medium and the porous matrix blocks are modelled as two separate overlapping continua, each with its own flow equation. The coupling of the two media is handled with a source/sink term in each equation. The exchange of flow is controlled by the local difference in potentials. Details and the development of the double porosity approach are described by Streltsova (1988), Sauveplane (1984) and Teutsch (1988). Narasimhan (1988) developed this concept further into multiple porosity systems and called the model MINC (multiple interacting continua).

The applicability of the distributed parameter approach to karst aquifers was described in detail by Thrailkill (1986) and it's appropriateness to conduit-flow aquifers in particular was examined.

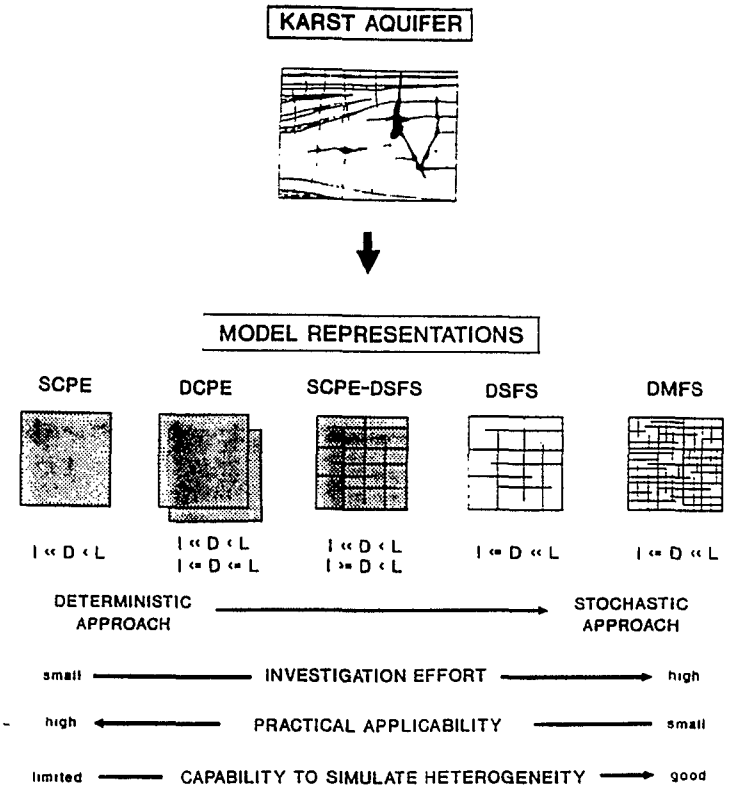

Fig. 3-2 Karst Aquifer Prototype and Five Possible Model Representations (Teutsch and Sauter, 1991)

3.4 Application of Distributed Parameter Models to Karst Aquifers

Teutsch and Sauter (1991) provided a conceptual framework for the classification of karst groundwater flow problems, employing the scale hierarchy approach (Fig. 3-2). In this diagram, four different main model representations could be identified, SCPE, the single continuum porous equivalent, DCPE, the double-continuum porous equivalent, DSFS, discrete singular fracture set and DMFS, the discrete multiple fracture set. This procedure allows the selection of an appropriate modelling strategy based on the analysis of the scale relationship between a) the length scale of the flow or transport domain (L), b) the length scale of the flow-dominating heterogeneities (I), and c) the length scale (averaging) of the detection method used (D). Below, some examples of karst groundwater models are described.

Single porosity models could be frequently and successfully employed in simulating karst groundwater systems, especially when dealing with water resources and water budget problems. (Teutsch, 1989; Baoren and Xuming, 1988; Maclay and Land, 1988; Tibbals, 1990). The high frequency of discharge and water level fluctuations in the Edwards aquifer (Maclay and Land, 1988) could not be simulated satisfactorily, which however was not required for the problem in question. As Thrailkill (1986) already predicted, could the Floridan aquifer be modelled with a single porosity approach (Tibbals, 1990).

Finite element models in which the matrix is represented by 3-D elements and fractures and conduits by 1-D and 2-D discrete line elements have been employed by Yusun and Ji (1988) and Kiraly (1984). In the example of Yusun and Ji (1988) the spring discharge and the model results do not appear to agree very well, which does not give any information on the modelling approach itself, rather more about the FE-grid or the calculation of the recharge input. Kiraly (1984), for example, could successfully apply a finite element model, representing the matrix blocks with a porous medium approach, with a superimposed discrete regular network of line elements, simulating the fast system.

If the karst aquifer model has to accommodate both, a regional flow system that is

slowly depleted and at the same time a fast transit system to simulate the rapid response after a rainfall event and tracer tests with high average velocities, double porosity/continuum models are the appropriate tool. Double porosity models have been used by Yilin et al. (1988) to simulate flow and by Teutsch (1988) and Sauter (1990) to model regional flow and transport.

For the work described, a double porosity model was chosen. It is considered suitable for the aquifer concerned, which is located at an intermediate position, possibly more towards the diffuse end member of the conduit-diffuse-flow spectrum (White, 1977). Here the physico-chemical characteristics of the spring water and tracer tests indicate that conduit flow is still an important factor. The discrete fracture approach is inapplicable, because the required data input (discrete geometry and effective hydraulic parameters) cannot be obtained.

Applied to a karst aquifer, the terminology of the double porosity or double continuum approach requires some further clarification. The terms fractures and conduits are used interchangeably for the fast transit system, and matrix and fissures are used to describe the slowly draining part of the aquifer system. Although generally used in the literature, it is preferred to use the term "fissured system" as opposed to "diffuse system", because "fissured system" describes the actual permeable pore space of the slow system, corresponding to the term "conduit system". The term "fractures" is used synonymously for conduits in order to reflect the duality fracture/matrix of the double-porosity/continuum approach. The same terms apply to the unsaturated zone, in particular to the epikarst (Chap. 4.1.3).

4 Provision of Data Input

This section demonstrates how the necessary input data for the double porosity modelling were obtained and in which form they can be included in the model. Main subsections are the calculation of recharge, the determination of the regional and local flow parameters (K, T and S) and transport parameters. Subsection 4.5 discusses the flow and transport dynamics of the aquifer under unsteady state conditions.

Emphasis is laid upon the scale, the respective measurement is taken at, and how that information can be converted to values applicable at the regional, i.e. modelling scale.

4.1 Recharge

The evaluation of recharge can be subdivided into the calculation of the daily recharge using some form of water balance method (Chap. 4.1.1-4.1.2) and the determination of the distribution function, according to which the recharge arrives at the groundwater table. The controlling element for the distribution of the recharge is the subcutaneous zone (Williams, 1983), presented in Chap. 4.1.3 and the parameters are quantified and distribution functions evaluated in Chap. 4.2 and 4.5.

4.1.1 Quantification of Groundwater Recharge

Groundwater recharge was computed on a daily basis, applying a soil water balance approach. Information at this level is a prerequisite for being able to simulate single recharge events, whose response on the groundwater, particularly the fast flow system, is registered in the order of one to two days after the event. It has also been shown by Howard and Lloyd (1979) that recharge calculations on a ten daily or monthly basis tend to systematically underestimate recharge.

Catchment Precipitation

The most important factor in the evaluation of groundwater recharge is the rainfall. The largest errors can be made with a bad estimate of the areal rainfall. Fig. 2-11 shows that the rain gauge density within the actual project area is fairly low. As shown in Chap. 2.5, the variation in average annual rainfall from 1050 mm in the north-west near the escarpment to 800 mm in the south-east is fairly high. The comparisons between recharge calculation and measured discharge, the procedure is shown below, revealed that a single rainfall station does not represent the whole area properly even if the rainfall depth is weighted by a factor. It can be assumed that site specific variations account for most of the discrepancies. Evaluation of an areal rainfall using Thiessen polygons is also inappropriate, because of their regional distribution.

Therefore, all seven stations, for which long term records existed were lumped together for an average areal rainfall. Fortunately, the gauges were evenly distributed over the whole range of topographic heights, so that the average of all stations could be expected to represent the catchment rainfall. Double mass analysis (Kelway, 1975, Linsley et al., 1982) between the individual raingauges and the average of all 7 stations did not reveal any significant deviation of any of them as a result of e.g. overshadowing by trees, relocation of the station or tree cutting. Only one rain gauge appears to exhibit some significant change in slope (Burladingen) from the year 1973 on, with the result of an increase in precipitation at the gauge location. Other gauges only display minor deviations from the straight line.

The Soil Moisture - Interception Water Balance

Potential evaporation was calculated with the Haude (1955) method, which requires air humidity and air temperature at 14:00h as input variables. The resulting values are corrected for the seasonally varying transpiration by plants. The soil moisture balance approach was carried out according to Uhlig (1959), a procedure, which is similar to that of Thornthwaite and Mather (1957), applying a field capacity of 75 mm (Hemme, 1970). The immobile water was determined at 20 mm (wilting point) which implies a depth of 55 mm of water, available to plants. Teutsch (1988) evaluated a quantity of 60 mm and Behringer (1988) of 50 mm for comparable situations in a karstified limestone terrain. *However, as a result of the dominance of the high percentage of woodland, interception becomes important, which is not corrected for in the Haude/Uhlig method. Therefore, three separate recharge calculations were performed, the first one for the forested area, with coniferous stands (42%), the second for deciduous stands (18%) and the third for the agriculturally*

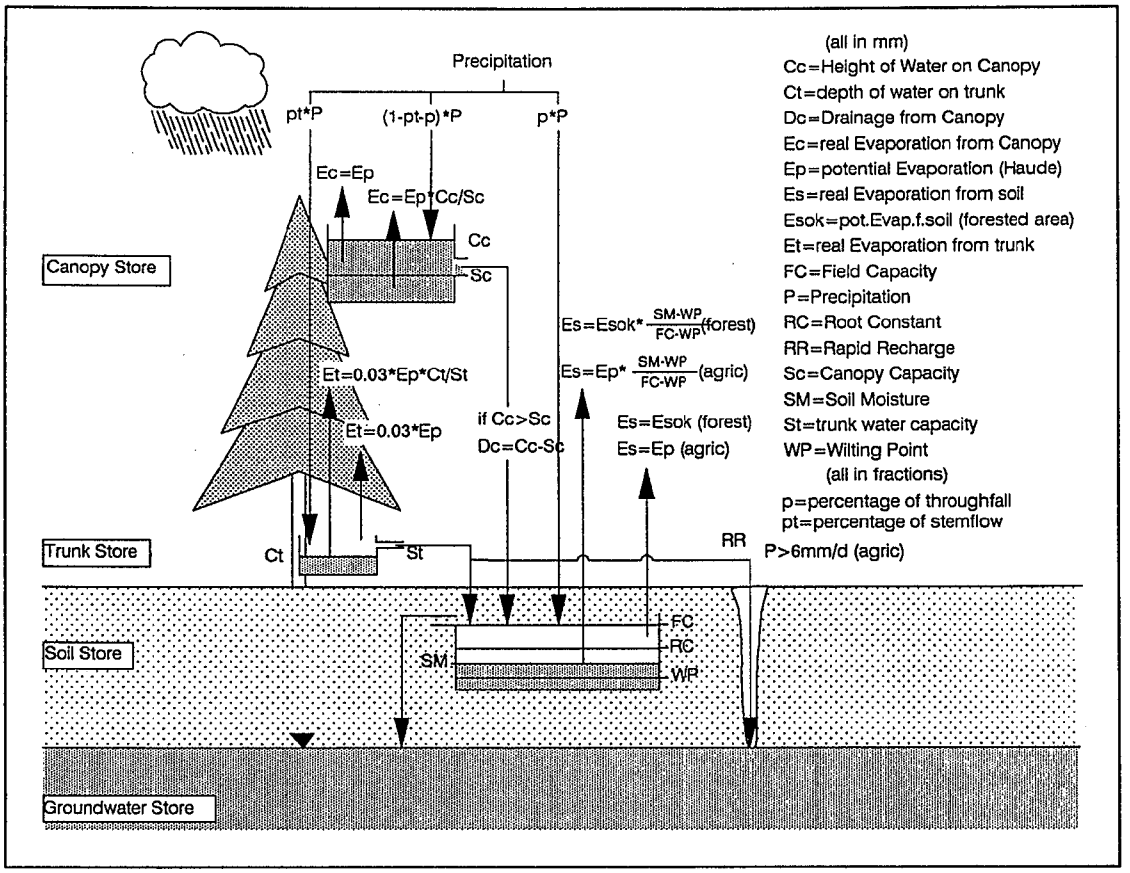

Fig. 4-1 Conceptual Model of Recharge Calculation Procedure

used land (40%) (Fig. 2-5). The conceptual model used is given in Fig. 4-1. The calculation procedures are identical for all three areas, except that for the forested part, the respective interception, stem flow and potential evapotranspiration were taken into account.

Soil Moisture Balance

There are several characteristic parameters that determine the flux components (evaporation, groundwater recharge) from the soil store. According to the model, groundwater recharge only occurs if the field capacity (FC, pF = 1.8 to 2.5) is exceeded. If the soil moisture (SM) drops below the field capacity (FC) and is still above the root constant (RC), evaporation can proceed at the full potential rate; below RC and above the wilting point (WP, pF = 4.2), evapotranspiration is reduced according to Es=Ep*(SM-WP)/(FC-WP), i.e. the potential evapotranspiration is multiplied by the ratio between the present and the maximum soil moisture, available to plants. This procedure accounts for the increasing difficulties for the plant to extract water from the soil. At the wilting point, transpiration by plants ceases. The field capacity and the wilting point parameters were derived from Hemme (1970), based on soil hydraulic studies on the various soil types of the Swabian Alb. The model parameter RC was extracted from Uhlig (1959) as 50 mm. In the respective diagram, displaying the cumulative potential water losses against the cumulative actual water losses from the soil, the potential loss equals the real loss for approximately the first 25 mm (FC=75 mm). Below RC, the losses were approximated with the above equation. The above procedure seems to represent better the physical basis of the gradual reduction of evaporation loss, than the more rigorous approach of Rushton and Ward (1979), where the evapotranspiration loss below the RC was reduced to 10% of the potential rate.

The above technique does not allow recharge to occur during the summer period, because

nearly always a substantial soil moisture deficit exists. Well hydrographs however show a response to recharge during the dry period, especially after heavy rainfall. It can be visualized that water bypasses the soil moisture store via dessication cracks and macropores without substantially reducing the soil moisture. The term rapid recharge was introduced by Rushton and Ward (1979) and their findings were supported by Beven (1981), Trudgill et al. (1983) and Smart and Friederich (1986). As suggested by Rushton and Ward (1979), the quantity of effective rainfall per day, exceeding a threshold of 6 mm is contributed directly to recharge. Rapid recharge is not included in the calculations for the forested areas because dessication cracks are unlikely to occur and the canopy and the thick organic cover are capable of delaying the input substantially. The recharge calculation applies to the catchment as a whole and the parameters determined apply to average conditions, i.e. they cannot discriminate into e.g. areas with thin or thick soil cover, which have been mapped in the catchment.

Interception Model

There are a number of attempts to calculate interception from forested areas. A review of the earlier work is given by Rutter et al. (1975). A very simple approach is presented by e.g. Flügel (1988), Benecke (1978) and Schroeder (1984), which is based on a regression analysis of measured total rainfall and throughfall of rainfall events. The method allows the determination of the interception loss and the canopy storage capacity, by determining the linear relationship between total rainfall and canopy throughfall for single events. Different equations are found for the summer and winter periods. Diagrams were developed for different tree species and summer and winter period by Brechtel and Pavlov (1977), that are however only applicable to the monthly sum of rainfall. The above methods either only apply on a large time scale i.e. monthly or half yearly time scale or to single rainfall events. If applied to daily rainfall, calculated interception becomes unrealistic, if on several consecutive days the canopy storage capacity is subtracted to account for interception. The error becomes particularly large if the evapotranspiration is reduced during the storm, as a result of high air humidity and if not enough time was available for the canopy to dry. Antecedent moisture conditions and climatic factors become important, if information is required on a daily or even hourly timescale.

These effects can be accounted for by applying a water balance for the canopy store and the trunk store (Rutter, 1975, 1971, Gash, 1978, Gash, 1980). The complete model, including the soil moisture water balance is schematised in Fig. 4-1, as well as the complete notation and the parameters used. The model was originally designed on an hourly basis, but modified for daily input in the present study. The drainage from the canopy cover was not defined by an exponential function, but it was assumed that after subtraction of evaporation losses, the water depth exceeding the canopy capacity could drain completely within that particular day. Because no input parameters for the interception were measured, the respective values were taken from the literature for the particular situation (Rutter et al., 1975; Gash and Morton, 1978; Baum-

Parameters used for Recharge Calculation

Parameter	Description	Value	Source
p	percentage throughfall of precipitation	25 %	Hr. Röther, Forstamt Gammertingen Dr. Schwarz, Forstl. Versuchsanstalt, Freiburg
Sc	Canopy Capacity	4.7 mm	Fleck (1987), Liebscher et al (1990) Calibration Parameter
St	Trunk Water Capacity	0.014 mm	Gash et al (1978), Rutter et al (1975)
Pt	Percentage Stemflow (of precip.)	1.6 %	Gash et al (1978), Rutter et al (1975)
FC	Field Capacity	75 mm	Hemme (1970) Calibration Parameter
RC	Root Constant	50 mm	Uhlig (1959)
WP	Wilting Point	10 mm	Hemme (1970)
RR	Rapid Recharge	forest: none agric: 6 mm	Rushton et al (1979) Calibration Parameter
P	Precipitation	variable	measured
Ep	Potential Evaporation (grass)	variable	calculated acc. to Haude (1955)
Esok (spruce, beech)	Potential Evaporation (forest)	variable	calculated acc. to Sokollek (1983)

Tab. 4-1 Input Parameters for Recharge Calculation for Agricultural and Forested Areas

gartner and Liebscher, 1990; Fleck, 1987) or derived from the characteristics of the stands (pers. communication, Mr. Röther, Forstamt, Gammertingen). The parameters chosen are given in Tab. 4-1.

There appears to be some confusion as to the definition of the values given for the canopy storage capacity, varying between 0.8 mm and 7.6 mm (Gash and Morton, 1978; Rutter et al., 1975; Baumgartner and Liebscher, 1990, p.321; Linsley et al., 1982; Chow et al., 1988, Schroeder, 1984), depending on the season. In some cases, the canopy capacity is related only to the drainage from the actual canopy cover and the throughfall that does not touch the canopy is considered separately, others lump both components together, or in some cases, no indication is given at all. For the investigations described, the canopy capacity only refers to the actual canopy, i.e, the throughfall is accounted for separately. Schroeder (1989) derived from lysimeter measurements that there is no significant difference in the canopy capacity if calculated on an event or daily basis.

For the water balance in the forested area, the potential evapotranspiration rates from the soil (E_{Sok}) were corrected according to Sokollek (1983).

Concerning the interception from a snow cover, the magnitude of interception measurements seems to vary greatly. It is frequently postulated that interception loss is determined to a great extent by the frequency of wetting of the canopy. Therefore, despite the reduced potential evaporation, interception loss seems to be in the same order as during the growing period (Baumgartner and Liebscher, 1990, p. 324; Rutter et al., 1975, p. 115). Interception storage is frequently extended to several days or even weeks. Satterlund et al. (1970) however determined evaporation from the crowns at 5% of the daily precipitation. In the model used, interception loss was tentatively set at 20% of the daily precipitation for the period of snow-cover. The specification of interception as a percentage of the daily precipitation is a very crude approximation and does not take into account the characteristics of the storm (intensities, spatial distribution) and neither the weather conditions, responsible for the duration, the snow is exposed to evaporation. Due to the lack of reliable and site specific data, such a procedure appears to be justified.

In the Rutter interception model, potential evaporation from the canopy is determined, applying the Monteith-Penman equations (Monteith, 1965). These equations allow an adaptation of the aerodynamic resistance of the vegetation cover to the conditions applicable at the tree tops. Due to the fact that the input data for the Monteith - Penman equation were not available, potential evaporation was calculated

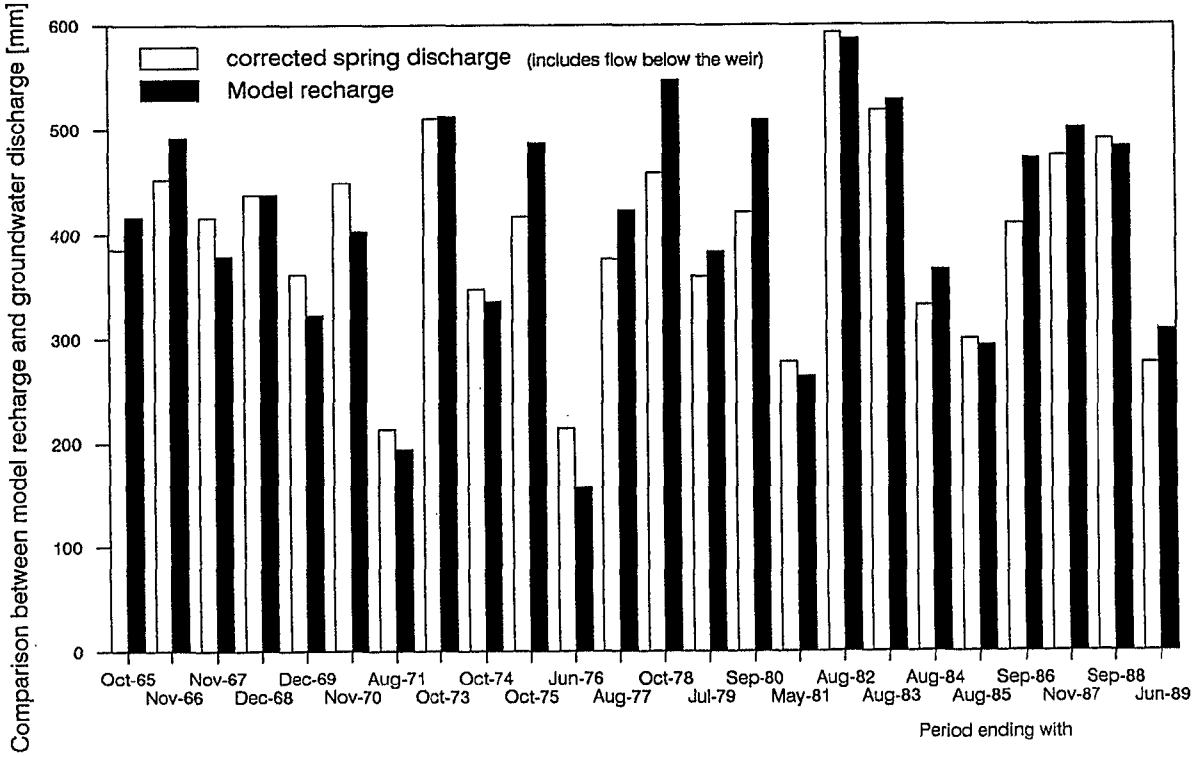

Fig. 4-2 Comparison Between Calculated and Actual Recharge (≈ discharge of Gallusquelle spring)

with the Haude Method. This might lead to a systematic underestimation of the evaporation from the crowns due to the neglect of wind effects.

Verification and Results of the Recharge Calculation

Tab. 4-2 and Fig. 4-2 show the results of the recharge calculation, presented above. The model results are compared with the average discharge of the Gallusquelle spring discharge and the Lauchert catchment discharge (App. 4-1), for periods of equal groundwater storage, derived from well hydrographs in the Gallusquelle catchment. Due to the absence of surface runoff, the spring/river discharge can be assumed to correspond to groundwater recharge if groundwater storage can be assumed to be zero. Differences between the sum of real evapotranspiration and groundwater recharge and rainfall in Tab. 4-2 are due to changes in the soil moisture.

The deviations between the average of spring discharge and Lauchert discharge, plus an estimated 50 l/s to account for the flow under the gauge (see below) and between the model results are acceptable and fluctuate within a range of ± 10% about the measured value, up until 1976. The larger discrepancies can probably be attributed to the inaccuracies in determining the stored groundwater and/or the unknown quantity stored within the epikarst and the unsaturated zone (see also Chap. 4.1.3). The comparison between uncorrected Lauchert discharge, spring discharge and model recharge is shown in App. 4-1. Between the years 1973 and 1976, no waterlevel measurements were available, which might explain the large differences for the periods beginning with the 5. Oct. 1974 and 5. Oct. 1975. The large deviations for the time between June 1976 and September 1980 can possibly be explained by the effect of rapid recharge in the model, because numerous heavy storms have been measured during that period (rapid recharge: Jun75: 40 mm, Jul76: 50 mm, Jun77: 40 mm, Sep77: 50 mm, May78: 60 mm, Aug78: 80 mm, Nov79: 50 mm, Jul to Aug80: 40 mm, Sep to Oct80: 40 mm). By increasing the threshold for rapid recharge however, recharge becomes far too low for the dry years, without having the desired effect of reducing the large deviations for the years 1975 to 1980.

There could however be another possible source of error, which lies in the discharge measurement itself. From June 1976 on, the

Results of Recharge Calculation, 1965-1990, "annual" values

field capacity	75 mm
interception capacity	4.7 mm
rapid recharge (agricultural land)	6mm

all in mm								E Haude	E Sok	E real			
Period		Spring discharge	Lauchert discharge	correct. disch	recharge model	Deviation (cor.dis -model)	Rainfall	Evapotranspirat.	Evapotranspirat.	Evapotranspirat.	Rapid Rech.	Inter-cept.	Snow-melt
01.03.65	19.10.65	370,4	357,3	386,1	416,5	-30,4	827,6	363,5	465,1	473,4	115,6	109,9	107,5
20.10.65	16.11.66	417,5	412,7	452,7	491,8	-39,1	1065,8	444,1	502,6	551,6	102,4	133,5	215,9
17.11.66	20.11.67	398,8	363,4	416,4	378,9	37,5	912,3	507,6	612,1	539,9	76,4	130,8	197,9
21.11.67	22.12.68	395,9	402,9	437,5	437,5	0,0	984,0	456,9	518,6	542,4	108,3	130,8	164,1
23.12.68	02.12.69	342,5	315,7	362,1	322,6	39,5	869,2	455,5	560,1	531,7	107,7	117,1	119,0
03.12.69	10.11.70	440,6	392,7	449,5	403,3	46,2	871,0	431,6	538,5	495,6	71,1	128,4	264,4
11.11.70	29.08.71	198,0	174,4	214,1	194,4	19,7	568,8	438,8	530,3	394,5	48,8	95,3	79,0
30.08.71	02.10.73	427,5	445,3	509,7	512,2	-2,5	1543,5	1038,0	1253,8	1030,0	123,4	255,0	310,3
03.10.73	04.10.74	363,9	260,2	347,2	335,5	11,7	857,3	472,6	564,3	512,7	85,3	136,1	136,5
05.10.74	04.10.75	403,8	359,3	416,5	486,6	-70,1	973,9	452,5	545,3	496,1	103,0	124,0	215,1
05.10.75	28.06.76	198,2	181,4	215,4	157,9	57,5	415,7	315,0	275,9	277,4	22,0	56,4	123,0
29.06.76	08.08.77	366,0	309,5	376,6	422,9	-46,3	1057,2	558,1	734,9	615,0	105,0	180,6	208,7
09.08.77	02.10.78	441,4	396,6	459,2	546,8	-87,6	1206,6	532,4	658,8	655,9	135,2	168,4	246,9
03.10.78	23.07.79	360,1	304,4	360,4	383,4	-23,0	727,5	318,2	328,9	354,5	58,9	108,2	219,5
24.07.79	08.09.80	405,6	357,2	421,0	508,7	-87,7	1157,6	555,8	719,2	652,2	104,9	179,2	231,9
09.09.80	25.05.81	259,3	247,4	278,1	264,5	13,6	537,2	241,2	208,1	242,8	39,4	80,6	181,0
26.05.81	23.08.82	541,4	556,3	592,4	586,4	6,0	1346,6	723,4	942,1	780,7	130,9	217,6	324,6
24.08.82	15.08.83	477,8	489,7	517,9	527,8	-9,9	951,9	524,4	651,2	453,9	91,3	138,9	224,6
16.08.83	13.08.84	269,2	325,0	331,9	366,3	-34,4	859,6	516,7	636,6	465,2	98,0	139,7	182,4
14.08.84	12.08.85	224,8	304,9	299,7	293,1	6,6	783,6	510,8	627,0	509,2	82,0	129,7	102,5
13.08.85	15.09.86	336,2	406,8	409,7	471,5	-61,8	1091,2	594,9	770,3	592,5	114,6	179,9	240,8
16.09.86	09.11.87	376,1	492,6	474,6	500,5	-25,9	1144,7	543,4	658,5	620,9	147,0	157,0	158,3
10.11.87	12.09.88	454,7	466,5	490,1	482,9	7,2	944,3	413,0	506,5	488,2	79,6	153,3	225,5
13.09.88	01.06.89	232,4	270,3	276,4	308,3	-31,9	568,1	248,7	212,5	269,2	56,2	77,8	113,3
sum			8702	8593	9495	9800							

Tab. 4-2 Results of Recharge Calculation (annual values)

deviations seem to be all more or less negative. Comparing the total discharge of the Gallusquelle with that of the Lauchert catchment, it is noted that the spring discharge is generally lower than surface water flow, whereas from 1965 on until 1980, the situation is reversed. It is plausible to assume that the Gallusquelle spring produces more water, per unit catchment area due to its north-western exposition (storm migration from north-west to south-east) than the Lauchert river discharge, which averages also over low recharge areas in the south-east. It could be observed that the water originating from the Gallusquelle spring could sometimes bypass the weir (pers. communication, Mr. Heinzelmann, Wasserwirtschaftsamt Sigmaringen), which leads to an underestimation of the total discharge.

One further unknown quantity is the discharge below the gauge. Merkel (1991) attempted a quantification of this unknown flow by impeller measurements and throughput analysis. Merkel (1991) evaluated this flow at 200 l/s for the Gallusquelle which corresponds to ca. 140 mm per year. Considering the inaccuracies in river stage measurements and the uncertainty regarding the recharge area, taking into account the flow from the Brunnhaldenquelle spring on the left river bank and assuming a more realistic hydraulic conductivity for the river sediments of perhaps $2*10^{-4}$m/s, this unknown flow would amount to 50 l/s or 35 mm/a. This estimate is backed up by comparing the flow duration curves of Gallusquelle and Lauchert (see below). The discharge below the Lauchert weir can be assumed to be much less because of the smaller cross section, which is only a fraction of the one for the Gallusquelle catchment. The measuring error in the Lauchert discharge is due to substantial abstraction by an industrial plant in the order of 1 m^3/s (pers. communication, Mr. Heinzelmann), which however is accounted for.

The largest source of error can be assumed in the estimation of areal rainfall (Chap. 4.1.1.1). A number of raingauges are situated in the north-west of the project area, i.e. within the high rainfall zone (Fig. 2-11). Although this geographical location does not appear to be prominent during average rainfall conditions, it might however be a major source of error if daily rainfall exceeds 30 mm/d, due to the overrepresentation of raingauges near the escarpment.

Nevertheless, the calculated values can be used further with some confidence and they can be assumed to be fairly close to the actual groundwater recharge with the added advantage of providing input on a daily time scale.

Snow Accumulation and Release of Melt

A very important factor for the distribution of groundwater recharge is the mechanism of snow accumulation and snow release through snow melt. In view of having to calculate recharge input on a daily basis for the

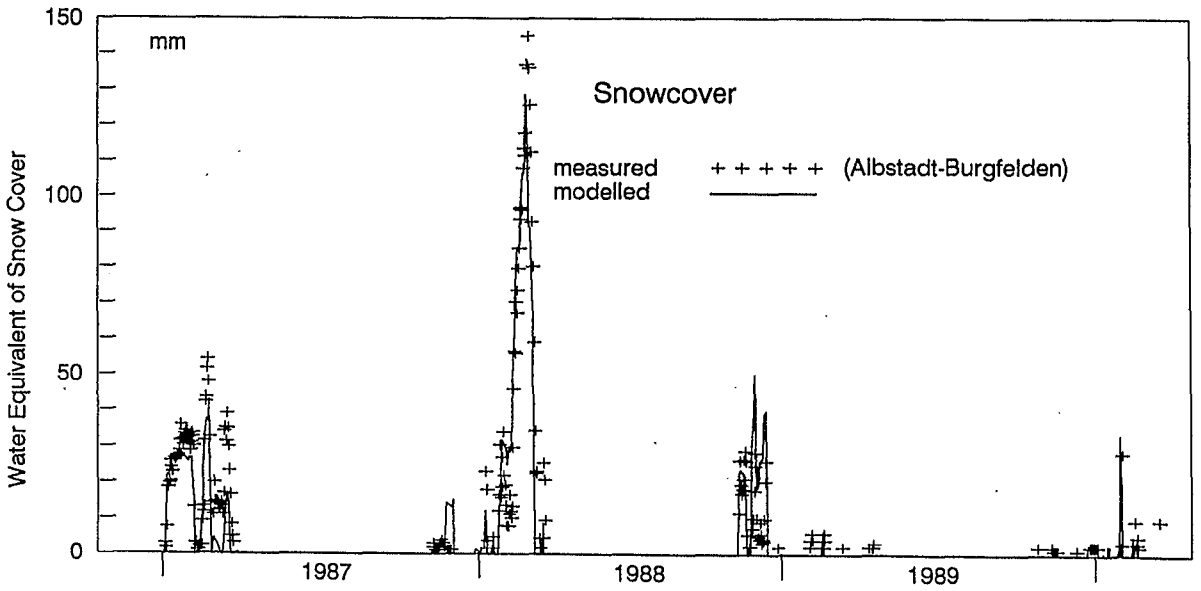

Fig. 4-3 Comparison Between Modelled and Measured Snowcover

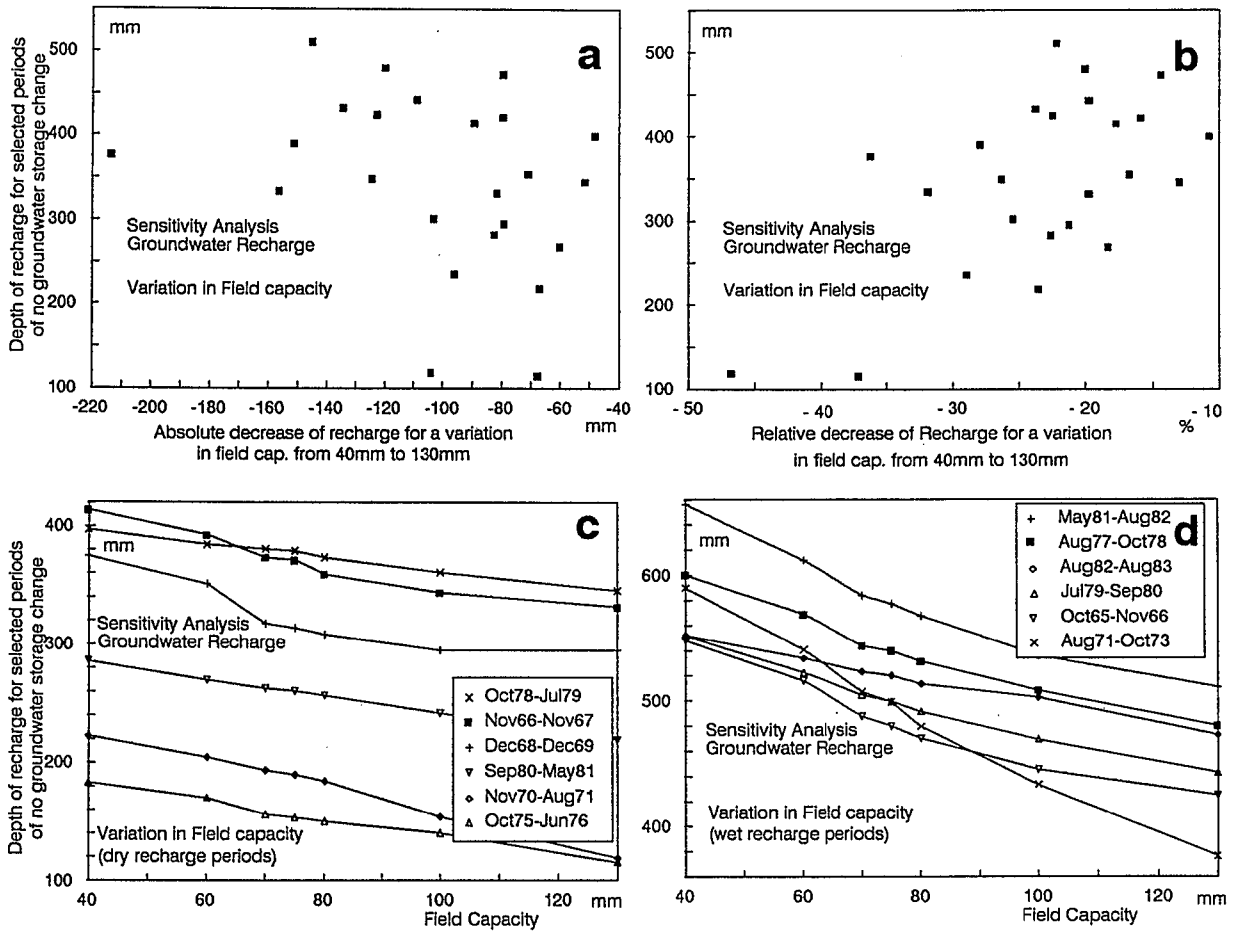

Fig. 4-4 Sensitivity Analysis of Recharge Calculation, Variation of Field Capacity

groundwater model, and in view of the winter recharge representing an important quantity, a snow cover budget calculation had to be included. This calculation was based on the simple procedure that snow is accumulated when precipitation was marked as snow fall or snow rain and with the daily average air temperature below 0°C. The release from the snow store was controlled with a melt-temperature relationship, using, after calibration, a degree day factor of 6 mm/°C, i.e. for an increase in average daily temperature by 1°C, the snow cover releases 6 mm of snow melt. The average daily air temperature was derived from own measurements for the period 1987-1990 and extrapolated into the past, using catchment corrected (regression analysis) temperature measurements of the Sigmaringen weather station.

Daily values of the water equivalent of the snowcover of the rain gauge Albstadt-Burgfelden were compared with the recharge model values (Fig. 4-3). The fit between measured and modelled data is very good, considering that the rain gauge is situated west of the project area at the foot of the escarpment and that it cannot necessarily be regarded as representative for the catchment area. The complete time series since the year 1965 is listed in App. 4-2. The differences between measured and modelled values are quite substantial for some of the years (1982, 1970, 1968). These differences can be explained by the quality of the measured data, i.e. the frequency of measuring. Whereas since 1983, snow depth readings were taken every other day, the responsible persons changed very frequently before that time and the depth readings were taken at very irregular intervals and for some periods, hardly any values exist. The single measurements were converted to a continuous series by using a cubic spline function. Some of the deviations can also be explained by site specific factors.

In any case, especially for the period 1983-1990, when the snowcover was carefully monitored, the fit between model and field data is good.

Sensitivity Analysis of the Recharge Calculation

A sensitivity analysis of the recharge cal-

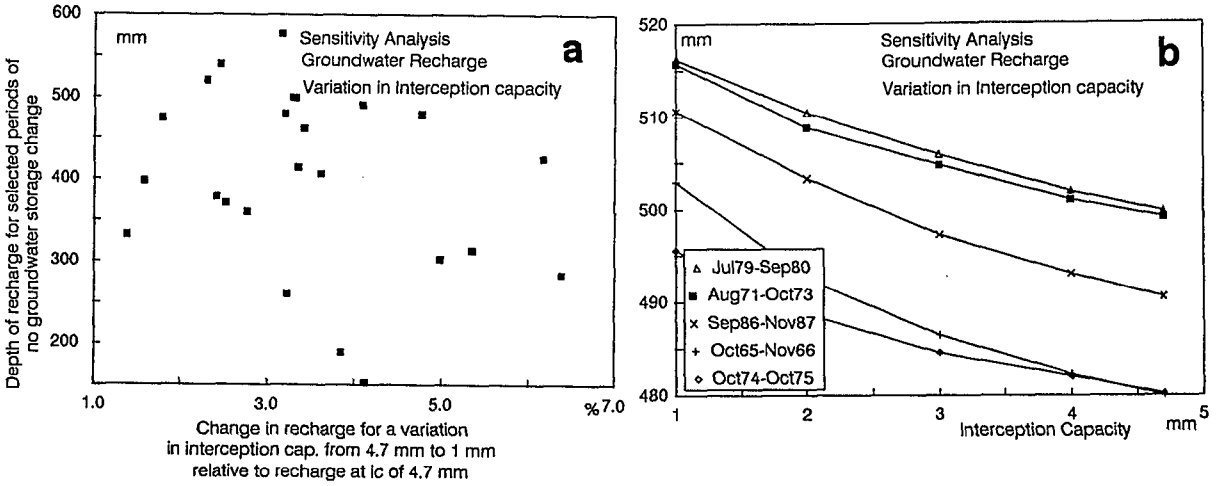

Fig. 4-5 Sensitivity Analysis of Recharge Calculation, Variation of Interception Capacity and Rapid Recharge Component

culation for the parameters field capacity (FC), interception capacity (canopy capacity) and rapid recharge was performed on an annual, monthly and daily time basis. The actual values are listed in App. 4-3. In order to save computing time, the forested area was assumed to only consist of coniferous stands. If the deciduous stands are included, the recharge increases by 3 mm to 12 mm per year. This value is very low compared to the large difference in canopy capacity between beech and spruce (2.7 mm for beech, 4.7 for spruce). The low percentage of deciduous stands in the catchment however explains the minor influence of deciduous stands on total recharge. Those three parameters mainly determine the total amount of groundwater recharge and its distribution with time. The effect of stem flow is negligible, it was only included for reasons of completeness.

By increasing the field capacity from 40 to 130 mm, the recharge is decreased by between 50 and 210 mm (Fig. 4-4 a and b) on an annual time scale, or between 10% and 45% of the recharge at a FC of 40 mm. The hypothesis was that during wet years, the reduction in recharge is larger if more soil water can be supplied to evapotranspiration. *It is apparent from Fig. 4-4 a and b that there is no significant correlation between the decrease in recharge and the total recharge for the specific period (no change in groundwater storage) considered. This observation can probably be explained by assuming that the decrease is more a function of the distribution of rainfall with time, rather than of the absolute height of rainfall. This demonstrates the effect of the rapid recharge component, the*

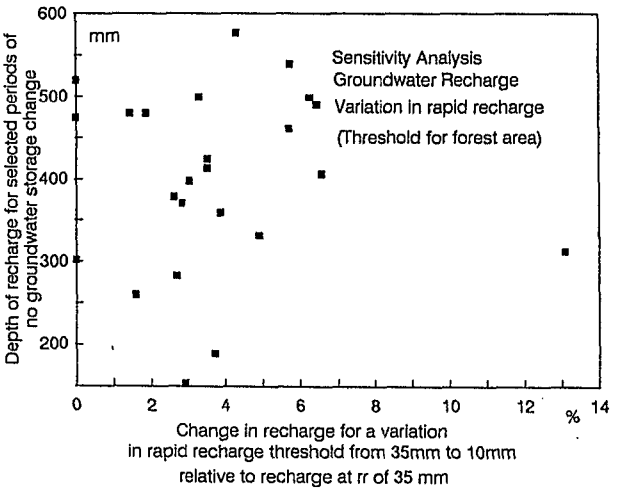

Fig. 4-6 Sensitivity Analysis of Recharge Calculation, Variation of Rapid Recharge

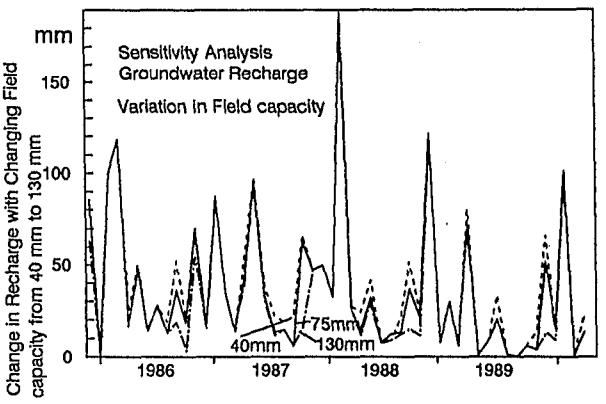

Fig. 4-7 Sensitivity Analysis of Recharge Calculation, Temporal variations due to changes in field capacity

magnitude of which is rather determined by the characteristics of the individual event, than by the weather conditions during that particular year. The same effect can be demonstrated in Figs. 4-4 c and 4-4 d in which the change in recharge is plotted against the change in FC for low and high recharge periods. The fact that the various lines do not run approximately parallel and even cross over illustrates again the above observation.

The stepwise change in canopy capacity from 4.7 mm to 1 mm, which is equivalent to a reduction in total interception, increased the total recharge by ca. 1.5% to 6.5% of the recharge at 4.7 mm canopy capacity, depending on the period considered. A similar lack of correlation between the change in recharge with the total

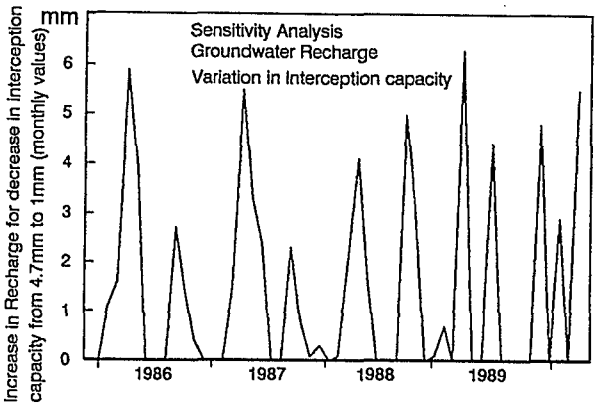

Fig. 4-8 Sensitivity Analysis of Recharge Calculation, Temporal variations due to changes in canopy capacity

recharge of the specific period is also observed (Fig. 4-5 a). The absolute change in recharge for the change in canopy capacity for selected periods is presented in Fig. 4-5 b. Gash and Morton (1978) also performed a sensitivity analysis of recharge estimates by varying the canopy capacity and the free throughfall coefficient p. They found that by varying the canopy capacity by 50%, the interception loss only changed by 15%. A change of 50% in p, the percentage of throughfall, produced a variation in the interception loss of 7%. The authors also attribute the low sensitivity to the relative magnitudes of rainfall and evaporation rates and their distribution over time.

Introducing rapid recharge also in the forested area and varying the threshold of the daily rainfall, Fig. 4-6, above which rapid recharge occurs from 35 mm to 10 mm, causes a change in the total recharge from 0% to 13%, related to the recharge with a threshold of 35 mm. Again, the magnitude of the change is, as was to be expected, unrelated to the total recharge of wet or dry periods, but a function of the temporal rainfall distribution and the respective rates.

The comparisons of the monthly values for field capacities 40, 75 and 130 mm (Fig. 4-7) reveal that the decrease in recharge for FC 75 mm and 130 mm as compared to a FC of 40 mm predominantly occurs during the spring summer and autumn, whereas during the winter period, when the soil storage is fully replenished, no difference is measured.

Fig. 4-8 illustrates the time variation in the increase in recharge due to the decrease in canopy capacity. It can be observed that maximum changes occur during spring and autumn months, when both, evapotranspiration and rainfall are high and more evenly distributed over a number of days. Due to the specific treatment of snow interception, as a result of the lack of data, no changes in recharge can be calculated by varying canopy capacity (crude approximation, 20% of daily precipitation).

The sensitivity analysis on a daily time basis was carried out for three months, the first one a winter month (Jan88), the second a summer month (Jun88) and the third one a spring month (Apr89). All the values are given in App. 4-3. The mechanisms, controlling the amount of recharge are the same as those discussed above. The change in daily recharge with a variation in rapid recharge is however somewhat more difficult to analyse. The amount of recharge is a function of the relative depth of rainfall, compared with the threshold of rapid recharge and the quantity of water left in the soil storage. It can therefore happen that on some days (e.g. 1 Apr89) recharge increases with a decrease in the threshold from 35 mm to 10 mm and on the next day (2 Apr89), the recharge decreases. The reason for that is that recharge occurs via rapid recharge and is released from the soil store, because field capacity is reached during either the 1st or the 2nd of April, depending on the amount of recharge.

4.1.2 Comparison of Results with Other Methods

There are numerous methods described in the literature for estimating groundwater recharge. However, only a number of them are applicable

Results of groundwater recharge estimates with and without interception and comparison with results from the Renger and Strebel (1980a) method

hydrolog. year 1.11.-31.10	rain-fall	evapo-transp. E Haude	dis-charge Lauchert	model recharge + ic + rr	Renger recharge	model recharge + ic - rr	model recharge - rr - ic	model recharge no red. in evapo	deviation Renger model	deviation +ic,+rr -ic,-rr
	mm	mm	mm	mm	mm	mm	mm	mm	%	%
1966	1040,6	430,4	400,9	485,0	502,9	470,4	601,0	597,6	4	-24
1967	886,7	503,5	362,9	382,2	475,0	357,1	440,3	409,4	24	-15
1968	990,9	451,0	379,0	428,5	493,6	415,8	553,9	518,2	15	-29
1969	830,0	449,4	333,9	328,5	433,8	306,4	416,4	402,2	32	-27
1970	942,2	437,5	400,2	409,9	471,8	396,9	494,1	475,8	15	-21
1971	637,5	545,1	198,7	198,6	386,2	171,1	213,7	176,3	94	-8
1972	627,5	471,8	152,9	146,0	355,5	126,5	185,0	129,2	143	-27
1973	960,4	480,0	290,2	422,1	493,4	393,3	498,5	440,8	17	-18
1974	847,8	461,4	259,9	335,6	445,1	316,4	405,5	380,5	33	-21
1975	913,7	460,8	355,5	432,4	469,8	412,4	499,7	458,9	9	-16
1976	690,8	538,1	219,8	200,0	407,5	180,4	246,5	197,7	104	-23
1977	973,2	417,7	303,3	422,8	475,6	413,5	562,0	551,5	12	-33
1978	1060,2	448,5	376,2	524,7	515,7	514,4	621,0	613,7	-2	-18
1979	851,9	469,0	321,2	377,9	449,4	356,1	438,7	396,3	19	-16
1980	1091,9	443,6	357,4	540,5	523,9	515,2	644,5	632,9	-3	-19
1981	897,1	495,1	323,6	388,4	475,9	358,2	442,6	395,4	23	-14
1982	1033,8	496,7	493,3	476,4	524,3	462,3	584,9	537,5	10	-23
1983	875,8	576,8	483,3	473,2	497,0	443,4	487,5	487,1	5	-3
1984	904,7	492,3	328,3	382,2	477,7	361,7	462,0	366,9	25	-21
1985	723,7	566,4	295,2	279,2	431,9	245,8	292,7	292,7	55	-5
1986	1113,6	467,6	397,5	501,0	539,2	470,4	624,4	572,0	8	-25
1987	1015,2	479,5	451,9	452,5	512,0	432,4	561,3	534,6	13	-24
1988	1084,1	458,3	510,2	532,1	526,8	513,8	623,4	624,1	-1	-17
1989	751,7	528,8	328,7	300,8	430,3	276,5	325,3	290,6	43	-8
mean (annual).	906	482	347	393	471	371	468	437		

remark: the discharge measurements cannot be directly compared with the recharge model results because of the neglect of groundwater storage change

abbrev.: - ic: no interception, - rr: no rapid recharge
no red. in evapo: no reduction in evapotranspiration below root constant.

Tab. 4-3 Results of Recharge Calculation and Comparison With the Renger (1980a) Method

to the recharge processes that occur in the project area and to the problem, which requires recharge on a daily base. Other methods that are based on the physics of evapotranspiration, i.e. using the atmospheric boundary layer approach (Black et al., 1987), demand climatic input data of high resolution and at different heights, only obtainable with meteorological balloons (Mawdsley, 1989). In order to account for the effect of different vegetation covers, particularly forested stands, heat balance methods on single tree trunks have been applied (Čermák and Kučera, 1987). The above review was intended to give an impression of the amount and number of different data that are necessary to accurately estimate evapotranspiration, which however are generally not available for most groundwater studies. Similar problems are encountered if the physics of snowmelt was to be taken into account. Other methods, e.g. Renger and Strebel (1980a), only allow the calculation of groundwater recharge on an annual level.

Therefore, the approach taken was a compromise between the available data and the daily resolution required. In the following, the importance of the estimation of interception is shown and the results of the recharge calculation are compared with the Renger and Strebel (1980a) method, which takes into account the increased evapotranspiration in forested areas. Renger and Strebel (1980a, 1980b) were able to develop the following relationship (eq. 4-1) by regression analysis. The authors calculated the soil water balance, using water content of the soil and suction potential measurements and compared it with rainfall, Haude potential evaporation and the quantity of water available to plants (i.e. the difference between field capacity (FC) and wilting point (WP)). E_{real} stands for the real evapotranspiration and P for the precipitation with all variables in mm.

Different equations were found for different vegetation covers of which eq. 4-1 applies to coniferous stands.

It can be demonstrated (Tab. 4-3) that by ignoring the effect of forest interception, recharge

$$E_{real} = 0.152\ P + 0.000382\ P^2 - 316.2 \log (FC-WP) - 0.651\ E_{Haude} + 1129.5 \qquad (4\text{-}1)$$

is generally grossly overestimated, providing the same field capacity is used. The increase varies from 0% to 143%. Generally, the overestimate lies in the range between 15% and 50%, which frequently exceeds the error given by Renger and Strebel (1980b) of ± 40 mm, with almost no difference during the wet years (1966, 1978, 1986, 1988) and a substantial overestimation during dry years (1971, 1972, 1976). The difference between a recharge model that takes into account the interception process (+ic) as compared to the one that does not (-ic, rapid recharge is not considered either), is a function of the relative magnitude of the rainfall and of the frequency of wetting of the canopy. The latter effect is not apparent when annual sums are compared. During dry years, the difference between the two models is smaller if interception is ignored and during high rainfall years, the recharge, calculated by the adopted model (+ic,+rr) is lower by about 25%.

The comparison is performed on the basis of the hydrological year, which lasts from the 1st November until the 31st October, the time when the change in stored groundwater, compared with the previous year is assumed to be negligible.

4.1.3 The Role of the Subcutaneous Zone

The recharge calculated in Chap. 4.1.1 does not usually reach the water table on the same day as the rainfall event occurred. A fast component leads to an increased discharge within a few days and a slow component is released within periods ranging from weeks to months (Chap. 4.5). A high storage, high permeability zone just below the soil, with a small thickness of only a few meters, is believed to be a controlling factor, determining temporal recharge distribution.

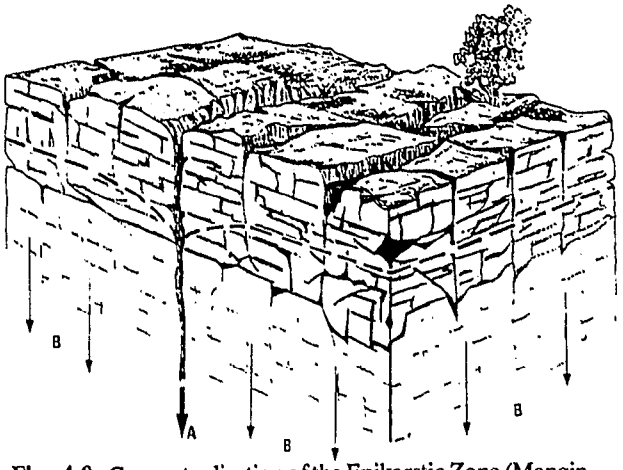

Fig. 4-9 Conceptualisation of the Epikarstic Zone (Mangin, 1975)

The existence of a horizon in the top part of the unsaturated zone of a limestone aquifer with an enhanced storage capacity, termed subcutaneous zone, has been strongly proposed by Williams (1983, 1985). Such a zone had already been introduced by Mangin (1975) as the "aquifère épikarstique" (Fig. 4-9). The subcutaneous zone is visualized as a horizon with thicknesses usually varying between two to three meters, having its origin in the increased solutional activity in the area of higher CO_2 supply. Further processes for the enhancement of the porosity of this zone are the near-surface tension release and the temperature variation. The base of the subcutaneous zone can be formed by a capillary barrier in narrow fissures or more frequently by clay residue of the solutional process (Fig. 4-10). This type of geometry leads to a subcutaneous water table and a substantial lateral flow towards large vertical shafts and conduits, conducting the water to the phreatic water table. Radial flow towards these preferential flow paths are believed to lead to the development of dolines and surface depressions (Williams, 1985). *The assumption of a subcutaneous zone is a prerequisite for the explanation of certain features in spring chemographs and temperature changes. Bakalowicz and Mangin (1980) identified in $\delta^{18}O$ spring water variations old water of earlier events with a marked deviation in ratio from the pre-event discharge and the new water input, causing strong fluctuations in the $\delta^{18}O$ at the beginning of the flood. Williams (1983) reinterpreted spring chemographs of Ashton (1966) by explaining an initial increase in electrical conductivity by associating this increase with a displacement of higher mineralised water of the subcutaneous zone.* Williams (1983) sees little evidence for hardness values in phreatic conduits being substantially higher than normal pre-event discharge. Frequently, this initial increase has been attributed to the flushing out of water from deeper sections of the phreatic zone.

The epikarst can also be visualized as a double-porosity system. The fast system (increase in electrical conductivity) is activated during the initial phase of the recharge event, whereas the slow system of the epikarstic zone works as the delaying factor on the recharge.

Renner (1991) found by repeated borehole fluid temperature logging after recharge events that surface temperature pulses were transmitted to the groundwater even up to one and a half months after the recharge event. Heat conduction can be excluded as a mechanism because of

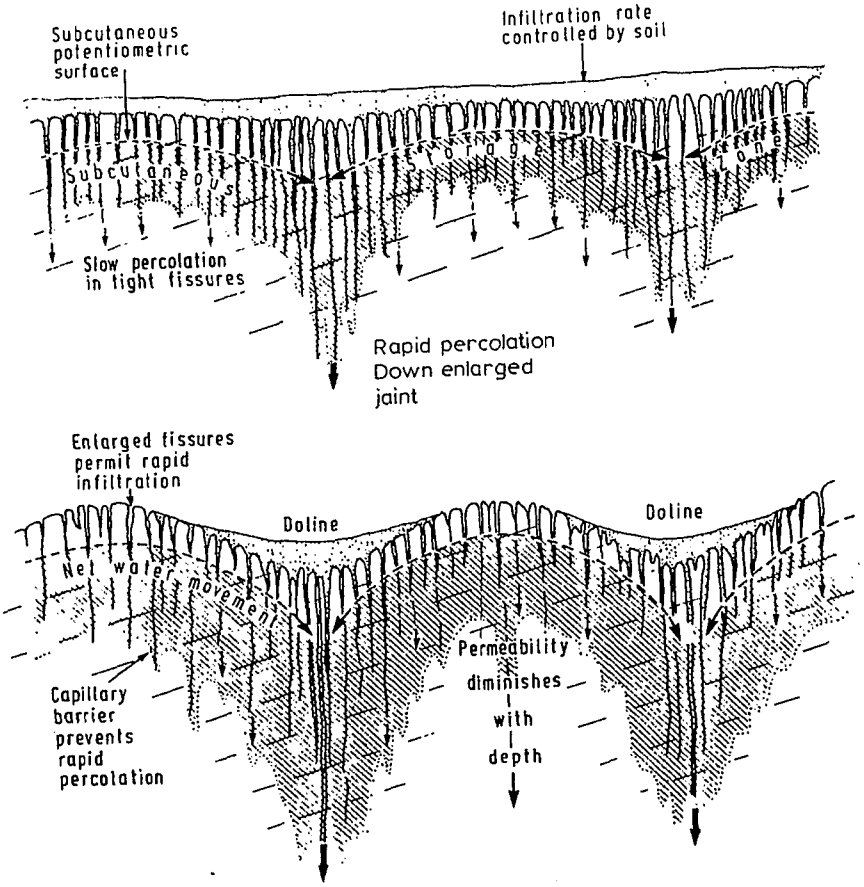

Fig. 4-10 Lateral Flow and Subcutaneous Storage in the Epikarstic Zone (Williams, 1983)

the high thickness of the unsaturated zone (100m). The only transport medium for the heat appeared to be the slowly drained water from the subcutaneous zone. Renner (1991) managed to locate the depth of the subcutaneous zone at 2-3 meters below the surface, by assuming the slow recharge rate, calculating the heat exchange in the phreatic zone induced by the slow drainage and correcting for heat gains/losses during the passage through the unsaturated zone. Fig. 4-11 displays the conceptual model of the heat transport from the surface to the groundwater incorporating the subcutaneous zone as an essential component.

One of the main functions of the subcutaneous zone is its influence on the delay and the distribution of the groundwater recharge as mentioned above. The knowledge of the distribution according to which recharge reaches the phreatic zone is essential for the calibration of a groundwater flow model (Sauter, 1990). It is attempted (Chap. 4.5) to quantify these distributions and the characteristic parameters of the epikarst by analysing time series of hydraulic and physicochemical parameters. Smart and Hobbs (1986) subdivided what is called in this study subcutaneous flow into four different components by investigating characteristic features of drip flow in a cave and their flow recession characteristics (Maillet, 1905). Smart and Friederich (1986) were able to directly measure the total drip flow of the cave and also associate a catchment area with it, which allowed the calculation of a storage coefficient of approximately 1% of the subcutaneous zone (see Chap. 4.2). The release of seepage flow from the subcutaneous zone can be described by a simple 1 or 2 component flow recession relationship. The recession constants of the fast draining seepage flows, which account for approximately 60% of the total flow are greater than 0.07 d^{-1}, while those with recession coefficients less than 0.03 d^{-1} provide 20% of the total flow. The remaining 20% have values of between 0.07 d^{-1} and 0.03 d^{-1}.

The time variation in the recharge input for the model calculations follows partly a recession relationship. A certain percentage is transferred directly to the water table as fast water (Chap. 4.5), the quantity exceeding the maximum storage capacity of the slow subcutaneous system of 30 mm is distributed following a separate function (intermediate component of the subcutaneous drainage, Chap. 4.5) and the subcutaneous storage is depleted following a recession constant of $\alpha = 0.05\ d^{-1}$. There is not enough information available in the project area to discriminate between several categories of subcutaneous flow. Further details regarding the development of the input function is discussed in Chap. 4.5 and the evaluation of the fast and

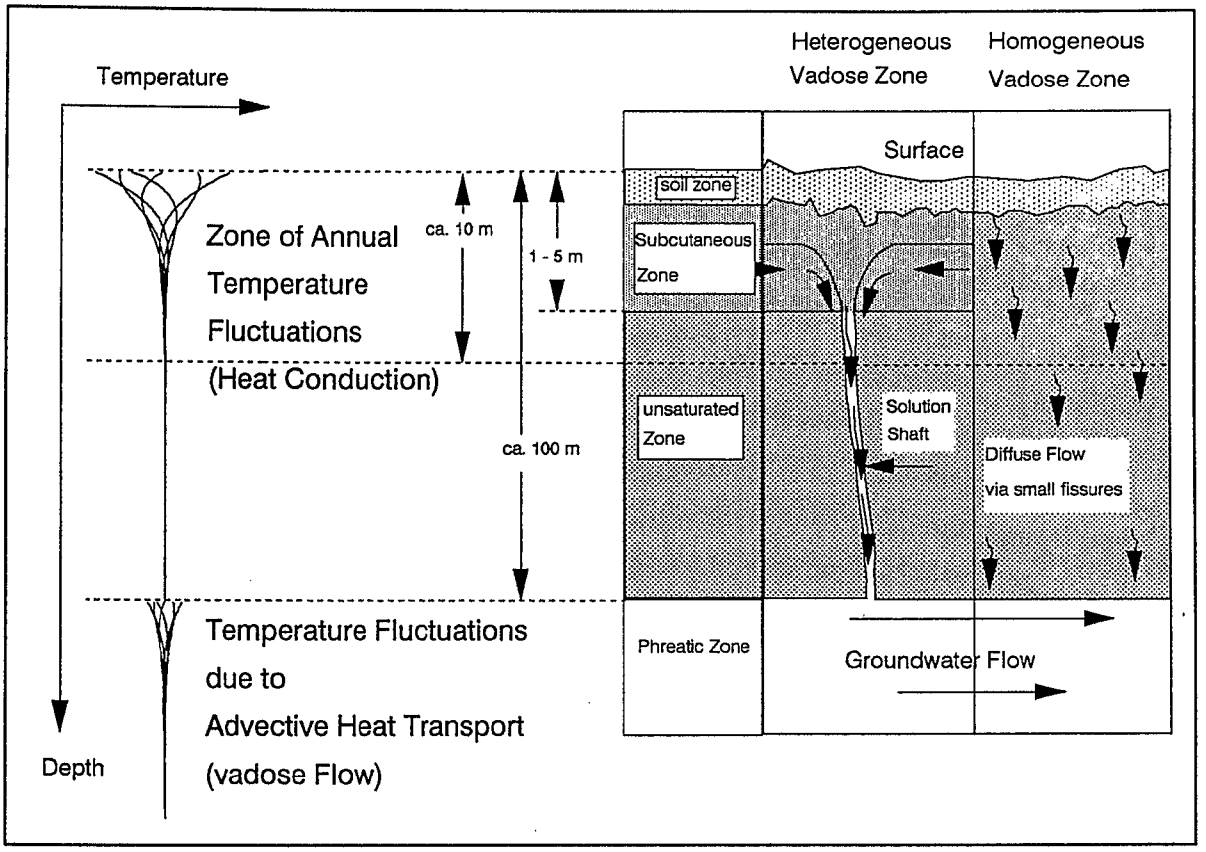

Fig. 4-11 Temperature Variations and Flow Pattern Within the Subcutaneous Zone and the Aquifer (Renner, 1991)

slow storage of the subcutaneous zone is demonstrated in Chap. 4.2.

4.2 Storage

In highly heterogeneous systems such as karst aquifers, parameters like porosity and the related storage coefficient are highly dependant upon the scale of the investigation method. Castany demonstrates (Fig. 4-12) how the porosity values obtained vary with the volume of rock sampled, expressed as the radius of investigation. Starting at a micro (laboratory) scale, where the porosity can vary from 0 (tight rock) to 1 (void), homogeneous values can be measured if a sufficiently large number of heterogeneities (fissures/fractures) are integrated within the sample volume. Castany (1984) does not observe any homogeneous behaviour on a meso scale (field hydraulic test), which is in the order of several hundred meters. Homogeneous behaviour prevails again if a sufficiently large number of large scale heterogeneities, such as conduits are included in the sample volume on a macro scale, visualized as a catchment or groundwater basin. However, even on a catchment scale the measured parameter can vary, depending on the presence of large faults, folds and lithostratigraphic variations. Domenico and Schwarz (1990) termed the different scales micro, macro and mega scale and applied similar principles to the hydraulic conductivity as will be shown under Chap. 4.3.1.

In this report, the different scales are subdivided into a) the laboratory, b) the local (borehole test) and c) the regional (catchment) scale, in order to include the dimension and the domain, the parameter applies to. Micro, macro and mega scales do not include this information because of their general formulation.

The relevant scale in porosity or storage for the groundwater models in question is the mega or regional scale.

It is useful to categorize storage into unsaturated and saturated storage, each of them again can be subdivided into different reservoirs, the soil zone and the epikarst (subcutaneous zone), the conduit storage and the water stored in microfractures and pores.

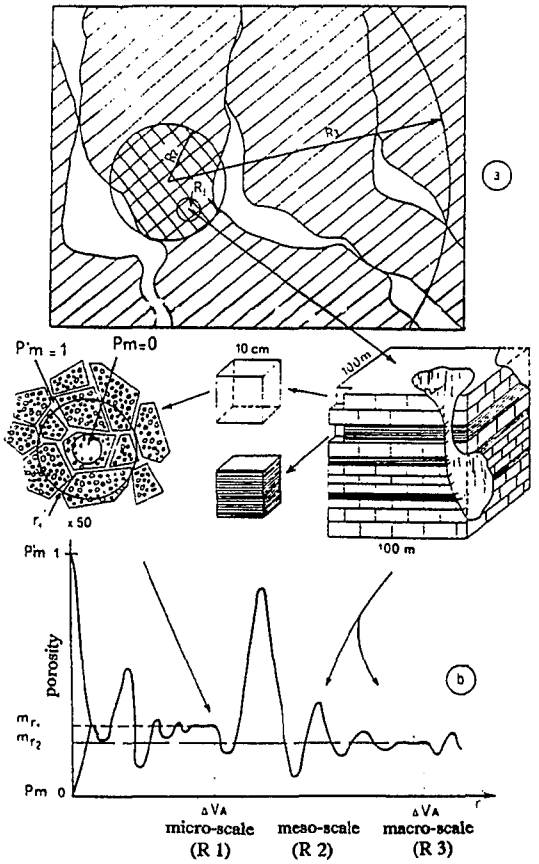

Fig. 4-12 Influence of Spatial Scale on Heterogeneity: a) Degrees of heterogeneity vs volume of rock, b) variation of total porosity with volume of rock

4.2.1 Unsaturated Storage

It can be assumed that the thin cover of orthic luvisols is unable to hold large quantities of water. Even after minor rainfall events, the soil is at field capacity. Soil physical examination *(Hemme, 1970), suggests a field capacity varying between 30 and 70 mm. Only in depressions, where brown earths prevail, does field capacity reach 180 mm.*

The storage capacity of the subcutaneous zone is difficult to assess. Through repeated borehole logging, temperature variations have been observed in the top 5 m of the phreatic zone (100 m b.g.l.) that are closely related to the surface air temperature, even after prolonged dry periods. *The only possible mode of heat transfer could be by water, temporarily stored in the unsaturated zone. These variations suggest that this type of recharge must be an important quantity, otherwise, it would have been buffered by the karst water stored in the saturated zone. Ongoing research is attempting some quantitative estimate of this type of recharge.*

Fast Subcutaneous Storage

After some recharge events, especially after prolonged dry periods, *it was observed that electrical conductivity of spring water increased for a short period followed by a rapid decrease (Chap. 4.5).* According to Ashton (1966), the water with the higher conductivity represents so-called deep phreatic water as a result of the longer reaction time between water and rock. *If however, this type of water is interpreted as water from the subcutaneous zone (Fig. 4-13, Williams, 1983), which is displaced by event water and discharged only via the conduit system, some estimate of the stored quantity can be made.*

This quantity however only represents the stored water of the fast system within the subcutaneous zone, i.e. the water that can be mobilized quickly within the fractures and fissures of the epikarst that drain the surrounding bulk subcutaneous zone (double-porosity concept). As will be shown in chapter 4.5, and already discussed above, rough estimates of the respective quantities, fast subcutaneous storage and conduit storage can be made. It has to be however noted that the discharged water is always a mixture of three components, the pre-event (conduit water), the subcutaneously stored and the new recharge water, because the piston flow approach as advocated by Ford and Williams (1989), Williams (1983) and Bonacci (1987) does not apply, rather an exponential model should be employed. The reason for that is that re-

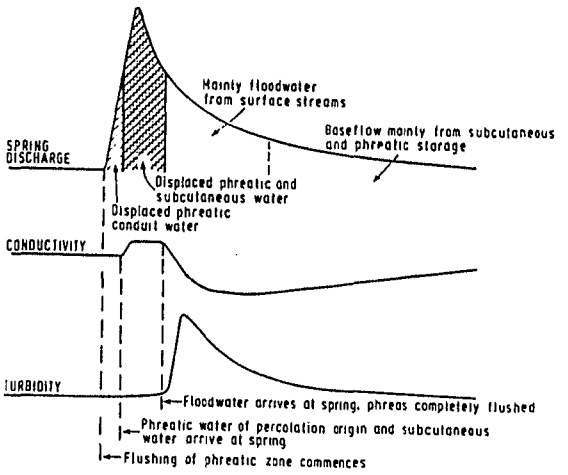

Fig. 4-13 Interpretation of a Karst Spring Hydrograph and Chemograph (Williams, 1983)

charge occurs at the same time close to the spring and at the distant water devide.

Tab. 4-4a shows the discharged quantities of the subcutaneous zone and the conduits. The storage of the fast system of the conduits is equal to the water volume, discharged between the increase in spring discharge and the arrival of the water from the subcutaneous zone, which is signalled by an increase in electrical conductivity and/or pH. Sometimes a slight increase in temperature can also be observed. The integrated discharge during the period of elevated electrical conductivity up until the arrival of the aggressive event water can be considered as the water stored within the fast system of the subcutaneous zone.

The time readings for the determination of the arrival of displaced phreatic conduit water, subcutaneous water or event water were based on half hourly data of an automatically recording datalogger, which allowed a satisfactory distinction between the different components. Pre-event discharge has not been extrapolated for the period of the flood because the contribution of the slow drainage into the fast path ways from the surrounding fractured rock is assumed to be negligible because of elevated potentials within the conduits.

Tab. 4-4a also lists the calculated recharge for the month and the week preceding the event. A hypothetical variable, constructed by these two values is thought to be a possible semiquantitative indicator of the stored water and the saturated thickness within the subcutaneous zone. *The values for the fast subcutaneous storage vary between 0.3 mm and 2 mm, which can be possibly extrapolated to 3 mm at maximum storage. Together with a 2 to 3 m thick epikarst and with plausible minimum saturated thicknesses in the order of several tens of centimeters a storage coefficient of approximately 0.001 can be obtained.*

It is however difficult to determine a storage coefficient for the fast system of the subcutaneous store, because the fractures cannot be assumed to be fully saturated before a rainfall event.

Calibration procedures for the distribution of the fast recharge input to the numerical model (Chap. 5), derived from the subcutaneous zone yielded a flow recession coefficient of about 0.4 d^{-1}, which describes the outflow relationship satisfactorily. This value compares well with the one obtained by Smart and Friederich (1986) for similarly fast subcutaneous flow components of 0.46 d^{-1}. This value however was not significant at the 5% level.

Slow Subcutaneous Storage

It was attempted to estimate the storage coefficient of the slow epikarstic system with a water balance approach, which can be expressed with the following formula (eq. 4-2),

$$S_{SC} = R - Q_{GW} - S_{GW} \pm S_S - Q_L \pm E \qquad (4\text{-}2)$$

where S_{SC}, S_S and S_{GW} represent the stored water in the subcutaneous zone, the soil zone and the aquifer respectively, R stands for the groundwater recharge, Q_{GW} for the groundwater discharge, Q_L for groundwater discharge which is not measured because of the flow below the weir and E for possible errors. The water balance is carried out after a certain period, when it can be assumed that no more recharge occurs, except from the slow drainage from the subcutaneous zone. The results vary between -19 and 27 mm (tab 4-4b). Considering the errors, inherent in the estimation of the phreatic storage coefficient and in the estimation of the regional increase in water level (both used to estimate quantities stored within the groundwater zone) and in the recharge calculation, maximum stored quantities can be estimated to range between 20 mm and 30 mm. Losses underneath the gauge (Q_L) are calculated assuming a constant rate of 50 l/s (Chap. 2.6.2). The change in soil moisture is taken from the recharge calculation. Only gains in soil moisture have to be considered in the water balance, because losses are due to evapotranspiration and not to drainage to the subcutaneous zone. Evaporation losses are already accounted for in the recharge calculation.

In order to be able to have a deficit of 20 mm, the subcutaneous store has to have at least a volume of 20 mm. The recharge calculation shows that the soil moisture is fully replenished before the event of Feb. 90 from the previous event and it can also be assumed that the subcutaneous store is fairly full, which is indicated by the high value of 1.4 mm for the fast subcutaneous store; a negative balance by the 30.7.90, i.e. the subcutaneous store contained 19 mm more water on the 12.2.90 than on the 30.7.90, can therefore be easily explained; one further indication that the subcutaneous store can take up more than 20 mm. *Assuming that the subcutaneous store can take up 30 mm (13.2.90) and that it was depleted by the 30.7.90 (1 mm),*

(a) Storage evaluation subcutaneous zone (fast system) and phreatic conduits

Date	storage sc zone	storage conduit	recharge previous month	recharge previous week	spring discharge	water-level (B7)
	mm	mm	mm	mm	m3/s	650m + .. m
24.12.88	0,6	2,3	113	3	0,79	12,28
11.12.88	0,7	1,3	70	48	0,70	10,72
13.6.88	0,3	1,5	30	14	0,69	11,92
7.6.88	0,9	0,5	14	3	0,67	12,07
1.3.90	2,0	0,6	84	10	0,66	11,20
18.4.89	0,8	0,9	37	5	0,46	10,93
18.12.89	0.4-c_s	?	30	30	0,34	7,61
2.4.89	1,1	0,9	9	0	0,33	10,91
10.10.88	0,9	0,3	14	8	0,32	9,35
5.12.88	0,8	0,2	22	21	0,29	8,80
5.9.88	0.5-c_s	?	6	0	0,28	10,28
11.7.89	0,4	0,3	14	4	0,23	9,90
14.2.90	1,4	0,5	17	2	0,17	7,68
16.12.89	0,4	0,2	3	2	0,12	7,54

Abbr.: sc zone: subcutaneous zone
Abbr.: c_s: conduit storage

(b) Storage evaluation subcutaneous zone (slow system)

Event Date	Excess/Deficit (Storage)	Recharge (calcul.)	Groundwater Discharge	Discharge Period	Groundwater Storage	Time of S Evaluation	Water level to preevent
	mm (S SC)	mm (R)	mm (Q GW)		mm (S GW)		+ ..m
Feb-90	-19	100	73	13.02.90-30.7.90	30	30.7.90	0,5
Dec-89	16	48	16	12.12.89-13.2.90	10	13.2.90	1,5
Dec-88	21	150	71	29.11.88-15.2.89	50	15.2.89	2,0
Apr-89	27	71	24	1.04.89-05.6.89	14	5.7.89	0,7

Rem.: For the evaluation of storage (water balance excess/deficit) a constant phreatic (slow system) storage coefficient of 0.02 was employed

Tab. 4-4 Storage Evaluation of the Subcutaneous Zone (a and b)

i.e. after 167 days, a recession coefficient of $\alpha = 0.02\ d^{-1}$ *can be evaluated, which is well in accordance with the values of Smart and Friederich (1986) for slowly draining subcutaneous flow components (*$\alpha < 0.03\ d^{-1}$*).*

Together with an assumed thickness of 2 to 3 m for the subcutaneous zone, a storage coefficient of 0.01 can be calculated for the slow (matrix) system of the subcutaneous zone, which is in agreement with the findings of Smart and Friederich (1986).

4.2.2 Groundwater Storage

Storage in the saturated zone can be subdivided at a regional scale into conduit and fissured system storage (Atkinson and Smart, 1981, Shuster and White, 1971, White, 1977).

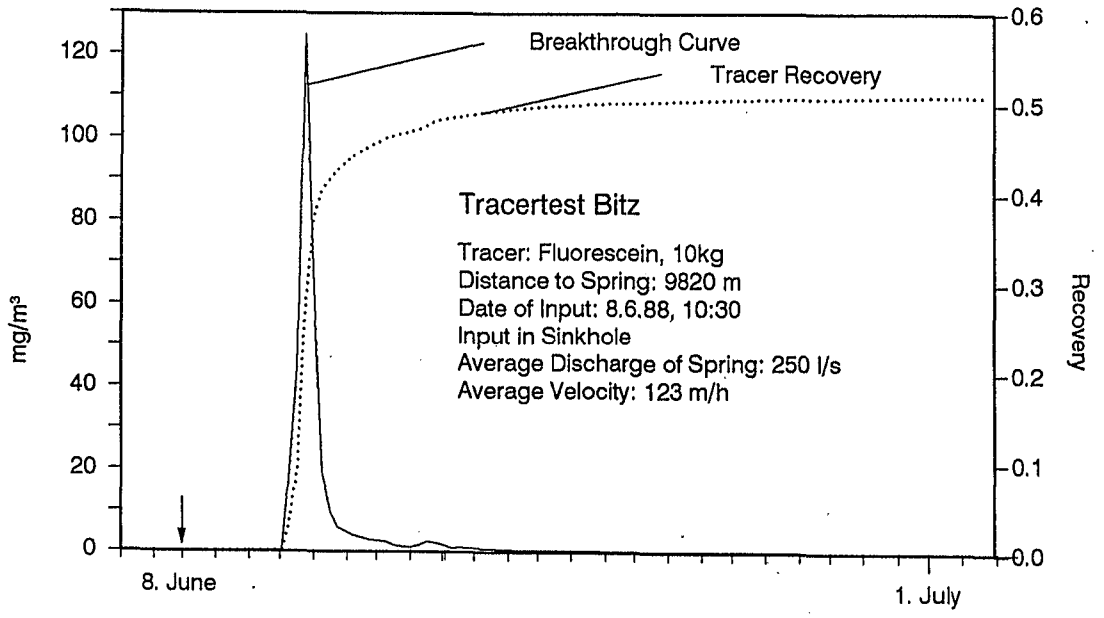

Fig. 4-14 Tracer Test With Tracer Injection Into Conduit System (data from Landesanstalt für Umweltschutz, unpublished)

Conduit Storage

Conduit storage could be evaluated with the approach suggested by Williams (1983) which is a modification of Ashton (1966) as outlined above. The events in Tab. 4-4a are ranked according to decreasing pre-event discharge. The spring discharge is taken as a measure for the unknown saturated thickness within the fast system of the aquifer. A similar parameter to the discharge is the waterlevel in borehole B7 and it becomes apparent that no simple relationship exists between spring flow and the potentials measured (see also Chap. 4.5). Generally, conduit storage ranges from 2.3 mm to 0.2 mm, with a variation, that is closely related to the saturated thickness of the fast groundwater system, indicated by either high spring discharge or high water levels or both. Bearing in mind the accuracy of the above method and assuming the saturated thickness of the conduit system to range between 2 m and 15 m (discharge varying between 0.12 m^3/s and 0.79 m^3/s), *the values obtained this way varied between 0.01% and 0.016%. The obtained storage coefficients are however a systematic underestimate of the true storage, because of the assumption of piston flow.* The estimation of the saturated thickness of the conduit system is based on water level readings in borehole B14, which is believed to be connected to the fast flow system (Fig. 2-22). The value of 15 m corresponds to water levels in B14 between the lowest discharge rate and average flood conditions. The value of 2 m corresponds to the difference in water levels at a spring discharge of 0.12 m^3/s and lowest discharge rate of 0.08 m^3/s. It is assumed that the base of the aquifer is more or less equal to the water level at the lowest flow conditions (≈ 0.08 m^3/s). These estimations are very tentative and the lower value of 2 m could be off the true value by several 100%. However, even assuming the largest error, the storage coefficient for the conduit system still remains in the order of 10^{-4}.

Another method employed are tracer tests, whereby the dye was injected into a doline connected to preferential flow paths (Fig. 4-14). The volume of groundwater discharged between the time of injection and the arrival of the dye, divided by the volume of the saturated rock, produced the figure between 0.00024 and 0.00039 for the conduit storage (Tab. 4-5). The tests with input into a sinkhole were time corrected, i.e. 6 hours were subtracted from the peak time to allow for the transfer of the dye through the unsaturated zone. The delay time of 6 hours was derived from the analysis of the time series (Chap. 4.5) as the difference between the highest intensity in rainfall and the highest water level in borehole B14 for event 14 February 1990 (Tab. 4.17), which is believed to respond to the fast groundwater system. The higher values, such as the one from test 782 and the borehole tests are not representative of the fast conduit system. It is possible that during low flow (0.12 m^3/s) the actual permeable aquifer is almost drained, especially further upgradient. Delayed transfer through the unsaturated zone is also a likely reason.

The values obtained from the borehole tests are a mixture between the storage of the slow and the fast groundwater flow system, whereby the relative proportions are unknown, because of the uncertainty of the distance from the input location to the nearest fracture/conduit.

Evaluation of storage coefficients of conduit system (regional)

Test	Source	Date of input	Input mode	Distance to spring [m]	Discharge [m3/s]	Time to peak [h]	satur. thickn. [m]	average velocity [m/h]	Storage
521	GLA	24.10.58	sinkhole	3026	0,490	31,5	20,0	96,1	0,00023
522	GLA	09.01.59	sinkhole	3026	0,690	21,0	25,0	144,1	0,00017
523	GLA	09.01.59	sinkhole	3026	0,690	23,0	25,0	131,6	0,00019
746	LfU	08.06.88	sinkhole	9820	0,760	79,5	27,0	123,5	0,00021
782	GLA	12.01.63	sinkhole	8730	0,120	283,0	15,0	30,8	0,00023
sw Bitz	Strayle(1970)	10.08.65	sinkhole	11100	0,700	98,0	25,0	113,3	0,00022
B25	GLA	01.08.67	borehole	5300	0,460	72,0	20,0	73,6	0,00028
B22	GLA	29.08.67	borehole	4500	0,340	119,0	18,0	37,8	0,00045
B19	GLA	20.10.67	borehole	5200	0,270	106,0	17,0	49,1	0,00029
B24	GLA	21.11.67	borehole	5900	0,220	123,0	16,0	48,0	0,00026
FV1	Merkel(1991)	26.04.89	borehole	4100	0,663	110,0	25,0	37,3	0,00064
FV2	Merkel(1991)	11.07.89	borehole	5300	0,351	77,5	18,0	68,4	0,00026
FV3	Merkel(1991)	07.02.90	borehole	6700	0,159	112,0	15,0	59,8	0,00016

Abbr.: GLA Geologisches Landesamt Baden-Württemberg
LfU Landesanstalt für Umweltschutz, Karlsruhe

Tab. 4-5 Evaluation of Storage of Regional Conduit System

Evaluation of storage coefficients of fissured system (regional)

	b7 m asl	b8 m asl	b25 m asl	b14 m asl	b17 m asl	Rockvol m3	Discharge m3	Storage	
25-Apr-88	666,96	672,12	676,30	697,60	737,21				FLOOD
02-Mai-88	665,18	669,81	675,30	695,79	734,59	8,67E+07	1,03E+06	0,012	CONDITIONS
09-Mai-88	664,86	667,83	674,99	693,93	732,26	7,01E+07	8,10E+05	0,012	
16-Mai-88	663,54	666,34	674,50	691,91	729,22	8,35E+07	5,72E+05	0,007	
							Average	0,010	
18-Jul-88	661,01	663,10	673,14	685,59	724,32				AVERAGE
25-Jul-88	660,98	662,80	673,12	685,48	723,41	1,23E+07	2,77E+05	0,023	FLOW
01-Aug-88	660,92	662,25	672,79	684,96	722,76	2,08E+07	2,45E+05	0,012	CONDITIONS
08-Aug-88	660,85	662,22	672,41	684,29	721,44	2,68E+07	2,21E+05	0,008	
15-Aug-88	660,75	661,90	672,05	683,65	720,67	2,31E+07	1,91E+05	0,008	
22-Aug-88	660,65	661,55	671,84	683,43	720,10	1,30E+07	1,89E+05	0,014	
29-Aug-88	660,55	661,22	671,61	683,40	719,69	8,19E+06	1,69E+05	0,021	
05-Sep-88	660,28	661,00	671,45	683,35	718,92	1,17E+07	1,58E+05	0,013	
12-Sep-88	659,91	660,77	671,25	683,30	718,72	7,50E+06	1,58E+05	0,021	
19-Sep-88	659,76	660,32	671,07	683,25	718,52	7,38E+06	1,26E+05	0,017	
26-Sep-88	659,59	660,22	670,95	683,20	718,31	5,13E+06	1,26E+05	0,025	
03-Okt-88	659,36	660,14	670,87	683,13	718,12	5,31E+06	9,45E+04	0,018	
							Average	0,016	
27-Jun-88	661,64	664,75	674,04	687,05	731,70				AVERAGE
04-Jul-88	661,62	664,09	673,70	686,96	728,20	3,92E+07	4,02E+05	0,010	FLOW
11-Jul-88	661,41	663,58	673,49	686,22	726,10	3,78E+07	3,55E+05	0,009	CONDITIONS
18-Jul-88	661,01	663,10	673,14	685,59	724,32	3,47E+07	3,09E+05	0,009	
25-Jul-88	660,98	662,80	673,12	685,48	723,41	1,23E+07	2,74E+05	0,022	
01-Aug-88	660,92	662,25	672,79	684,96	722,76	2,08E+07	2,43E+05	0,012	
							Average	0,013	

Tab. 4-6 Evaluation of Storage of Regional Fissured System for Flood (top) and Average Flow Conditions

The most critical source of error in the above procedures is the estimation of the saturated thickness and the determination of the drained rock volume. In order to be consistent, the saturated thickness was related to the discharge (2 m at 0.12 m^3/s and 15 m at 0.79 m^3/s) and the width of the drained rock volume was kept constant at 4000 m, derived from the equipotential map (Fig. 2-21). As already mentioned above, the storage coefficients determined with the Williams (1983) method are an underestimate of the actual storage and therefore, a value of 0.0003 is a plausible storage coefficient, which corresponds to a value of 0.00031, obtained by Atkinson (1977) and a value of 0.00035 of Pfaff (1988). The method applied by Pfaff (1988) assumes that the integrated volume under the flow recession curve for the fast flow, subtracting the volume under the recession curve for the slow flow is equal to the water stored in the conduit system, which is only true for two totally disconnected systems, joining at the spring. The error made however is likely to be negligible in karst systems where the slow system dominates after a few days.

Fissured System Storage

The storage of the whole aquifer system, which mainly consists of fissured system storage, could be similarly evaluated by deviding the water volume discharged by the volume of the aquifer drained. The drained rock volume could be calculated using the waterlevel changes in the boreholes. Tab. 4-6 displays data from three recession periods, the first one during extremely high water levels (25-Apr-88), the second during average conditions (18-Jul-88) and the last one during a period, when it was assumed that the high storage/transmissivity horizon, described in Chap. 2.6 was activated. The boreholes selected for the evaluation procedure were those believed to be representative for a larger area. For the determination of the rock volumes, weighting factors were allocated to the data from the respective piezometers, i.e. the average of B7, B8 and B25 were given a weight of 2/5, those of B14 a weight of 2/5 as well and the values of B17 were multiplied by 1/5.

The storage coefficients obtained varied somewhat, which was to be expected, but it can be assumed that the storage varies between 0.01 for high water levels and 0.017 for intermediate water levels. Taking into account the flow under the weir of estimated 50 l/s, the storage is increased at intermediate conditions and not affected at high levels.

The effect of the high storage/permeability horizon did not materialize in a high storage coefficient because the borehole B17 shows a very high change in water level, not necessarily representative, which substantially increases the

rock volume and decreases the storage accordingly.

It can be concluded that a value of about 2% represents the fissured system storage coefficient with a somewhat lower (1% to 1.5%) value during high water levels, which was already suspected from the water level information (Chap. 2.6.3). These findings compare reasonably well with those of Villinger (1977)

Storage at a Local Scale

Storage at a local scale can usually be derived from hydraulic tests. The slug and injection tests of Chap. 4.3.1.2 do not deliver reliable results as discussed below and most of the pumping tests have been analyzed with a steady state approach. *The pumping test in the borehole Veringenstadt however yielded an unconfined storage coefficient of 0.0001, a value that can be assumed to represent the storage of the local conduit system (short test duration, Chap. 4.3.1.2.1).* The relatively high transmissivity suggests that there is a direct connection to the fast system.

Stober (1991) determined an effective porosity of approximately 2.5% for a doublette tracer test in Saulgau geothermal wells (distance between wells: 430 m). Taking the same approach as described above for evaluating conduit storage using information from tracer tests, an effective porosity of approximately 1% was determined using $n_e = (Q\,t)/(2\pi\,r^2\,h)$. *This value of 1% storage can be considered to represent the local storage parameter for the slow system indicated by the tracer breakthrough curve (Fig. 6-2) characteristic for a homogeneous medium. The probability to encounter a direct conduit/fracture connection between the two wells is very improbable and therefore only the local fissured system was tested.*

Laboratory Measurements

Weiß (1987) measured porosity and permeability of the Upper Jurassic limestone sequence in the southern Franconian Alb, which is geologically comparable to the Swabian Alb. The values obtained as effective porosities in the bedded facies of the ki2 varied from 0 % to 12 % with a mode at 3%. The core samples used had a diameter of approximately 3 cm and an equal length. No representative samples could be obtained from the bioherm facies, which is frequently dolomitised and dedolomitised and the porosities can be assumed to be generally higher.

4.3 Flow within the Aquifer

A similar approach to Castany (1984) to describe the effect of scale on the measured parameter in heterogeneous flow systems has been taken by the Department of Energy (1986). Fig. 4-15 shows how the measured hydraulic conductivity varies with the radius of influence of the investigation method. Although the diagram applies to flows of basalt, it can easily be transferred to the flow in karstified carbonate rocks. The highly permeable flow tops can be visualized as conduits and the hydraulic characteristics within a single basalt flow as interconduit fractured blocks, where fissured system flow prevails.

The graph illustrates how large the representative elementary volume has to be in order for continuum conditions to apply. Contrary to the porosity, the hydraulic conductivity increases at a larger scale (domain of multiple flows, D), which is plausible because of the added effect of the high permeability flow tops. The porosity can also be assumed to increase but only very slightly, which however cannot be measured. This different behaviour could be explained by the cubic law (Snow, 1965), which describes the relationship between permeability and the fracture aperture. Porosity increases linearly with the fracture aperture, whereas the permeability increases with the cube of the distance between the two fracture faces.

In Fig. 4-16 hydraulic conductivity distributions are plotted against the size of the sampled volume in karst aquifers, which ranges from between fractions of a meter and 10000 m. It is illustrated by Kiraly (1975, in Ford and Williams, 1989) how the effect of various fissure and fracture discontinuities increases the overall hydraulic conductivities.

In a numerical model, simulating groundwater flow and transport, the hydraulic parameters dedicated to the respective discretised unit (element/cell), are a result of the sum (arithmetic/harmonic/geometric) of the parameters of the identified sub-systems, weighted by their respective proportions within the particular model unit. The problem of accommodating a number of flow sub-systems in a numerical model can be approached by either employing models, incorporating multiple continua such as MINC (Narasimhan and Pruess, 1988) or by determining the representative parameter at the modelled scale of a double-continuum model. The

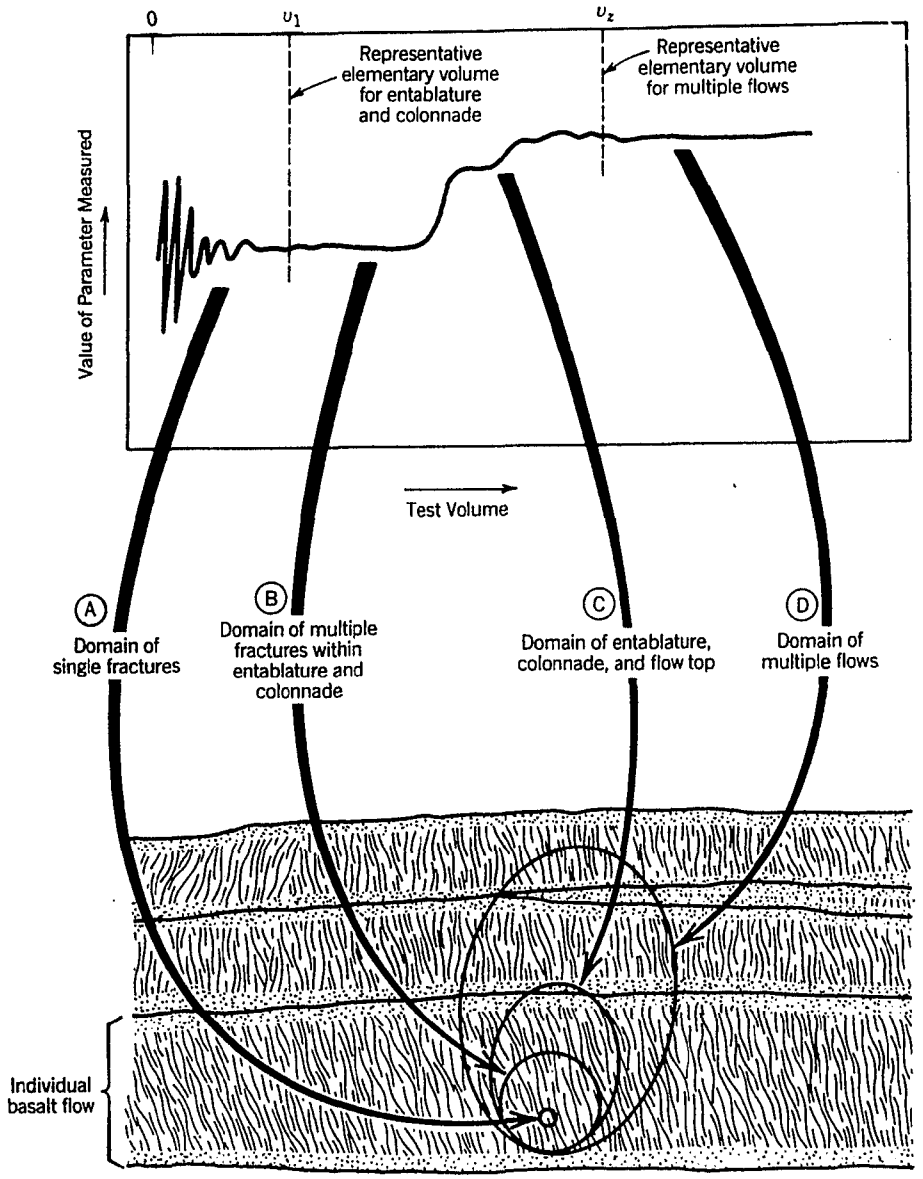

Fig. 4-15 Schematic Definition of a Representative Elementary Volume as Applied to Basalt (Department of Energy, 1986)

structure of the MINC model, applied to a karst aquifer, could be visualized as an intertwined system of fast (fracture, conduit) and slow (matrix, fissure) flow, i.e. double-continuum systems, whereby each slow system can again be split into a conduit and fissure flow continuum.

The fractured continuum of the lowest manageable double-continuum sub-system could be visualized as the joints, spaced at decimeter intervals (10 cm - 30 cm) and frequently measured in quarries. The complimentary parameters of the matrix (fissure) continuum can be measured in the laboratory on cores with dimensions of several centimeters. The above described double-continuum system could be regarded as the lowest in the hierarchy of multiple interacting continua. It forms the matrix continuum of the next higher double-continuum system, where the higher permeable set of fractures and the solution widened fissures are spaced apart between one and several meters. The double-continuum system can be investigated at this level in the hierarchy by double packer tests, where the packers enclose a test interval of less than one meter. Slug and injection tests with a test interval and radius of investigation of several tens and pumping tests with a scale of investigation of several hundreds of meters can identify the double-continuum systems at the respective scales.

At the regional, i.e. catchment scale, where conduits and caves represent the fracture continuum, the hydraulics of the matrix continuum could possibly be derived from pumping tests, which are, as outlined above, the result of the hydraulic characteristics and the interaction of

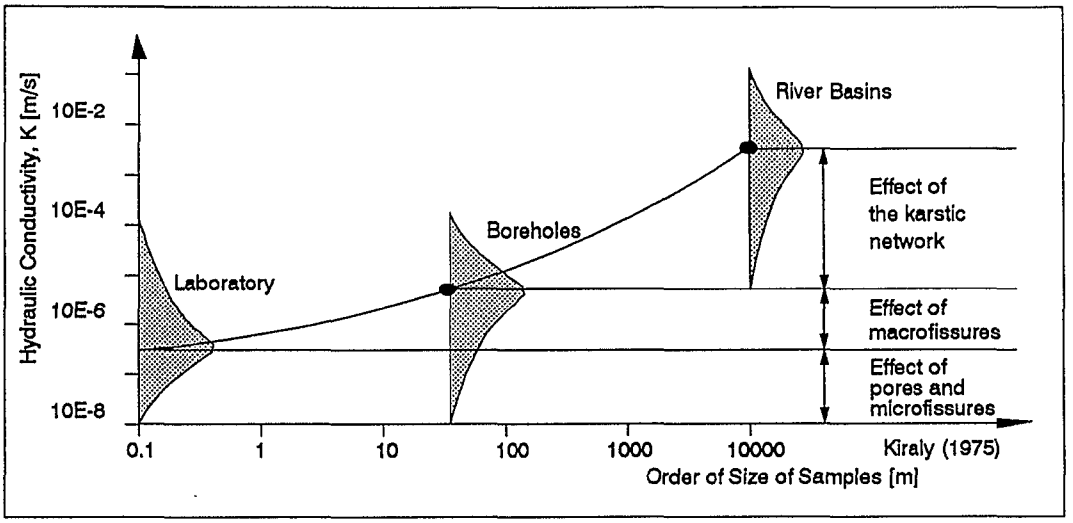

Fig. 4-16 Schematic Representation of the Effect of Scale on the Hydraulic Conductivity of Karst (Kiraly, 1975)

all the lower scale double-continuum flow systems.

For practical purposes, if the problem in question asks for answers at regional scale, no information is required on e.g. the potential change over a distance of several meters. It is also difficult to obtain all the relevant input data at every scale. Therefore, the flow system can be conveniently simplified to a single double-continuum model, assuming that the parameters can be determined at the modelling scale.

Within the context of this study, the model was designed to simulate regional flow and transport and the breakthrough of tracer tests with travel distances of several thousands of meters. Therefore, the nodes of the model grid were spaced 500 m apart (Chap. 5), which was a compromise between the lowest resolution of information on aquifer geometry, and the radius of investigation of a large scale pumping test.

It is attempted in this chapter to demonstrate how the hydraulic parameters were obtained, taking into account the various scales at which they were measured. The idea was to evaluate the hydraulic conductivity at the lower scales in order to be able to derive the resulting hydraulic conductivity at the next larger scale, together with a knowledge of the various proportions of fast and slow flow system, which exist at every scale. Fig. 4-17 illustrates how in a karst aquifer, the three different scales can be visualized, the regional, local and laboratory scale.

4.3.1 Hydraulic Parameters of the Aquifer

The evaluation of hydraulic parameters was subdivided into a regional assessment, taking into account the existence of the fast and the slow flow system, local scale tests in boreholes and laboratory measurements, derived from the literature. Particular emphasis has been put on the separate evaluation of fast and slow flow characteristics.

4.3.1.1 Regional Approach

Common hydraulic testing methods such as slug tests, packer tests and pumping tests, usually have a limited testing radius, which is usually in the order of several tens to hundreds of meters, depending on the nature of aquifer material. For regional flow models especially heterogeneous ones like a karst aquifer, an REV (Bear, 1972) can be estimated to be in the order of 1 km, a scale for which no testing methods are available.

The only signal, activating larger regions of the aquifer system are natural pulses, such as rainfall events, which can be evaluated by applying recession analysis to the output signal, i.e. the spring discharge. This method has the advantage that information can be gained over a large area, but because the registration of the output signal can only be measured at the spring, a differentiation into regionally varying parameters is generally not possible.

If however the regional hydraulic conductivity varies laterally and with depth (Chap. 2.6.1, 2.6.3), the value of the parameter obtained depends on the intensity of the signal (recharge depth) and only reflects the hydraulic characteristics of that portion of the aquifer, dominating the flow.

The approach taken for the evaluation of the

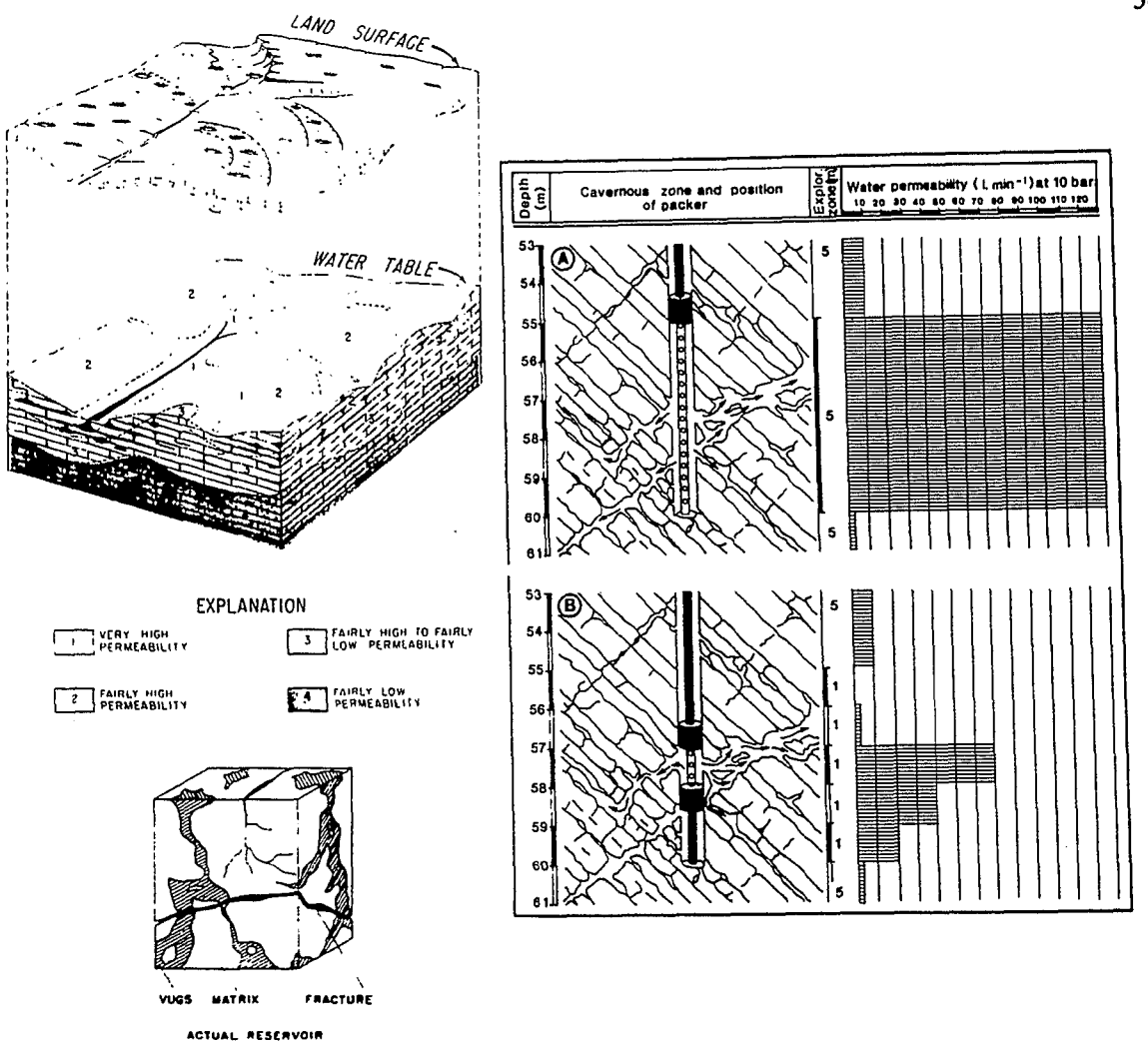

Fig. 4-17 Conceptualisation of Heterogeneities at Different Scales, a) regional (Legrand and Stringfield, 1973), b) local (Milanovic, 1981) c) laboratory (Warren et al, 1963)

regional hydraulic conductivity (K_{reg}) was first to measure average regional gradients in the south-eastern, central and north-western part of the Gallusquelle catchment during three different flow conditions, low (0.12 - 0.36 m^3/s), intermediate (0.47 - 0.99 m^3/s and high flow (1.25 - 2.66 m^3/s). Assuming that there is no more recharge to the aquifer together with a knowledge of the respective discharge and the saturated thickness, values can be calculated for T and K. Secondly, the recession coefficients α (Mail-let, 1905), derived from spring discharge measurements were used to calculate average transmissivities at different fill levels of the aquifer, using the formula developed by Rorabaugh (1964) for groundwater discharge from bank storage (further details see below).

Gradient (Darcy) approach

Fig. 4-18 shows a block diagram of the aquifer, subdivided into three different areas, a highly conductive one in the south-east, a low conductive one in the central, and an intermediately conductive one in the north-western part. The respective discharge is allocated as a fraction of the total, according to the three different surface areas. The base of the aquifer was taken from Fig. 2-17 and the saturated thickness varied according to the waterlevel in the boreholes.

Tab. 4-7 displays the results of the gradient method. The slope of the watertable was determined using the waterlevels in boreholes B7 and the spring for the south-east and that in B25 and B21 for the central region. Because of the lack of borehole information, an average regional gradient was taken from Villinger (1977) and Sauter (1990) for the north-west.

The hydraulic conductivities varied between 2 and $13*10^{-4}$ m/s for the south-east and $2*10^{-5}$ and $3*10^{-4}$ m/s for the central region. An average hydraulic conductivity of approximately $1.5*10^{-4}$ m/s was determined for the north-

Evaluation of Regional Hydraulic Conductivity

(a) (CENTRAL, LOW CONDUCTIVITY RANGE)

Width of crossection: 4500 m
Saturated thickness: related to wlevel in B25, base of permeable zone: 640 m
Throughput: 3/5 of spring discharge

	Wlevel B25 [m a.s.l.]	Wlevel B21 [m a.s.l.]	Spring discharge [m3/s]	Gradient	K [m/s]	TENTATIVE VALUES
25.11.85	669,62	718,15	0,12	0,024	0,00002	0,00002 m/s at 100 l/s
29.10.79	670,04	716,86	0,17	0,023	0,00003	
27.11.78	670,25	717,86	0,20	0,024	0,00004	"regional fissure" hydraulic conductivity
27.9.82	670,58	717,96	0,22	0,024	0,00004	(low flow conditions)
29.11.76	670,04	718,29	0,24	0,024	0,00004	
17.10.83	670,09	717,80	0,30	0,024	0,00006	
24.11.80	670,20	717,94	0,36	0,024	0,00007	
2.7.84	672,42	718,06	0,47	0,023	0,00008	0,0001 m/s at 600 l/s
31.5.82	673,07	718,32	0,55	0,023	0,00010	
5.5.80	673,66	718,22	0,60	0,022	0,00011	"mixed conduit-fissure" hydraulic conductivity
27.6.83	672,95	718,07	0,62	0,023	0,00011	(intermediate flow conditions)
16.5.77	673,58	718,63	0,65	0,023	0,00011	
7.7.86	674,49	718,54	0,73	0,022	0,00013	
30.6.86	674,70	718,52	0,79	0,022	0,00014	
5.6.78	674,07	718,34	0,99	0,022	0,00018	
28.2.77	674,19	719,66	1,23	0,023	0,00021	0,0003 m/s at 1500 l/s
5.4.82	676,03	718,54	1,57	0,021	0,00027	
3.4.78	674,67	718,54	1,57	0,022	0,00028	"mixed conduit-fissure" hydraulic conductivity
19.3.79	675,00	720,00	2,28	0,023	0,00039	(high flow conditions)
28.3.88	678,16	720,28	2,66	0,021	0,00044	

(b) (SOUTH-EASTERN, HIGH CONDUCTIVITY RANGE)

Width of crossection: 3500 m
Saturated thickness: related to wlevel in B7, basis of permeable zone: 630 m
Throughput: 5/5 of spring discharge

	Wlevel B7 [m a.s.l.]	Wlevel Spring [m a.s.l.]	Spring discharge [m3/s]	Gradient	K [m/s]	
25.11.85	657,73	640,00	0,12	0,005	0,00019	0,0002 m/s at 100 l/s
29.10.79	657,79	640,00	0,17	0,005	0,00027	
16.9.79	657,93	640,00	0,20	0,005	0,00031	"regional fissure" hydraulic conductivity
29.11.76	657,69	640,00	0,24	0,005	0,00038	(low flow conditions)
16.1.84	657,41	640,00	0,25	0,005	0,00041	
25.3.85	656,90	640,00	0,26	0,005	0,00044	
6.7.81	657,67	640,00	0,30	0,005	0,00048	
14.11.77	658,93	640,00	0,31	0,005	0,00044	
2.7.84	661,14	640,00	0,47	0,006	0,00056	0,0007 m/s at 600 l/s
31.5.82	660,97	640,00	0,55	0,006	0,00066	
27.6.83	661,36	640,00	0,62	0,006	0,00072	"mixed conduit-fissure" hydraulic conductivity
16.5.77	662,02	640,00	0,65	0,006	0,00072	(intermediate flow conditions)
7.7.86	663,02	640,00	0,73	0,007	0,00075	
5.6.78	662,55	640,00	0,99	0,006	0,00105	
17.2.80	664,97	640,00	1,15	0,007	0,00102	0,0013 m/s at 1500 l/s
28.2.77	663,18	640,00	1,23	0,007	0,00124	
12.4.82	665,73	640,00	1,58	0,007	0,00134	"mixed conduit-fissure" hydraulic conductivity
27.3.78	664,38	640,00	1,63	0,007	0,00151	(high flow conditions)
18.4.83	664,20	640,00	2,01	0,007	0,00189	
19.3.79	664,84	640,00	2,28	0,007	0,00205	
28.3.88	677,18	640,00	2,66	0,011	0,00118	

(c) (NORTH-EASTERN, LOW CONDUCTIVITY RANGE)

Width of crossection: 3500 m
Saturated thickness: 30 m at 400 l/s
Throughput: 2/5 of spring discharge

	Spring discharge [m3/s]	Gradient	K [m/s]	
(Sauter, 1991)	0,40	0,008	0,00020	"average"
(Villinger, 1979)	0,50	0,018	0,00011	"flow conditions"

Tab. 4-7 Results of Evaluation of Regional Hydraulic Conductivity (Darcy, Gradient Approach)

western region. The lower value was generally calculated during low flow conditions, which is believed to represent "regional matrix (fissured system)" hydraulic conductivity, employing double porosity terminology. The more conduits (fractures) are included at higher saturated thicknesses, the higher the resulting K_{reg}. During intermediate flow conditions, the higher permeable zone, identified in Chap. 2.6.1, is partly saturated, derived from the water level in B7 (above 660 m), and is therefore contributing to the flow. Above a level of 663 m, permeability is reduced again. As could already be expected from the information on waterlevels and aquifer geometry in Chap. 2.6., the hydraulic conductivity is lowest within the high gradient area and highest within the south-eastern area close to the spring.

The main source of error lies in the estimation of the saturated thickness. It was however not possible to use transmissivities because of prevailing unconfined conditions and because the waterlevel fluctuations (min.-max.) amount to a considerable fraction of the total saturated thickness of flow conditions of an average year.

The hydraulic conductivities obtained are a result of the varying contributions of fracture (conduit) and regional matrix system. At low flow conditions it can however be assumed that the effect of the regional fracture system is minimal because all the flow stems from the matrix blocks and that the measured gradients are mainly determined by the hydraulic conductivity of the regional fissured system (K_{regfis}). At higher flow and flood conditions the regional hydraulic conductivities are dominated by the fractures/conduits.

Evaluation of Fracture Contribution to the Hydraulic Conductivity

With a knowledge of the hydraulic conductivity of the regional fissured system (K_{regfis}), together with an estimation of the hydraulic conductivity of the total system (K_{reg}), a volume percentage of the fractures/conduits per unit volume permeable rock (%frac) can be determined (eq. 4-3, 4-4).

$$K_{reg} = K_{regfis} \, (\, 1 \, - \, \%frac \,) \, + \, K_{regcond} \cdot \%frac \qquad (4\text{-}3)$$

This approach however requires information on the hydraulic conductivity of the conduit system ($K_{regcond}$), *which can be derived from the average velocity* v_a *of tracer breakthrough curves (Chap. 4.4 and 4.5). Tracer tests with input into sinkholes selectively test only the fast flow system. The arithmetic average of the relative proportions of the two systems was used for the calculations. Because the effective porosity* (n_e) *is unity in fractures/conduits, the only unknown in the calculation of* $K_{regcond}$ *is the hydraulic gradient in the fractures/conduits. The maximum gradients likely to occur within the fractures/conduits are those of the regional fissured system/matrix and the minimum gradient is parallel to the aquifer base, derived from Fig. 2-17. Lower gradients are unlikely to occur.* The aquifer below the base level can still be assumed to be permeable but cannot contribute to the flow to a major extent because of its low permeability. With the approach described above, $K_{regcond}$ can be narrowed down to one order of magnitude.

$$K_{regcond} = \frac{v_a}{n_e} \cdot \left(\frac{\partial h}{\partial x}\right)^{-1} \qquad (4\text{-}4)$$

Tab. 4-8 lists the results of the calculation and it becomes apparent that the hydraulic conductivity of the fractures/conduits is likely to range between a few and approximately 10 m/s, depending on the gradient and the flow conditions. Correspondingly, the volume percentage of the fracture contribution to the sytem hydraulic conductivity can be estimated to range between 0.005% and 0.01%, which compares well with the conduit storage evaluated using time series of physico-chemical parameters and spring discharge (Chap. 4.2.2).

Gale (1984) analyzed the morphology of the conduit-bottom beds (e.g. scallops), composed

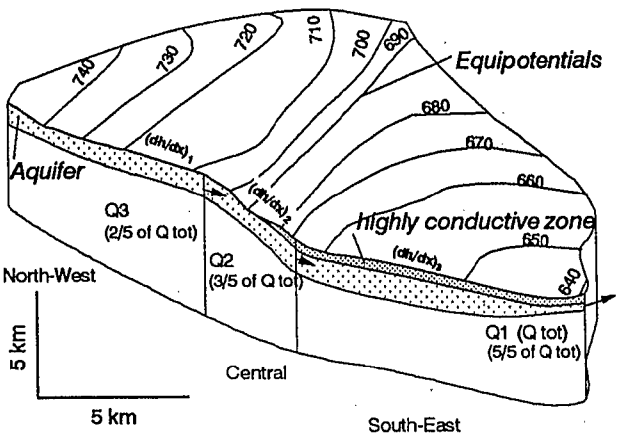

Fig. 4-18 Block Diagram of the Gallusquelle Catchment

Regional Hydraulic Parameters (Darcy Approach)

		Gradient: low (parallel aquifer base)				Gradient: high (equal to fissure gradient)			
		low	interm.	high		low	interm.	high	
	Va		110	250			110	250	
	flow:	100	600	1500	l/s	100	600	1500	l/s
South-East	K regcond:		7,6	17,4	m/s		5,1	9,9	m/s
	%frac		0,00007	0,00006	%		0,00010	0,00011	%
	K reg	0,0002	0,0007	0,0013	m/s	0,0002	0,0007	0,0013	m/s
	Gradient		0,004	0,004	-		0,006	0,007	-
Central	K regcond:		3,1	6,9	m/s		1,3	3,0	m/s
	%frac		0,00003	0,00004	%		0,00006	0,00009	%
	K reg	0,00002	0,0001	0,0003	m/s	0,00002	0,0001	0,0003	m/s
	Gradient		0,01	0,01	-		0,023	0,023	-
North-west	K regcond:				m/s				m/s
	%frac				%				%
	K reg		0,00015		m/s		0,00015		m/s
	Gradient				-				-

Tab. 4-8 Evaluation of Regional Conduit Hydraulic Conductivity (Gradient/Darcy Approach)

of hydraulically transported sediments and the solutionally developed bedforms of accessible conduit walls. The author was able to derive mean values of flow velocity and other hydraulic parameters such as boundary-shear stress, conduit Reynolds and Froude number, boundary friction factor, boundary roughness and flow power. Mean conduit flow velocities, which were partly derived from literature varied between 0.43 m/s and 0.03 m/s. The flow velocities derived from tracer tests in the study area and used for the evaluation of hydraulic conductivity (Tab. 4-8) range at the lower end of this spectrum, i.e. between 0.07 m/s and 0.03 m/s. These flow velocities are however an underestimate of the actual mean velocity in the channels and conduits, because of the tortuous nature of the flow paths. On the other hand, the karstification is much less developed in the project area than in the catchments discussed in Gale (1984). Thrailkill et al. (1991) determined flow velocities in the Inner Bluegrass Karst, Kentucky to range between 0.04 m/s and 0.16 m/s, which compare well with those determined in this study.

Baseflow Recession Method (Rorabaugh, 1964)

Rorabaugh (1964) showed that the slope of base flow recession curves of water released from bank storage after flood events plotted on a log-lin diagram (discharge - log) is proportional to aquifer diffusivity. With a knowledge of the groundwater basin geometries (L=average distance to the groundwater devide) and the storage coefficient, transmissivities and hydraulic conductivities can be evaluated according to the following eq. 4-5

$$T = \frac{\alpha \, 4 \, S \, L^2}{\pi^2} \qquad (4\text{-}5)$$

with α representing the base flow recession coefficient.

Atkinson (1977) and Trainer and Watkins (1974) successfully applied this method to evaluate regional average transmissivities for limestone aquifers. Trainer and Watkins (1974) also discussed the effects of lateral and vertical heterogeneities in the aquifer characteristics and their influence on the base flow recession. As discussed at the beginning of this chapter, horizontal variations in aquifer characteristics cannot be assumed to be detected with this method, because the dependant variable - discharge - can only be measured at one single point. However, because of the decline in water level, a recession curve reveals information on lower zones of the aquifer with decreasing discharge.

Fig. 4-19 displays the recession characteristics of the Gallusquelle groundwater catchment over two and a half years. It can be observed that the recession coefficient decreases from ca. 0.25 d^{-1} to 0.0018 d^{-1}. *It is believed that the value of 0.0018 represents the "pure fissured system" and the value of 0.25 d^{-1} the "pure conduit system" recession, because in both cases, the other flow component is negligible. The values of 0.017 d^{-1} and 0.006 d^{-1} can be assumed to be a combination of $K_{regcond}$ and K_{regfis} with varying proportions.*

The change in slope between α = 0.017 d^{-1} and α = 0.006 d^{-1} occurs synchroneously with

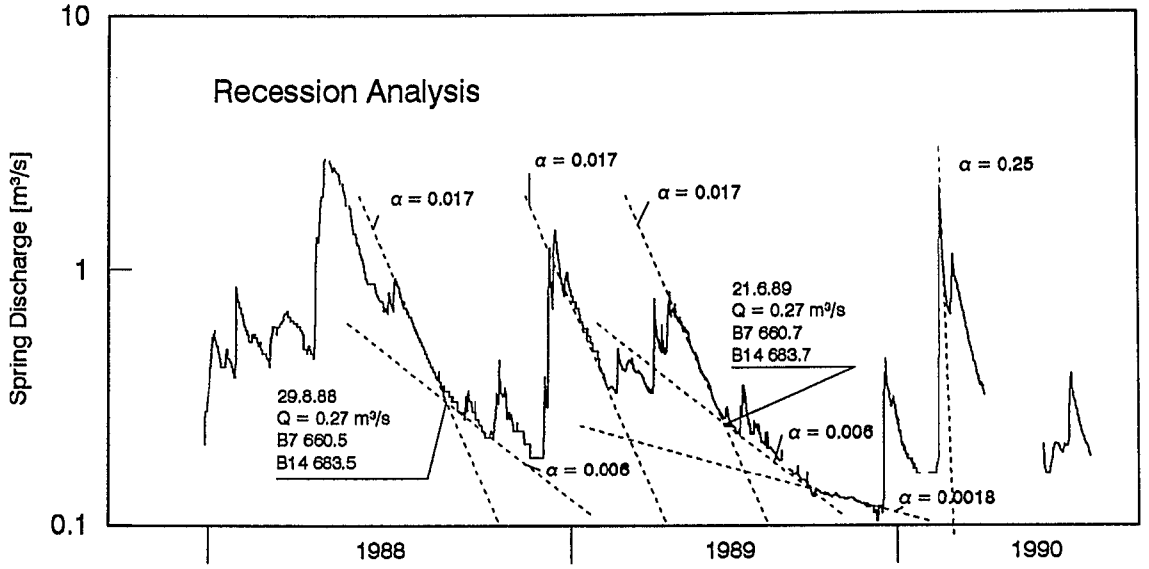

Fig. 4-19 Evaluation of Regional Hydraulic Conductivity, Recession Analysis

the water level dropping below the highly conductive horizon, identified in Chap. 2.6. during two consecutive years. It is not surprising that the increase in K is more prominent than in storage, considering the above explanation.

Tab. 4-9 summarizes the results and lists the respective hydraulic conductivities. The fissured system value of 0.0002 m/s corresponds to the fissured system value of the highly permeable south-east region, which is plausible, considering that during low flow conditions that region is dominating the flow due to its higher storage and transmissivity. Further upgradient it can be assumed that the actual permeable zone of the aquifer is completely drained. The conduit hydraulic conductivity also corresponds to values determined with the gradient method. The value for the recession coefficient was determined in February 1990 during a time period, when the contribution of the fissured system could be assumed to be negligible during initial recession. This particular event was ideal for such an evaluation because of its clean and sharp input function. The mixed values determined are about twice as high as the hydraulic conductivities determined with the gradient method. This might be caused by the fact that a fixed value of saturated thickness is used to calculate K. Transmissivities compare somewhat better. Another source for differences could be that with the gradient method, hydraulic conductivities are determined for a fixed discharge, whereas the hydraulic parameters, calculated using the recession method, apply to a range of discharges.

Summary

Combining the above results, regional hydraulic conductivities of the regional fissured system/matrix ranges between $2*10^{-5}$ m/s and $2*10^{-4}$ m/s and of the fractures/conduits ($K_{regcond}$) between approximately 2 m/s and 10 m/s. The relative proportion of the fractures/con-

Regional Hydraulic Parameters (Rorabaugh, 1964)

	Recession Constant alpha -	Storage Coeff. S -	Distance to Water Devide L [m]	Transmissivity T [m2/d]	Saturated Thickness m [m]	Hydraulic Conductivity K [m/s]
"fissures"	0,0018	0,010	11000	8,83E+02	50	0,0002
"mixed"	0,0060	0,016	11000	4,71E+03	30	0,0018
"mixed"	0,0170	0,012	11000	1,00E+04	30	0,0039
"conduits"	0,25	1	11000	1,23E+07	15	9,0

Tab. 4-9 Results of Evaluation of Regional Hydraulic Conductivity, Recession Method

duits per unit rock volume (%frac) most likely ranges between 0.005% and 0.01%.

4.3.1.2 Local Scale Tests

Local scale tests can be subdivided into an actual local scale test, in the present study a pumping test and a sublocal test, e.g slug, injection and double packer tests. This subdivision was made in order to account for the different testing radii of the different methods.

The subscripts for the parameters obtained are consistent with the regional parameters (fis, cond). On a local scale, "l" stands for local, "sl" for sublocal.

4.3.1.2.1 Pumping Tests

Only a small number of full scale pumping tests are reported (archive of the Geologisches Landesamt, Baden-Württemberg), that had been conducted in or close to the project area. The tested boreholes are usually located close to the river valleys, where most of the settlements are located. The risk is lowest to drill a dry hole (area of flow concentration close to the springs and regional outlets, encouraging solution processes) and where also the drilling costs are lowest because of the thinner unsaturated zone.

Tab. 4-10 summarizes test data of historical pumping tests, for which no time-drawdown data are available. They were therefore analyzed, using the iterative method of Walton (1970), employing eq. 4-6,

$$T^n = \frac{2.3\ Q}{2\ s} \log \left(\frac{2.25\ T^{n-1}\ t}{r_w^2\ S}\right) \qquad (4\text{-}6)$$

with s representing the steady state drawdown and t the time after the drawdown was measured. Transmissivity is not very sensitive to S and t, very sensitive however to the drawdown, which in a fractured or karstified aquifer is mainly determined by the well-loss, difficult to quantify with the information available. A storage coefficient of 0.01 and a well-loss of 60% were assumed, based on Lloyd et al. (1981) and Sauter (1981). The resulting hydraulic conductivity ranged between $4*10^{-5}$ m/s and $1*10^{-3}$ m/s, which is in the range of regional hydraulic conductivities, determined for the fissured system of the highly permeable southeastern area of the Gallusquelle catchment.

For comparison, the test results of a pumping test in compact, non-karstified limestone at Meßkirch (approx. 30 km south of the Gallusquelle) were included as well as an example of a test in a non-karstified limestone, with a hydraulic conductivity of the local fissured system of $1*10^{-6}$ m/s.

Villinger (1988) determined hydraulic parameters for a production and an observation well, drilled in the Lauchert valley near Veringenstadt (Ahlenbergquelle) and obtained hydraulic conductivities, that varied by more than an order of magnitude although the wells were only 25 m apart (Tab. 4-11). The hydraulic conductivity of the observation well corresponds to the values generally determined in valleys and that of the production well to the K of the "regional fissured system" of the central low permeable area of the catchment. The storage coefficient appears to characterize confined conditions, which is also suggested by the geological logs. The determination of S, however, was performed on the time-drawdown curve, when the water level

Pumping test evaluation (Walton, 1970, single readings)

	Q [m3/s]	t [s]	s [m]	r [m]	h [m]	K l [m/s]	Position		
Test1 (b5) Hettingen	0,0068	36000 *	22,35	0,200 *	35,4	3,8E-05	valley	welloss	60%
Test2 (b4) Hettingen	0,0360	36000 *	12,50	0,200	17,0 *	8,7E-04	valley	storage init. T	0,001 1,0E-05
Kämmerles-quelle	0,0320	36000 *	9,20	0,200 *	20,0 *	9,1E-04	valley		
Messkirch	0,0020	18000	185,00	0,175	30,0	1,2E-06			
Messkirch	0,0018	9000	180,00	0,175	30,0	9,9E-07			
Veringendorf b2,b1	0,0780	666000	1,50	5,000	20,0 *	obs.well			
Veringendorf b2,b2	0,0780	666000	56,00	0,200	20,0 *	4,1E-04	valley		

* estimated or read from map

Tab. 4-10 Evaluation of Local Hydraulic Conductivity, Pumping Tests

Pumping test evaluation - Bitz		
	K 1 [m/s]	
Jacob/Theis Recovery	3,0E-06	Skin not taken into account
Numerical homogeneous Model	6,7E-06	Skin not taken into account
Numerical Double Porosity Model	1,0E-05	

Pumping test evaluation - Veringenstadt (Villinger, 1988)		
	K 1 [m/s]	S -
Veringenstadt, Well 1	2,0E-05	0,0001
Veringenstadt, Observ. well 1	1,0E-04	?

Tab. 4-11 Results of Evaluation of Local Hydraulic Conductivity, Pumping Tests, Unsteady State

had already dropped below the base of the sealing clay (Pleistocene Lauchert lake). The storage coefficient of 0.0001 therefore more or less corresponds to the fraction of the local conduits per unit volume rock, determined in Chap. 4.3.1.1 and 4.2.2.

As indicated above, a pumping test was performed by the Landesanstalt für Umweltschutz in borehole Bitz as well and a hydraulic conductivity of $1*10^{-5}$ m/s could be evaluated, employing a double-porosity groundwater flow model (TRAFRAP-WT, Huyacorn, 1983).

The values determined by large scale pumping tests are believed to represent the hydraulic characteristics of the "regional fissured system", because their radius of influence, given a sufficiently long pumping period, is estimated in the order of several hundreds of meters using various approximations. The borehole Bitz, situated in the north-western area of the Gallusquelle catchment seems to reflect the hydraulic characteristics of the low permeability "regional fissured system" and the results from the wells in the valleys, those of the high permeability "regional fissured system".

4.3.1.2.2 Slug Tests

The low conductivity end of the spectrum, not taking into account laboratory measurements, could only be evaluated from boreholes further upgradient. Because the unsaturated thickness is very high (≈100m) and the 2.5" casing could not accommodate powerful pumps, it was impossible to conduct full scale pumping tests. Considering the low hydraulic conductivities that had to be expected within the lower part of the aquifer, tapped by the piezometers (screened 6m), and in view of the difficulty involved in assessing high well losses, it was decided to conduct slug tests. The parameters determined by slug tests and injection tests are classed as sub-local values in order to account for their smaller volume of integration.

Developments in Slug Test Analysis

There are a number of different small scale borehole hydraulic tests such as slug tests and packer tests. The data are interpreted using a variety of different analytical procedures, based on various assumptions. In order to be able to describe and quantify the tested system at the appropriate scale requires an understanding of the simplifications involved in order to be able to select the appropriate method for analysis. Here, emphasis is put on the quantification of the hydraulic parameters of a double continuum system. It is tried to highlight the advantages/disadvantages of certain methods and to point out possible errors made by choosing the inappropriate method.

In a slug test, an instantaneous change in pressure or fluid head is imposed on a well penetrating an aquifer. This change can be created by suddenly removing or adding a volume of fluid to the well. The water bearing formation can respond either by producing formation fluid or by taking up the excess fluid from the well. The response of the head, as a function of time is used for the estimation of aquifer transmissivity and borehole conditions.

In recent years, the employment of slug tests for the determination of aquifer hydraulic parameters became very popular, especially because they do not require the same organizational effort as do full scale pumping tests and they deliver rapid results especially in low permeability environments. A particularly important aspect on contaminated sites is that

no contaminated water is removed from the aquifer, thereby avoiding all ensuing problems.

Slug tests however suffer various drawbacks, to be further discussed below, including their inability to deliver reliable storage coefficients, due to the fact that no water is abstracted and that the tested volume is relatively small.

Ferris and Knowles (1954) probably first applied slug tests for the determination of aquifer transmissivity, based on the solution of Theis (1935). Cooper et al. (1967) applied the analogous solution to a heat conduction problem by Carslaw and Jaeger (1960), which included heat storage in the line source, to aquifer flow problems and developed a semilog type curve matching technique. Papadopulos et al. (1973) extended the family of type curves for higher α values. The concept of skin effect was introduced by Van Everdingen (1953) and applied to the fluid flow field in a slug test by Ramey et al. (1975). The solution by Ramey et al. (1975) is based on the previous work in the heat flow area by Jaeger (1956), which includes well storage and skin effect. Ramey et al. (1975) also looked at the radius of investigation, however without skin. Faust et al. (1984) and Moench and Hsieh (1985) further investigated the effects of a finite thickness skin in the well bore and found that the early time response is mainly dominated by the hydraulic characteristics of the skin zone and that the late time response is determined by the aquifer properties. Sageev (1986) also included well bore storage and skin effects in their solution. He examined early and late time response and came to the conclusion that up to three sets of type curves should be used for the analysis, depending on the presence of skin. By converting slug test head data to equivalent head data for a constant discharge of a well, Peres et al. (1989) made the modern procedures, used in the petroleum industry available for slug test analysis.

Widdowson et al. (1990) were able to present analytical procedures by calculating dimensionless discharge for a range of slug test geometries. The advantage of this method is that the evaluation of effective radii (R_e) and the use of match points of type curves are not required.

If inertial effects of the aquifer are important, the water level response displays a characteristic damped oscillation. Solutions for this kind of curves were presented by Krauss (1974), Van der Kamp (1976), Kipp (1985) and Kabala (1985).

In the area of soil hydrology, two methods of evaluating transmissivity from slug tests were developed by Hvorslev (1951) and by Bouwer and Rice (1976). The Hvorslev method, which

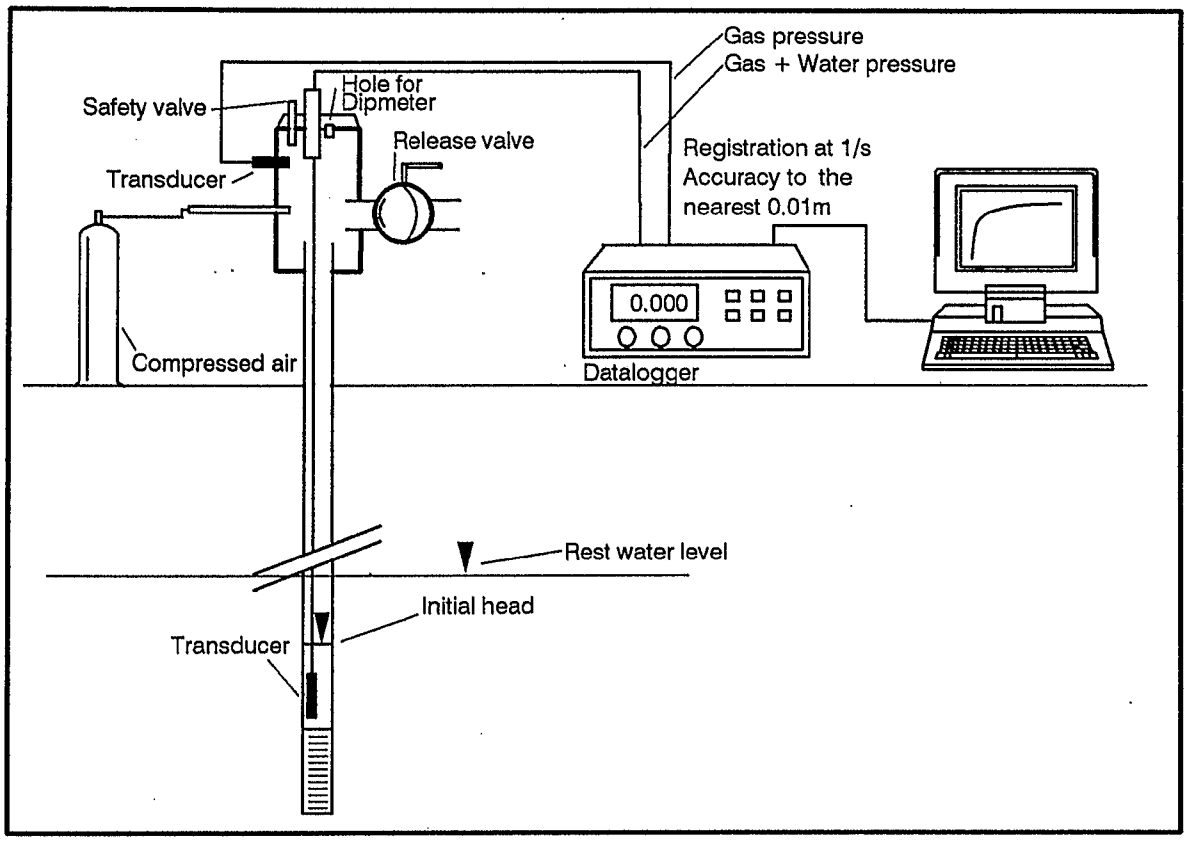

Fig. 4-20 Experimental Setup for Slug Tests

strictly only applies to point piezometers, was extended by NAVFAC (1971) and Cedergren (1977) to allow for different borehole and aquifer geometries. The Bouwer & Rice method applies to unconfined aquifer conditions and partially penetrating wells and assumes steady flow. Different flow geometries were accounted for by deriving the necessary constants, using an electrical analogue model. Both approaches are based on the equation of Thiem and do not consider compressive storage within the aquifer. Chirlin (1989) examines the effects of the violation of the above assumption. A number of computer codes were developed for a more efficient analysis (Thompson, 1987; Kemblowski and Klein, 1988).

The application of slug tests to fractured systems was investigated by Barker and Black (1983); Dougherty and Babu (1984) and Karasaki et al. (1988). Barker and Black (1983) pointed out the nonuniqueness of type curves with respect to determining reservoir parameters, apart from hydraulic conductivity and storage coefficients. The unknowns include fissure densities, apertures and the hydraulic parameters of the rock matrix.

They found that the Cooper method systematically overestimates aquifer transmissivities by a factor of up to three. This figure however applies to a fairly homogeneously fissured aquifer such as the English Chalk.

Dougherty and Babu (1984) examined in detail the effects of partial penetration, different skin factors and mass exchange coefficients in a double porosity system. They did however not present any parameter estimation solution. Karasaki et al. (1988) developed type curves for heterogeneous aquifer systems and came to the conclusion that "slug tests suffer problems of nonuniqueness to a greater extent than other well tests".

Slug Test Performance and Data Recovery

In the present study, slug tests were conducted by displacing the water within the borehole by compressed air. The experimental setup is given in Fig. 4-20. The compressed air was supplied via a tank and after the well was put under a predetermined pressure, no more air was added until equilibrium was reached between well and formation head. This could take up to 45 minutes, depending on the initial change in water column. Progress of the equilibration could be monitored with two pressure transducers, the first one was placed below the lowest expected water level, the second measured gas pressure. The compressed air within the well was allowed to suddenly escape via a large valve, which did not take longer than approximately 2 seconds, and the recovery of the water level was digitally recorded. *The tests were repeated at several different pressures in order to test the dependance of the test on the particular conditions of the well (Streltsova, 1988, p. 367). The base data for the tests are given in Tab. 4-12.*

Estimation of Hydraulic Parameters from the Test Data

Apart from the tests in well B7, all the tests produced recovery curves that could be expected to be analyzed by commonly available methods. The tests in B7 exhibited an initial rapid increase up to 20% of the initial displacement. The observed deviation can be attributed to either a rapid drainage of the gravelpack or a highly permeable zone, surrounding the well. At the depths of 134 and 137 m two large fractures (aperture 1 cm), plugged with residual loam, were observed during drilling, which could also be responsible for the rapid initial flow.

The approach taken in the analysis of the tests was, to firstly apply well established methods of analysis, considering also the effect of partial penetration, and secondly to compare the results with those of a numerical model, capable of incorporating double porosity effects and complex boundary conditions. The numerical model also allows to test the results for the relative importance of various parameters and boundary conditions. Examples are presented for the tests in borehole B8 (Fig. 4-21), because they display also the effects of the double porosity system. The other results are presented in App. 4-4. All results, including those of the numerical model are compiled in Tab. 4-13.

The data obtained from the various tests were first analyzed for homogeneous aquifer conditions using the Cooper et al. (1967) method. Reasonable fits could be obtained for all tests, apart from B7, from about $H/H_0 = 0.6$ down to $H/H_0 = 0.1$. At the beginning, the measured curve systematically stays below the theoretical one, towards the end of the tests, the drawdown within the aquifer might not be negligible anymore; the Cooper method only applies to confined conditions, whereas the tests were conducted in an unconfined aquifer.

The deviation from the theoretical curve is generally larger, the larger the initial displa-

cement, and the values of hydraulic conductivity obtained are higher, the larger the displacement. These features will be discussed in a final analysis of the tests. The values (Tab. 4-13) varied from $1*10^{-4}$ to $1.3*10^{-5}$ m/s; storage coefficients were not determined because they were totally unrealistic, which might be due to the fact, that hardly any water is withdrawn from the aquifer. Barker and Black (1983) also point out that they are usually a gross underestimate, even by a factor of 10^6.

The same data were also analyzed with the method presented by Ramey (1975) and the fit appeared to be somewhat better, with however the same problems, concerning early and late data, as observed before. The results obtained did not vary as extremely as with the Cooper method and all the curves revealed positive skin factors. The variations within the skin factors cannot be considered as significant, because the type curves have a fairly similar shape within the range where the match was obtained. The hydraulic conductivity varied between $1*10^{-5}$ and $6*10^{-5}$ m/s, the skin factors between 4 and 45.

Dougherty and Babu (1984) presented a sensitivity analysis of the effect of inner boundary conditions as there are, well storage, skin effect and partial penetration and also the effect of a different aquifer model, i.e. a double porosity system, by varying the matrix-fracture exchange coefficient. Well storage and skin effect are accounted for by the Ramey method. The neglect of partial penetration tends to overestimate hydraulic conductivity by a factor of about 6 - 7, assuming that only a quarter of the aquifer thickness is open to the well, which is probably the case in the tested aquifer.

The data were therefore analyzed with the procedure described by Bouwer and Rice (1976) and Bouwer (1989) and outlined in the previous section. The data are plotted on a semilogarithmic scale with the time on the linear axis. A straight line is drawn through the data points (slope: $1/t \ln (y_o / y_t)$) and the hydraulic conductivity is evaluated with the following formula

$$K = \frac{r_c^2 \ln (R_e / r_w)}{2 L} \frac{1}{t} \ln (\frac{y_0}{y_t}) \qquad (4\text{-}7)$$

with

$$\ln (R_e / r_w) = [\frac{1.1}{\ln (H / r_w)} + \frac{C}{L / r_w}]^{-1} \qquad (4\text{-}8)$$

whereby r_c and r_w are the radii of casing and borehole, L stands for the length of the tested section, H for the aquifer thickness and C represents a geometrical factor for well-aquifer geometry taken from a diagram, based on evaluation of various geometries using an electrical analogue.

The tests in boreholes B8 and B7 were corrected for the initial rapid increase, which is assumed to be caused by the fast drainage of the highly permeable area immediately surrounding the well (Bouwer, 1989). By evaluating the volume of water that suddenly entered the well, an equivalent corrected casing radius can be calculated for the initial head (eq. 4-9).

$$r_{ck}^2 = \frac{V_{sud}}{\pi h_{ic}} + r_w^2 \qquad (4\text{-}9)$$

with r_{ck} as the corrected casing radius, V_{sud} the volume of water that was suddenly drained and h_{ic} the new corrected initial head. The data for the tests in B8 and B7, where this initial drop was most significant are given in Tab. 4-14. The hydraulic conductivities, evaluated with the Bouwer and Rice method (Tab. 4-13) were as

Test Data (Slugtests)

well	B7	B8	B14	B25	B17	Unit
r c (casing radius)	0,034	0,034	0,034	0,034	0,034	m
r w (borehole radius)	0,055	0,055	0,055	0,055	0,055	m
surface level	770,71	759,92	782,09			m asl
screened section	139-142 m	125-131 m	154-160 m	118-124 m	113-119 m	m bgl
rest water level						
test 1	660,92	662,25			660,92	m asl
test 2	660,92	662,25			660,92	m asl
test 3	660,92	662,25	687,14		660,92	m asl
test 4			684,96		660,92	m asl
test 5			684,96			m asl
test 6			684,96			m asl

Tab. 4-12 Base Data for Slug Tests

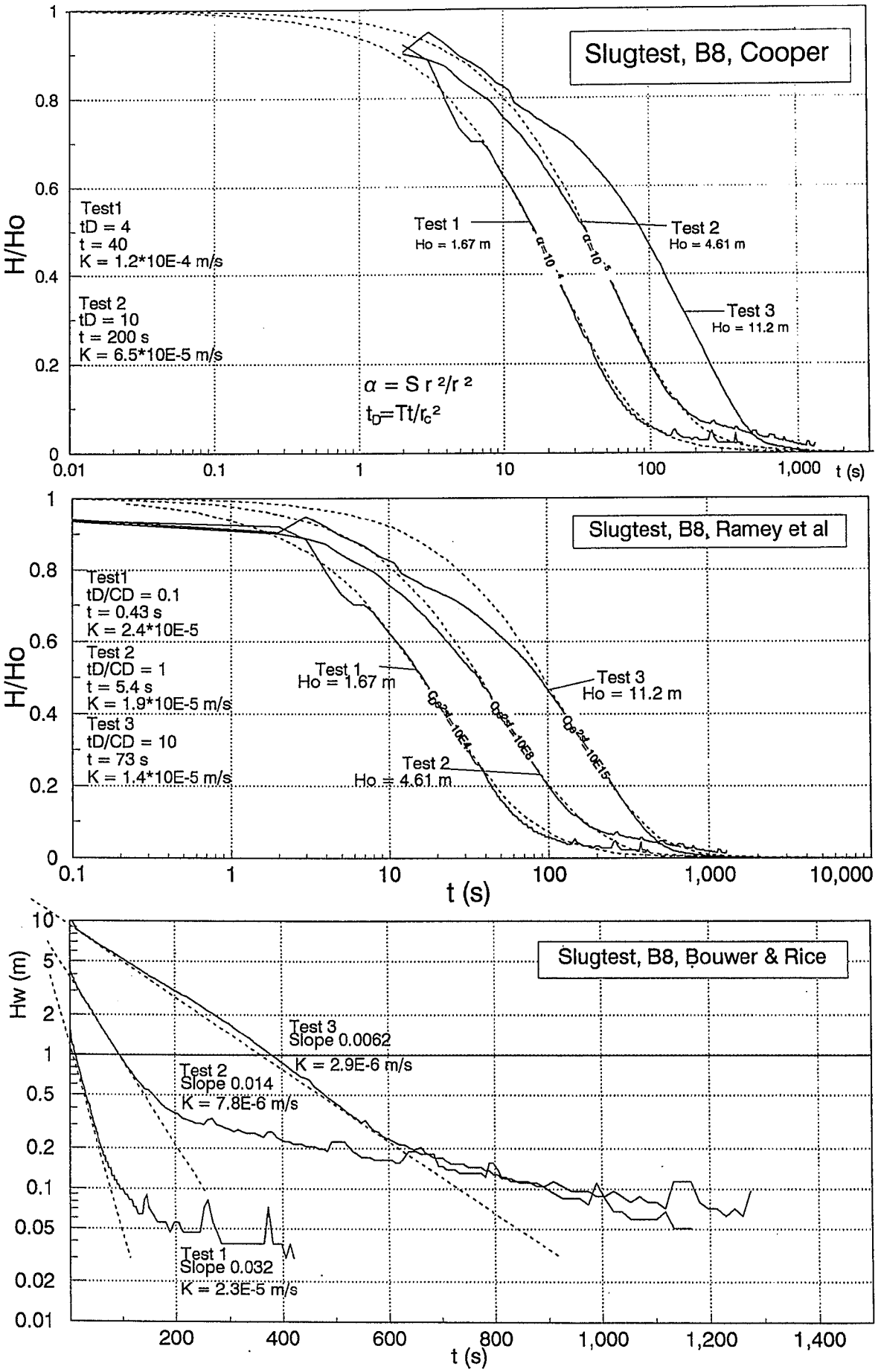

Fig. 4-21 Slug Test Evaluation Using Type Curve Matching and Analytical Approaches (B8)

Slugtest Results HYDRAULIC CONDUCTIVITIES (Summary)

well diameter: 0.11m
tested section: 6 m
casing diameter: 0.07 m

Well	B7			B8			Unit
Test	Test 1	Test 2	Test 3	Test 1	Test 2	Test 3	
Displacement [m]	1	2,76	7,35	1,67	4,61	11,2	m
K sl (Cooper, 1967)			3,7E-05	1,2E-04	6,5E-05	bad fit	m/s
K sl (Ramey et al, 1975)			1,2E-05	2,4E-05	1,9E-05	1,4E-05	m/s
CDe-2SF			1E+15	1E+04	1E+08	1E+15	
SF (CD=1/2S=25)			17	4	9	17	
K sl (Bouwer et al, 1973)	2,2E-06	1,3E-06	1,8E-06	2,3E-05	7,8E-06	2,9E-06	m/s
Model Results (TRAFRAP-WT, Huyacorn, 1983)							
K slcond			2,2E-03	1,2E-02	4,0E-03	2,2E-03	m/s
% frac			0,0025	0,0025	0,0025	0,0025	
K slfis			1,0E-06	5,0E-06	3,0E-06	1,0E-09	m/s
Skin (interporosity)			1E+06				
K sl (conduits+fissures)			5,0E-06	3,0E-05	1,0E-05	5,0E-06	m/s

Well	B14					B17				
Test	Test 1	Test 3	Test 4	Test 5	Test 6	Test 1	Test 2	Test 3	Test 4	
Displacement [m]	2,69	2,25	1,33	6,51	3,65	1,1	2,9	6,95	8,74	m
K sl (Cooper, 1967)	2,2E-05	1,3E-05	2,6E-05	1,6E-05	1,5E-05	6,0E-05	7,8E-05	3,2E-05	3,2E-05	m/s
K sl (Ramey et al, 1975)	2,4E-05	1,6E-05	1,9E-05	1,4E-05	1,3E-05	5,7E-05	4,6E-05	4,1E-05	4,1E-05	m/s
CDe-2SF	1E+40	1E+35	1E+35	1E+35	1E+35	1E+40	1E+40	1E+40	1E+40	
SF (CD=1/2S=25)	45	40	40	40	40	45	45	45	45	
K sl (Bouwer et al, 1973)	1,2E-06	2,2E-06	1,8E-06	1,4E-06	1,6E-06	1,8E-05	4,2E-06	3,8E-06	3,7E-06	m/s
Model Results (TRAFRAP-WT, Huyacorn, 1983)										
K slcond				1,1E-03	1,2E-03	3,9E-03	3,9E-03	3,0E-03	3,0E-03	m/s
% frac				0,0025	0,0025	0,0025	0,0025	0,0025	0,0025	
K slfis				1,0E-09	1,0E-09	1,0E-09	1,0E-09	1,0E-09	1,0E-09	m/s
Skin (interporosity)				5E+08	2E+07	5E+08	5E+08	1E+08	1E+08	
K sl (conduits+fissures)				3,0E-06	3,0E-06	1,0E-05	1,0E-05	7,0E-06	7,0E-06	m/s

Tab. 4-13 Summary of Results from Slug Tests

expected much lower and varied from $1*10^{-6}$ to $2*10^{-5}$ m/s.

Dougherty and Babu (1984) also investigated the effects of a decrease in the matrix - fracture exchange coefficient λ by decreasing λ. The field data curves tend to be steeper near the inflection point (H/H_o - lin tD/C_D). Therefore, if the Cooper or Ramey type curves are used, and the early time data are considered less important (well storage, skin, partial penetration), the hydraulic conductivity is underestimated.

In order to be able to account for the geometry of the well and its boundary condition, a numerical finite element model (double porosity) was used to simulate the recovery data (TRAFRAP-WT, Huyacorn, 1983). The fluid exchange between fractures and matrix can be modelled as transient flow (de Swaan, 1976) and a skin surrounding the matrix blocks (interporosity skin) is integrated as well (Moench, 1984). As will be demonstrated below, a pseudo-steady state matrix to fissure flow (Barenblatt et al., 1960) frequently represents the field data better, which can be achieved by setting the skin around the matrix blocks to a high value. The model also allows the choice of spherical, prismatic or arbitrary shaped matrix blocks. For the present model, slab shaped matrix blocks were chosen.

The rectangular finite element model grid is given in Fig. 4-22. The model consists of 8 nodal rows and 13 nodal columns, i.e. 84 elements. The well was represented with a storage coefficient of 1.0 and a high hydraulic conductivity of 10 m/s and the unperforated steel casing by a very low hydraulic conductivity (10^{-10} m/s). The extreme gradients and the enormous difference between the hydraulic conductivities caused some problems with stability of the solution. Therefore, the area next to the well was finely discretised, to allow a gradual change of the hydraulic parameters, which resolved stability problems. Next to the well, a high

permeability zone was included as well, corresponding to the gravel pack. This feature was hoped to help with the simulation of some observed fast initial recoveries, as observed in well B7.

The slug tests were modelled by setting the head in the well area to the lowered test water level (no gradient within the well) and calculating the head distribution within the modelled area at time steps, starting with 1 s and gradually increasing the interval by multiplying the previous interval by 1.025.

Results of the Model Simulations and Sensitivity Analysis

The important calibrated model parameters are given in Tab. 4-13. The model results vary for the tests with the highest initial displacement within a very narrow range, i.e. hydraulic conductivities between $0.3*10^{-5}$ m/s (B14) and $0.7*10^{-5}$ m/s (B17). The fit between model and field data is generally very good (Fig. 4-23, App. 4-5). Initial fluctuations of the test data could be either caused by the system itself that reacts underdamped or by the test procedure. The compressed air requires a finite time to escape and a standing wave might develop with compression and decompression cycles. It was not attempted to optimize test B7_3 any further, because there are numerous variables, especially unknown geometry that causes an initial fast recovery. Fig. 4-23 shows in principle how a fit can be obtained between field data and model data. In this particular case, the annulus was simulated with a very high hydraulic conductivity.

Test data for slug test B8_3, during which the double porosity became fairly prominent, is displayed in Fig. 4-23. In order to simulate pseudo-steady state flow between matrix and fracture, the interporosity skin (Moench, 1984) was set to a high value (B14, B17). Most of the tests could be simulated without having to add any noticable matrix contribution ($K_m = 1*10^{-9}$ m/s). Only in tests B8_1 and B8_2, where the initial displacement was lower and where the double porosity effects were detected, higher K_{slfis}-values (sub-local fissured system (matrix) hydraulic conductivity) were used to improve the fit at early and late times. K_{slcond} (sub-local conduit (fracture) hydraulic conductivity) and %frac (the volume percentage of the conduits per unit rock volume) are interrelated, i.e. their product has to be the same, which is the continuum hydraulic conductivity of the fractured system.

A sensitivity analysis was conducted of the calibrated test results of B8_3, which reveal double porosity effects (Fig. 4-24). The model runs were plotted on a lin-log scale. Then a shift parallel to the time axis translates directly to a change in hydraulic conductivity. A curve further to the right means a lower hydraulic conductivity. The dominant parameter is obviously the sublocal conduit (fracture) hydraulic conductivity. A skin, if present can also have a major effect on the test data. In none of the tests was it necessary to use a borehole skin to improve the fit; which however does not ex-

Slugtest Evaluation (Bouwer & Rice, 1973)

		B 8						B7					
	Unit	Test 3	Test 3e	Test 2	Test 2e	Test 1	Test 1e	Test 3e	Test 3	Test 2e	Test 2	Test 1e	Test 1
L	m	6	6	6	6	6	6	6	6	6	6	6	6
H	m	30	30	30	30	30	30	30	30	30	30	30	30
rw	m	0,055	0,055	0,055	0,055	0,055	0,055	0,055	0,055	0,055	0,055	0,055	0,055
rc	m	0,035	0,041	0,035	0,038	0,035	0,043	0,083	0,035	0,075	0,035	0,097	0,035
D	m	30	30	30	30	30	30	30	30	30	30	30	30
L/rw		109,1	109,1	109,1	109,1	109,1	109,1	109,1	109,1	109,1	109,1	109,1	109,1
A		4,5	4,5	4,5	4,5	4,5	4,5	4,5	4,5	4,5	4,5	4,5	4,5
B		0,75	0,75	0,75	0,75	0,75	0,75	0,75	0,75	0,75	0,75	0,75	0,75
C		4,2	4,2	4,2	4,2	4,2	4,2	4,2	4,2	4,2	4,2	4,2	4,2
ln(Re/rw) D=H		4,694	4,694	4,694	4,694	4,694	4,694	4,694	4,694	4,694	4,694	4,694	4,694
Slope ln(Yo/Yt)/t		0,004	0,004	0,014	0,014	0,032	0,032	0,001	0,003	0,001	0,002	0,001	0,003
K sl	m/s	2,1E-06	2,9E-06	6,6E-06	7,8E-06	1,6E-05	2,3E-05	1,8E-06	1,5E-06	1,3E-06	1,1E-06	2,2E-06	1,5E-06

Extension: "e" : corrected, effective, casing radius

Tab. 4-14 Effect of Correction of Effective Well Radius on the Results From Slug Tests

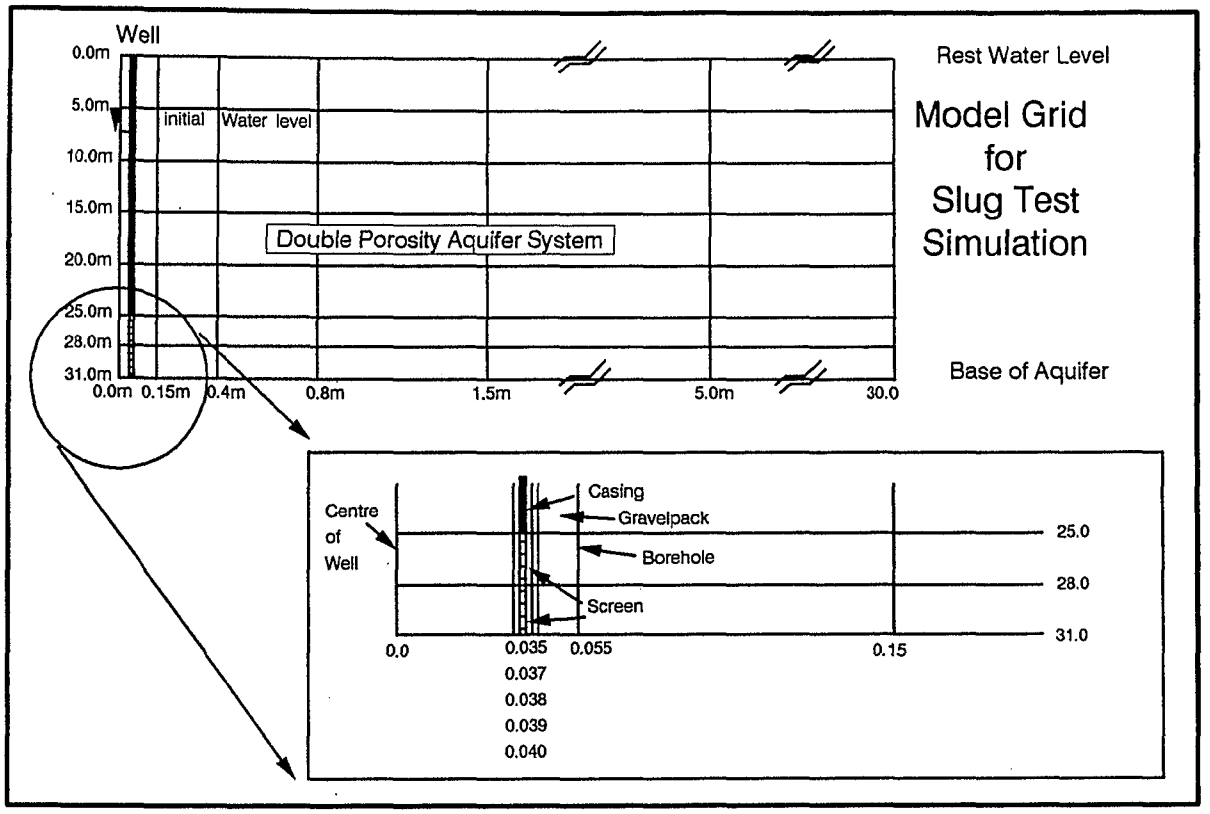

Fig. 4-22 Model Grid Used for Slug Test Simulation

clude the presence of such a low/high permeability zone either. A skin generally delays the initial drop/recovery of the water level and tends to steepen the curve. According to Hawkins (1956) the skin factor s_f is defined as (eq. 4-10), with K_{sl} and K_{Skin} as the hydraulic conductivities of total sub-local system (matrix + fractures) and skin zone and r_{Skin} and r_w as the radius of the skin zone and the borehole, measured from the centre of the borehole.

$$s_f = \left(\frac{K_{sl}}{K_{Skin}} - 1\right) \cdot \ln\frac{r_{Skin}}{r_w} \qquad (4\text{-}10)$$

It was avoided to use too many fitting parameters in order to optimize the model/field data fit. In order to demonstrate the effect of a highly permeable matrix, K_m was varied as well. A decrease of the hydraulic conductivity of the matrix to a tenth of the calibrated value still has a noticable effect, if matrix hydraulic conductivity is increased by a factor of 10^3 and 10^5, the hydraulic conductivity of the matrix becomes dominant over that of the fractured system. A variation of the interporosity skin is shown in Fig 4-24, although not applicable to test B8_3, because of the low K_{slfis} value, used for calibration. The interporosity skin (s_{ip}) (Moench, 1984) is defined as in eq. 4-11, with K_{slfis} and b_{slfis} as the hydraulic conductivity of the matrix blocks and the distance from the centre of the matrix block to the fracture and b_{Skin} the thickness of the skin.

$$s_{ip} = \frac{K_{slfis} b_{skin}}{K_{Skin} b_{slfis}} \qquad (4\text{-}11)$$

A variation in matrix block size and in storage coefficient of the matrix and the fractures does not have a marked effect on the hydraulic conductivity of the total system.

Radius of Influence and Effect of Displacement Depth

In trying to assess how representative the above tests are for the aquifer in question and to assist in allocating an appropriate scale of investigation to slug tests, it is important to determine a radius of influence. Ramey (1975) and Sageev (1986) investigated the radius of influence of slug tests and developed appropriate diagrams. A critical parameter in this assessment is the scale of resolution of the recovery measurements, which however can be easily dealt with by using pressure transducer readings. For resolutions of H/H_o (relative residual head) < 0.01 and a C_D value (dimen-

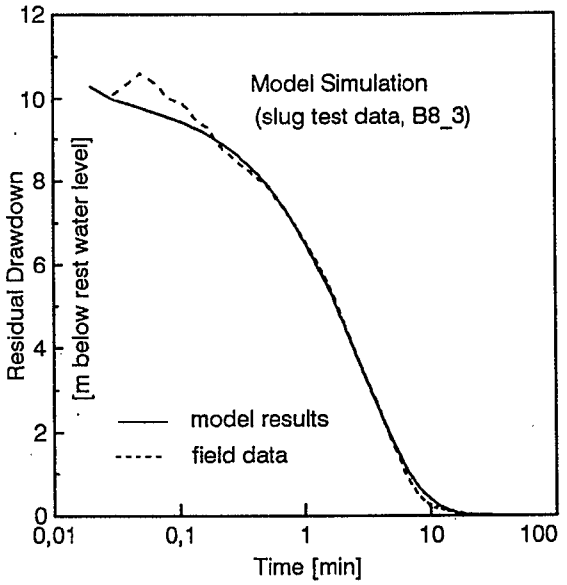

Fig. 4-23 Comparison Between Field and Model Data for Slug Test B8_3

sionless well storage) of 100 (to which the result is not very sensitive), *the radius of investigation is 1000 times that of the well radius, i.e. approximately 10 - 20 m.*

It was mentioned earlier on that the hydraulic conductivity of the tests is dependant on the displacement depth, i.e. the duration of the test. This feature, which is attributed to the heterogeneous characteristics of the matrix/fracture system, has also been described by Streltsova (1988), who observed it whenever "the formation volume, influenced by the test is smaller than the representative formation volume required for fracture pattern replication" (p.366). The following conceptual model might explain this hydraulic behaviour. If the well is drilled within a compact matrix block, the hydraulic response of an aquifer section is mainly determined by the low matrix conductivity near the well. If however the well is connected to the fracture network, short tests will only excite the highly conductive fractures, and the longer the duration of the test, the more will the less conductive fractures and matrix contribute to the test result. Therefore a systematic decrease in the hydraulic conductivity obtained with increasing test duration (displacement), can be observed. K can be assumed to tend towards an asymptotic value.

4.3.1.2.3 Injection Tests

Slug tests suffer certain limitations; their radius of influence is fairly moderate due to the small volume of water displaced during the test. Therefore, and in order to crosscheck the slug test results, injection tests (Lugeon or borehole recharge tests) were conducted as well, whereby the injected rate was kept constant and it was attempted to obtain steady state conditions.

Methods Available for the Evaluation of Injection Tests

The most widely used methods, which are based on the work of Dupuit (1863) and Thiem (1906) such as the formula according to the U.S. Bureau of Reclamation (1963), generally assume a homogeneous and isotropic aquifer and also steady state conditions. In case steady state conditions cannot be achieved, the usual pumping test evaluation methods (Krusemann and de Ridder, 1990) can be applied, which however also assume a homogeneous and isotropic aquifer. When dealing with fractured media and if skin and well storage become important, the above methods generally fail.

Since the early seventies, substantial progress has been made within the area of reservoir engineering in the evaluation of hydraulic tests for the hydraulic characteristics of oil reservoirs. A detailed review of the approach taken for evaluation is presented by Gringarten (1982). The paper describes, how the theoretical models are constructed, which are composed of the aquifer model (homogeneous - heterogeneous, confined - unconfined) itself and inner (well, i.e. skin, well storage, partial penetration etc.) and outer (impermeable, recharge boundary) boundary conditions and how type curves are developed. The Theis (1935) method is a special case of such a model without inner and outer boundary conditions, applicable to a homogeneous, confined aquifer.

There are two types of plots that are used for flow test evaluation, a specialized and a diagnostic plot. A specialized plot is specific to a given flow regime, i.e. the test data plot on a straight line, when particular flow regimes prevail. Well bore storage is for example revealed on a plot of lin Δh (head) versus lin Δt (time) and also when log Δh is plotted against log Δt. Because of the fact that during well bore storage flow regime the head change is proportional to the change in time that particular regime is revealed as a straight line of slope 1 in both plots. The specialized plot can be used for parameter estimation; the Horner or Theis recovery plot, where the head change (lin) is plotted against the logarithm of a dimensionless time function, the radial flow regime is charac-

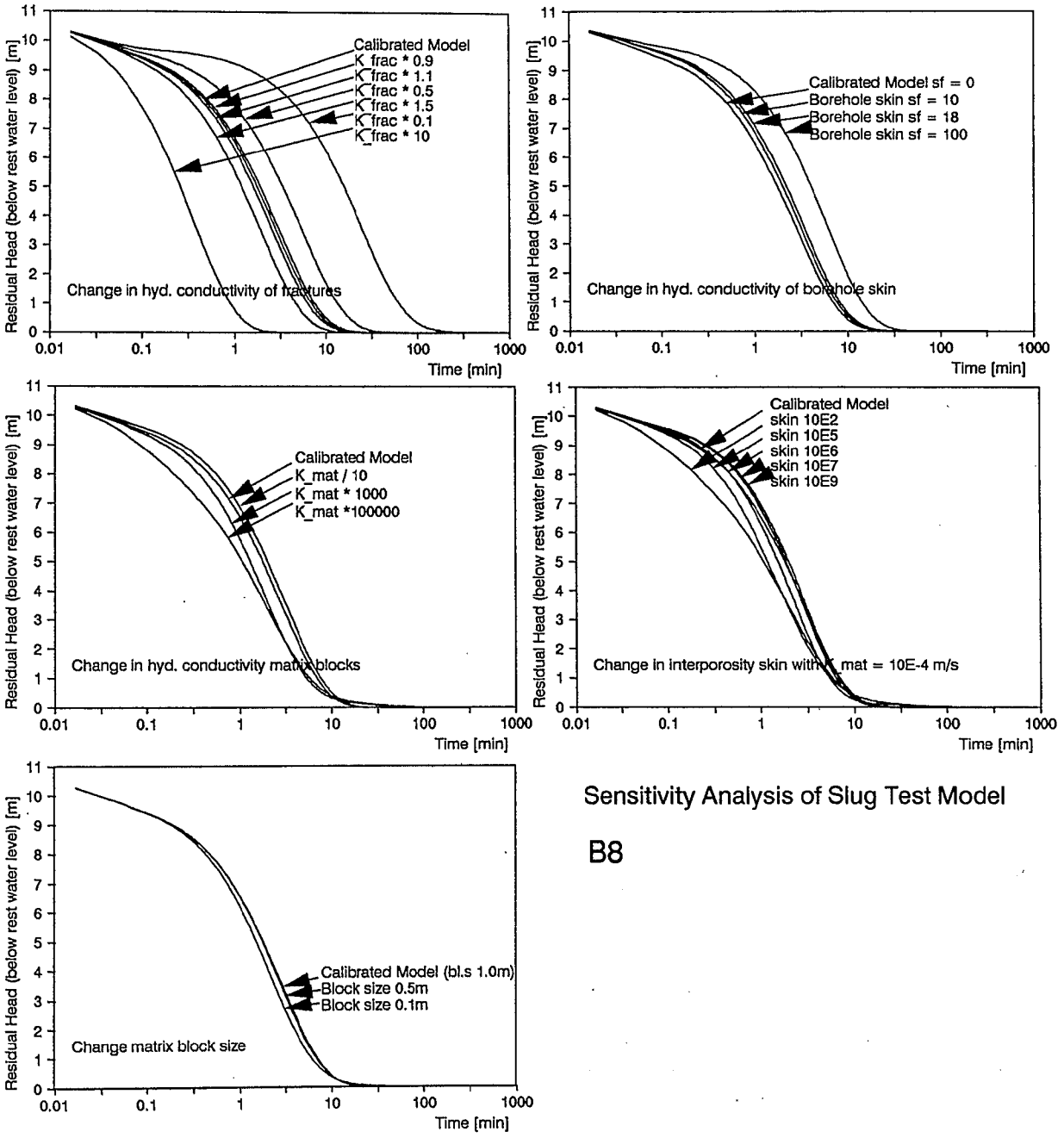

Fig. 4-24 Sensitivity Analysis of Slug Test Model

terized by the straight line period. A number of other flow geometries and fracture flow can be evaluated by the following plots:

Δh *vs* $\sqrt{\Delta t}$ (high conductivity fracture, half unit slope, Gringarten et al. 1975) (4-12)

Δh *vs* $\sqrt[4]{\Delta t}$ (low conductivity fracture, one-fourth slope, Cinco and Samaniego, 1978) (4-13)

Δh *vs* $1/\sqrt{\Delta t}$ (spherical flow, Moran and Finklea, 1962) (4-14)

Δh *vs* Δt (pseudo steady state flow, Jones, 1956) (4-15)

Karasaki et al. (1985) published a model that is composed of a finite linear flow area surrounding the well and an outer radial flow region. The model can be used to find the extent and the flow parameters of the fractures near the well and average values for the entire sys-

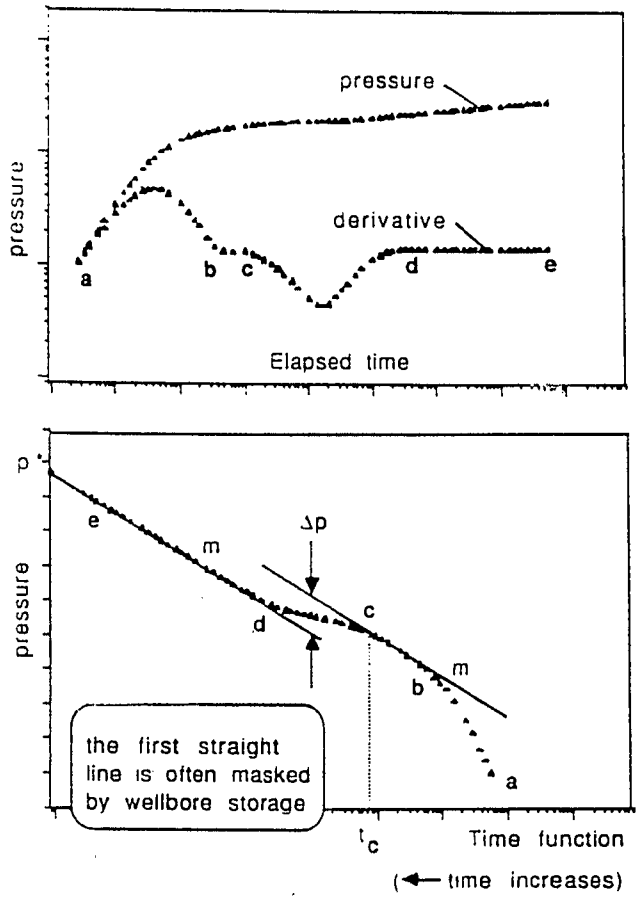

Fig. 4-25 Build-up Pressure Response of a Double Porosity Reservoir in a Diagnostic and Specialized Plot (Leach, 1990, Schlumberger)

tem.

The diagnostic plot is a log - log plot that allows the identification of the various flow regimes, which plot as straight lines on specialized plots. By superposition of the log-log behaviour of every component of the model (basic model, inner and outer boundary conditions) a type curve is obtained, representing the particular theoretical model, which can then be used for parameter identification. However, the type curve matching procedure suffers one drawback; particularly in wells with high well bore storage and dominant skin, the type curves are very similar, so that a unique match is almost impossible. It was therefore suggested by Bourdet et al. (1983a) to use not only the head change, but also the differential of the head change for the type curves, which is much more sensitive to different flow regimes. The above paper deals with homogeneous reservoirs, whereas Bourdet et al. (1983b) and Alagoa et al. (1985) treat double porosity reservoirs and fractured well tests respectively. The double porosity approach assumes two overlapping continua, one representing the fractured and the other the matrix, low permeability system. They are both connected by an exchange term and the flow between them is controlled by the head. For a detailed review of the double porosity approach, the reader is referred to Streltsova (1988), Sauveplane (1984) and Teutsch (1988).

Because of its applicability to the tests performed, the double porosity model is discussed in detail.

When water is withdrawn or injected via a well into a double porosity system, only the highly conductive fracture system is activated first, the low permeability matrix does not respond as quickly and therefore does not contribute to the flow during early times. Finally, after a differential head has been established between fracture and matrix, the matrix blocks contribute a significant flow proportion. When the head slowly equilibrates between fractures and matrix, no heterogeneity in head distribution can be measured anymore within the aquifer. Therefore, the hydraulic response of a double porosity system can be devided into three typical flow regimes, an initial flow, characterizing the fractured system, a transition period, when matrix and fracture systems contribute to the hydraulic response and finally a homogeneous behaviour, describing the entire system.

The heterogeneous nature of the aquifer can be described by two parameters (eq. 16 and eq. 17, Warren and Root, 1963), where ω is the ratio of the storage coefficient of the fractured system, λ the interporosity pseudo-steady-state flow parameter, α a geometric factor of the matrix block shape (m^{-2}) and r_w the well radius.

$$\omega = \frac{S_f}{S_f + S_m} \tag{4-16}$$

$$\lambda = \alpha r_w^2 \frac{K_m}{K_f} \tag{4-17}$$

Subscripts "m" and "f" represent the matrix and the fracture parameters. Fig. 4-25 a,b dissect the head (pressure) response of a double porosity system (by Dr. Leach, unpubl. material, Schlumberger, The Hague), by using a diagnostic (Fig. 4-25 a) and a specialized plot (Fig. 4-25 b). From time a to b, the response is mainly dominated by the well storage (straight line, slope 1 in diagnostic plot) and during period bc, which is frequently camouflaged by long lasting

well storage effects, radial flow within the fractured system is established (straight line in the specialized and constant derivative in the diagnostic plot). The transition period can be described by a decrease in the derivative values and during the transition, the pressure (head) curve follows one of the λe^{-2S} (S = skin factor) curves (Fig. 4-26a). These typecurves were developed by Bourdet and Gringarten (1980). When finally homogeneous conditions across the whole reservoir are established and radial flow conditions prevail, the specialized plot (Horner plot) reveals a straight line, the derivative is constant, and the pressure (head) curve characterizes the flow behaviour of the whole system. Fig. 4-26b represents an application of the above type curves and displays well test data of a fractured oil reservoir. t_D/C_D represents the dimensionless time variable and p_{tD} the dimensionless pressure of the type curve.

The advantage of the head derivative curve is that it helps to obtain a unique match of the data with the type curves due to its high sensitivity to the various parameters. The numerical values of different sections of the type curves and the values Δp, m and t_c of the specialized plot are used for parameter evaluation, i.e. T, S, ω, and λ.

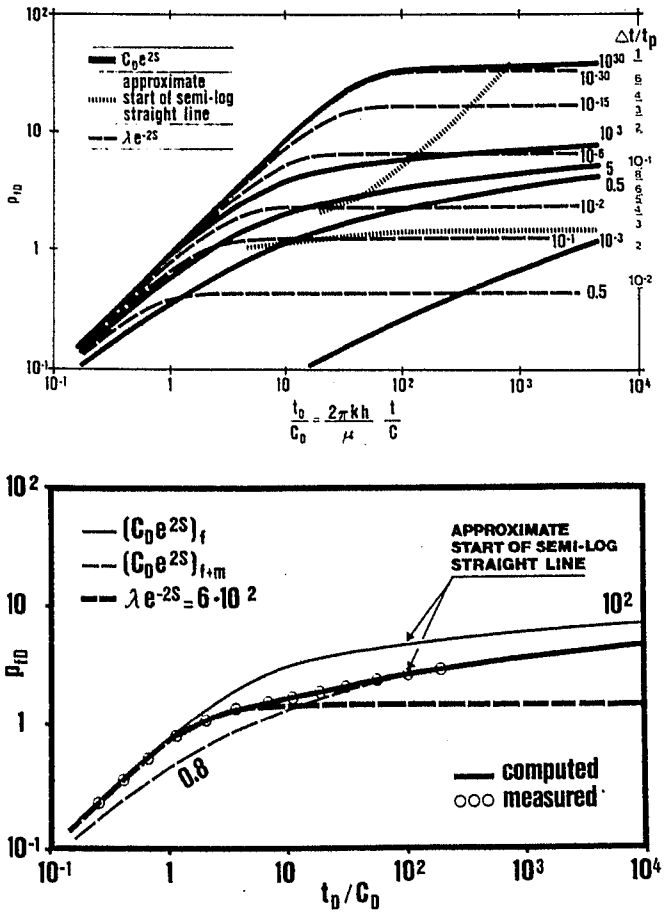

Fig. 4-26 Log-Log Type Curves for a Well in a Double-Porosity Fractured Reservoir (a) and Well Test Data (b) (Bourdet et al, 1980)

Performance of Injection Tests and Data Recovery

Two kinds of injection tests were used for parameter estimation. The first ones, conducted within the context of the study consisted of the injection of water into cased boreholes (B7, B25, B14, B8) with a screened section at the bottom of the hole of approximately 6 m (oral communication, Dr. Koerner, Geol. Landesamt Baden Württemberg, also checked with borehole temperature logs). The test data are given in Tab. 4-15 and the head change vs time in Fig. 4-27. Steady state conditions could be achieved for tests B8 and B25, the tests in wells B14 and B7 however failed to deliver reliable results, because the head build up during the injection phase was extremely rapid, although the hydraulic conductivities from all the slug tests were in the same order of magnitude for all tests. This behaviour is attributed to the clogging of the permeable parts of the formation as a result of the reversed flow direction into the formation.

In order to circumvent the inconsistencies in flow during the injection phase, only the recovery period was used for analysis. As will be discussed in the next chapter, some interference between the water running down the side of the casing (100m) after injection ceased and the decline of the head could be detected. The interference becomes apparent, when the velocity of the water seeping down the casing is higher than the head change per time and results in a slight peak or a delay in the head drop.

The second kind of test are double packer tests in an uncased hole near the village Bitz (unpublished data, Mr. Straßburger, Landesanstalt für Umweltschutz, Karlsruhe), investigating vertical hydraulic conductivity distribution. The profile within the saturated zone was not complete because of packer leakage and therefore did not sample the sections with high hydraulic conductivities.

The Deutsche Bundesbahn also kindly gave permission to use their data from double-packer tests, performed in a series of boreholes in the eastern Swabian Alb, drilled for investigatory purposes for a planned tunneling project.

Test Data (Injection Tests)						
well	B7	B8	B14	B25	B17	Unit
r c (casing radius)	0,034	0,034	0,034	0,034	0,034	m
r w (borehole radius)	0,055	0,055	0,055	0,055	0,055	m
Injection Rate	0,5	1,3	1,5	1,4		l/s
Injection Head	42	13,8	45	14,3		m

Tab. 4-15 Base Data of Injection Tests

Test Results and Hydraulic Parameters of Tests B7, B8, B14 and B25

The test results, using various methods are summarized in Tab. 4-16.

The tests in boreholes B7, B8, B14, B25 were analyzed first using the traditional evaluation method for Lugeon tests (Houlsby, 1976) using eq. 4-18

$$K = \frac{Q}{2 \pi L h} \ln \left(\frac{L}{r_w}\right) \qquad (4\text{-}18)$$

with L as the length of the tested section, h the injection head and Q the injection rate. Another standard method is the Theis recovery or Horner plot, where the section of the time drawdown curve is used for the analysis when radial flow conditions can be assumed. Barker (1981) developed an analytical technique, specifically designed for tests in fractured rocks. Transmissivity is evaluated by an iterative method using eq. 4-19

$$T^{(n)} = \frac{Q}{2 \pi h} \ln \frac{T^{(n-1)}}{C r_w \sqrt{K_v K_h}} \qquad (4\text{-}19)$$

with C as a constant (1.781), K_h and K_v the horizontal and the vertical hydraulic conductivity of the matrix.

Only tests B8 and B25 could be analyzed by a Horner plot. Fig. 4-28 displays the plot for borehole B8, and the plots for B25, B14 and B7 are included in App. 4-6. The tests B8 and B25 display a certain feature, that has already been described above, i.e. the delayed recovery, which is caused by water running down the side of the steel casing. By the time the drop of the water level in the borehole is slower than the speed of the water seeping down the casing, the rate in head drop is reduced in B25 substantially or even inversed (i.e. head increase in B8): The results are however not influenced to a major degree, because the effect ceases before the onset of the infinite acting radial flow period. The S-shaped curve, a typical characteristic of double porosity aquifer tests, also becomes apparent in test B8. The result obtained from test B8 can be used further with some confidence, the plot of test data B25 however does not yield a definite straight line. The transmissivity appears to decrease towards lower water levels, which might be traced back to the head falling below the top of the open section. This fact, however, should have the opposite effect, because the test section is reduced. The most likely explanation is that the hydraulic conductivity is higher within the lower part of the screened section. The transmissivity obtained, using the method of Barker (1981) is dependant on the unknown hydraulic conductivity of the matrix. Although the result varies linearly only with the natural logarithm of the inverse of the matrix hydraulic conductivity, an increase from 10^{-9} m/s to 10^{-6} m/s changes K_{tot} in B8 and B25 to 2.8 and $2.5*10^{-5}$ m/s respectively.

Hydraulic conductivities, obtained from the type curve analysis, using Bourdet and Gringarten (1980) method are generally substantially higher than those from the other methods. As an example, test data and fitted type curve for test B8 are shown in Fig. 4-29.

Test B8 was also analyzed employing the well test analysis program STAR, developed by Schlumberger. The field data could be fitted without using any skin, on the contrary, a negative skin of -4 was obtained from the model fit (Fig. 4-30, p_D = dimensionless pressure). This observation could possibly explain the high hydraulic conductivity obtained by Bourdet and Gringarten (1980), because very high $C_D e^{2S}$ (C_D, dimensionless well storage constant; S, skin factor) values were the result of that particular method. The peak observed in the pressure derivative at 0.1 hr is caused by the above described delayed seepage down the side of the casing.

The field data of test B14 (App. 4-7) show an initial half unit slope, which could possibly indicate a fracture, intersecting the well (Gri-

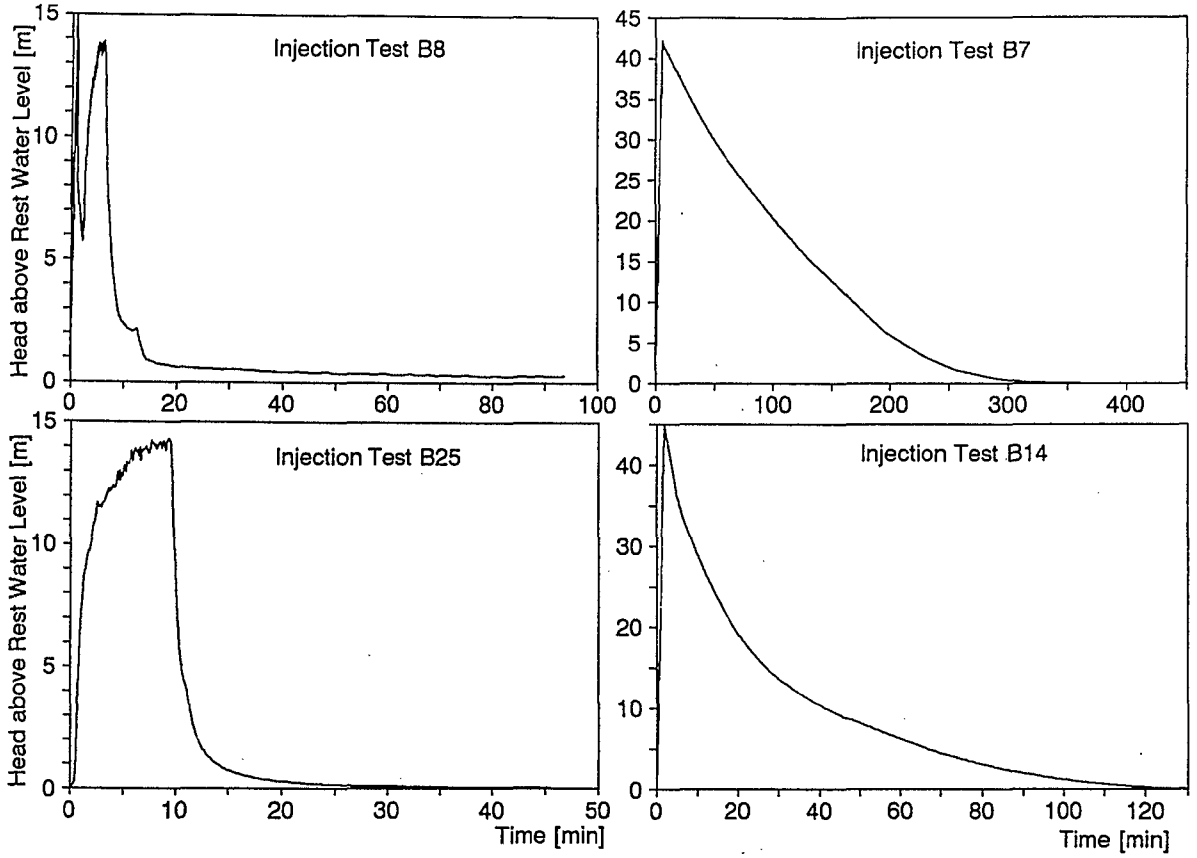

Fig. 4-27 Changes of Water Levels During Injection Tests

ngarten et al., 1975).

The bottom line in Tab. 4-16 summarizes estimated test results. These tentative estimations take into account the above considerations and drawbacks of certain methods and that Bourdet and Gringarten (1980) appears to overestimate the hydraulic conductivity in the test setup used for the present study.

In sum, hydraulic conductivities for the injection tests in B7, B8, B14 and B25 seem to vary between $5*10^{-6}$ m/s and $5*10^{-5}$ m/s, depending on the borehole tested. The radius of investigation can be calculated according to Streltsova (1988, p. 79) according to the eq. 4-20, with R_i as the radius of investigation, η as the diffusivity, and t the flow period. A and c_2 are constants, that

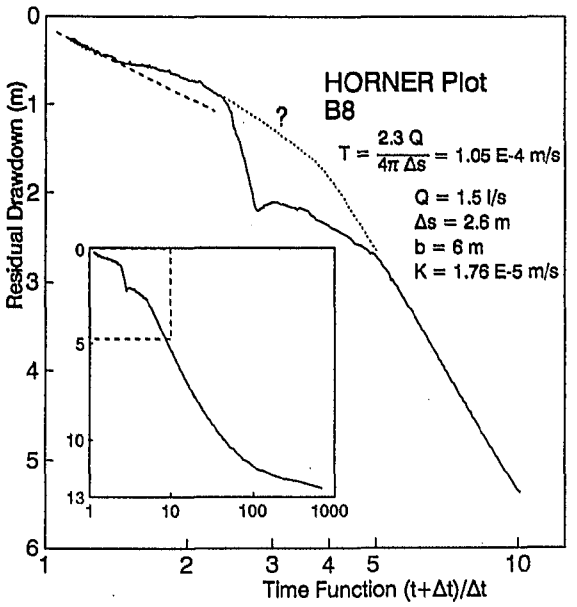

Fig. 4-28 Horner Plot of Injection Test B8

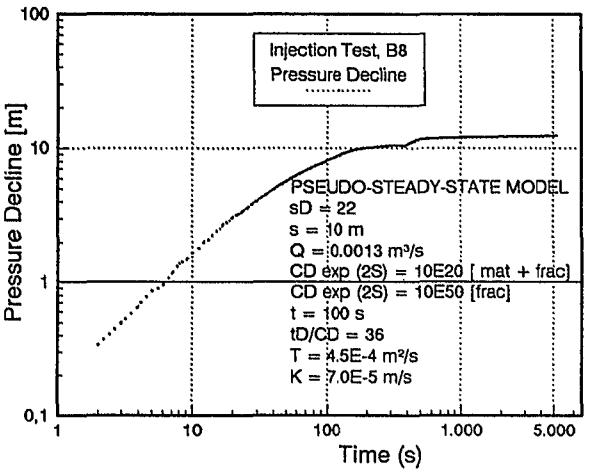

Fig. 4-29 Log-Log Plot of B8 Injection Tests Data

Injection Tests (Summary)	Hydraulic Conductivities				
	B7	B8	B14	B25	
Houlsby (1976)		1,5E-05		1,3E-05	m/s
Horner plot		1,8E-05		3,3E-05	
Barker (1981)		4,4E-05		3,9E-05	m/s
Bourdet et al (1980)	1,7E-05	7,0E-05	1,5E-06	5,0E-05	m/s
Bourdet et al (1983a)		1,2E-05			m/s
	7E-06	2E-05	5E-06	3E-05	m/s

Tab. 4-16 Summary of Results of Injection Tests

depend on the definition of the radius and the system of units used. The radius of influence calculated with the above method, with c_2 being unity and A equal to 4.781, ranges between 10 and 20 m depending on the diffusivity (m^2/d) and the time (d) used.

$$R_i = A \sqrt{c_2 \eta t} \qquad (4\text{-}20)$$

Test Results and Hydraulic Parameters of Double Packer Tests in the Borehole Bitz

The data from double packer tests (Sauter, 1989) in the borehole Bitz, situated in the northwestern low permeable zone of the catchment were evaluated using steady state (Houlsby, 1976) and unsteady state procedures for parameter determination (Bourdet and Gringarten, 1980). The test sections were preferentially located in horizons where fractures and solution channels could be detected, using a selecion of borehole logs and borehole television inspection. However, highly productive zones could not be tested because of packer leakage and the limited injection rate of the testing equipment. This explains hydraulic conductivities ranging between $1*10^{-5}$ m/s and $3*10^{-4}$ m/s. A pumping

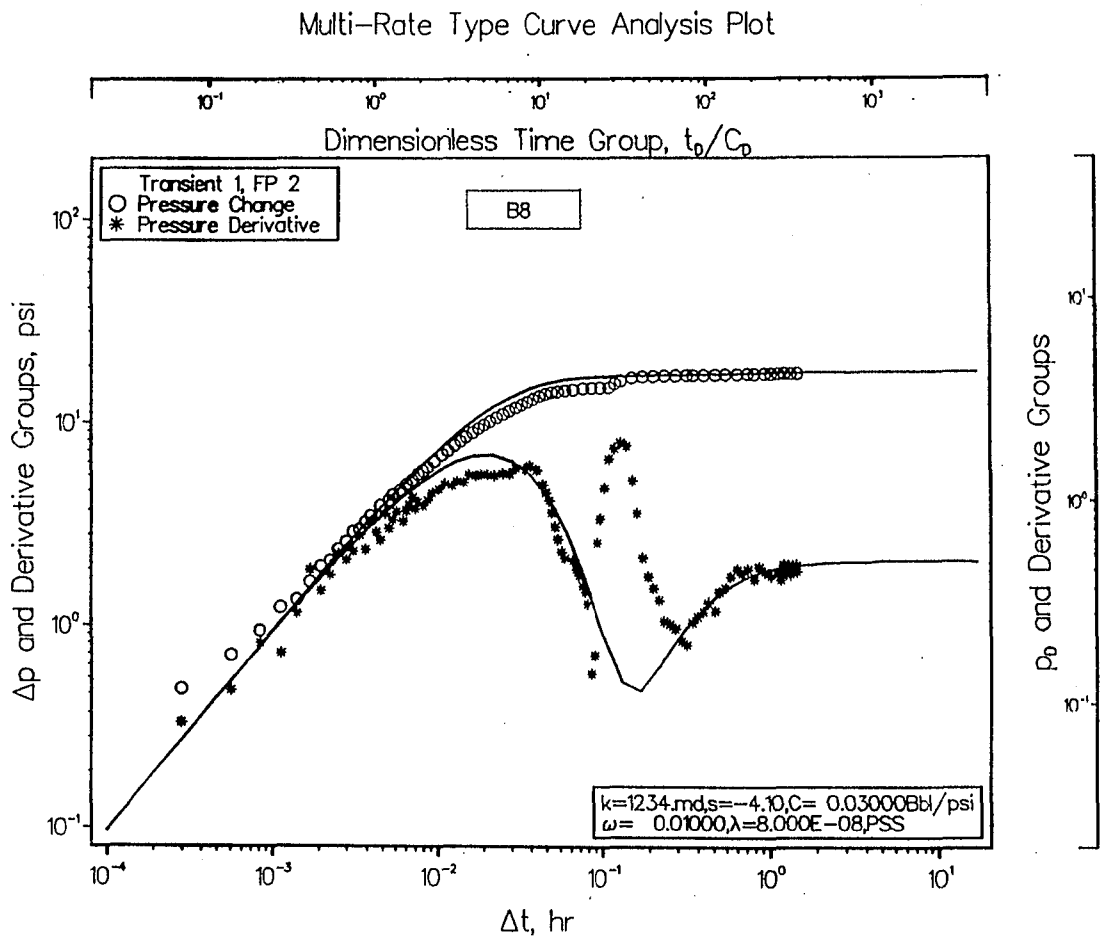

Fig. 4-30 Evaluation of B8 Injection Test Using Pressure Derivative

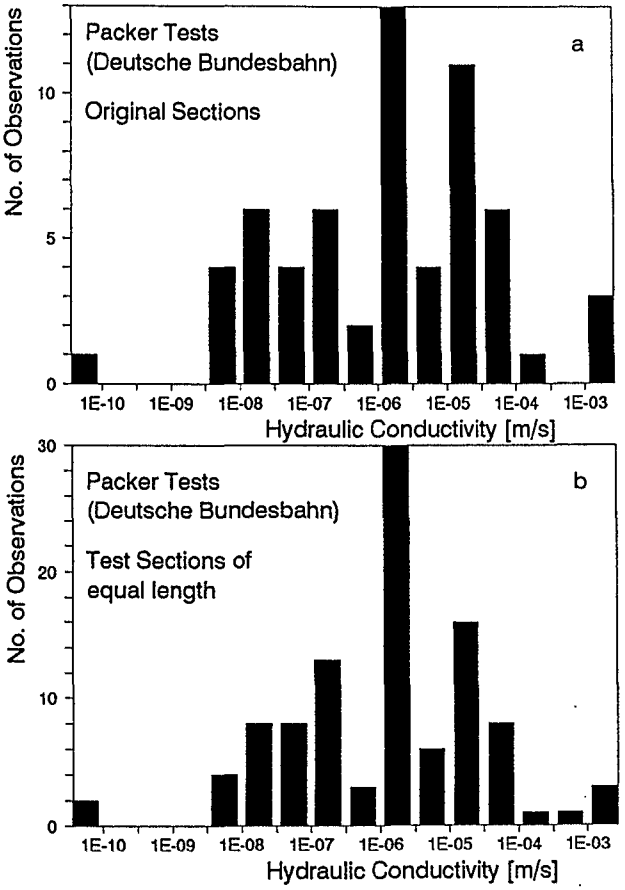

Fig. 4-31 Histograms of Hydraulic Conductivity Distribution from Double Packer Tests (Deutsche Bundesbahn)

test, performed in the same well and discussed below, gives results of the total saturated thickness of the aquifer, extending over approximately 30 m.

Test Results and Hydraulic Parameters of Double Packer Tests in the Eastern Swabian Alb (Deutsche Bundesbahn)

Fig. 4-31 depicts frequency distributions of double packer tests, conducted in boreholes of the Deutsche Bundesbahn. The wells were drilled during investigatory works for a planned tunneling project. The projected tunnel transects a karst aquifer with the same geological strata as in the study area, for a substantial distance.

The tests were performed using different test section lengths, ranging between 5 and 40 m. In order to correct for the different lengths, the longer sections were weighted higher, i.e. counted more frequently (Fig. 4-31). The tests were evaluated by the Deutsche Bundesbahn, using the steady state (Houlsby, 1976) and unsteady state (Bourdet and Gringarten, 1980, and similar procedures) method. Maximum hydraulic conductivity can be localized between $1*10^{-6}$ m/s and $5*10^{-5}$ m/s. There might however be a systematic underestimate of the hydraulic conductivity, indicated by the frequency distribution because a relatively high number of tests were conducted within the unsaturated zone.

The hydraulic conductivities, however, demonstrate that comparable values can be obtained for geologically similar situations. The tests, plotted in Fig. 4-31, apply to the ki2/3 massive limestones. A smaller number of tests were carried out in non-karstified kil marly limestones and yielded values between $5*10^{-8}$ m/s and $5*10^{-7}$ m/s and a maximum at $5*10^{-8}$ m/s. Occasionally, hydraulic conductivities between $1*10^{-6}$ m/s and $5*10^{-5}$ m/s were reported.

4.3.1.3 Laboratory Scale Measurements

In order to complete the spectrum of hydraulic conductivities, measured at various scales, some data could be found in Weiß (1987), which however only cover the bedded facies of the carbonate series of the Upper Jurassic (Franconian Alb). A very definite maximum was measured between 10^{-8} m/s and 10^{-9} m/s for bedded limestone. For dolomite beds, the hydraulic conductivities varied from 10^{-4} m/s to 10^{-8} m/s at the measured scale of 3 cm diameter cores. It is however difficult to take samples of the massive karstified limestone. Hydraulic conductivities can be assumed to vary by many orders of magnitudes, in the extreme case no porous or fractured medium is encountered at all, if e.g. a "sample" is taken in the centre of a cavity.

4.3.2 Summary

Fig. 4-32 displays the karst system hydraulic conductivities of all the hydraulic tests and the regional evaluation. It is apparent that the hydraulic conductivity increases with an increasing scale of investigation. Lowest values are determined in the laboratory and the highest on a catchment scale. The values are categorized into a socalled "common range", i.e. hydraulic conductivities, that are most frequently measured and "low conductivities", which usually give an indication of the hydraulic conductivity of the fissure system at the respective scale. The range of variation of hydraulic conductivity is indicated tentatively with dashed lines. Among double packer tests, the higher values are usually underrepresented, which is generally a result

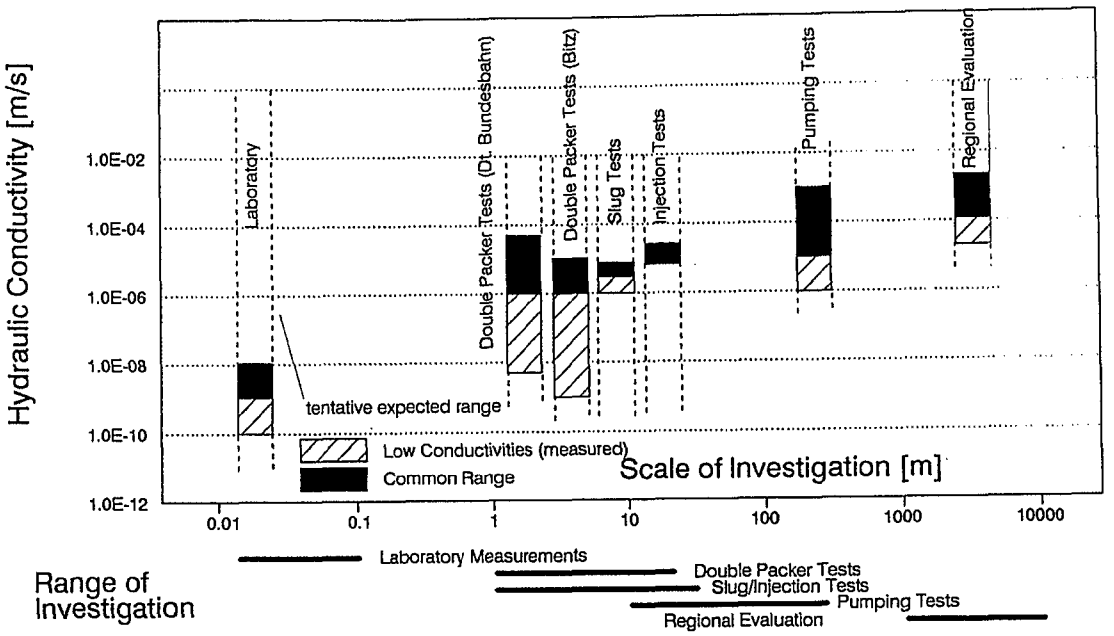

Fig. 4-32 Relationship Between Hydraulic Conductivity and Scale of Investigation

of the testing equipment with its limited injection rate.

It is interesting to note that system hydraulic conductivities, measured at a certain scale (e.g. local scale) seem to correspond to the hydraulic conductivity of the fissured system at the next higher scale (i.e. regional scale). Slug tests and injection tests produced fissure hydraulic conductivities of between 10^{-6} m/s and 10^{-9} m/s, which correspond approximately to the total hydraulic conductivity measured in the laboratory. The "common range" of the laboratory tests are probably an underestimate, because samples have only been taken from the bedded facies. This range can probably be extended by one order of magnitude to 10^{-7} m/s. The fissure system values, resulting from slug and injection tests (K_{slfis}) correspond to the permeabilities, measured in less karstified, i.e. fissured zones of the double packer tests. Average hydraulic conductivities measured between $1*10^{-5}$ m/s and $1*10^{-6}$ m/s by slug tests correspond to fissure system values of pumping tests (K_{lfis}), identified as hydraulic conductivities of unkarstified limestone. A similar relationship applies, if the pumping test results are compared with the regional fissure system values (K_{regfis}).

Fig. 4-33 graphically summarises the above observations, and shows that hydraulic conductivity (fissures + conduits) of the lower scale can serve as input for fissure hydraulic conductivity at the next higher scale. Storage values do not vary to a major degree and can be estimated at 0.015% ± 0.01% for the conduits and at 1% to 2% ± 0.5% for the fissures.

These findings have been used as input for a regional double-continuum flow and transport model.

4.4 Transport Parameters

Numerous tracer tests were carried out in karst aquifers of the Swabian Alb, mainly for the purpose of delineating catchment boundaries, protection areas for drinking water abstraction, and to determine average transport velocities.

Generally, in a specific catchment, a linear relationship between spring discharge and average velocity of the pore water can be observed (Fig. 4-34, Merkel, 1991, Teutsch, 1988, tracer tests in sinkholes), which is less expressed if borehole tracer tests are examined (Merkel, 1991).

Only recently (e.g. Schädel and Stober, 1988, Seiler et al., 1989) had it been attempted to apply analytical methods to the tracer breakthrough curves and to evaluate dispersivities and to derive from the data information on the type and the degree of karstification. The specification of dispersivities for karst areas has to be treated with caution. They only apply to an equivalent porous medium and to homogeneous and isotropic conditions. Stober (1991) distinguished (Fig. 4-35) between dye traces, conducted in highly karstified aquifers with large

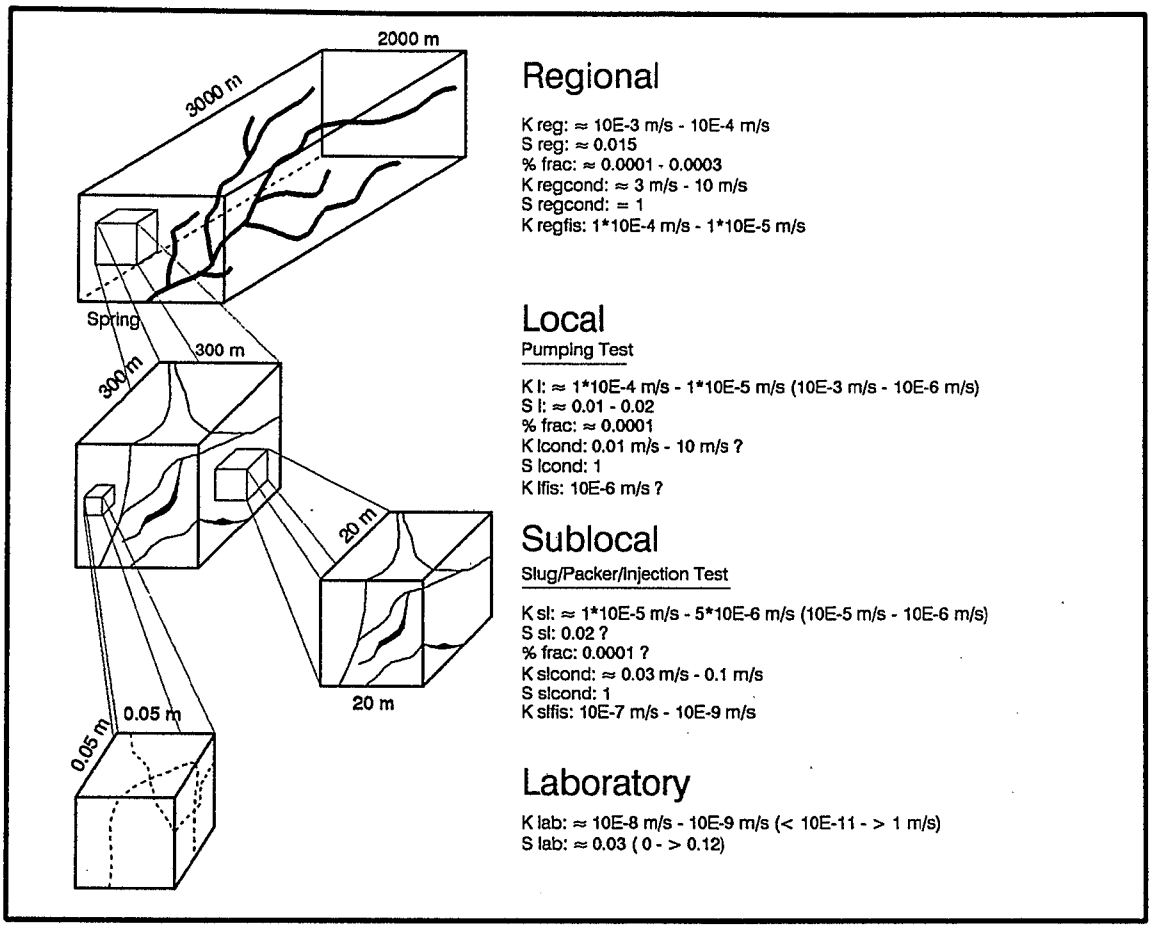

Fig. 4-33 Geometrical Relationships and Hydraulic Parameters at Different Scales in the Study Area

conduits and caves (Bereich 1) and others with input in boreholes (Bereich 4). Longitudinal dispersivities vary between 3.8 m and 1180 m. It can however be assumed that dispersivities, derived from tests in sinkholes and activating the fast system, are usually an overestimate, compared to the true conduit dispersivities, because the flow of the dye through the highly heterogeneous unsaturated zone causes the dispersion to increase.

Tracer tests, performed in boreholes of the Gallusquelle catchment (B19, B24, B25), known for their direct connection to the conduit system, because of the close distance to the Hohenzollern graben, produced dispersivities between 5 m and 9 m (Merkel, 1991). In the above borehole tests, the dispersion, caused by the unsaturated zone, can be excluded. The dispersivities, determined by Seiler et al. (1989), derived from tracer tests in the conduit system, all ranged below 20 m.

Teutsch (1988) fitted numerically generated (double-porosity model) breakthrough curves to field data from tracer tests in the highly karstified shallow karst of the Reutlinger Alb. Dispersivities in the order of 150 m were obtained for the conduit system and it can be assumed that the dispersion is mainly caused by the heterogeneities within the thick unsaturated zone.

Dispersivities, determined from borehole tracer tests are always a result of both, the dispersivity derived from the fissured system blocks and that, due to the conduit system. The parameter therefore depends on the geometry of the fissured system blocks, i.e. the distance travelled within the "regional fissured system". Therefore, no single value can be given for fissured system dispersivities, they probably range between 50 m and several hundred meters (Merkel, 1991, Stober, 1991, Schädel and Stober, 1988).

4.5 Dynamic Analysis of Recharge and Aquifer Flow

The hydrological response of a karst aquifer is strongly controlled by the geological structure of the aquifer and the mode and time variation of the recharge input. With water flowing at different rates through a karst aquifer, slowly through small fissures and very rapidly through

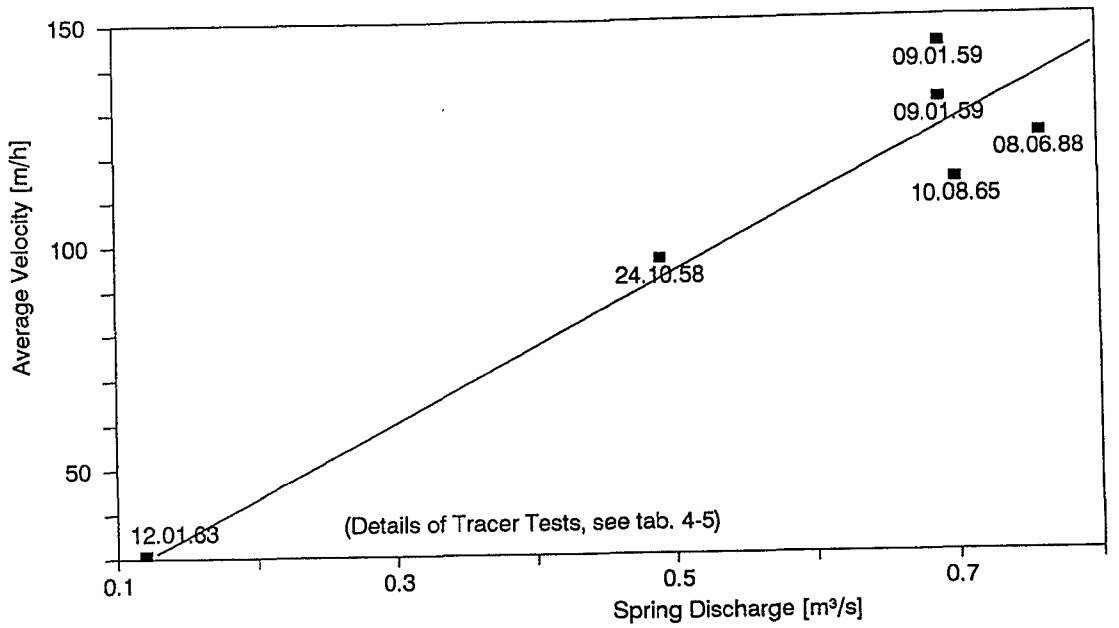

Fig. 4-34 Relationship Between Spring Discharge and Average Velocity of Tracer

large fractures and solution enlarged channels, the simulation of the flow and transport requires information on both systems and their interaction as well as quantitative estimates of quantity and distribution of groundwater recharge.

On the scale from conduit to diffuse flow, the aquifer investigated can be placed on an intermediate position (mixed-flow), Chap. 3.1. Whereas the water quality parameters and the discharge react "flashy", and the response to storms is still very rapid, the determining part of the aquifer really is the matrix blocks (fissured/diffuse system), that store and release the water over several months. Nevertheless, it is understood that the drainage is still via a tributary network of conduits. As can be shown below, following storms, approximately 5-10% of the total flow reaches the spring directly via the conduit network.

Such a variable flow behaviour cannot be described by average conditions. It rather requires an understanding of also extreme conditions, such as floods and drought periods. A model claiming to simulate the karst aquifer should also be capable of satisfactorily representing these extreme situations.

Detailed information on the response of the Gallusquelle karst aquifer can be obtained from the time series analysis of hydrological and physicochemical parameters. The time series serve on the one hand to build a conceptual model of the aquifer, to provide necessary input data and to also deliver field data for model calibration on a time variant basis.

4.5.1 Previous Related Work

It has been recognized for some time that spring water quality variations provide valuable information on the flow system within a karst aquifer. Shuster and White (1971) could distin-

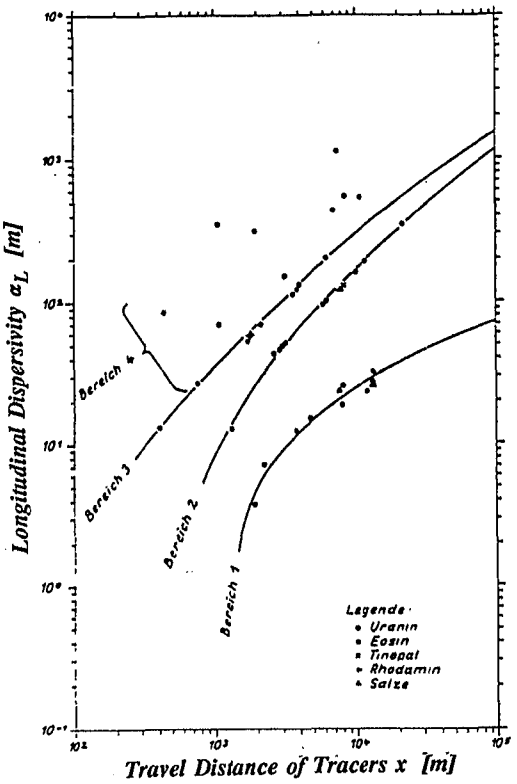

Fig. 4-35 Variation of Longitudinal Dispersivity of Karst Aquifers and Travel Distance of Tracers (Stober, 1991)

guish between fast and slow groundwater based on variations in Ca/Mg ratio temperature and hardness. Hanshaw and Back (1974), Scanlon and Thrailkill (1987), Back et al. (1979), Kastrinos and White (1986) and Rothermel and Ogden (1986) were able to use longterm temporal and spatial variations of chemical parameters to evaluate aquifer characteristics and groundwater velocities and to distinguish between different types of springs. Frequently, especially in connection with contaminant transport analysis, short term fluctuations of water quality and spring flow have been analyzed by Quinlan and Alexander (1987), Steele et al. (1985) and Hallberg et al. (1985), with the aim of designing appropriate groundwater monitoring strategies.

Hallberg et al. (1983) analyzed the spring discharge during flood events using various hydrograph separation methods to distinguish between pre-event and event water of a karst spring.

Hess and White (1974, 1988) attempted to interpret high frequency fluctuations in spring water chemistry by attributing them to different arrival times of water from tributaries at the main conduit. Dreiss (1989a) explains rapid changes in water quality by surface water entry to the groundwater system close to the spring. The complexity of karst chemograph responses have also been recognized by Dreiss (1989a), Bakalowicz and Mangin (1980) and Williams (1983).

Bakalowicz and Mangin (1980) and Williams (1983) include the unsaturated zone and in particular the epikarstic zone in their interpretation and they were able to explain frequently observed initial increases in total dissolved solids (TDS) before the arrival of the newly recharged water. Dreiss (1989a) comments on the lack of detailed examination of storm responses on both, short and longterm basis. Many karst springs display both, a fast initial response and also a longterm memory effect after recharge events. A proper understanding of the aquifer system therefore asks for measurements on both time scales. Vervier (1990), Dreiss (1989a), Behringer (1988), Meiman et al. (1988) and the present study attempted to fill this gap. The studies of Vervier (1990) and Meiman et al. (1988) display very complex output signals of flood pulses, difficult to interpret, caused by the additional influence of sinking streams and maturely karstified aquifers. In the present study, the dominant factors determining the output are only the conduit and the fissured (diffuse) system with areal autogenic (Williams, 1983) recharge input.

4.5.2 Methodological Aspects

It was attempted to measure all the time variant parameters on a continuous basis. Therefore, automatic digital dataloggers (PHYTEC, PRODATA) were installed to measure spring discharge (pressure transducer), groundwater levels (pressure transducer), electrical conductivity (WTW LA 1/T-) and temperature (PT100) at half hourly intervals. Turbidity values were provided by the Zweckverband Zollernalb, representative measurements could however only be obtained during pumping hours, because the readings were taken at the waterworks and not directly at the spring. Turbidity data can be regarded as a measure for the quantity of suspended solids in spring water. Rainfall was also measured continuously in order to be able to exactly determine the highest intensity of rainfall with an hourly resolution (LAMBRECHT, automatic raingauge).

Due to the fact that electrical conductivity cannot be considered as a conservative parameter, regarding possible chemical changes on the passage from the surface to the water table and also within the phreatic zone, a suitable conservative tracer was important for the analysis of hydrograph data. Therefore, based on the experiences of Zeidler (1987) in shallow and deep karst aquifers (Teutsch, 1989) in adjacent areas, the relative abundance of ^{18}O in rain and spring water was measured as well, in order to be able to identify new and old groundwater components in spring water. $\delta^{18}O$ has been frequently used as a tracer for the separation of the groundwater component in surface discharge (Fritz et al., 1976; Herrmann et al., 1978; Sklash and Farvolden, 1979; Herrmann and Stichler, 1980; Körner et al., 1986). In karst groundwater systems, the relative abundance of oxygen isotopes has been employed to determine mean transit times (Bertleff, 1986; Geyh and Groschopf, 1978) and to analyse single storm events (Bakalowicz and Mangin, 1980; Hallberg et al., 1983). Samples were collected at 16 hourly intervals, which was determined by the sampling intervals of the automatic sampler (0.25, 0.5, 1, 2, 4, 8, 16 h). The samples were analyzed by the Institut für Hydrologie, Gesellschaft für Strahlen- und Umweltforschung, Neuherberg.

In the following graphical presentations, groundwater recharge (Chap. 4.1) is displayed instead of precipitation, in order to only show those events, with their respective intensity,

actually contributing to groundwater recharge. This procedure implies that local storms, which might have some effect on the spring water quality and flow, do not show up as groundwater recharge because of averaging out and the recharge calculation method.

Groundwater levels can be measured at a resolution of 0.01 m, electrical conductivity at 0.1 µS/cm and the temperature at 0.01°C. The electrical conductivity values are temperature corrected for 25°C.

Although $\delta^{18}O$ can usually be measured at an accuracy of ± 0.15‰, it can be assumed that, if whole time series are measured, the accuracy can be improved substantially (oral communication, Prof. Seiler, GSF). This point is critical, because frequently it has been attempted to interpret $\delta^{18}O$ fluctuations in spring water as significant, although they ranged within the error bars. However, in combination with the information from the other parameters, such assumptions appear to be justified.

4.5.3 Discussion of Typical Recharge Events

The analysis of natural pulses have a major advantage compared to local tests, because they deliver results, that are representative for the whole catchment and these pulses also activate parts of the groundwater system, that are very difficult to test with local field methods, such as the dominant conduit network.

The analysis however requires clean, sharp inputs, that do not show any spatial and temporal variation. The major drawback, however, is the overlapping and superposition of the signals of several events, which makes detailed examination and interpretation often difficult and ambiguous.

Summary of Observations

The variations in parameters and different effects, described below, can be summarized in an idealized rainfall event and its idealized responses (Fig. 4-36). The various stages are described in the following in chronological order.

The fast water component of a sharp input pulse of recharge water arrives at the water table, which leads to an increase in discharge induced by the pressure pulse in the conduit system. This increase in the potential is indicated by the peak in the water levels in B7 and B14, and the high flow velocities in the conduit network by the elevated turbidity. The arrival of the fast water components at the spring is schematised in Fig. 4-37. Between the time of discharge increase and the increase in electrical conductivity, groundwater, displaced from the conduits arrives at the spring. After that, the discharge of fast subcutaneous water is sometimes signalled by a slight increase in electrical conductivity and the arrival of the new fast recharge water commences with the rapid drop in electrical conductivity. The negative offset in $\delta^{18}O$ represents subcutaneous water, that stems from a previous, less important isotopically light rainfall event. Isotopically light water is displaced from the fast subcutaneous zone. The slow event water component, delayed by the "fissured system" of the subcutaneous zone, leads to an increase in the regional water levels and a second maximum in spring water $\delta^{18}O$, once it is discharged at the spring.

With the above conceptual model in mind, the actual field data can be understood better. Deviations of the real data from the idealized model are explained below. In the diagrams (Fig. 4-38 to 4-41) "scw" stands for subcutaneous water, "fw." and "sw." for fast and slow event water, with the figure indicating the chronological order, the rainstorm occurred in.

Fig. 4-38 to 4-41 display time series of four periods during which recharge events of various importance occur. The graphical presentations of the remaining periods can be found in App. 4-8. The selected series include three winter and one autumn recharge event. All the events display superposition of different storms to a more or lesser degree and although the Oct. 88 event cannot be quantitatively evaluated, it is believed to be fairly typical of a summer/autumn event.

The presentation of all the parameters is selfexplanatory. The plotting of the ^{18}O data require some further clarification. The ^{18}O graph contains two sets of information, the relative abundance of ^{18}O in the spring water (left ordinate), represented as squares and crosses and the $\delta^{18}O$ in rainfall input as bars (right ordinate). The length of the bars indicates the deviation of the isotope ratio in the rainfall from the baseline (see below) and the shading of the bar the intensity of the respective recharge. The spring water samples were distinguished as to their time of collection. It is suspected that abstraction, which is in the order of 100 l/s might influence the $\delta^{18}O$ as a result of mobilisation of deeper phreatic groundwater, close to the spring. The $^{18}O/^{16}O$ ratio in precipitation was plotted relative to the deviation of

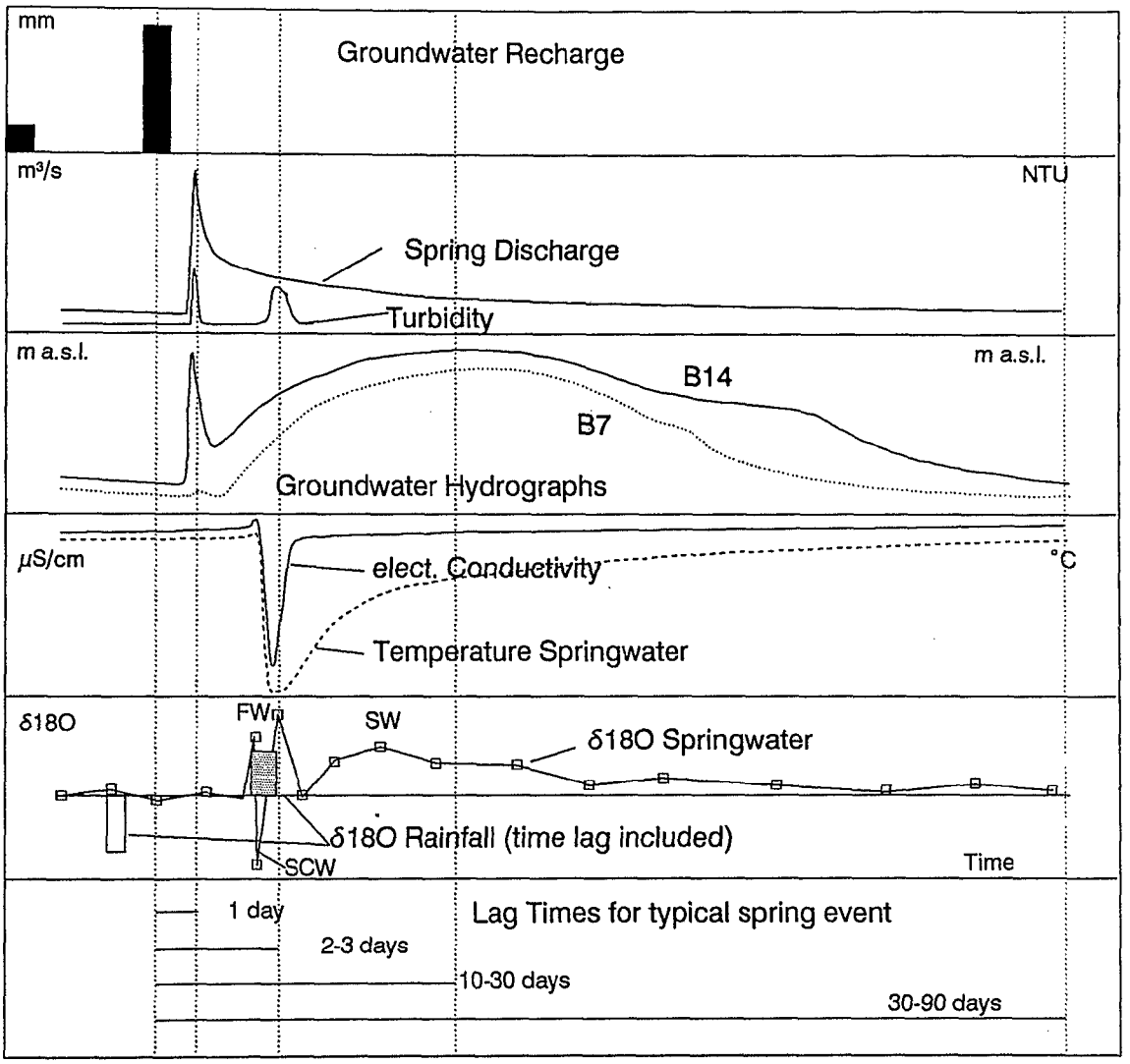

Fig. 4-36 Schematised Response of Hydraulic and Physico-Chemical Parameters to an Idealised Rainfall Event

the $\delta^{18}O$ (rainfall) from a value of -10.55‰. This value was evaluated as a base value, the $\delta^{18}O$ appears to tend to after rainfall events (Aug88, Nov88, May89, Aug89, Nov89, Dec89, Jan90). This base level also corresponds to the recharge weighted average $\delta^{18}O$ in the input throughout the observation period (Jan88-Jan90) and the $\delta^{18}O$ level at the end of the 1989 drought period in Oct/Nov 89. The relative depth of recharge is indicated as the intensity of shading of the respective bar and distinguishes between < 5 mm and > 20 mm in categories of 5 mm. The lag time between rainfall and recharge appearing at the spring has already been taken into account, by shifting the bars by the respective lag.

The Feb90 event includes data of volatile chlorinated hydrocarbons. No $\delta^{18}O$ values have been measured for that period yet.

All events, apart from some summer and autumn events display some common features in their hydraulic and physico-chemical behaviour. A sharp increase in spring flow, with a peak discharge of 1 - 2 days after the highest intensity in rainfall is followed by a less rapid drop in discharge. The actual event water reaches the spring approximately 0.5 to 2 days later, which implies that peak discharge consists mainly of pre-event water, as has also been described by Williams (1983) and Dreiss (1989a). The maximum water level in the aquifer was read between 1 and 4 weeks after the event. The highest groundwater levels in the boreholes are not measured simultaneously with peak discharge. The bulk of the recharge water arrives at the water table delayed by the epikarst and the hydraulic conductivity of the aquifer fissured system and therefore distributed over several

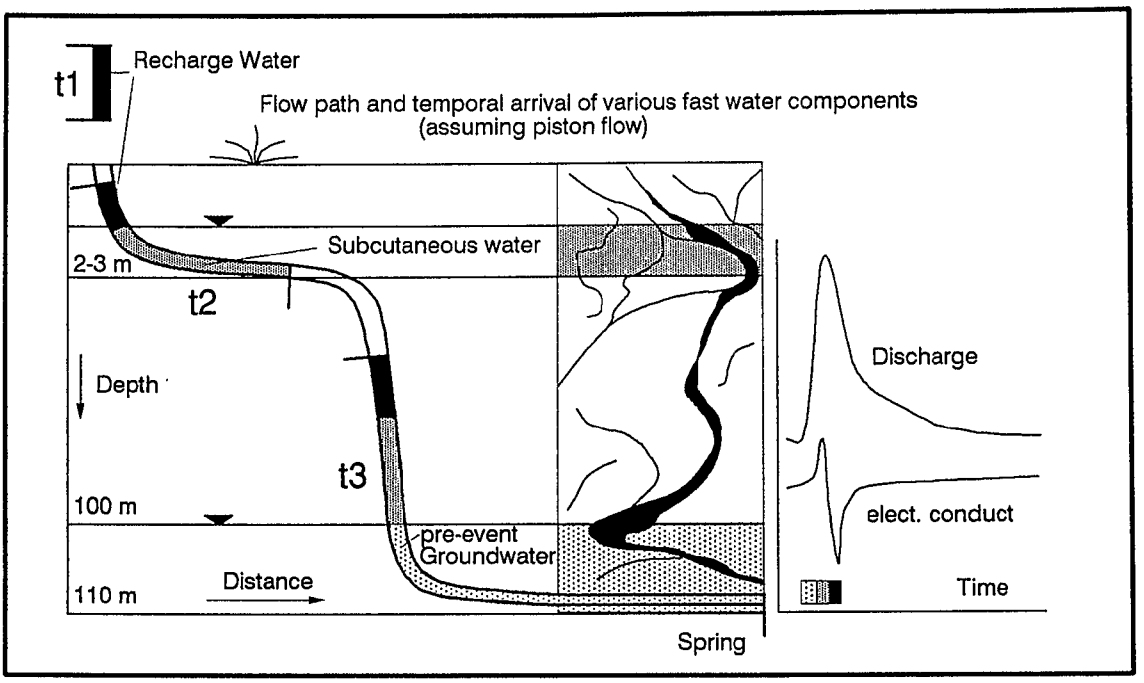

Fig. 4-37 Conceptualisation of Flow Path and Change in Spring Water Parameters to Different Recharge Water Components

weeks to months (see below). Increased, and frequently the highest values in spring water turbidity were observed contemporaneously with peak discharge, i.e. the turbid water consists mainly of pre-event water.

The groundwater hydrographs show a response, that suggests that two distinct flow systems exist. Some intermediate maxima could be measured in both boreholes simultaneously with peak discharge. These might reflect the maximum potential in the fracture system, which dissipates quickly, due to the inherent high hydraulic conductivity. These maxima are particularly apparent in B14, where hydraulically effective fractures have been suspected (Chap. 4.3.1.2). A tracer test in borehole B14 displays high (60 m/h) average velocities but not conduit velocities (100 m/h), which might be due to the prevailing low flow conditions (0.16 m^3/s, FV3, Tab. 4-5). Artefacts as a result of borehole completion, i.e. that recharge water runs down the annulus, can probably be excluded. An experiment, whereby approximately 250 l of water were poured down the annulus of the borehole only had a minor effect on the waterlevel, the increase of which disappeared within a few of hours. The decrease in water level after the injection test (Chap. 4.3.1.2) was also completed after one hour. These observations lead to the conclusion, that the observed intermediate maxima, attributed to the hydraulic reaction of the fracture/conduit system, which lasts throughout several days, cannot solely be explained by a direct connection between surface and open section of the piezometer via the annulus.

The turbidity is probably the most suitable parameter to distinguish between the fast and the slow event water component. In order to keep the clay particles in suspension, a minimum of hydraulic energy and turbulence is required, a criterion, which allows the distinction between the two flow components. It also enables the determination of the time, when the fraction of the fast water, arriving at the water table becomes zero.

Another indicator for the fast water component is the variation of the electrical conductivity of the spring water. Considering that the chemical reactions between recharge water and carbonate rocks are very fast (hours to days), it can be assumed, that as long as a substantial deviation from background levels can be measured, most of the discharge water must be fast water, moving rapidly through unsaturated and saturated zone.

The temperature of the spring water behaves somewhat differently. The initial rapid change in temperature at the time of arrival of fast water at the spring occurs simultaneously with

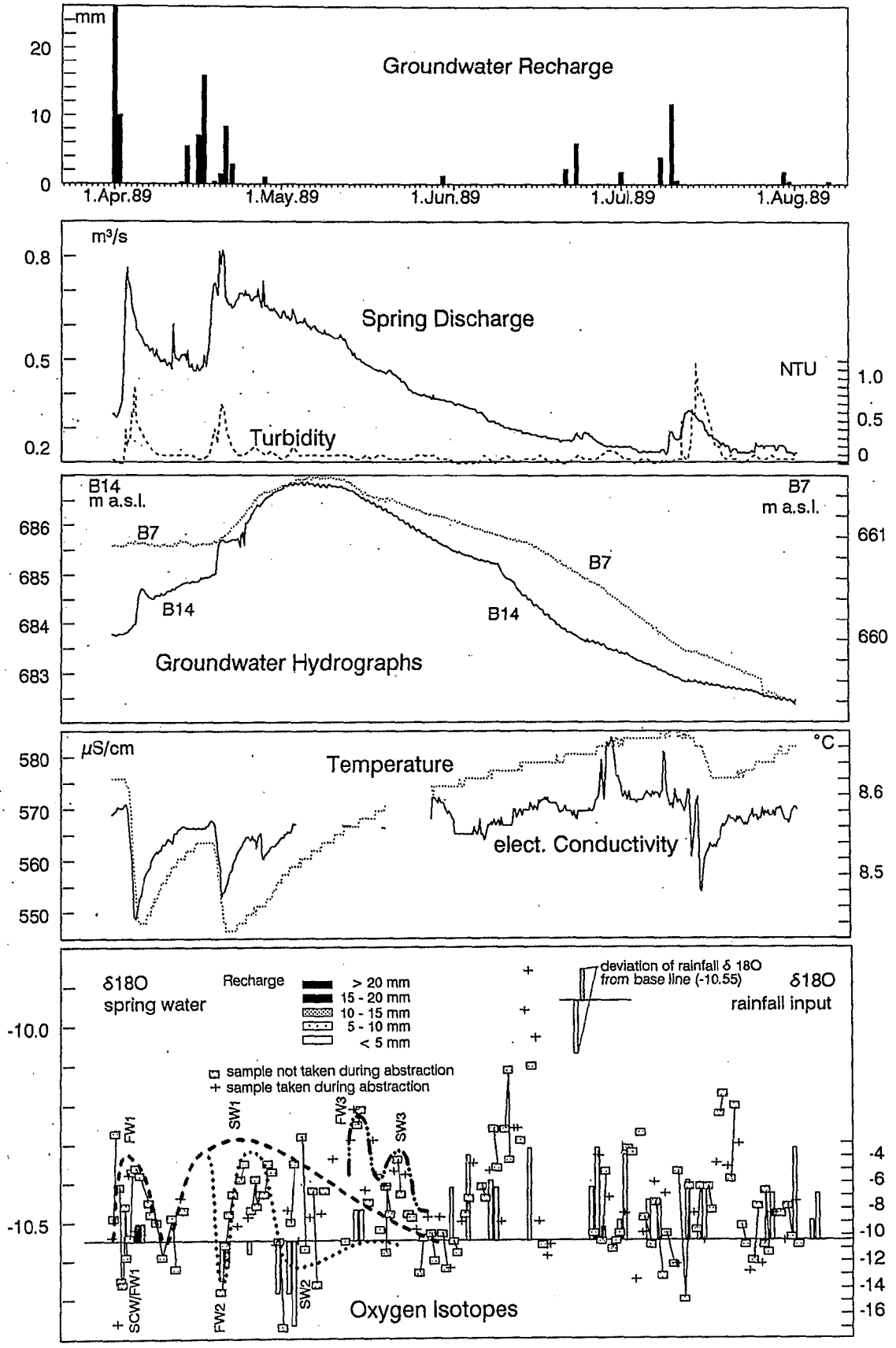

Fig. 4-38 Time Series of Hydraulic and Physico-Chemical Parameters of in the Gallusquelle Karst Aquifer (April 1989)

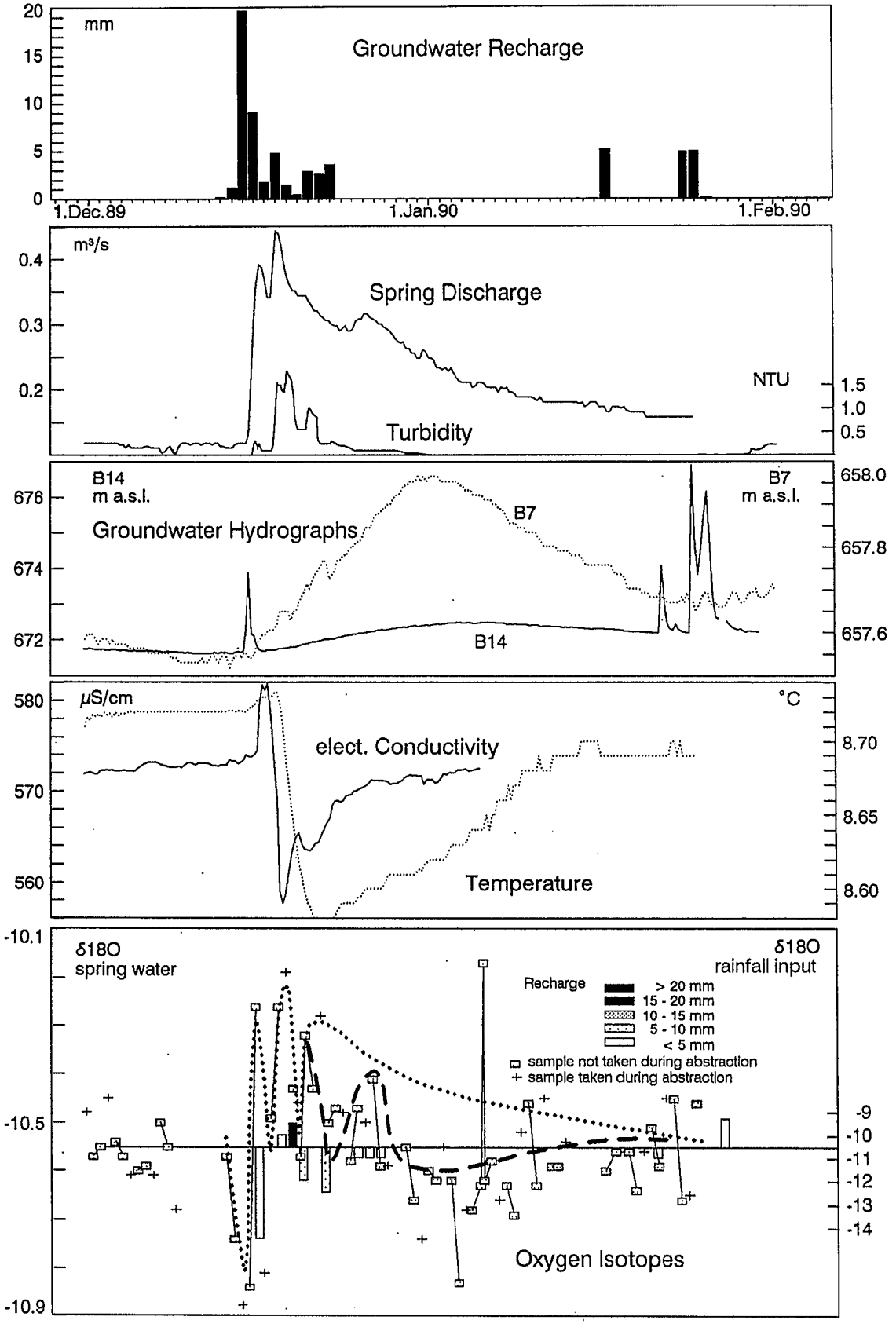

Fig. 4-39 Time Series of Hydraulic and Physico-Chemical Parameters in the Gallusquelle Karst Aquifer (December 1989)

the change in electrical conductivity. The temperature minimum however, difficult to determine, because of the resolution of only 0.01°C, is generally delayed by an estimated lag of 0 - 20 hours. This difference can be explained by comparing the relative quantities of fast and slow water components (see below). Considering that the fast water amounts to an average of 6% of the recharge water and that faster components of the slow water arrive at the spring within 2 - 3 days, the temperature parameter responds with a further decrease because of the high heat capacity of the water. The change in heat content of the water is less sensitive to time than the chemical reactions between rock and water, that increase TDS. The same physical property of the water can also help to explain the substantial memory effect of the aquifer with regard to the temperature deviation from background, caused by the recharge event. It can frequently take up to several months, especially after spring events, for spring water temperatures to return to pre-event levels. By that time, spring discharge and aquifer storage also returned to values, measured before the storm. These observations show that temperature could possibly be regarded as a more or less conservative tracer, particularly for the fast flow component.

One further feature in the chemograph of the electrical conductivity is common to a number of events, depending on the season. Frequently an initial increase in electrical conductivity, particularly after long dry periods, is observed, which had also been noted by Ashton (1966) and Williams (1983). As already discussed in Chap. 4.2.1, the water discharged during increased electrical conductivity can be interpreted as old water from the subcutaneous zone, displaced by fast event water.

$^{18}O/^{16}O$ ratios were analyzed in order to circumvent problems, associated with the changes, the new event water is subjected to, i.e. changes in its dissolved mineral content and temperature during its passage through unsaturated and saturated zone. However, the measured values display variations, that are frequently difficult to analyse due to the superposition of several events and small, high frequency variations in $\delta^{18}O$, which are often within the range of the analytical error. However, the Apr89 event (Fig. 4-38) also reveals the distinction between the two flow components, the fast and the slow. The broken line indicates an interpretation of the expected bimodal breakthrough of $\delta^{18}O$ as a response to the event of 1st April, the first peak indicating the arrival of the fast component, the second broader maximum the delayed slow event water (further details see below). Before the actual arrival of the fast water, frequently, an offset in the $\delta^{18}O$ is observed, which occurs simultaneously with the arrival of the subcutaneous water at the spring.

Event of April 1989

The Apr89 event (Fig. 4-38) is well documented with data and has been discussed in detail by Sauter (1990). There is however one drawback that several other rainfall events camouflage the signal of the 1st April. The observed data are generally in accordance with the model, but the $\delta^{18}O$ values display substantial scattering. The described offset, indicative of subcutaneous water (scw) is not very clear. Positive and negative (in relation to the base line) deviations were measured, which could be the result of the large variation in $\delta^{18}O$ in rainfall since 1st March 89. Spring water values, that were higher in $\delta^{18}O$ could also be explained by rapid recharge water, entering the conduit system close to the spring. By mid-April, $\delta^{18}O$ values deviate from the expected breakthrough due to the interference from the event of 15/16 April with a fairly negative input of around -13‰. At the end of April, rainfall input with $\delta^{18}O$ of even -17‰ was measured.

During summer, increases in electrical conductivity are frequently measured (event of Oct88). The increases at the end of June 89, however, are caused by a spill of sewage water due to a blocked pipeline.

Event of December 1989

The event of Dec89 (Fig. 4-39) is a relatively unimportant storm. It shows, however some interesting features. It is composed of at least three small storms. The electrical conductivity distinguishes most clearly between the 3 different fast water components. The arrival of the subcutaneous water is marked even by a slight increase in spring water temperature, followed by the arrival of the fast water of the first event. The decrease in electrical conductivity is further accelerated (steeper slope), which marks the arrival of the fast water of the second event and finally the third pulse is marked by a broader minimum, which had to be expected from the information on recharge, which was drawn

out over three days.

The first minimum and maximum of the $\delta^{18}O$ breakthrough (dotted line) shows the arrival of lighter recharge and subcutaneous water (isotopically heavier than the event water). Changes to the isotope ratios could also be due to melt water released from surface ice. Ponding of melt water was observed before the actual event and this water might have rapidly found its way to the conduit network, whereas the slow water was still immobilized in the ice cover. This concentrated input can then evoke a drop in the $\delta^{18}O$ and a peak in the water level of B14, probably connected to the solution enlarged channels. Similar conditions prevail towards the end of Jan90.

The dotted and the broken line attempt to reconstruct the breakthrough of the two main events 2 and 3. The interpretation however was only possible in combination with the information from electrical conductivity, temperature, water levels and pH (not shown on the graphs).

Event of February 1990

The output signals of the Feb90 event (Fig. 4-40), characterized by a sharp input, display all the elements described in the previous events. No information however on $\delta^{18}O$ is available yet. Additional information represented by pH of spring water and contents in volatile chlorinated hydrocarbons has been included. The ph equivalent as Volts has been displayed instead of the actual pH, because the values were initially discarded due to large drifts in the measurements and no calibrated values exist. The pH of spring water generally fluctuates around 7.35. The pH-equivalent was corrected for drift, but there are still large scale fluctuations. Nevertheless, some interesting information can be deduced from the measurements. As described in the discussion of the events Apr89 and Dec89, it was suspected that some water, recharged rapidly close to the spring causes some early deviations in spring water chemistry. This assumption is substantiated by the pH information. Before the arrival of the subcutaneous water, indicated by the increase in electrical conductivity (pre-event level appr. 575 µS/cm) and the increase in TCE, a small quantity of aggressive, undersaturated water, which is low in pH, arrives at the spring, which can only be newly recharged water because of the solutional equilibration process between water and rock being very fast. Similar pulses of new water before the arrival of subcutaneous water can also be detected in the pH variations of Apr89 and Dec89 events (not displayed).

The levels of Trichloroethylene (TCE) and Perchloroethylene (PCE) in spring water of Feb90-May90 (Fig. 4-40) and Dec89-Jan90 (App. 4-8) also show some interesting features. The samples were analyzed by the Landesanstalt für Umweltschutz, Karlsruhe. The levels in both types of organics are also strongly influenced by recharge events. During arrival of new water, the concentrations are reduced due to dilution, and appear to return to a more or less constant background level of approximately 0.8µg/l (TCE) and 17-18 µg/l (PCE). The initial increase in both contaminants, synchroneously with the arrival of subcutaneous water can serve as an indication, that PCE and TCE stem from the same compartment of the aquifer system. Similar increases are measured, when melt water, released from the ice cover (Dec89, Jan90) is discharged at the spring.

The more or less constant background level is somewhat more difficult to explain, because the concentrations remain the same even with decreasing discharge. It could be assumed that the whole aquifer is "homogeneously" contaminated, which however is unlikely, because of the relatively low storage volume and the event water being much lower concentrated. It is also unlikely that the organics are sorbed within the aquifer because of its low content in naturally occurring organic material, providing sorption capacities. The controlling element could be the epikarst with its high water storage volume and high organic matter content within the range of the soil zone, which also releases recharge water over long periods, thereby keeping up the discharge in the spring. The constant concentration in chlorinated hydrocarbons could therefore be controlled by the equilibrium kinetics of the diffusion process. Rates of contaminant discharge vary from approximately 0.1 kg/day to ca. 1 kg/day.

Event of October 1988

The event of Oct88 (Fig. 4-41) is a typical summer/autumn event with several small events in short succession. Electrical conductivity increases instead of decreasing which is probably due to mixing with subcutaneous water. The $\delta^{18}O$ variations show a fairly complex pattern, because of the overlapping of events, with very large variations during the discharge

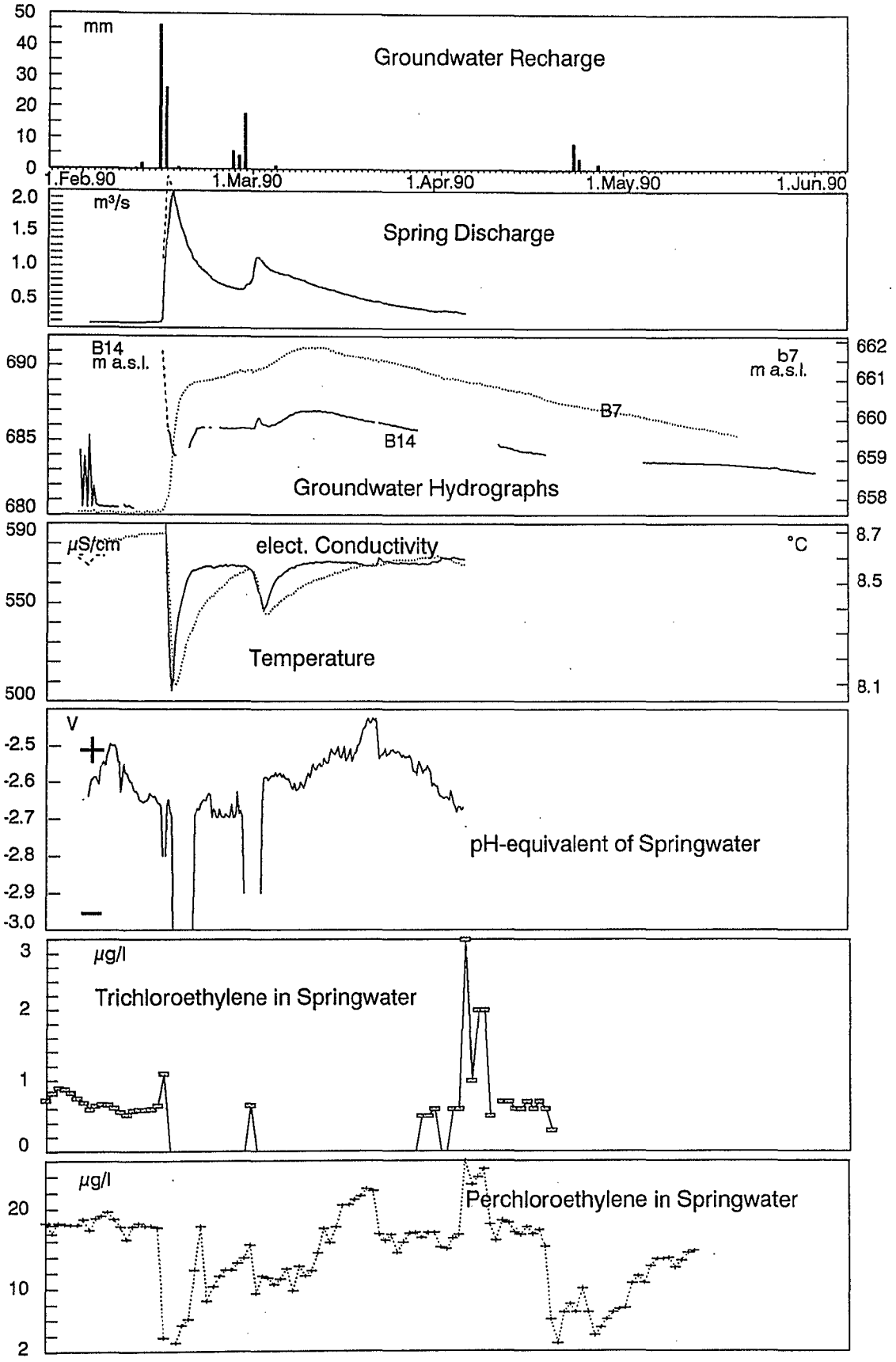

Fig. 4-40 Time Series of Hydraulic and Physico-Chemical Parameters in the Gallusquelle Karst Aquifer (February 1990)

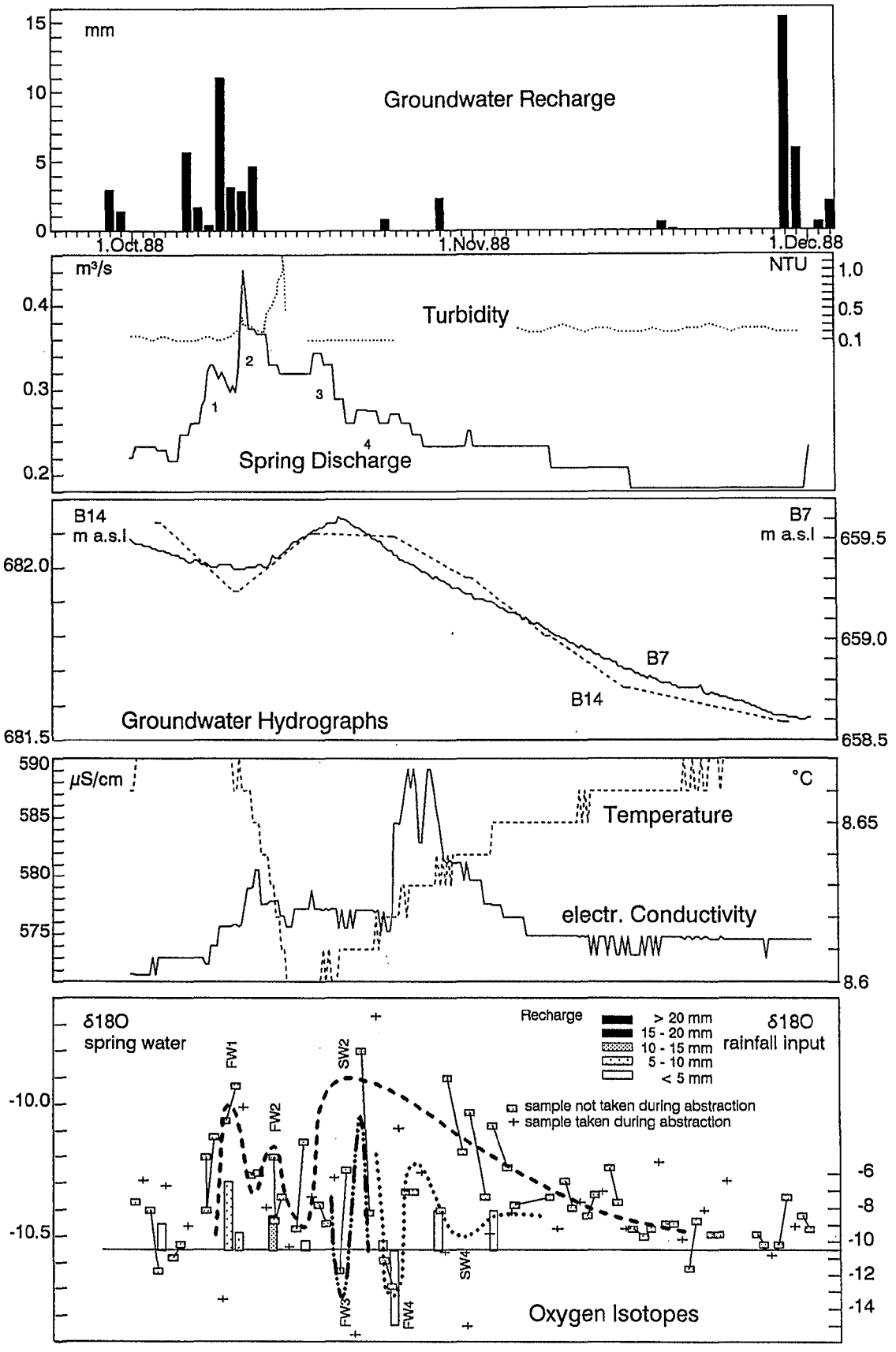

Fig. 4-41 Time Series of Hydraulic and Physico-Chemical Parameters in the Gallusquelle Karst Catchment (October 1988)

of event water in the second half of October. These high frequency changes however cease in November 1988.

The variations in spring discharge indicate at least 4 events, which however are not very well documented in isotope and $\delta^{18}O$ variations. Tentative breakthrough curves for two events are indicated as a broken and dotted lines.

One particular feature of late summer events does not become apparent in 1988. In September 1989 (App. 4-8) isotopically very light (-10.7‰ and less) water is discharged at the spring, although sporadically occurring recharge events (do not show up in calculated recharge) are all, without exception, more positive than the baseline. This feature becomes also apparent in the longterm spring $\delta^{18}O$ graph of Fig. 2-19. The water, discharged towards the end of the 1989 drought is interpreted as very old water, originating from deep aquifer horizons and recharged during the winters of previous years. During drought periods in late summer and autumn, the interference by isotopically heavy event water is minimal and heavier spring and summer recharge has already been discharged. Therefore the relatively small quantity of light winter water (with probably an age of several years) can dominate the $^{18}O/^{16}O$ ratio at the spring. Only during winter recharge periods, characterized by low $\delta^{18}O$ were the potentials high, so that water could penetrate deeper, low permeability sections of the aquifer. It can therefore be assumed that all the water in lower aquifer zones consists of isotopically light winter water. This low $\delta^{18}O$ groundwater becomes an important component in spring discharge during low flow conditions, e.g. during the drought of 1989.

Events of Mar88, Jun88, Aug88, Dec88, Aug89, Oct89

In the following the remaining events of the observation period are discussed.

Unfortunately, the large snowmelt event of Mar88 is only partly documented with field data; no measurements of temperature and electrical conductivity exist and for the water levels, no continuous readings are available. Although large quantities of low $\delta^{18}O$ snow accumulated during Feb88 and Mar88, the chemograph of $\delta^{18}O$ does not show any clear depression, which could be associated with the melt water. This observation is attributed to the influence of the fairly heavy rain, which actually induced the snowmelt. As apparent from the spring discharge and the groundwater hydrographs, the recharge input is not sharp, but drawn out over several weeks. The large variation in $\delta^{18}O$ indicates also incomplete mixing within the aquifer.

At the beginning of June 1988, two events are registered, which show two overlapping, but very distinct responses. The first one is isotopically negative the second positive with respect to the base line. They generally display the features described in the idealised model, the variations in the relative abundance of the oxygen isotopes, however, are probably very strongly influenced by the winter recharge water (times of spring discharge, $Q > 700$ l/s). As indicated by the dotted and broken lines, some interpretation of the breakthrough curves is still attempted.

The summer events of Aug88, Aug89 and Oct89 do not produce sharp and unique responses; they have however several features in common that the $\delta^{18}O$ variation is large, ranging from -10.9‰ to -9.9‰, and that the slow water breakthrough is not very well developed. The large variations can be explained by small quantities of heavy recharge, frequently as short thunderstorms and the mobilisation of deep light winter groundwater, which despite its small rate can become dominant during low flow conditions. The fact that the slow water component is less expressed is probably due to rapid recharge via desiccation cracks, which does not give the subcutaneous zone and the soil sufficient time to become saturated. Additional reduction of the slow recharge might also be the result of evapotranspiration even from the subcutaneous zone.

Although the $\delta^{18}O$ of Dec88 was positive (relative to base level) and although the total quantity of new water is high, the $\delta^{18}O$ curve does not indicate large quantities of slow water. One could speculate that the subcutaneous store was fairly depleted (0.6 mm, fast subcutaneous store, Tab. 4-4a), or that the water level in the aquifer was low, i.e. that the new slow recharge water replenishes low permeability horizons. The relatively fast recovery of the spring water temperature supports that theory.

4.5.4 Quantitative Evaluation of Time Series

Next to the qualitative analysis of spring flow and water quality variations to understand how the system responds and to derive from the response information on aquifer characteristics, it was attempted to deduce quantitative esti-

mates of the different proportions of fast and slow flow components and their respective time variations, according to which recharge enters the aquifer.

Lag Times and Average Velocities

An important criterion for quantitative analysis are lag times of peak values. They reflect how fast the aquifer responds to inputs and reveal transit times of the fast water through unsaturated and saturated zone. Tab. 4-17 summarizes the lag times between the highest intensity in rainfall and the maxima of discharge, electrical conductivity, temperature and both water levels, i.e. the one of the fast and the slow system. Some of the information has already been included in the discussion of the different events. The temperature minimum has been determined by extrapolating rising and falling limb of the temperature curve, because during the lowest temperature, the digital values remain the same over a number of hours. A source of error in the determination of the values in the table is that sometimes, especially after thunderstorms during summer, temperature and electrical conductivity minima cannot be traced back unambiguously to a certain storm, which might be very local or not even registered by the automatic rain gauges.

The discharge maximum of the event of 14 February 1990 occurs very late, considering the sharp and large input. The maximum had to be extrapolated, because spring water had to be abstracted in substantial quantities (≈ 400 l/s) in order to avoid flooding of the area near the spring. The lag time of 48 hours however appears to be too large, the error possibly caused by the assumption that the additional abstraction was constant. Corrections were made, based on the discharge of the Lauchert river at Gammertingen, which resulted in a corrected time lag of 35 hours, producing also acceptable average velocities.

Averages were also calculated for the lag times, although these lags should rather be treated individually. They are determined by a number of factors, such as spatial and temporal distribution of rainfall, saturation level of soil and subcutaneous zone, pre-event and event discharge and the aquifer characteristics. The last factor becomes apparent when average velocities are calculated for the transport of fresh water through the conduit system. The time difference between the maximum discharge (arrival of the water at the water table) and the minimum of electrical conductivity (arrival of new water at the spring) is assumed to be the time for the transit of the fast water through the conduit system of the aquifer. However, the resulting average velocities are too high, compared with those determined by tracer tests (Fig. 4-34, Tab. 4-5), if half the distance to the water devide (5500 m) is taken as the transport distance. Considering that the south-eastern part of the aquifer (Fig. 2-17) is capable of conveying the new recharge water considerably faster to the spring than the remaining part, it is reasonable to assume that the peak values are applicable to an average distance of 3500 m. The average velocity ranges between 60 m/h and approximately 250 m/h. The higher values are thought not to be representative, because in the case of event 11 July 1989, a thunderstorm,

Event	Precipitation [time]	Q [h]	Conductivity [h]	Temperature [h]	"frac." Level [h]	"matr." Level [d]	peak velocity [m/h]	Spring Discharge Peak [m3/s]	Preevent [m3/s]
06.06.88	08:00	28	77	79	28	23	71	0,812	0,67
12.06.88	20:00	24	49	72		23	140	0,925	0,69
03.08.88	10:00	17							
02.09.88	04:00	22	58				97	0,335	0,28
04.09.88	04:00	45							
07.10.88	04:00	25	63	63		9	92	0,322	0,32
10.10.88	03:00								
05.12.88	00:00	38	56	70			194	1,213	0,29
11.12.88	12:00	24	32	42	24	27	438	1,415	0,7
24.12.88	12:00	36	66	66			117	0,975	0,79
01.04.89	17:00	42	83	98	85	32	85	0,767	0,33
17.04.89	01:00	53	85	97	77	24	109	0,816	0,34
11.07.89	01:00	39	48	60			389	0,351	0,23
15.12.89	12:00	33	74	91	35	18	85	0,391	0,12
17.12.89	06:00	26	84	103			60	0,443	0,34
14.02.90	06:00	35	51	61	6	16	219	2,074	0,17
01.03.90	02:00	20	51	58	28	9	113	1,123	0,66
	Averages	32	63	74	40	20			

Tab. 4-17 Lag Times and Peak Velocities of Different Flood Water Components

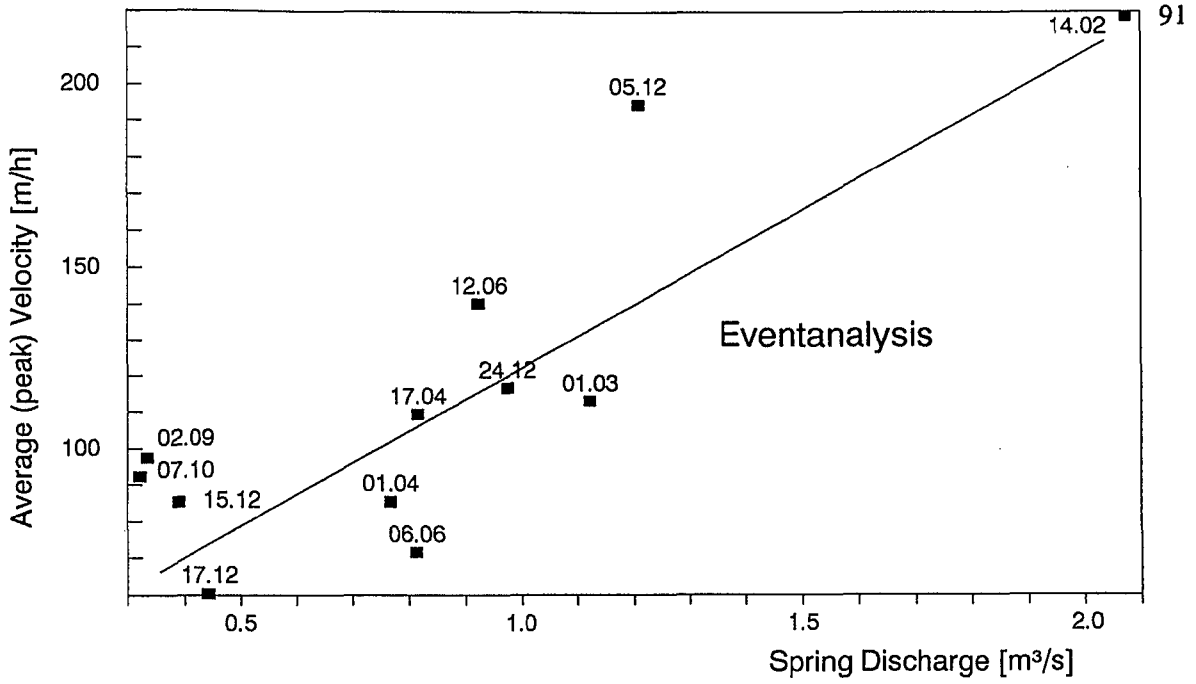

Fig. 4-42 Relationship Between Spring Discharge and Peak Velocity of New Recharge Water

which might have occurred close to the spring, induced the signals, and on the 11 December 1988, a gap in the measurements might have been the cause for an overestimate.

The average velocities are plotted against the maxima of discharge in Fig. 4-42. It becomes apparent that there is a more or less linear relationship between Q and v_a at low discharge, which seems to deviate from the straight line during extreme events, such as the one of 14 February 1990. Comparison of the results with tracer tests shows a similar relationship (Fig. 4-34). A comparison between the Q/v_a relationship for tracer tests in the Echaz catchment (Teutsch, 1988) and the above results shows that the change in conduit transport velocity in the Echaz catchment is approximately three times as high as the change in velocity in the Gallusquelle catchment for the same change in spring discharge. The mean discharge (0.67 m^3/s) and the catchment area (90 km^2) of the Echaz springs are somewhat higher than those of the Gallusquelle spring. The large difference in velocities can be explained by the higher degree in karstification and the large gradient in the conduit system of the Echaz catchment.

Assessment of the Fraction of the Fast Flow Component

As outlined previously (Chap. 4.5.3), the maximum discharge and the prominent changes in electrical conductivity and temperature are caused by a fraction of the recharge water, travelling very rapidly through subcutaneous and unsaturated zone and conduit system of the aquifer. It is therefore essential to accurately determine that particular quantity as a model input. Several methods were applied to quantify fast recharge. Sauter (1990) already attempted to calculate the fast components for the 1st and 14 April 1989 events. A similar approach was taken, some of the assumptions, however, were modified in the light of further knowledge, gained from additional measurements.

Tab. 4-18 lists the relevant cutoff times and the results of the different methods used for the quantification of the fast water percentage.

As outlined in Chap. 4.5.2, electrical conductivity can be used as an excellent tracer for fast water, assuming that the total spring flow consists of fast water, after subtraction of the pre-event discharge rate. This assumption is justified, because during the discharge of fast flow, somewhat higher potentials prevail within the conduit system, so that the contribution of slow water is somewhat reduced. *Fig. 4-43 demonstrates the idealised separation of the spring hydrograph, although the fast water separated, is in reality a mixture of several components, in which the fast water component is dominant (see also Williams, 1983, Fig. 4-13). The above procedure strictly speaking only applies to piston flow conditions.*

As discussed above, spring water temperature can be regarded as a fairly conservative tracer,

Event Analysis											Depth of fast water component					
Event	Increase discharge		Maximum Discharge		low Turbidity		Increase Elect. Cond.		Minimum Temperature		hydr [mm]	cond [mm]	temp [mm]	rech [mm]	fast water [mm]	% of rech
06.06.88	07.06	02:00	07.06	11:00	07.06	23:00	07.06	20:00	10.06	18:00	1,2	0,6		16,5	1,0	6,1
12.06.88	13.06	03:00	13.06	12:00	14.06	01:00	13.06	09:00	16.06	07:00	1,2	1,5		14,7	1,4	9,5
03.08.88																
02.09.88																
04.09.88																
07.10.88																
10.10.88																
05.12.88	05.12	03:00	06.12	14:00	07.12	06:00	05.12	21:00	07.12	21:00	3,2	2,9	3,1	47,7	3,0	6,3
10.12.88	10.12	17:00	11.12	04:00	11.12	19:00	11.12	15:00	13.12	05:00	4,1	3,3		40,7	3,5	8,6
24.12.88																
01.04.89	02.04	13:00	03.04	11:00	04.04	05:00	03.04	12:00	06.04	03:00	1,6	1,6	1,2	31,3	1,6	5,1
17.04.89	18.04	05:00	19.04	06:00	20.04	10:00	18.04	18:00	21.04	03:00	2,1	1,1		26,4	1,5	5,7
11.07.89	11.07	13:00	12.07	16:00	13.07	05:00	12.07	03:00	15.07	13:00	1,2	0,4		12,2	0,8	6,6
15.12.89	15.12	17:00	16.12	20:00	17.12	00:00	16.12	16:00	18.12	22:00	0,8	1,6		31,2	1,2	3,8
17.12.89	17.12	21:00	18.12	08:00	18.12	21:00	20.12	18:00	21.12	17:00				9,2		
14.02.90	14.02	12:00	15.02	17:00	17.02	00:00	15.02	08:00	17.02	03:00	6,4	6,3	5,8	72,1	6,2	8,6
01.03.90																

Tab. 4-18 Cutoff Times Used for Hydrograph Separation Methods (Fig. 4-43)

which is particularly applicable to the temperature change, induced by the fast water. Based on the criterion that the fast water component, displaced from the conduits, is negligible by the time the electrical conductivity recovered, a recession relationship can be used to separate the temperature changes, caused by the fast and the slow water. Assuming that during the lowest temperature the fast component represents 100% of the total flow, established component separation methods (Sklash and Farvolden, 1979, Pinder et al., 1969) can be applied to evaluate the fraction of the fast component on the total recharge (Fig. 4-43c).

A common approach to distinguish between two components is the simple recession analysis, assuming a distinct hydraulic response for each of the two systems (Maillet, 1905; Atkinson, 1977). Whereas the previously described methods quantify the event water components directly, i.e. the spring water analyzed, represents event water, the recession analysis considers the change in discharge as a result of the pressure pulse induced by the new recharge water, i.e. the change in discharge reflects the arrival of the fast event water component at the water table. This feature is very useful, because it helps to describe the time variation in the input to the groundwater system (Fig. 4-43a). The assumption, concerning the recession coefficient in Sauter (1990) is changed somewhat. It is assumed, as indicated above, that the return to more or less pre-event values of the turbidity (not considering the turbidity of the actual new water) determines the time when the proportion of the fast component, arriving at the water table becomes zero (Fig. 4-43a).

The results of the three methods are listed in Tab. 4-18, together with the recharge, applicable to the respective storm. However, depending on the event, one or the other method under- or overestimates that particular fraction. The separation method, using the temperature as a tracer should only be applied to the first storm of a series, because of the increased contribution of slow water during the later events.

The 1.2 mm of fast water (event 6.6.88), evaluated with the hydraulic method is probably too high. It cannot necessarily be assumed that all the water during the selected period is fast water, because the pre-event flow rate is a relatively large proportion of the total flood flow, i.e. the ratio - total/pre-event flow - is low. The end of the recovery of the electrical conductivity, difficult to determine, was estimated conservatively, which might have led to underestimates. The temperature method is somewhat arbitrary when the temperature change does not show a well developed peak. Taking into account the above, the fast water was estimated at 1 mm.

The high percentage of 9.5% of fast water, resulting from the event of 12 June 1988, can be explained by thunderstorms. The 1.5 mm, estimated with the electrical conductivity method are probably too high, because only the lower pre-event discharge of 6 June 1988 has been subtracted.

The average of all three methods was taken to determine fast flow for 5 December 1988 as well as for 10 December 1988. The higher percentage for the latter event can be explained by the assumption that the subcutaneous zone was

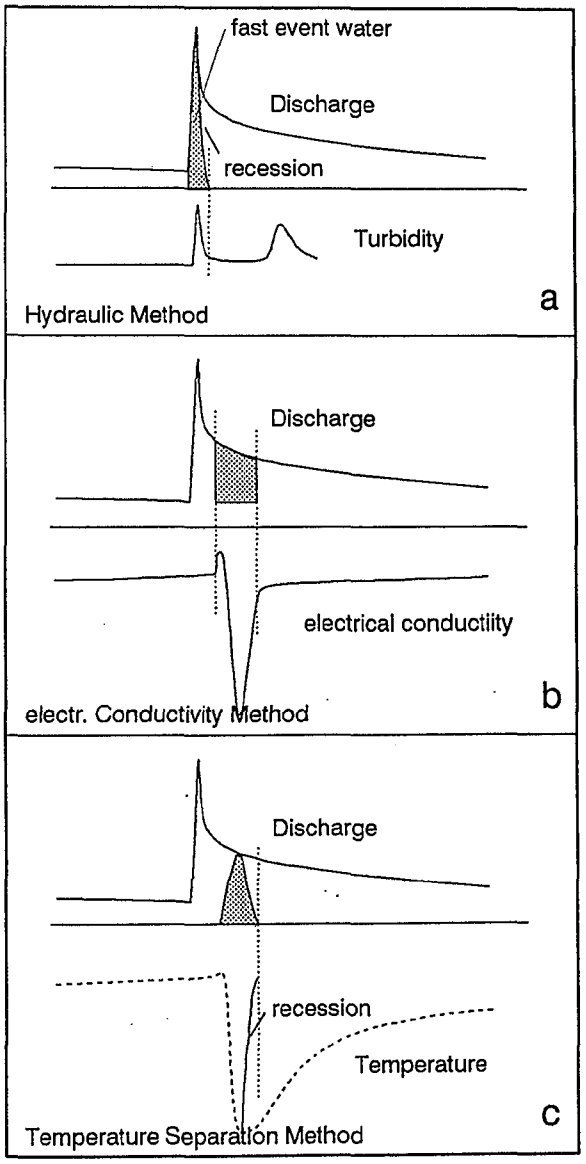

Fig. 4-43 Methods Used in Hydrograph Separation for Fast Water Component (Shaded)

still replenished from the previous event.

On the 1 April 1989 event, electrical conductivity and hydraulic method agree well and preference was given to those two values, because the assumption on 100% fast flow during minimum temperature might be difficult to uphold at low ratios of event/pre-event flow.

On the 17 April 1989, the subcutaneous zone is relatively full, however, because of the low event/pre-event discharge ratio, the hydraulic method might overestimate the fast component. The percentage of 5.7% might be somewhat too low. Local raingauges indicate that the recharge evaluated using areal values (Chap. 2.5) at 26.4 mm is probably too high.

The average of all methods used was taken for the determination of the fast component of the events of 11 July 1989, 15 December 1989 and 14 February 1990.

Generally the results of all three methods agree very well and a value of between 5% and 9%, depending on the specific circumstances, such as season and rainfall intensity, can be assumed with confidence to represent the fast flow component of a particular recharge event.

The definition of "short-term" recharge differs between different authors. Dreiss (1989a) defines that quantity as water causing some physical dilution of old background discharge, measured with the concentrations of Ca^{2+}, Mg^{2+} *and* HCO_3^-. *Dissolution at the surface and in the subsurface as well as contributions from surface storage and redistribution in the vadose zone (i.e. effects from subcutaneous zone are considered negligible). These assumptions are probably only valid in dolomite aquifers, such as the catchments of the described Missouri springs. Applying the same hydrological separation procedure as used in the electrical conductivity method, the author calculates the proportion of new water in the total discharge at 25%, assuming that the chemical composition of the water, discharged at the end of a drought represents the concentration of the old "long-term" water. In Dreiss (1989b), a seasonally varying concentration of old water was applied in connection with the evaluation of kernel functions, however no totals were calculated. The variations in Ca, Mg and* HCO_3 *appear to be of a similar shape to the temperature series measured in the present study. Dreiss (1989a) did not distinguish between fast and slow event water, although the responses of the aquifers appear to be comparable to the Gallusquelle catchment.*

Behringer (1988) evaluated short-term event discharges in carbonate aquifers, using Mg^{2+} *as a tracer. Similar percentages, varying between 6% and 42% and an arithmetic mean of 20%, for hydrologically comparable springs (deep karst, Teutsch, 1989) were determined for shallow and deep karst aquifers.*

Using temperature as a tracer, the short-term component of the discharge at the Gallusquelle can be calculated by assuming that the Nov89 temperature of 8.73°C represents the temperature of old water, that the minimum temperature of the respective event indicates the input temperature of the respective recharge water,

and by extrapolating successively every temperature anomaly, using a recession relationship, to the assymptotic temperature of 8.73°C. A percentage of approximately 30% of the total flow is computed, which is well in the range of percentages, calculated by Behringer (1988) and Dreiss (1989a).

The significance of this percentage is however somewhat questionable, because it does not necessarily give any quantitative information on the hydraulic and transport characteristics of the aquifer, nor any information on turnover times. It is predominantly determined by the chemical solution kinetics within the aquifer (Behringer, 1988, Dreiss, 1989a), by the heat transfer between water and aquifer material (present study) and by the processes in the subcutaneous and vadose zone, if longer periods than a few days are considered. The values however can be used as a qualitative measure for hydraulic response characteristics, to compare aquifers of similar mineralogical composition.

Longterm Aquifer Response and Turnover Times

The temperature variation of the observation period, as displayed in Fig. 2-19, is a good indicator for the longterm aquifer behaviour. Depending on the input temperature of the event water, the memory effect of a particular event, i.e. the time period during which aquifer response can be traced back to a certain recharge event varies between two and three months. This period is less in summer and up to approximately five months after winter recharge events. The long-term temperature effects are usually due to the slow release of water from groundwater storage.

Frequently, longterm seasonal variations in the $\delta^{18}O$ of spring or surface water are compared with the variation of $\delta^{18}O$ in rainfall input. The damping of the amplitude of the input function, assuming a completely mixed aquifer, can be used to calculate turnover times (Stichler et al., 1984). *However, Fig. 2-19, representing the longterm variations in $\delta^{18}O$ of spring water does not indicate any long-term regular seasonal variations. The relative abundance of ^{18}O appears to be rather determined by the short-term effect of the previous recharge event.*

Fig. 4-44 displays the monthly averages of spring flow $\delta^{18}O$ and rainfall $\delta^{18}O$, together with the respective monthly discharge, recharge and precipitation. It is apparent, that $\delta^{18}O$ in precipitation is lower in winter and higher in summer, which is obvious. However, no regular pattern can be deduced from the input $\delta^{18}O$ graph. The response function from spring water reveals also the same effects as observed in the non-averaged $\delta^{18}O$ graph that the spring $\delta^{18}O$ is determined by the $\delta^{18}O$ of the most recent recharge water.

The $\delta^{18}O$ spring water graph shows an interesting feature, which might have become apparent solely because of the low recharge in 1989. This feature consists of a general tendency of the $\delta^{18}O$ to lower values, reaching a minimum in Oct89. Water, which is relatively light in $\delta^{18}O$ is discharged at low groundwater levels. When there is no interference with isotopically heavy summer recharge, the $\delta^{18}O$ drops to even -10.9‰. This low rate, isotopically light discharge is interpreted, as already discussed above, as very old (several years) winter recharge, which could penetrate into lower aquifer zones, due to the then prevailing high groundwater potentials. During low flow conditions, this old groundwater is released from storage, which is most likely located further upgradient in the central and north-western part of the catchment. The observed behaviour of the spring water $\delta^{18}O$ indicates a pronounced layering in isotope ratios, which invalidates assumptions of homogeneously mixed aquifers, which is a prerequisite for applying the hydraulic exponential model.

Assessment of the Temporal Distribution of Recharge Input

A similar approach for the determination of the temporal distribution of groundwater recharge as described by Sauter (1990) was taken.

The input to the system can be derived from hydraulic considerations for both components, fast and slow spring flow. The spring discharge and the response of the groundwater hydrographs reflect the interplay between input to and outflow from the aquifer and can be used for a description of the input.

Fast Recharge Input

The event of February 1990 is used to demonstrate the procedure, because the storm of 14 February 1990 occurs as a sharp signal and it can be assumed that the subcutaneous store is fully replenished. There is however some interference by an event at the end of February 1990.

The pressure pulse, due to the fast water,

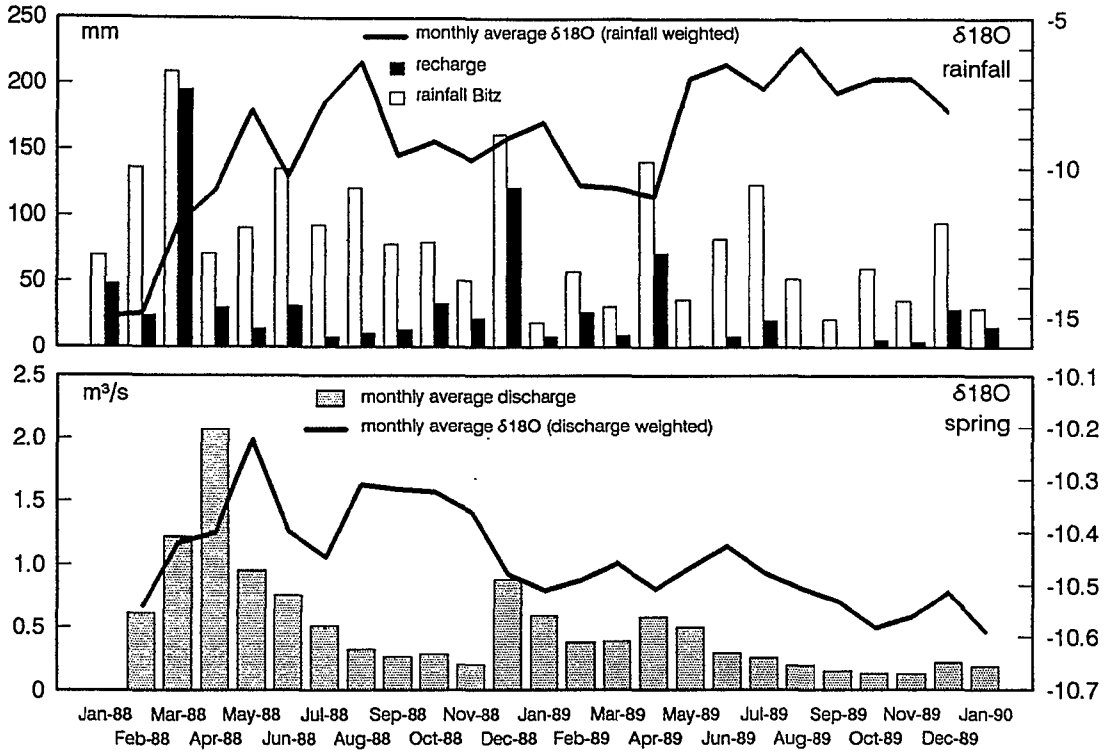

Fig. 4-44 Longterm Variations in Relative Abundance of Oxygen Isotopes in Rainfall and Spring Water

analyzed above (Fig. 4-43a), is closely related to spring discharge during the first few days. Most of the fast input (Fig. 4-45) occurs two to three days after the storm, approximately 2/3 on day two and 1/3 on day three. Although the analysis of the hydrograph gives more detailed information on the distribution of fast input, the model (Chap. 5) requires input on a daily basis.

Slow Recharge Input

The arrival of the slow recharge input at the water table can be described by comparing spring discharge (slow flow) and groundwater hydrographs (Fig. 4-45). The rate of water released from the subcutaneous zone is higher than the discharge (slow flow) during periods of rising water level and lower, when the potentials drop. At times of no head change, both quantities are equal.

The total volume of slow spring discharge (output) and the total volume of subcutaneous flow must be equal for a particular event. Considering that fast flow amounts to approximately 6 mm (Tab. 4-18) and that the calculated recharge is 72 mm, the total slow spring discharge should amount to 66 mm. By extrapolating the groundwater hydrographs and correcting for the event of 26-28 February 1990, stored groundwater due to the event of 14 February 1990, is found to have returned to zero by the end of June 1990. The extrapolated slow spring flow volume (Fig. 4-45) amounts to approximately 60 mm by the middle of June, which is sufficiently accurate, taking into account the relatively crude extrapolation methods.

For the construction of the total subcutaneous flow curve, several assumptions have to be fulfilled:

1.) The total subcutaneous flow volume is equal to the slow spring flow volume

2.) The total subcutaneous flow rate is equal to the slow spring flow rate during periods of negligible head change, which is the case between the 22nd and the 28th February 1990.

The observations of Renner (1991) (Chap. 4.1.3) indicate that there is still some noticable drainage from the subcutaneous zone after 1.5 months. The information from Tab. 4-4a on fast subcutaneous storage reveals that, if 0.4 mm is assumed to be the minimum fast subcutaneous storage, the drainage from slow subcutaneous zone is negligible after 2.5 months (18.4.89 - 11.7.89), assuming that the slow subcutaneous

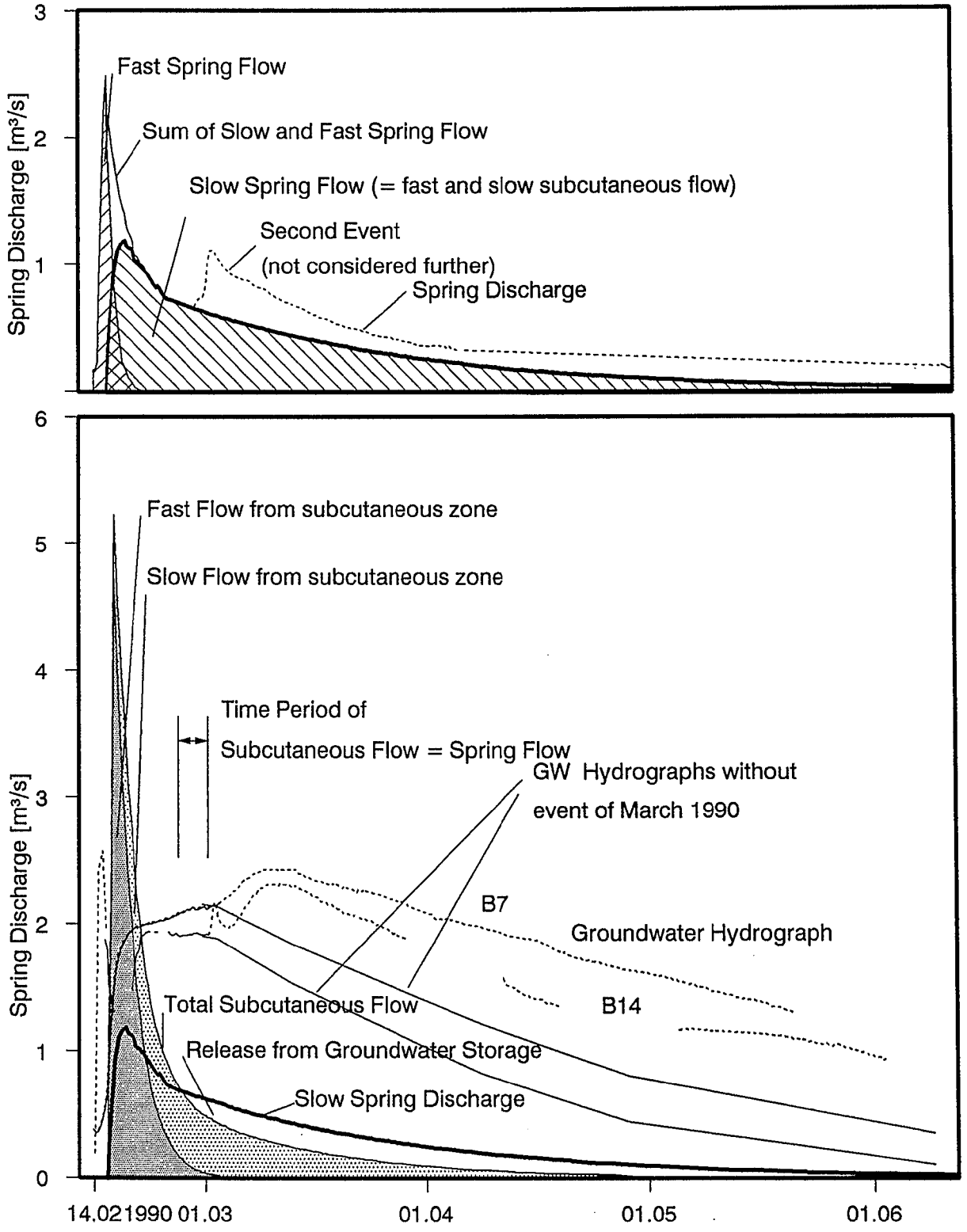

Fig. 4-45 Quantification of Temporal Distribution of Slow Recharge Component

store is replenished on 18 April 1989. Smart and Friederich (1986) also evaluated a drainage period from the slow subcutaneous store in the order of 2 months.

The implications for the subcutaneous flow rate curve are therefore that the flow is negligible after 2 months, providing the slow subcutaneous store is full (30 mm, see Chap. 4.2.1) and that the flow from fast subcutaneous storage exceeds the rate of the slow spring flow with a maximum coinciding with the time of the inflection point of the groundwater hydrograph.

The use of the hydrograph as a qualitative indicator for the subcutaneous flow rate assumes that there is no vertical change in hydraulic conductivity and storage within the phreatic zone. It has however been shown (Chap. 2.6.1) that there is a high storage/hydraulic conductivity horizon within the area surrounding B14 (685 m - 689 m) and B7 (660 m - 663 m). During the event of 14 February 1990, the water levels during the time of no potential change lie well within that zone, which implies that, although the head is less sensitive to a change in subcutaneous flow rate, the groundwater head is still a very good indicator for the relative subcutaneous flow, i.e. the slow recharge input.

Smart and Friederich (1986) demonstrated that the drainage from the subcutaneous zone follows an exponential relationship. However, a fast initial drainage and a subcutaneous flow lasting over several months cannot be described with a single recession curve. Therefore, the total subcutaneous flow is calculated by the superposition of slow and fast subcutaneous flow (Fig. 4-45), which also has a physical basis as discussed in Chap. 4.1.3, using a double porosity approach. Each of these recession curves requires information on the capacity of the respective store (initial flow, Q_o) and the recession coefficient. The initial storage volume for the slow subcutaneous zone was determined in Chap. 4.2.1 at approximately 30 mm and the recession constant can be calibrated so that there is negligible flow after approximately 2 months.

The fast subcutaneous flow determines the time, during which slow spring discharge and total subcutaneous flow are equal. The flow from the slow subcutaneous store is relatively constant, compared with the change in flow rate from the fast subcutaneous store. The capacity (initial flow) is however difficult to determine. For the above analysis, the difference between the slow spring discharge volume and the slow subcutaneous flow volume (30 mm) was used. Although this figure might vary, depending on the event, implying some consequential changes to the recession coefficient, but because the fast recession coefficient is relatively high, the shift in the time of equal subcutaneous flow and spring flow lies in the order of hours to a day.

The recession coefficients α (Maillet, 1905) were determined at 0.05 day^{-1} for the slow and at 0.38 day^{-1} for the fast subcutaneous flow system. These parameters can be used to the percentual recharge distribution of an idealised sharp recharge event on a daily basis.

5 Flow Modelling

As outlined in Chap. 3.4, a double porosity or double continuum approach is the most appropriate for the modelling of groundwater flow in the Gallusquelle catchment or generally karstified limestone aquifers, especially if there are not enough data available for modelling discrete discontinuities. The data, gathered on aquifer geometry (Chap. 2.6.1) hydraulic parameters (Chap. 4.2, 4.3), recharge input and its temporal variation (Chap. 4.1, 4.5) were used as model input.

5.1 Model Geometry and Boundary Conditions

A one-dimensional double-continuum model (Teutsch, 1988) was chosen because the modelled area can be approximated by a strip of approximately 4200 m with the exception of the area of flow convergence near the spring and because the information on the lateral variation of aquifer parameters and aquifer geometry is very scarce. At the development stage, it also helps to keep the model as simple as possible in order to be able to concentrate on modelling the dominant effects. The model described by Teutsch (1988) was modified in order to include the variable aquifer bottom, determined in Chap. 2.6.1 and to allow recharge into both, the conduit and the fissured system (Fig. 5-3a). It was found (Chap. 4.5) that a significant fraction of the total recharge (5%-10%) reaches the water table directly via solution shafts, without being substantially delayed by the subcutaneous zone. Contrary to the model of Teutsch (1988), no flow reached the spring via the matrix system, i.e. all the water had to pass via the conduits, which corresponds to the field situation. The interval between model nodes was fixed at 500 m, which is a result of the scale of resolution of aquifer geometry and the detection scale at which regional variations in aquifer parameters can be observed. The discretisation interval does not reflect any lithological units within the aquifer, e.g. the average block size, because in a continuum approach, the model does not incorporate such features per definition.

Although observed in the field, vertical changes in aquifer parameters, i.e. discrete horizons, were not included in the model, because the available data did not allow the specification of all the heterogeneities within the aquifer. It was also attempted to construct the model at the same time as realistic as necessary and as simple as possible for practical application. A reduction in hydraulic conductivity near the aquifer base had to be introduced into the model, in order to be able to simulate low flow, while at the same time high gradients had to be kept up within the aquifer. Initially, this change was integrated into the model by reducing the hydraulic conductivity to a fraction of the initial value below a certain threshold. This approach led to convergence problems, especially in the area where the highest change in gradient occurs, because between iterations, the calculated head oscillated between the high and low K horizon, a behaviour, which was particularly expressed around km 4 and km 7. In this region, it is very likely that neighbouring cells have water levels in the high and the low K zone. In order to avoid the abrupt change in K, the hydraulic conductivity was gradually reduced with decreasing saturated thickness (m_{sat}) ($K_{new}=-K_{old}*m_{sat}/20$). The constant "20" indicates that below a threshold of 20 m, the new hydraulic conductivity is gradually reduced, a value, which is within the observed range of the identified active aquifer. The spring was simulated as a fixed head.

The distribution of recharge, as evaluated in Chap 4.1.3 was used in the model.

5.2 Unsteady Simulations

In calibrating the numerical model, the following steps were taken. First of all, in order to save computing time and because the data base, i.e. recharge and its temporal distribution, spring flow and hydrograph readings was far superior to other time periods, the simulation of the period 1987 to 1990 was first attempted. A new weir was installed at the Gallusquelle spring in 1987, which guaranteed accurate measurements at least for that particular period. In previous years, water could frequently bypass the gauge, particularly during flood and low flow conditions. The continuous readings of groundwater hydrographs between 1988 and 1990 previously measured at weekly intervals guaranteed the registration of also minor recharge events.

After the initial calibration, performed with a time step of 1 day, the modelled period was extended to 25 years (1965-1990) and examined for major and significant and systematic deviations.

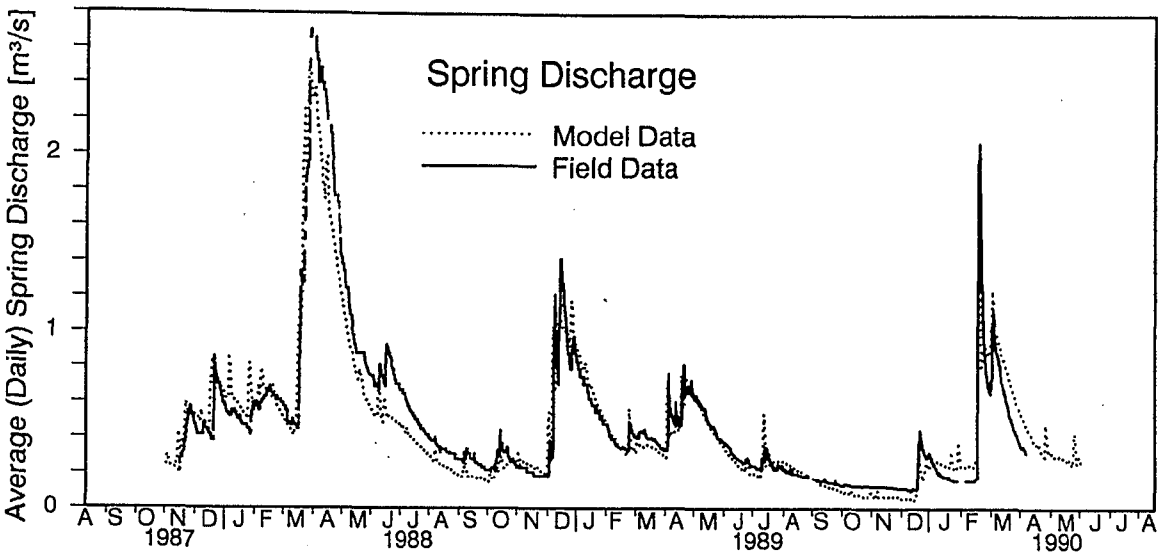

Fig. 5-1 Comparison Between Model and Field Spring Discharge (Period 1987-1990)

5.2.1 Period 1987-1990

Fig. 5-1 and 5-2 display a comparison between modelled and field data of spring flow and groundwater hydrographs. It is apparent that the fit between both time series is very good, considering the type and number of assumptions made in connection with the recharge calculation, the distribution of recharge over time (subcutaneous zone), including the distribution of snow melt, parameter evaluation and aquifer geometry.

The head deviations during the snow melt event of April 1988 in spring flow can possibly be explained by an underestimate of the total recharge. The evaporation from a snow cover is not very well understood and because of a high spatial variability difficult to assess.The differences in modelled and measured hydrographs are a result of the fact that the model does not include a vertical change in the storage coefficient, which had been observed in the field. It can be seen that the change in head is larger in the field than in the model data during April 1988 up to a level of approximately 662 m asl in well B7, which implies that the model storage coefficient is too high for levels above this threshold, considering that the flow is modelled accurately. Below 660 m asl, the selected model storage is too low. Therefore, the calibrated storage coefficient is an average for the entire aquifer thickness. There are not enough data available to include a threshold for a change in storage in the vertical dimension in the model. The large lateral variation in the parameters makes it impossible to allocate a definite value to a certain cell.

Fig 5-3 demonstrates that the regional gradient and the observed range of water level fluctuations could be reproduced.

In well B14, the water level decline could be reproduced better, because the aquifer appears to behave more homogeneously in the surroundings of this particular piezometer.

5.2.2 Period 1965-1990

Fig. 5-4 and 5-5 display the comparisons between modelled and field data (discharge and groundwater hydrographs) for the period 1976 to 1987. The results of the period 1965 to 1975 are included in app. 5-1. The match between both sets of data is generally good. The main features in the hydraulic responses could be reproduced, such as the recession, the variation between minimum and maximum discharge and the variation of groundwater levels. Observed differences can be explained by the absolute recharge depth (Chap. 4.1.1.5) and by the temporal distribution of groundwater recharge, in particular the snowmelt. It is believed that the match could be further improved by examining the water release of snowmelt in detail, which however requires further substantial research efforts and is beyond the scope of the present project. It generally appears that water is released too early from the snowpack (Dec 1972, Dec 1976, Jan 1980, Feb 1986) so that modelled recharge is too low in late spring. These minor inconsistencies are also reflected in the responses of the groundwater hydrographs.

The differences between model and field

data at low flow conditions (1969, 1981, 1983) are also most likely connected to the temporal distribution of recharge and to the characteristics of individual rainfall events, that could not be reproduced by the areal recharge estimation. The approach used in the evaluation of areal groundwater recharge does not make allowances for processes, that are specific to a particular season.

5.3 Calibrated Model Parameters

Tab. 5-1 lists the model parameters required for unsteady state simulation of a karst aquifer employing a double continuum approach.

As will be shown in Chap. 5.4, the variation in discharge measured at the spring is highly sensitive to the hydraulic parameter, controlling the exchange between slow and fast system and not very sensitive to the hydraulic conductivity of the fast flow system itself.

The advantage of the definition of the exchange term in the double-continuum approach is that it does not require the evaluation of the geometry of the blocks of the slow system. The exchange term includes an expression, consisting of the hydraulic conductivity, the distance across which the potential drop occurs and the throughput area. Together with the knowledge of the model calculated head difference between fissured and conduit system, the cross-flow rate can be calculated. The fact that the hydraulic conductivity of the fissured system cannot be singled out from the exchange term implies that model hydraulic conductivities can only be evaluated by making certain assumptions concerning the dimensions of the fissured system blocks. As described in Chap. 4.3.1, this particular length scale can be estimated for the Gallusquelle spring catchment in the order of 500 - 1000 m. The hydraulic conductivities for the slow system were evaluated using the flow from the fissured to the conduit system for a particular time step, normalizing it per square meter and extracting the potential difference from the model. The length over which this potential drop occurs was assumed to be 1000 m.

The hydraulic conductivities (K_{regfis}) vary within a very narrow range of 1 to $5*10^{-6}$ m/s and the difference between the three different areas is not very large. These values correspond to hydraulic conductivities measured by large scale pumping tests (Chap. 4.3.1.2) which ranged from $1*10^{-6}$ m/s for more or less unkarstified rock to $1*10^{-5}$ m/s, representing average hydraulic conductivities. Higher values were determined in valleys where a major component of the flow occurs in the conduit system. The values of the regional evaluation of the hydraulic conductivity of the fissured system produced slightly higher values than the model. This could be a result of the assumption that at low flow conditions the total throughput of all three zones occurs only in the regional fissured system, which is physically probably not very realistic, because the drainage is primarily towards the respective conduits. This means that the water derived from the fissure system of the north-western area does not flow through the fissure system of the central region, but bypasses it via the conduits. The same reasoning applies to the

Parameters Used for Model Calibration
FLOW MODEL
1. Hydraulic Conductivity of Fissured System
2. Hydraulic Conductivity of Conduit System
3. Storage Coefficient of Fissured System
4. Storage Coefficient of Conduit System
5. Elevation of Aquifer Base
6. Threshold for Reduction in Fissured System Hydraulic Conductivity Close to Aquifer Base
7. Throughput Area for Conduit Flow System at the Spring (Transmissivity, together with (2.))
8. Recharge Input (see Parameter List of Tab. 4-1)
additionally
a. Snow Accumulation and Melt Release (Degree Day Factor)
b. Temporal Distribution (Storage and Flow Recession Parameters of Subcutaneous Zone)
c. Rapid Recharge Threshold
d. Ratio Fast / Slow Recharge Component
TRANSPORT MODEL (additional parameters)
1. Dispersivity of Fissured System
2. Dispersivity of Conduit System

Tab. 5-1 Parameters Used for Model Calibrations

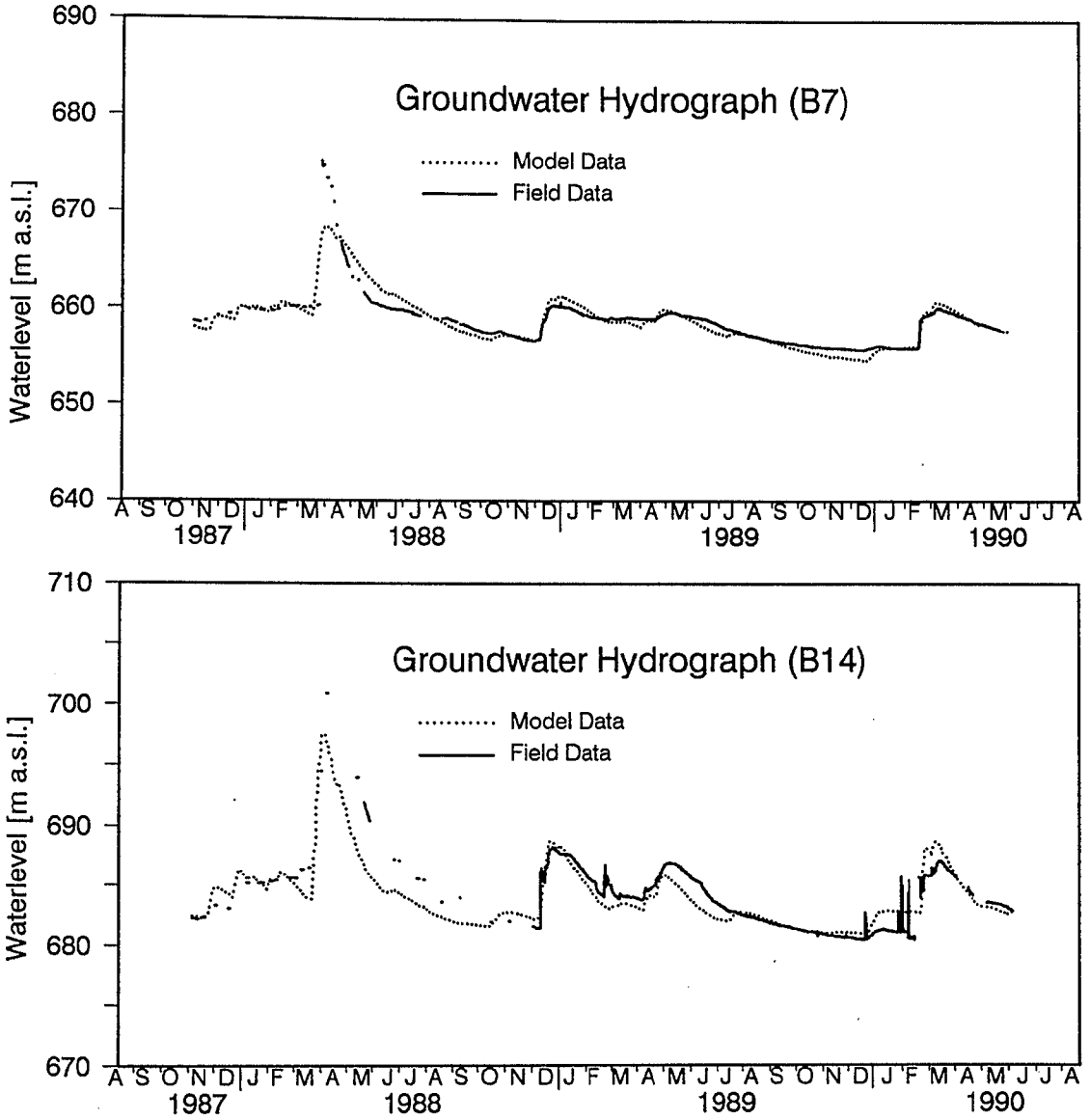

Fig. 5-2 Comparison Between Model and Field Groundwater Hydrographs (Period 1987-1990)

hydraulic conductivity of the central and south-eastern region.

There is also a major unknown in the estimation of the regional hydraulic conductivity, i.e. the estimation of the saturated thickness, which has been estimated somewhat low (conservatively), based on the information on aquifer geometry, implying a higher K_{regfis}.

In the south-eastern area, the contribution of the conduit system can be assumed to be higher, and in the north-western region, the karstified ox2 limestones might have a major influence on the flow.

All these effects generally lead to a higher regional hydraulic conductivity of the fissured system and therefore a possible overestimation of the hydraulic conductivity of the fissured system.

In sum, the above considerations possibly lead to a reevaluation of the analysis of the field data and by applying some further corrections to the field values, the hydraulic conductivity of the slow flow system can probably be ranged between 10^{-5} m/s and 10^{-6} m/s, which is the same order of magnitude as the model parameters. A detailed analysis, of the contributions of the different flow systems requires further research into the inherent scale dependencies.

The model continuum hydraulic conductivities of the fast (conduit) system can be ranged somewhere between 0.035 m/s and 0.052 m/s at the model gradient of 0.0001. As shown in Fig. 5-3, the basis of the conduit system is horizontal and set below the level of the spring. Therefore, in order to be able to convey the water to the spring at such a low gradient, the hydraulic conductivity had to be increased to an unrealistically high value. Assuming a realistic gradient of approximately

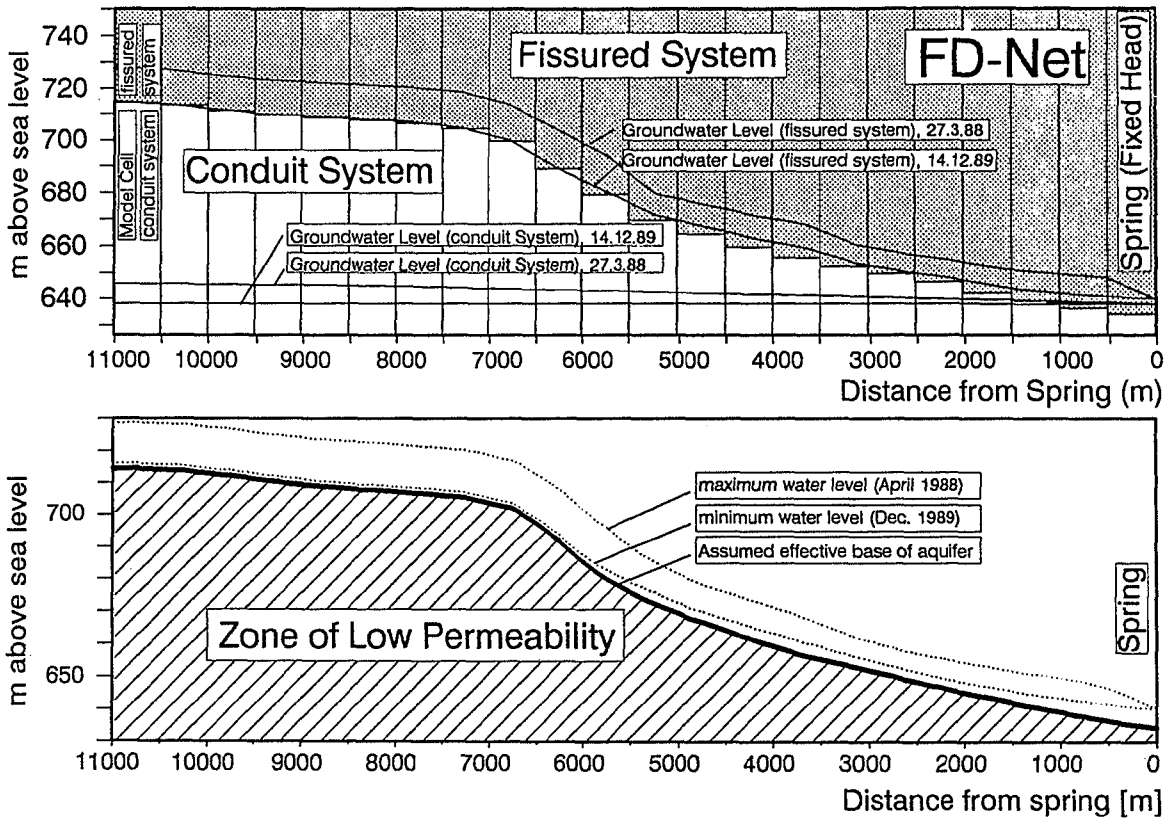

Fig. 5-3 Model Discretisation and Regional Head Variation in the Model

0.0075 (Chap. 2.6.1, parallel to the base of the aquifer), continuum hydraulic conductivities (conduit system) of between 0.00045 m/s and 0.0007 can be calculated. These values compare well, with those, determined in the regional assessment of hydraulic conductivity (Chap. 4.3.1.1) of between 10^{-3} m/s and 10^{-4} m/s. As long as the product of hydraulic conductivity and gradient is constant, such a procedure is viable. As shown in Chap. 5.4, the flow is not very sensitive to this parameter and only the velocities from tracer tests in the fast

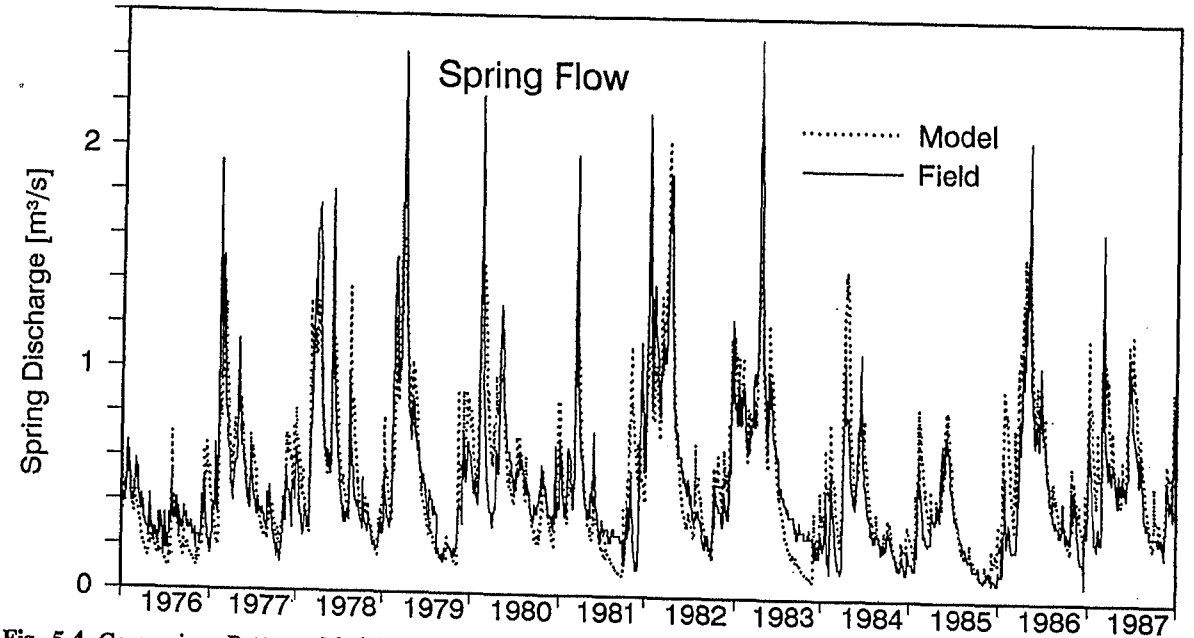

Fig. 5-4 Comparison Between Model and Field Discharge for a Longterm Record (1976-1987)

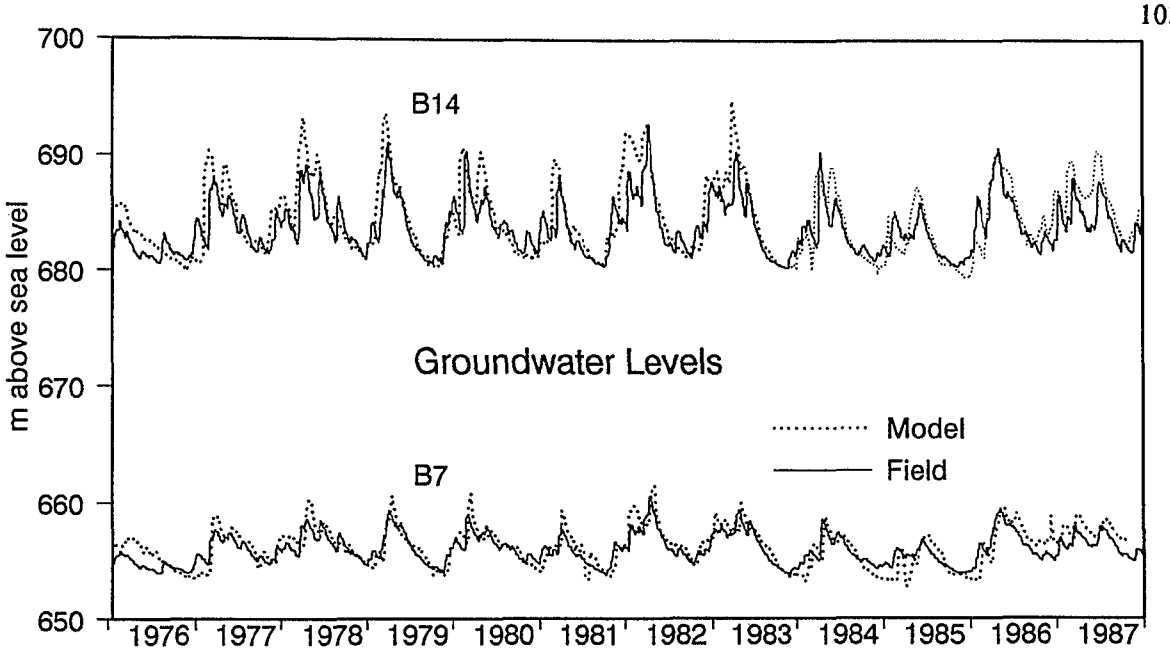

Fig. 5-5 Comparison Between Model and Field Groundwater Hydrographs for a Longterm Record (1976-1987)

system help to narrow down this parameter. The velocities, obtained from these tests however depend on the hydraulic gradient, which in turn depends on the unknown geometry of the base of the conduit system. In the model, this base was kept just below spring level, which is unrealistic, but because of the lack of detailed information and due to the lack of sensitivity to $K_{regcond}$, the above solution was accepted. Despite these simplifications, the model is capable of simulating both, flow and transport through both, slow and fast system, by applying physical deterministic principles. Further work is required to better include the geometry of the fast system in the model.

Model storage coefficients vary between 0.008 and 0.025 for the slow fissured system with the lower values upgradient in the northwest. In the conduit system, $S_{regcond}$ was assumed to be constant using a value of 0.0001

5.4 Sensitivity Analysis

A groundwater flow model, capable of accurately simulating aquifer flow and potential changes has to necessarily be sensitive to changes in the hydraulic parameters. The sensitivity to either hydraulic conductivity or storage coefficient reflects how accurately a model can be tuned and how useful it might be as a predictive tool.

In total, six different variables were selected, which were increased and decreased in order to test the response of the flow and the water level changes as compared to the calibrated model. Those were:

- storage coefficient, fissured system (S_{regfis})
- hydraulic conductivity, fissured system (K_{regfis}, flow only in fissures)
- fissure-conduit exchange coefficient (actual K_{regfis})
- transmissivity, conduit system ($T_{regcond}$ at spring)
- hydraulic conductivity, conduit system ($K_{regcond}$)
- storage coefficient, conduit system ($S_{regcond}$)

The difference between the 2nd and the 3rd parameter is that the fissure-conduit exchange coefficient actually represents the hydraulic conductivity of the fissured system, due to the flow pattern within the karst aquifer from the slow to the fast system, i.e. there is no substantial quantity of water, that only flows within the fissured system and discharges at the spring. The hydraulic conductivity of the fissured system in the model is very low, which is the reason why a variation in this parameter did not significantly affect the model output.

Fig. 5-6 a,b and 5-7 a,b show the variations of spring flow and groundwater hydrographs to changes in the storage and the hydraulic conductivity of the slow/fissured system respectively. A two fold increase in K_{regfis} or S_{regfis} has more or less the same effect on the spring flow as does the halving of S_{regfis} and

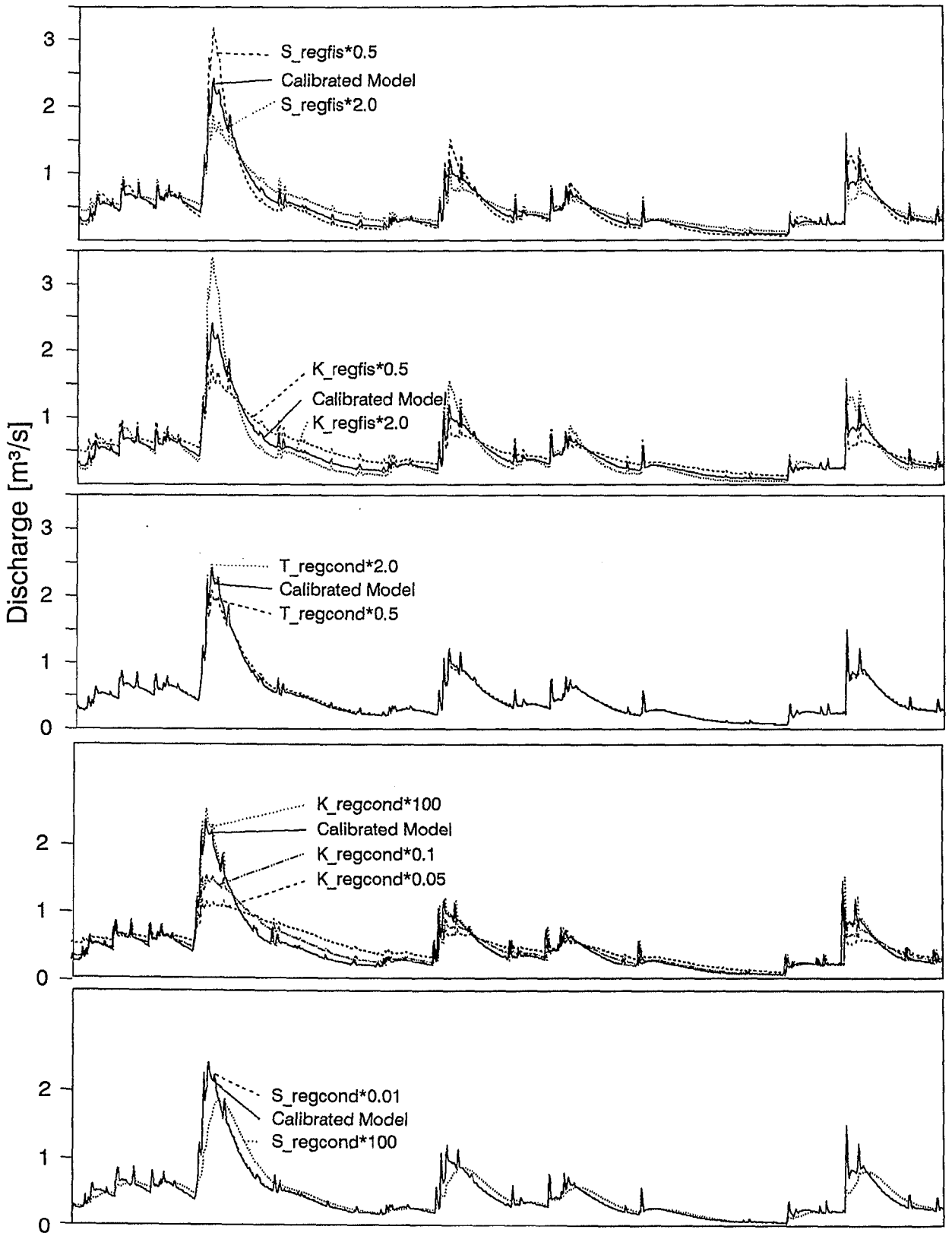

Fig. 5-6 Sensitivity Analysis for the Variation in Spring Discharge with Changing Hydraulic Parameters

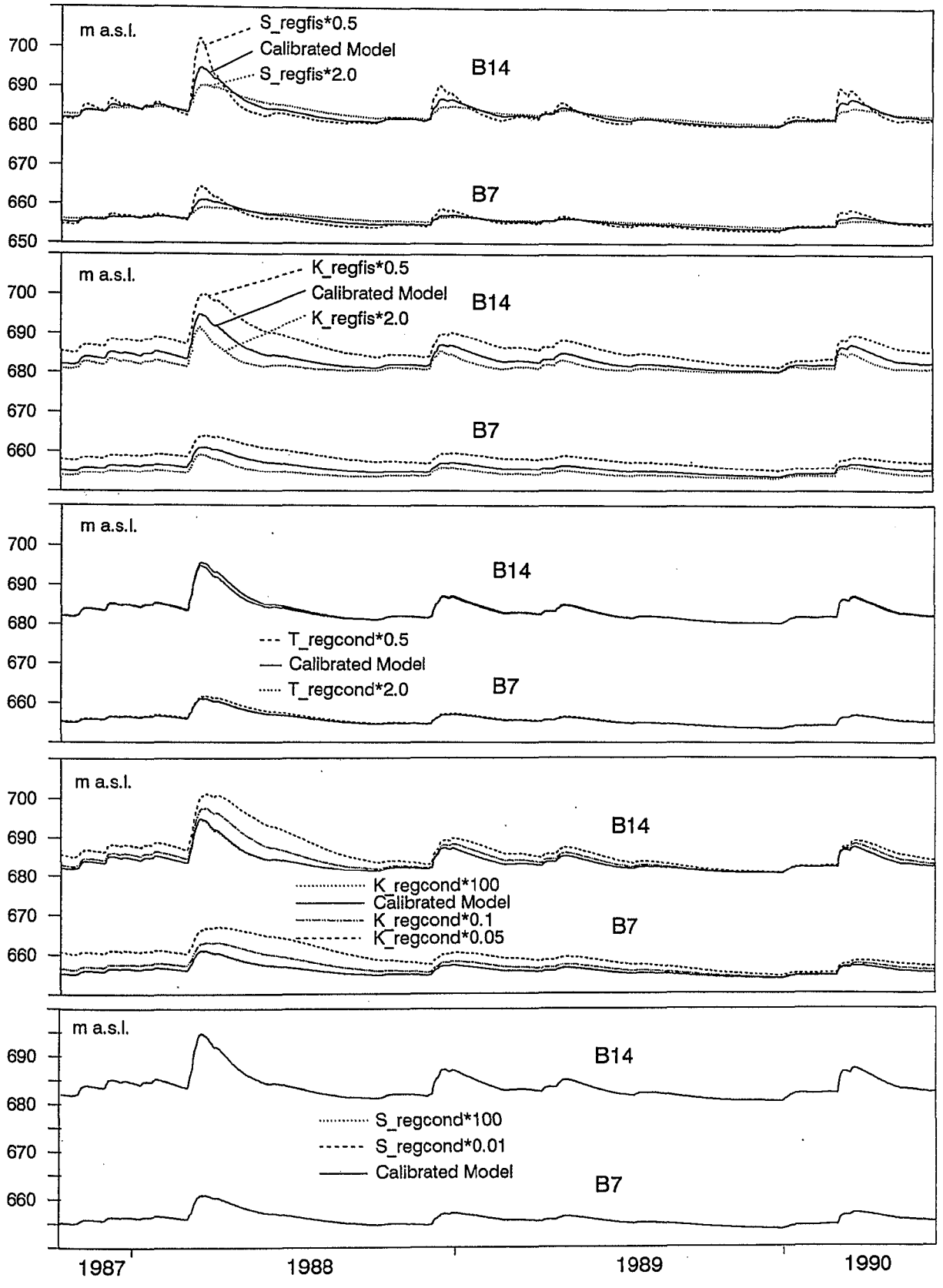

Fig. 5-7 · Sensitivity Analysis for the Variation in Groundwater Hydrographs with Changing Hydraulic Parameters

K_{regfis}. The comparison of the groundwater hydrographs for the same set of sensitivity runs however reveals a marked difference. Whereas an increase in S_{regfis} causes, as expected, a damping of the water level fluctuations, leads an increase in K_{regfis} not to a change in the shape of the hydrograph but to more or less a decrease in the absolute level and a slight decrease in the amplitude. *This different response in the water levels helps to eliminate ambiguities that result from a simultaneous change in S and K and enables the individual selective calibration of each hydraulic parameter.*

The variation in the crossectional area at the spring, i.e. the change in transmissivity at the spring (simulated as fixed head), hardly had any influence on the discharge and groundwater hydrographs. The reduction in transmissivity could be compensated by an increase in gradient in the conduits.

In order to have any response in spring flow and the groundwater hydrographs, the $K_{regcond}$ had to be increased or decreased substantially. Fig. 5-6d, Fig. 5-7d display the change in hydrographs as a result of a ten fold in/decrease and a twenty fold decrease. The variations are comparable to those of Fig. 5-6b and Fig 5-7b in K_{regfis}. The lowest value ($K_{regcond}$ multiplied by a factor of 0.05) is in the same order of magnitude (5 times higher) as the hydraulic conductivity of the fissured system. *It has to be noted that an increase in $K_{regcond}$ by a factor of ten causes hardly any increase in discharge. This demonstrates that the controlling part of the system, as far as flow is concerned, is the fissured system.*

A change in the storage of the conduit system (Fig. 5-6e, 5-7e) did not affect the model flow and the hydrographs either because only a small percentage of the recharge reaches the fast system directly and there is hardly any head build-up in the conduits due to their high hydraulic conductivity. The influence of a change in $S_{regcond}$ did not affect the spring discharge and the groundwater hydrographs except when the storage of the conduits was increased by a factor of 100, which is the same order of magnitude as that of the fissured system.

6 Transport Modelling

The simulation of the transport of a certain compound in groundwater represents an integrated analysis of a groundwater system. It requires the simulation of the hydraulics of the aquifer as well as the recognition and the quantification of the different transport processes. In order to be able to model transport in a karst aquifer and to calibrate the model results, the different output signals from transport processes need to be categorized and analyzed with respect to the part of the whole system, that influences the signal the most.

Primarily it has to be distinguished between areal source and point source input (Teutsch and Sauter, 1991). Some of the parameters used in areal source transport, such as turbidity and electrical conductivity are more selective for the fast system and some provide information on both systems and their interaction ($\delta^{18}O$, temperature, (Chap. 4.5)). Point source tracer tests can reflect the characteristics of the conduits (input in sinkhole), the diffuse/fissured system (forced gradient test between two boreholes) or a combination of both (test with input in borehole and tracer breakthrough monitored at spring).

The response of the model to all these different situations can be considered as the criterion for the versatility and usefulness of the model for different conditions.

6.1 Model Selection, Geometry and Boundary Conditions

In order to guarantee numerically stable solutions of groundwater transport simulations in advection dominated problems, a particle tracking method was selected. Models, solving the actual transport equations with the Finite Element or Finite Difference method would require very small discretisation intervals and consequently large storage and computing times. The model of Teutsch (1988) was selected and modified in order to allow for areal source input, including the temporal variation, a sloping base of the aquifer and a spatial variation in parameters.

The transport simulation is based on the hydraulic model, described in Chap. 5. The tracer input was generated based on the delayed recharge input under the assumption of a conservative tracer.

6.2 Unsteady Simulations

As previously described, the transport model can be applied to several different test situations:

- point source input into sinkhole, sampling at the spring (test for conduit system).
- point source input into borehole, sampling at the spring (test for mixed conduit/fissured system).
- point source input into borehole, sampling at borehole (test for fissured system).
- areal source input, sampling at spring (test for mixed conduit/fissured system).

In the project area, there are no two boreholes available, that would allow a tracer test solely of the fissured system (Stober, 1991, Teutsch and Sauter, 1991). Although this type of test was not modelled within the context of this study, the regional transport model would be able to simulate the corresponding breakthrough curve without having to make any significant changes, that would affect the regional transport model. The remaining three types of tracer breakthrough curves, together with their respective numerical simulation are discussed below. The model approaches and their limitations are also addressed.

6.2.1 Conduit System

Fig. 6-1 shows the breakthrough of a tracer test, conducted close to a dry valley near the town Bitz in the north-west of the project area. The input location guaranteed a direct connection to the conduit system and the relatively small sampling intervals, compared to previous tests made a definite sharp peak of the breakthrough curve visible. The field data were compared with the model data generated for hourly time steps. The fluctuations of the model curve is a result of the statistical generation of the dispersion, using the random walk method. The input mass of the model was evaluated from the dye recovery of the field test, because it can be assumed that a substantial fraction of the dye remained within the unsaturated zone as a result of the mode of injection, the slow release of which is probably responsible for the tailing in Fig. 6-1.

The model fit was achieved using a dispersivity of 10 m, most of which can probably be associated with the flow through the heterogeneous unsaturated zone.

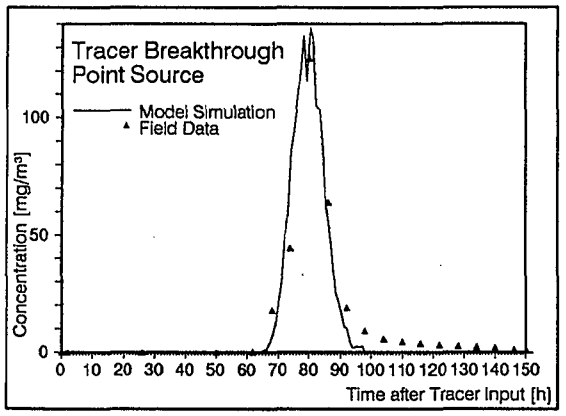

Fig. 6-1 Comparison Between Model and Field Breakthrough Curve for a Tracer Test with Input into Conduit System

The fit is good and highly sensitive to the transmissivity of the conduit system at the spring and the resulting hydraulic gradient. A porosity of 0.0001 and a transmissivity (at the spring) of 0.28 m^2/s were used for the simulation of the calibrated model breakthrough. Due to the lack of a realistic representation of the basis of the conduit system (see above, Fig. 5-3), a gradient of 0.00013 was produced by the model. Such a value does not correspond to the field situation. Using the gradient variation, evaluated in Chap. 2.6.1, an average transmissivity of 0.0063 m^2/s would be the result for the calibrated model. In the model, the height of the cross-sectional area is 8 m, i.e the continuum hydraulic conductivity of the regional conduit system could be fixed at around 0.0008 m/s, with higher values close to the spring.

The above results, i.e. low sensitivity of flow and high sensitivity of the breakthrough to $T_{regcond}$ *imply that the calibration of the fast/conduit system of the groundwater flow model requires a number of tracer tests (conduit system) to obtain a consistent hydraulic parameter set.*

6.2.2 Fissured System

Stober (1991) presented a tracer breakthrough of a test, conducted between two geothermal wells, completed in karstified limestones of the Upper Jurassic in the area of Saulgau, situated approximately 50 km south of the Swabian Alb (Fig. 6-2). The wells are 430 m apart. Correcting for interferences from a third well, the breakthrough curve coincides with the theoretical curve for porous media. Because of the low probability of a direct connection between input and output well via a conduit, the test results clearly reflect the characteristics of the fissured system, which obviously can be represented by a simple porous continuum approach. The average pore water velocity was determined at less than 0.2 m/h. Hydraulic conductivity was determined for the above test at 0.00018 m/s and the storage coefficient varied between 0.01 and 0.025, depending on the method used (Chap. 4.2.2.)

The simulation of the above breakthrough curve is straightforward, because the shape of the curve suggests a homogeneous medium. Although the above model is capable of simulating the arrival of the dye, the specific features of a double continuum model however are not required.

6.2.3 Mixed Fissured-Conduit System

Merkel (1991) performed a number of tracer tests with the input in some of the boreholes of the Gallusquelle catchment. Samples were taken at the spring, which implies that the breakthrough is a result of the influence of the fissured and the conduit system. The curves are characterized by relatively high peak velocities (35 m/h - 70 m/h) and a long drawn-out tailing (e.g. Fig. 6-3). Because the dye was injected directly into the groundwater, the unsaturated zone does have no effect on the breakthrough. The shape of the curve is mainly determined by the properties of the fissured system, whereas the variation in peak velocity depends on the distance between the input location and the point where the dye enters the conduit system. *This fact implies that the simulation of this kind of breakthrough curve demands the integration of geometrical features, i.e. the specification of the exact distance between the point of the tracer injection and the nearest conduit.*

Although theoretically and practically possible, the simulation of such tests does not comply to the philosophy and the characteristics of double-continuum models, i.e. that the flow and the transport do not depend on the geometry of the matrix-fracture system. Every one of the fissured system/conduit tests would require the specification of the borehole-conduit distance, i.e. one further calibration parameter. Thus the solution becomes non-unique and the information content of the

modeling exercise is reduced. Therefore, such a hybrid simulation was not attempted.

6.2.4 Areal Source Input

The typical breakthrough signal for areal source input are the time series of hydraulic and physico-chemical parameters, measured at the spring, as discussed extensively in Chap. 4.5.

The relative abundance of oxygen isotopes can be employed as well as a regional tracer and displays a bimodal breakthrough after recharge events. The respective time series however reveal very complex patterns due to the superposition of several events, the influence of the subcutaneous zone and the variations in input $\delta^{18}O$.

Fig. 6-4 displays the model simulation of the variation in the relative abundance of the oxygen isotopes in the spring water of the Gallusquelle over a two month period, starting with the beginning of April 1989. The model is based on the calibrated flow model, described in Chap. 5, without any further changes and the dispersivities of 10 m for the conduit and 70 m for the fissured system. The dispersivities were evaluated from tracer tests (Merkel, 1991), that tested the respective system. The tracer test in Stober (1991), Fig. 6-2, yielded a dispersivity of 90 m.

The model curve is a result of the superposition of 10 model runs, one per recharge event, the first one from the beginning of March 1989. The "input concentration" was determined based on recharge depth and the $\delta^{18}O$ relative to the base level of -10.55‰.

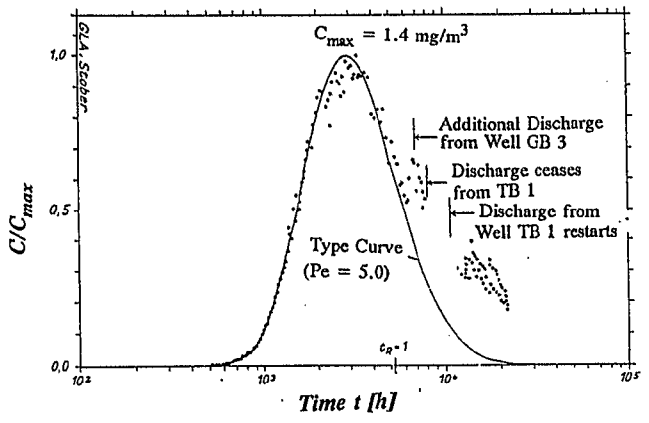

Fig. 6-2 Example of a Forced Gradient Tracer Test Sampling Solely the Fissured System (Stober, 1991)

The comparison between model and field data demonstrates that the model is capable of reproducing the range of fluctuations, the negative or positive (relative to base level) peaks and also the general trend of the areal input breakthrough curve. The model also reproduces the return to base level at the beginning of June 1989. Deviations of the field data from the model can be explained as follows. The initial fast drop of $\delta^{18}O$ at the 2 April 1989 is probably the result of relatively light water (in $\delta^{18}O$), caused by the early March events, which is displaced from the subcutaneous zone (Chap. 4.5). The model does not yet include the simulation of the epikarst with respect to its $\delta^{18}O$ variation.

The high fluctuations of the field data in May 1989 are most likely the result of incomplete mixing within the aquifer. The model assumes complete mixing and therefore shows an average $\delta^{18}O$ value.

As apparent from Fig. 4-36, the recharge calculation did not produce any groundwater recharge for the middle of May 1989, although an increase in the $\delta^{18}O$ was registered (Fig. 6-4) and rainfall isotope data were obtained for that particular event. Due to the averaging over a large area, no recharge could be calculated and therefore no positive increase in $\delta^{18}O$ was produced by the model.

The simulation of the regional transport through the karst aquifer shows that only the numerical model allows the interpretation of such a complex breakthrough signal, especially if the breakthrough curves of several events are superimposed. It also demonstrates that a number of variations in the isotope ratios, although frequently within the error bars, can be interpreted as significant.

6.3 Sensitivity Analysis

The sensitivity analysis of the transport model only concentrated on the areal source input problems, because the point source (conduit) tracer test simulation is mainly dependent on the hydraulic gradient and the storage within the conduits and therefore does not reflect the properties of the entire system.

The sensitivity analysis of a regional transport model is not as straight forward to interpret as that of a flow model, because of the interaction between fissured and conduit system, which becomes more apparent in the areal transport signal than in the hydrographs. Moreover, the effects of the subcutaneous

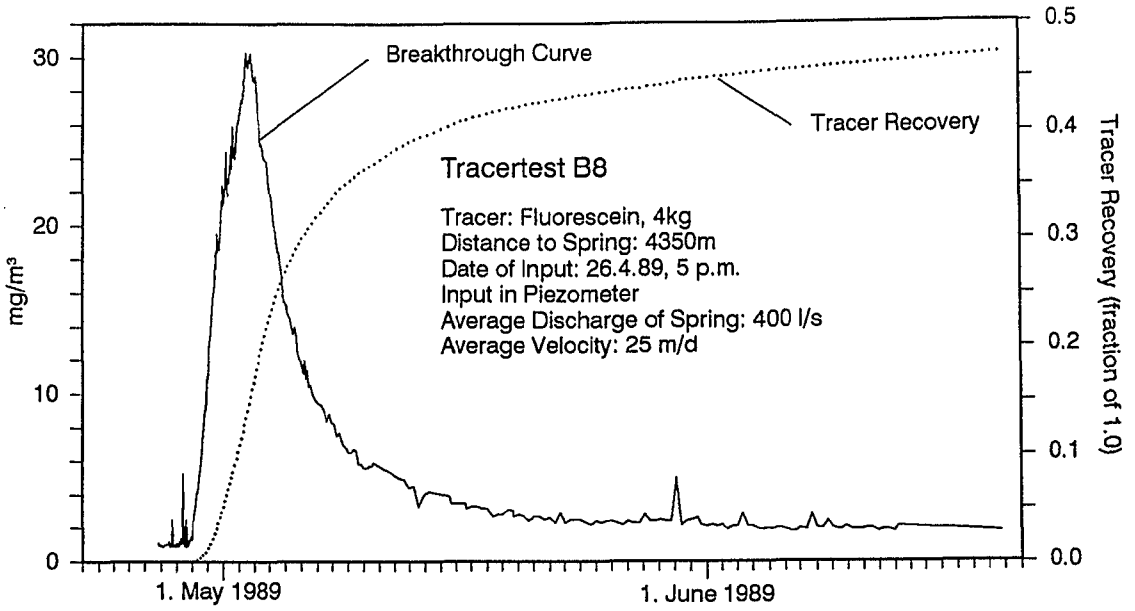

Fig. 6-3 Example of a Tracer Test Sampling a Mixed Fissured-Conduit System (Merkel, 1991)

zone on the magnitude and time variation of recharge input influence the output signal to a major degree. Considering the field evidence, it is assumed as known.

The areal breakthrough curve is a result of the time variation in the recharge input (subcutaneous zone, although with constant concentration), the preevent flow and storage in both systems and the relative event flow from conduit and fissured system.

An exhaustive testing of all relevant parameters with and without time variation is beyond the scope of this study, the main effects are however discussed. Figs. 6-5 a to e display the change of the calibrated breakthrough curve with the change in various parameters as a result of tracer input due to one single rainfall event (1/2 April 1989) and dilution effects of later recharge. Especially because of this dilution effect, separate sensitivity runs were calculated, so that the various mechanisms, controlling the changes could be identified. The corresponding simulations for the whole series of events with varying $\delta^{18}O$ input are included in App 6-1.

Fig. 6-5 a shows the variation of the curve as a result of a change in S_{regfis}. By doubling the storage coefficient of the fissured system, the maximum concentration of peak one (conduit system) is decreased and that of peak two (fissured system) increased. The maximum concentration of the peak is also shifted towards earlier times as compared with the calibrated model. Due to the higher, zero concentration pre-event discharge, the concentration of peak one is lower, and due to the larger quantity of higher concentrated water in the fissured system (compared with the calibrated model), the event of 20 April 1989 is unable to substantially dilute the groundwater stored in the fissured system.

Doubling the hydraulic conductivity of the matrix/fracture exchange coefficient (Fig. 6-5 b), reverses the effects on the breakthrough curve, observed above. The maximum concentration of peak 1 is slightly increased, because of the increased contribution of the fissured system and almost merges with the peak two (fissured system). The quicker release of water from the slow system storage causes a substantial increase in the peak concentration of the second peak. An increase of the gradient in the conduits by the flow from the slow system causes higher flow velocities and therefore a substantial shift in the second peak.

A similar response of the breakthrough signal can be seen in Fig. 6-5 c. In this case however, a similar change in concentration can be observed as a result of halving the crossectional area (transmissivity) at the spring. This leads to an increased gradient in the conduits further upgradient and to increased velocities. Because the head within the conduit system, close to the spring affects the head within the fissured zone (Fig. 5-3, potential difference controlled flow between the two systems, when water level in conduits not below base of fissured zone), the general head increase within the fissured system augments the flow from the slow to the fast system. The general increase in the width of the peak with increasing

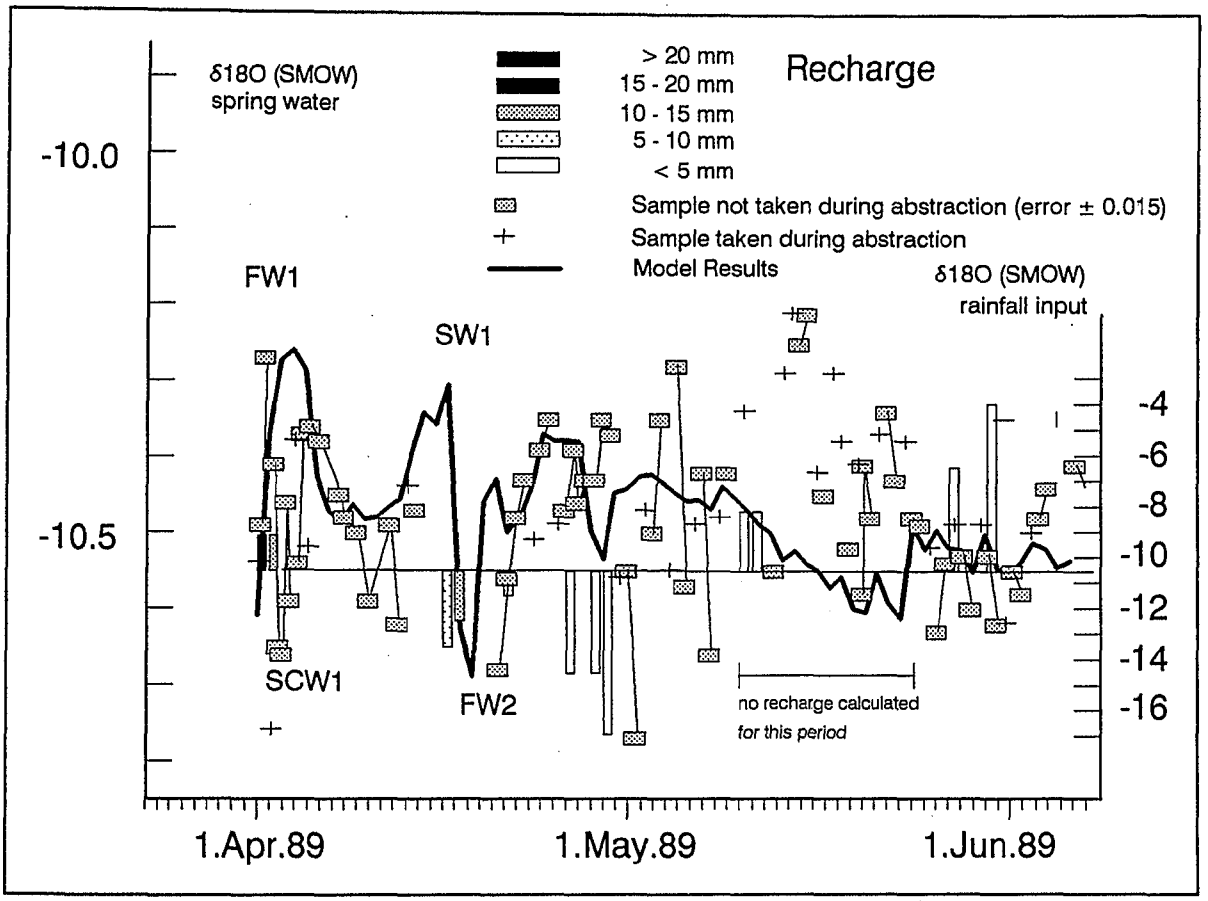

Fig. 6-4 Comparison Between Field Variation of Oxygen Isotope Ratios in Spring Water After a Recharge Event and Model Simulated Data

transmissivity can probably be attributed to the larger volume of water available in the conduits, which recharge water is diluted in.

In order to obtain any significant response in the areal-input breakthrough by changing the hydraulic conductivity of the conduit system, the $K_{regcond}$ had to be multiplied by factors of 10, 100, 0.1 and 0.05 (Fig. 6-5 d). A decrease in $K_{regcond}$ causes the maximum concentration of the first conduit peak to slightly increase, whereas an increase in $K_{regcond}$ leads to a slight decrease. The second peak displays a slight increase in concentration with increasing $K_{regcond}$ and vice versa. A plateau concentration is reached earlier with higher conduit hydraulic conductivity.

The variation in $S_{regcond}$ hardly displayed any response in the breakthrough curve, except when the conduit storage was increased by a factor of a hundred, i.e. to 1%, which is in the same order as that of the fissured system. In this case, the concentration of peak 1 is increased substantially.

The main hydraulic parameters dominating the transport through a karst aquifer have been identified as the hydraulic conductivity of the fissured system, controlling the release of water from the slow into the fast system and the transmissivity of the conduit system. Because of the complex interaction between both systems, only a numerical transport model allows the interpretation of the importance of every single parameter in determining the shape of the breakthrough curve. This statement applies in particular, if the breakthrough is modified by the superposition of several rainfall events.

The above analysis ignores the effects of the change in the recharge input function, i.e. a variation in the hydraulic parameters of the epikarstic zone. The release of water from the subcutaneous zone is controlled by a number

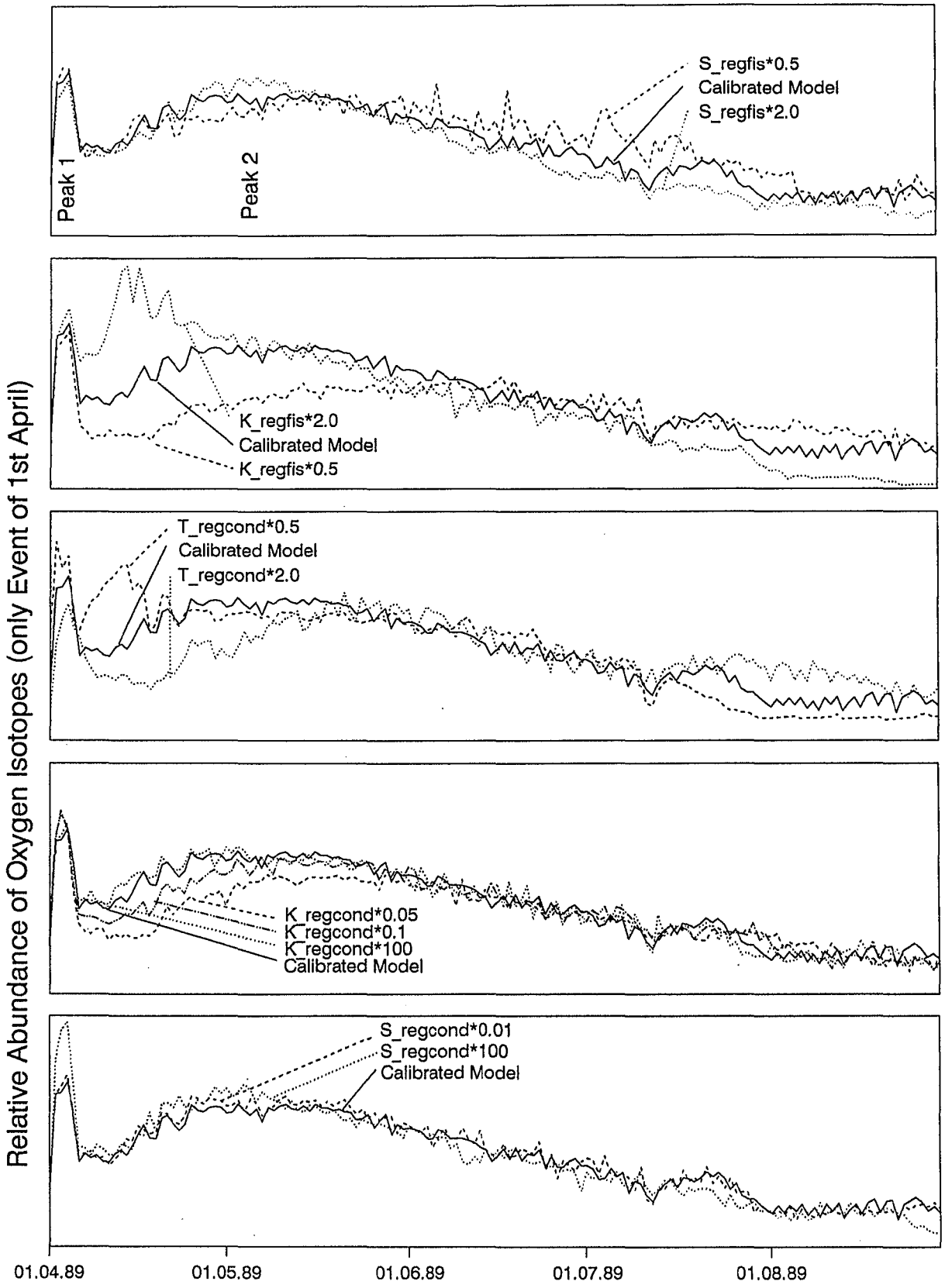

Fig. 6-5 Sensitivity Analysis for the Variation in Concentration of an Areal Tracer (e.g. Oxygen Isotopes) with Changing Hydraulic Parameters

of parameters. In the simplest case, the subcutaneous system can be described by two storage, two resistance parameters and the relative distribution of fast and slow recharge water. However, because of the lack of interaction with another system, the change in the outflow of recharge as a result of a change in parameters is straightforward. It can be described by a respective change in the height and/or width of the fast and the slow peak.

7 Conclusions

This study concerns two main aspects: firstly, the selection of an appropriate modelling tool for the simulation and prediction of groundwater flow and transport in a karst aquifer system, the construction, testing as well as validation of the model. Secondly, the provision of data input, required for the modelling of such a complex flow system.

Flow and Transport Modelling

A combined flow and transport model represents the complete integration of the determining processes in a karst aquifer and allows the examination and evaluation of the dominant effects.

- A Double-Continuum Porous Equivalent Model (Teutsch and Sauter, 1991) was found to be the most appropriate for the study area. Each of the two flow systems of the aquifer, the fast flow, i.e. conduit system, and the slow, i.e. fissured system, is simulated with a separate continuum, and both are coupled by an exchange term. The model applies to flow from a catchment, that discharges at a spring, or where the flow into a river via alluvial deposits can be quantified. The integration of a zone of lower hydraulic conductivity close to the base of the aquifer guaranteed the upkeep of the observed steep regional gradient, even during low flow conditions.
- The hydraulic and hydrological responses of the aquifer could be reproduced very well, considering the number of assumptions and simplifications introduced. The model can be used for short term (range of days) as well as long term (tens of years) problems. The model also incorporates a realistic aquifer base.
- Extreme conditions, such as floods and droughts could be modelled with very good accuracy (ratio of high to low flow: 30:1), whereby the waterlevel fluctuations could be simulated very well. Generally, the model runs demonstrate the applicability of the tool.
- The dominant hydraulic parameters in the flow simulation are the storage coefficient and the hydraulic conductivity of the fissured system, that control the storage and release of groundwater over time. Calibrated fissured system hydraulic conductivities vary between $1*10^{-6}$ m/s and $5*10^{-6}$ m/s and the storage coefficients range between 0.008 and 0.025. The model showed that due to their different response on water levels, the two parameters can be tuned more or less independantly, thereby reducing ambiguities. The fissured system acts like a buffer, and because of their high hydraulic conductivity, the conduits do not represent a limiting factor in the flow simulation.
- The transport model is applicable to point-source and nonpoint-source input, which also allows the modelling of complex recharge events, where a number of events of different intensity and different $\delta^{18}O$ are superimposed.
- The dominant hydraulic parameters in the transport simulation have been identified as the hydraulic conductivity of the fissured system and the transmissivity of the conduit system. It was preferred to specify conduit transmissivity instead of hydraulic conductivity in order to avoid the specification of the unknown throughput area as one further parameter. The conduit (continuum) transmissivity at the spring was calibrated with a value of 0.0063 m^2/s. Because of the complex interaction between both systems, only a numerical transport model allows the interpretation of the importance of every single parameter in determining the shape of the breakthrough curve. This statement applies in particular, if the breakthrough is modified by the superposition of several rainfall events.
- The model has been validated and can be employed for predictive purposes, i.e. without any further corrections and calibration, the model could reproduce time variant fluctuations of $\delta^{18}O$, a nonpoint-source tracer.

Data Provision

The validation of the model for field situations depends highly on the available hydraulic parameters from field tests, on the aquifer geometry and the shape of the aquifer base, as well as on the evaluation of daily recharge, which includes the determination of its temporal distribution.

- A large number of borehole logs together with information from water level fluctuations and fluvial history allowed the identification of aquifer base and zones of higher and lower hydraulic conductivities.
- A soil moisture balance approach together with a water balance for the canopy (accounting for interception loss) produced sufficiently accurate values for groundwater re-

charge. Calculated recharge was compared with spring discharge (for periods of zero groundwater storage change), which, after corrections for losses below the gauge, represents actual recharge in this particular karst area (no surface runoff). Annual recharge varies between 146 and 540 mm with a mean of 390 mm/a. Important parameters in the recharge calculation are the field capacity (75 mm), the interception capacity (4.7 mm) and the rapid recharge threshold (6 mm). Although the rapid recharge component as a total percentage of the annual recharge is of only minor importance (increase of between 5% and 10%), it provides recharge for periods, where otherwise no recharge would have been calculated, although observed in the field.

■ The importance of the influence of the epikarstic zone on the temporal distribution of recharge input and the relative distribution of recharge between fast and slow system needs to be stressed. The analysis of time series of hydraulic and physico-chemical parameters yielded storage and recession constants for the drainage from the subcutaneous zone, which could be divided into a fast and a slow recharge component. The fast flow component, that discharges within 2 to 3 days, ranges between approximately 4% and 10% of the total recharge, depending on the season and the characteristics of the events. The slow flow, discharging within several weeks to several months is believed to be controlled by the hydraulic properties of the epikarstic/subcutaneous zone. It can be further subdivided into slow and fast subcutaneous flow with flow recession coefficients (Maillet, 1905) of 0.03/d for the slow and 0.46/d for the fast subcutaneous flow component. The maximum stored water volume of the slow subcutaneous system could be estimated at 30 mm.

■ The analysis of spring flow, temporal and spatial variation of groundwater levels, borehole hydraulic tests and also the time series of physico-chemical parameters of spring water allowed the quantification of storage and hydraulic conductivity for both, the slow (fissured) and the fast (conduit) system, for flood as well as drought conditions. The importance of the dependance of the above parameters on the measurement scale due to the heterogeneous distribution of fast and slow flow paths was recognized. The relationship between hydraulic conductivity and the sampled volume could be determined by evaluating the parameters at the catchment, several different borehole and laboratory scales. This procedure allowed the allocation of hydraulic conductivity at the modeling scale The total system (fissured and conduit system) hydraulic conductivity roughly varies between 10^{-3} m/s and 10^{-4} m/s for the regional scale (regional gradient, km to several kilometers), 10^{-4} m/s and 10^{-5} m/s for the local scale (pumping tests, 100 m to several hundreds of meters) and between 10^{-5} m/s and 10^{-6} for the sublocal scale (borehole hydraulic tests, 10 m to several tens of meters). The system hydraulic conductivity is generally determined by the conduits, which represent approximately 0.01% to 0.03% of the total rock volume, depending on scale and spatial variation. The fissured system hydraulic conductivity at every scale was determined to be lower than the corresponding conduit hydraulic conductivity (expressed as the equivalent continuum value) by approximately 1 order of magnitude, which can be considered as a general guideline. Total system storage coefficients, as far as they could be determined at the respective scale, ranged between 1% and 2%, with very little variation between scales. It is interesting to note that system hydraulic conductivities, measured at a certain scale (e.g. local scale) seem to correspond to the hydraulic conductivity of the fissured system at the next higher scale (i.e. regional scale). Slug tests and injection tests produced fissure hydraulic conductivities of between 10^{-6} m/s and 10^{-9} m/s, which correspond approximately to the total hydraulic conductivity measured in the laboratory.

■ The analysis of the various time series provided an insight into the different processes affecting the recharge and groundwater circulation. The chronology of the different parameter variations helped to understand the sequence of events. Depending on the season and the characteristics of the event, maximum discharge is measured on average 30 h after maximum intensity in rainfall , minimum electrical conductivity 60 h and minimum temperature 70 h after maximum precipitation. The maximum waterlevel in the conduits is read betwen 30 and 40 h and in the fissured system on average 20 days after the event. As apparent, the maximum waterlevel in the fissured system does not occur simultaneously with peak discharge, which is attributed to the delaying effect of the epikarst. The difference between minimum electrical conductivity and minimum temperature can be explained by the fact that the conductivity peak is solely a re-

sult of the fast water component, whereas the temperature peak also includes some slow water. This type of analysis allowed the differentiation of the flood pulse into the fast and slow event component, as well as the identification of pre-event conduit stored and subcutaneously stored water. The time series analysis also provided the data ($\delta^{18}O$) for the bimodal breakthrough of fast and slow groundwater components of a regional tracer. These data could be used to compare the model results with. Although the $\delta^{18}O$ data could not be used to quantitatively separate fast and slow flow components, the values demonstrate the complicated pattern in the breakthrough signal of superimposed events, the impact of pre-event subcutaneous water and the layering of different age water within the aquifer.

Suggestions for Further Research

In order to improve the model results, some further research efforts would be required in the area of aquifer zonation, groundwater recharge, parameter estimation, the model calibration and the modelling tool itself.

- From an economical point of view it would not be very wise to drill further boreholes for the identification of aquifer zones of different hydraulic conductivity. The variability between boreholes is so extreme that unambiguous results cannot be obtained. It is rather recommended to derive well developed and less well developed aquifer zones from the geological history. The spatial distribution of dolomitized and dedolomitized horizons, as well as the evolution of the fluvial system are believed to give valuable information on the location of the actual aquifer. It is assumed that the main solutional processes take place within the zone of annual water level fluctuations.
- The accuracy of the recharge calculation might be somewhat improved by employing an alternative and more deterministic procedure for the evaluation of the potential evapotranspiration, such as the Penman or the modified Penman method (Gash and Morton, 1978) to account for forest evapotranspiration. Some attempt should also be made at assessing the loss under the spring gauge more precisely. Efforts should particularly be put on the determination of the hydraulic characteristics and dominant flow processes within the epikarst. The epikarstic zone determines the period of time over which recharge water is released into the aquifer and represents an important element in the recharge process. One approach could be the monitoring of seepage water rates in caves, as done by Smart and Friederich (1986). However, caves frequently develop their own hydrology, i.e. due to precipitation of carbonate, the seepage water might be guided around the cavern and therefore cave seepage is not necessarily representative of seepage from the subcutaneous zone. An alternative approach could consist of the observation and analysis of hydraulic and physico-chemical parameters of small springs, fed by water from the subcutaneous zone, that sometimes occur even in the Gallusquelle catchment, or in an artificial trench, dug into the epikarst.
- The conduction of large scale, long term pumping tests in large diameter boreholes at some distance from the spring might give some further information on the effective or representative hydraulic parameters of the conduits and fissured system at the modelling scale. This applies particularly if the tests are interpreted using modern techniques, which take into account the double porosity effects and if early and late data are examined separately.
- For the calibration of the conduit system response, the availability of a piezometer, tapping the fast system would be essential. It has been demonstrated (Dr. Quinlan, pers. communication) that by employing geophysical methods, boreholes can be drilled precisely into a conduit. This method however can only be employed in a karst aquifer with shallow groundwater table. The identification of a more sensitive nonpoint-source tracer (instead of $\delta^{18}O$) would be of enormous help in the calibration of the transport model. The ubiquitous chloro-fluoro hydrocarbons might prove to be very valuable. Alternatively, temperature could be used as a tracer. This method however would require the simulation of the heat exchange between water and rock within the subcutaneous zone, within the solution shafts, that convey recharge water to the water table, as well as within the aquifer. Investigations in more mature karst areas, where the fast water component represents a larger fraction of total recharge are believed to reveal more pronounced $\delta^{18}O$ signals. Finally, the realistic integration of the conduit system base into the model should be aimed at.

8 References

Agsten, K., 1977, Zur Entwicklung und Vergesellschaftung der Böden in traufnahen Bereichen der westlichen Schwäbis chen Alb (Balinger Berge). Geol. Jb., F, 5, 84p.

Aiguang, C., Hanchen, L., Juanming, X. & S. Jinli, 1988, Stochastic Modelling of the Karst Spring of Xin'an, Shanxi Province, in: Karst Hydrogeology and Karst Environment Protection, Proc. of the 21st Congress of the Int. Assoc. o. Hydrogeologists, Guilin, China, 621-628.

Alagoa, A., Bourdet, D. & J.A., Ayoub, 1985, How to simplify the analysis of fractured well tests. World Oil, October 1985.

Ashton, K., 1966, The analysis of flow data from karst drainage systems. Trans. Cave Research Group, G.B., 7, 161-203.

Atkinson, T.C. & P.L. Smart, 1981, Artificial Tracers in Hydrogeology, in: A Survey of British Hydrogeology 1980. The Royal Society, London, 173-190.

Atkinson, T.C., 1977, Diffuse flow and conduit flow in a limestone terrain in the Mendip Hills, Somerset, J. Hydrol., 19, 323-349.

Avias, J. & C. Joseph, 1984, Modélisation des systemes karstiques, in: A. Burger & L. Dubertret. (eds), Hydrogeology of Karstic Terraines, International Contributions to Hydrogeology, Heise, Hannover.

Back, W., Hanshaw, B.B., Pyle, T.E., Plummer, L.N. & A.E. Weidie, 1979, Geochemical significance of groundwater discharge and carbonate dissolution to the formation of Caleta Xel Ha, Quintana ROO, Mexico. Water Res. Res., 15, 1521-1535.

Bakalowicz, M. & A. Mangin, 1980, L'aquifère karstique. Sa définition, ses charactèristiques et son identification. Mm. L. sr. Soc. geol. France, 11, 71-79.

Baoren, C. & Z. Xuming, 1988, The mathematical simulation of hydrological regime of Chaohua spring in Mixian County. Karst Hydrogeology and Karst Environment Protection, Proc. of the 21st Congress of the Int. Assoc. o.Hydrogeologists, Guilin, China.

Barenblatt, G.E., Zheltov, I.P. & I.N. Kochina, 1960, Basic concepts in the theory of homogeneous liquids in fissured rocks. J. Appl. Math. Mech. (USSR), 24, 1286-1303.

Barker, J.A. & J.H. Black, 1983, Slug Tests in Fissured Aquifers, Water Res. Res., 19, 1558-1564.

Baumgartner, H.-J. & A. Liebscher, 1990, Lehrbuch der Hydrologie, Band1, Allgemeine Hydrologie - Quantitative Hy drologie, Borntraeger, Berlin, 673p.

Bear, J., 1988, Dynamics of Fluids in Porous Media, Dover, New York, 764p.

Behringer, J., 1988, Hydrochemische Kurz- und Langzeitstudien im Malmaquifer der Mittleren Schwäbischen Alb. Ph. D. Thesis, Universität Tübingen, 222p.

Benecke, P., 1978, Der Wasserumsatz eines Buchen- und eines Fichtenwaldökosystems im Hochsolling (Methoden und Ergebnisse), Universität Göttingen, Göttingen, 225p.

Bertleff, B.W., 1986, Das Strömungssystem der Grundwässer im Malmkarst des westlichen Teils des süddeutschen Molassebeckens. Abh. Geol. Landesamt, Baden-Württemberg, 12, 1-271.

Beven, K., 1981, Micro, meso, macroporosity and channeling flow phenomena in soils. J. Soil Sci., Soc. Am., 45, 1245.

Black, T.A., Spittlehouse, D.L., Novak, M.D. & D.T. Price, 1989, Estimation of areal evaporation, IAHS Publ. 177.

Bonacci, O., 1987, Karst Hydrology, Springer, Berlin-Heidelberg, 184pp.

Bourdet, D., Ayoub, J.A., Whittle, T.M., Pirard, Y.M. & V. Kniazeff, 1983, Interpreting well tests in fractured reser voirs. World Oil, October 1983.

Bourdet, D. & A.C. Gringarten, 1980, Determination of fissure volume and block size in fractured reservoirs by type curve analysis, presented at the SPE-AIME 55th Annual Technical Conference and Exhibition, Dallas, Texas. Society of Petroleum Engineers, SPE-9293.

Bourdet, D., Whittle, T.M. Douglas, A.A. & Y.M. Pirard, 1983, A new set of type curves simplifies well test analysis. World Oil, May 1983.

Bouwer, H., 1989, The Bouwer & Rice slug test - An update. Ground Water, 27, 304-309.

Bouwer, H. & R.C. Rice, 1976, A slug-test for determining hydraulic conductivity with completely or partially penetrating wells. Water Res. Res., 12, 423-428.

Brechtel, H.M. & M.B. Pavlov, 1977, Niederschlagsbilanz von Waldbeständen verschiedener Baumarten und Altersklassen in der Rhein-Main Ebene. Arb. d. DVWK, Bonn und Hess. Forst. Vers. Anst. Hann.- Münden.

Burdon, D.J. & N. Papakis, 1963, Handbook of karst hydrology, Athens. Institute for Geology and Subsurface Research, FAO.

Carslaw H.S. & J.C. Jaeger, 1960, Conduction of heat in solids. 2nd ed., Oxford Univ. Press, London.

Castany, G., 1984, Hydrogeological features of carbonate rocks. in: Unesco, Guide to the hydrology of carbonate rocks, Studies and Reports in Hydrology, vol 41, 47-61.

Cedergren, H.R., 1977, Seepage, drainage and flow nets. 2nd ed. Wiley, 534pp.

Čermák, J. & J. Kučera, 1987, Transpiration of mature stands of spruce as estimated by the tree-trunk heat balance me thod, IAHS Publ. 167, 311-317.

Chirlin, G.R., 1989, A critique of the Hvorslev method for slug test analysis: the fully penetrating well. Groudwater Mo nitoring Review, 9, 130-138.

Chow, V.T., Maidment, D.R. & L.W. Mays, 1988, Applied Hydrology. Mc Graw Hill, N.Y., 572pp.
Cinco, H. & Samaniego, F., 1978, Transient pressure analysis for fractured wells, Soc. Petr. Eng., SPE-7490.
Cooper, H.H., Jr., Bredehoeft, J.D. & I.S. Papadopulos, 1967, Response of a finite diameter well to an istantaneous charge of water. Wat. Res. Res., 3, 263-269.
Cullen, J.J.IV & R.G. LaFleur, 1984, Theoretical considerations on simulation of karstic aquifers. In: R.G. LaFleur (ed), Groundwater as a geomorphic agent, Allen & Unwin, Boston, 249-280.
Cvijic, J., 1918, Hydrographie souterraine et evolution morphologique du karst. Rec. Trav. Inst. Geog. Alpine, 375-426.
Darcy, H., 1856, Les fontaines publiques de la ville de Dijon, Paris, Dalmont.
Department of Energy, 1986, Environmental assessment, reference repository location, Hanford site, Washington, DC, US. DOE/RW-0070.
Domenico, P.A. & F.W. Schwartz, 1990, Physical and chemical hydrogeology. Wiley, N.Y., 824p.
Dougherty, D.E. & D.K. Babu, 1984, Flow to a partially penetrating well in a Double Porosity Reservoir, Water Res. Res., 20, 1116-1122.
Dreiss, S.J., 1989a, Regional scale transport in a karst aquifer, 1. Component separation of spring flow hydrographs, Water Res. Res., 25, 117-125.
Dreiss, S.J., 1989b, Regional scale transport in a karst aquifer, 2. Linear systems and time moment analysis, Water Res. Res., 25, 126-134.
Dreybrodt, W., 1988, Processes in karst systems, Physics, chemistry and geology. Springer, Berlin, 288p.
Drogue, C. & A. Guilbot, 1977, Représentativité d`un bassin témoin en hydrogéologie karstique: Application a`la modélisation des écoulements souterrains d`un aquifère de grande extension. J. Hydrol., 32, 57-70.
Duffy, C.J. & L.W. Gelhar, 1986, A frequency domain analysis of groundwater quality fluctuations: Interpretation of field data. Wat. Res. Res., 22, 1115-1128.
Duffy, C.J. & J. Harrison, 1987, The statistical structure and filter characteristics of tritium fluctuations in fractured ba salts, Wat. Res. Res., 23, 894-902.
Duguid, J.O. & P.C.Y. Lee, 1977, Flow in fractured porous media, Water Res. Res., 13, 558-566.
Dupuit, J., 1863, Etudes théorétiques et practiques sur le mouvement des eaux dans les canaux découverts et à travers les terrains perméables. Dunod, Paris.
Etzold, A., Hahn, W. & U. Koerner, 1975, Keuper, Jura und Tertiär in Bohrungen der Planungsgemeinschaft Bodensee-Neckar-Stollen zwischen Bodensee und Neckar. Jh. Geol. Landesamt Baden-Württemberg, 17, 89-255.
Van Everdingen, A.F., 1953, The skin effect and its influence on the productive capacity of a well. Trans. Inst. Min. Metall., 198, 171-176.
Faust C.R. & J.W. Mercer, 1984, Evaluation of slug tests in wells containing a finite-thickness skin. Water Res. Res., 20, 504-506.
Ferris, J.G. & D.B. Knowles, 1954, The slug test for estimating transmissibility. US. Geol. Surv. Ground Water Note, 26, 1-7.
Fleck, W., 1987, Einfluß des Bodenaufbaus und des Waldbestandes auf Verdunstung und Abflußbildung im Naturpark Schönbuch bei Tübingen. Ph.D. Thesis, Universität Tübingen, 111p.
Flügel, W.-A., 1988, Interzeptionsverluste und Niederschlagsbilanzen für Fichten und Buchenbestände aus dem "Holl muth", Kleiner Odenwald. Heidelberger Geogr. Arb., 66, 83-100.
Ford, D. & P. Williams, 1989, Karst geomorphology and hydrology. Unwin, London, 601pp.
Fritz, P., J.A. Cherry, K.V. Weyer and M.G. Sklash, 1976, Runoff analyses using environmental isotopes and major ions. In: IAEA, Interpretation of environmental isotope and hydrochemical data in groundwater hydrology. Vienna, 111-130.
Gale, S.J., 1984, The hydraulics of conduit flow in carbonate aquifers. J. Hydrol., 70, 309-327.
Gascoyne, M., Ford, D.C. & H.P. Schwarcz, 1983, Rates of cave and land form development in the Yorkshire Dales from speleothem age data. Earth Surf. Proc. Landforms, 8, 557-568.
Gash, J.H.C. & A.J. Morton, 1978, An application of the Rutter model to the estimation of the interception loss from Thetford forest, J. Hydrol., 38, 49-58.
Gash, J.H.C., Wright, I.R. & C.R. Lloyd, 1980, Comparative estimates of interception loss from three coniferous forests in Great Britain. J. Hydrol., 48, 89-105.
Geyh, M.A. & P. Groschopf, 1978, Isotopenphysikalische Studie zur Karsthydrologie der Schwäbischen Alb. Abh. Geol. Landesamt, Baden-Württemberg, 8, 7-58.
Göttlich K.H. and J. Werner, 1968, Zur Flußgeschichte der Lauchert. Jber. u. Mitt. oberrh. geol. Ver., N.F. 50, 115-126.
Golwer, A., 1978, Geologische Karte von Baden-Württemberg 1:25000, Blatt 7821, Veringenstadt, Erläuterungen, Lan desvermessungsamt Baden-Württemberg, Stuttgart, 151p.
Gradmann, R., 1931, Süddeutschland. 1-2, J. Engelhorns Nachf., Stuttgart.
Gringarten, A.C., 1982, Flow-test evaluation of fractured reservoirs. in: T.N. Narasimhan, Recent trends in hydrogeo logy, GSA, Special Paper, 189, 237-263.
Gringarten, A.C., Ramey, H.J.jr. & P. Raghavan, 1975, Applied pressure analysis for fractured wells, J. Petr. Tech.., 27, p887.

Gwinner, M.P., 1976, Origin of the Upper Jurassic limestones of the Swabian Alb (Southwest Germany). Contributions to Sedimentology, 5, 75pp.

Gwinner, M.P., 1973, Geologische Karte von Baden-Württemberg, Blatt 7721, Gammertingen, Erläuterungen, Landesvermessungsamt Baden-Württemberg, Stuttgart.

Hagen, G., 1839, Über die Bewegung des Wassers in engen cylindrischen Rohren. Poggendorff Annalen, 46, 423-442.

Hallberg, G.R., Libra, R.D., Bettis, E.A. & B.E.Hoyer, 1983, Hydrogeologic and water quality investigations in the Big Spring Basin, Clayton County, Iowa. Open File Rep. 84-4, Iowa Geol. Surv.

Hanshaw, B.B. & W. Back, 1979, Major geochemical processes in the evolution of carbonate aquifer systems. J. Hydrol., 43, 278-312.

Hanshaw, B.B. & W. Back, 1974, Determination of typical hydraulic conductivity through use of ^{14}C dating of ground water. In: Extrait des Mémoires del l`Association Internationale des Hydrogeologues, Congrès de Montpellier, France, 195-198.

Haude, W., 1955, Zur Bestimmung der Verdunstung auf möglichst einfache Weise, Mitt. d. Dt. Wetterdienstes, 11, Bd2, Bad Kissingen.

Hawkins, M.F., 1956, A note on the skin effect. Trans. AIME, 207, 357-358.

Hebestreit, Ch., 1990, Untersuchungen über fluviatile Geodynamik, Sedimentologie und Subrosion im Rahmen der jung pleistozänen Klima- und Landschaftsgeschichte der Oberen Wutach im Kiesabbau Großwald, Gem. Reiselfingen. Diplom-thesis, Geologisches Institut, Universität Tübingen, 116p.

Herrmann, A., J. Martinec and Stichler, W., 1978, Study of snow melt-runoff components using isotope measurements. Proc. Modeling of Snow Cover Runoff, U.S. Army Cold Regions Research and Engineering Laboratory, Hanover, New Hampshire, 26-28 Sep. 1978, 288-296.

Herrmann, A. and Stichler, W., 1980, Groundwater - runoff relationships. Catena, 7, 251-263.

Hess, J.W. & W.B. White, 1974, Hydrograph analysis of carbonate aquifers, Res. Pub. 83, Inst. Res. Land and Water Resourc., Pa State University, 63p.

Hess, J.W. & W.B. White, 1988, Storm response of the karstic carbonate aquifer of south-central Kentucky. J. Hydrol., 99, 235-252.

Hemme, H., 1970, Die Stellung der "lassivierten" Terra fusca in der Bodengesellschaft der Schwäbischen Alb, Ph.D. Thesis, Univ. Hohenheim, 77p.

Houlsby, A.C., 1976, Routine interpretation of the Lugeon water test. Q.J.Eng.Geol., 9, 303-313.

Howard, K.W.F. & J.W. Lloyd, 1979, The sensitivity of parameters in the Penman evaporation equations and direct re charge balance. J. Hydrol., 41, 329-344.

Huyakorn, P.S., Lester, B.H. & C.R. Faust, 1983, Finite Element techniques for modelling groundwater flow in fractured aquifers. Water Res. Res., 19, 1019-1035.

Hvorslev, M.J., 1951, Time lag and soil permeability in groundwater observations. U.S. Army Corps of Engineers Waterways Experiment Station Bulletin, 36, Visocksburg, Miss..

Irmay, 1984, Theoretical models of flow through porous media. RILEM symp. on the transfer of water in porous media, Paris.

Jaeger, J.C., 1956, Conduction of heat in an infinite region bounded interval by a circular cylinder of a perfect conductor. Anst. J. Phys., 9, 167-179.

James, N.P. & P.W. Choquette, 1988, Paleokarst. Springer, N.Y., 416pp.

James, N.P. & P.W. Choquette, 1984, Limestones - the meteoric diagenetic environment. Geo-science Canada, 11, 161-194.

Jones, P., 1956, Reservoir limits tests. Oil & Gas J., 54, p184.

Kabala, Z.J., Pinder, G.F. & P.C.D. Milly, 1985, Analysis of well - aquifer response to a slug test. Wat. Res. Res., 21, 1433-1436.

Van der Kamp, G., 1976, Determining aquifer transmissivity by means of well response tests. The underdamped case. Wat. Res. Res., 12, 71-77.

Karasaki, K, Long, J.C.S. & P.A. Witherspoon, 1988, Analytical models of slug tests. Wat.Res.Res., 24, 115-126.

Karasaki, K., Witherspoon, P.A. & J.C.S. Long, 1985, A new analytical model for fracture dominated reservoirs. Soc. Petr. Eng., SPE-14171.

Kastrinos, J.R. & W.B. White, 1986, Seasonal hydrogeologic and land-use controls on nitrate contamination of carbonate groundwaters. Proc. of the Environmental Problems in Karst Terranes and their Solutions Conference, National Water Well Association, Bowling Green, Kentucky, 88-114.

Katzer, F., 1909, Karst- und Karsthydrographie. Zur Kunde der Balkanhalbinsel, 8. Sarajevo.

Kelway, P.S., 1975, The rainfall recorder problem. J. Hydrol., 26, 55-77.

Kemblowsky, M.W. & C.L. Klein, 1988, An automated numerical evaluation of slug test data. Ground Water, 26, 435-438.

Kipp, K.L., 1985, Type curve analysis of inertial effects in the response of a well to a slug test. Wat. Res. Res., 21, 1397-1408.

Kiraly, L., 1984, La régularisation de l`Areuse (Jura Suisse), simulée par modèle mathematique. in: A. Burger & L. Dubertret. eds, Hydrogeology of Karstic Terraines, Int. Contributions to Hydrogeology, Heise, Hannover, 94-99.

Kiraly, L., 1975, Rapport sur l'état actuel des connaissances dans le domaine des charactères physiques des roches karstiques. In Hydrogeology of karstic terraines. A. Burger und L. Dubertret (eds), International Union of Geol. Sci, Series B, 3, 53-67.

Koerner, U., 1965, Report of the Geologisches Landesamt Baden-Württemberg, no. IV/1-909/65.

Kraemer, S.R. & H.M. Haitjema, 1989, Regional Modelling of fractured rock aquifers. in: G. Jousma, J. Bear, Y.Y. Haimes & F. Walter, Groundwater Contamination: Use of models in decision making, Kluwer, Dordrecht, 467-476.

Krauss, I., 1974, Die Bestimmung der Transmissivität von Grundwasserleitern aus dem Einschwingverhalten des Brunnen-Grundwasserleitersystems. J. Geophys., 40, 381-400.

Kriele, W., 1969, Tektonische Untersuchungen auf der Zollernalb. Unpubl. Diplom-thesis, Geologisches Institut, Univer sität Tübingen.

Krusemann, G.P. & N.A. de Ridder, 1990, Analysis of pumping test data. Int. Inst. for Land Reclamation and Improve ment, publ. 42, 377p.

Legrand, H.E. & V.T. Stringfield, 1973, Karst Hydrology - a review. J. Hydrol., 20, 97-120.

Linsley, R.K., Kohler, M.A. & J.L. Paulhus, 1982, Hydrology for Engineers. McGraw Hill, N.Y., 508p.

Lloyd, W., Harker, D. & R.A. Baxendale, 1981, Recharge mechanism and groundwater flow in the chalk and drift de posits of southern East Anglia. Q.J. Eng. Geol., 14, 87-96.

Long, J.C.S., Gilmour, P. & P.A. Witherspoon, 1985, A model for steady fluid flow in random three-dimensional net works of disc-shaped fractures. Water Res. Res., 21, 645-658.

Maclay, R.W. & L.F. Land, 1988, Simulation of flow in the Edwards aquifer, San Antonio region, Texas, and refine ments of storage and flow concepts. U.S.G.S. Water Supply Papers, 2336.

Maillet, E., 1905, Essais hydraulique souterraine et fluviale. Hermann, Paris, 218p.

Maloszewski, P. & A. Zuber, 1985, On the theory of tracer experiments in fissured rocks with a porous matrix. J. Hy drol., 79, 333-358.

Mangin, A., 1984, Ecoulement en milieu karstique. Ann. des Mines (mai-juin), 1-8.

Mangin, A., 1975, Contribution à l'étude hydrodynamique des aquifères karstiques. Ph.D. thesis, Univ. Dijon, France, Ann. Spéléol., 30, 21-124.

Mawdsley, J.A., 1989, The accuracy of regional evapotranspiration estimates made using the atmospheric boundary layer bulk transfer method. in: T.A. Black, D.L. Spittlehouse, M.D. Novak, & D.T. Price, Estimation of areal evapotrans-piration. IAHS Publ., 177, 105-116.

Meiman, J., Ewers, R.O. & J.F. Quinlan, 1988, Investigation of flood pulse movement through a maturely karstified aquifer at Mammoth Cave National Park: a new approach. Proc. Second Conference on Environmental Problems in Karst Terranes and their Solutions, Nashville, Nov. 1988, 227-263.

Merkel, P., 1991, Karsthydrologische Untersuchungen im Lauchertgebiet (westl. Schwäbische Alb). Diplom thesis, Geo logisches Institut, Universität Tübingen, 108p.

Milanovic, P.T., 1981, Karst Hydrogeology. Colorado, Water Resources Publications.

Moench, A.F. & P.A. Hsieh, 1985, Analysis of slug test data in a well with finite thickness skin. Mm. 17th Int Congress on the Hydrogeology of Rocks of Low Permeability. IAH, Tucson, Ariz., 17, 17-29.

Moench, A.F., 1984, Double-Porosity models for a fissured groundwater reservoir with fracture skin. Wat. Res. Res., 20, 831-846.

Monteith, J.L., 1965, Evaporation and environment. Symp. Soc. Exp. Biol., 19, 205-234.

Moran, J.H. & E.E. Finklea, 1962, Theoretical analysis of pressure phenomena associated with the wireline formation tester. J. Petr. Tech., 14, p889.

Morrow, D.W., 1982, Diagenesis 1. Dolomite. Part 1: The chemistry of dolomitisation and dolomite precipitation. Part 2: Dolomitisation models and ancient dolostones. Geoscience Canada, 9, 5-13, 95-105.

Müller, S., 1963, Bodenentwicklung aus verkarsteten Weißjurakalken der mittleren Schwäbischen Alb. Jh. Karst und Höh-lenkunde, 4, 45-56.

NAVFAC (Naval Facilities Engineering Command), 1971, Chpt. 4, Field tests and measurements. Design Manual - Soil Mechanics, Foundations and Earth Structures. Dept. of the Navy, Alexandria, Virginia.

Narasimhan, T.N. & K. Pruess, 1988, MINC: an approach for analysing transport in strongly heterogeneous systems. in: E. Custodio, A. Gurgui & J.P. Lobo Ferreira (eds.), Groundwater flow and quality modeling, Reidel Dordrecht, 375-391.

Neuman, S.P., 1987, Stochastic continuum representation of fractured rock permeability as an alternative to the REV and fracture network concepts. in: Custodio, E., Gurgui, A. & J.P. Lobo-Ferreira (eds.), Groundwater flow and quality modeling, Reidel Publ., Dordrecht, 331-362.

Obarti, F.J., Garay, P. & I. Morell, 1988, An attempt to karst classification in Spain based on system analysis. in: Karst Hydrogeology and Karst Environment Protection, Proc. of the 21st Congress of the Int. Assoc. o. Hydrogeologists, Guilin, China, 328-336.

Pankow J.F., Johnson R.L., Hewetson J.P. & J.A. Cherry, 1986, An evaluation of contaminant migration patterns at two waste disposal sites on fractured porous media in terms of the equivalent porous medium (EPM) Model. J. Cont. Hyd., 1/1: 65 - 76.

Papadopulos, I.S., Bredehoeft, J.D. & H.H. Cooper, 1973, On the analysis of slugtest data. Wat. Res. Res., 9, 1087-1089.

Peres, A.M. Onur. M. & A.C. Reynolds, 1989, A new analysis procedure for determining aquifer properties from slug test data. Wat. Res. Res., 25, 1591-1602.

Pfaff, T., 1987, Grundwasserumsatzräume im Karst der Südlichen Frankenalb. Berichte GSF No. 3/87, Neuherberg, 132p.

Pinder, G.F. & J.F. Jones, 1969, Determination of the groundwater component of peak discharge from the chemistry of total runoff. Wat. Res. Res., 5, 438-445.

Poiseuille, J.M.L., 1846, Recherches experimentales sur le mouvement des liquides dans les tubes de tres petits diametres. Acad. Science Paris Mem. sav. etr., 9, 433-545.

Pulido-Bosch, A. & A. Padilla, 1988, Some considerations about the simulation of karstic aquifers. in: Karst Hydrogeo logy and Karst Environment Protection, Proc. of the 21st Congress of the Int. Assoc. o. Hydrogeologists, Guilin, China. , 583-588.

Quinlan, J.F. & R.O. Ewers, 1985, Groundwater flow in limestone terranes: Strategy rationale and procedure for reliable efficient monitoring of groundwater quality in karst areas. 5th Nat. Symp. and Exp. on Aquifer Restoration and Groundwater Monitoring, Columbus Ohio, May 1985, 197-234.

Quinlan, J.F. & E.C. Alexander, 1987, How often should samples be taken at relevant locations for reliable monitoring of pollutants from an agricultural, waste disposal, or spill site in a karst terrane?. Proc. 2nd Multidisciplinary Conf. on Sinkholes and Env. Impacts of Karst, Florida Sinkhole Res. Inst., Orlando, Florida, 277-286.

Ramey, H.J. jr., Agarwal, R.G. & I. Martin, 1975, Analysis of "slug" test or DST flow period data. J.Can.Petr.Technol., 37-47.

Renger, M. & O. Strebel, 1980a, Jährliche Grundwasserneubildung in Abhängigkeit von Bodennutzung und Bodeneigen schaften. Wasser und Boden, 32, 362-366.

Renger, M. & O. Strebel, 1980b, Beregnungsbedarf landwirtschaftlicher Kulturen in Abhängigkeit vom Boden. Wasser und Boden, 32, 572-575.

Renner, S., 1991, Temperaturuntersuchungen im Karstaquifer der westlichen Schwäbischen Alb. Unpubl. Diplom Thesis University of Tübingen, 92p.

Rinaldo, A. & G. Gambolati, 1987, Basin scale transport of dissolved species in groundwater. Adv. Res. workshop, NATO, Lisbon, Portugal.

Romm, E.S., 1966, Fluid flow in fractured rocks, Nedra, Moscow.

Rorabough, M.J., 1953, Graphical and theoretical analysis of step-drawdown test of artesian well. Proc. Am. Soc. Civ. Eng., 79, No. 362, 23p.

Rothermel, S.R. & A.E. Ogden, 1986, Time series analysis of Edwards aquifer springs in Comal County, Texas. Proc. of the Environmental Problems in Karst Terranes and their Solutions Conference, National Water Well Association, Bowling Green, Kentucky, 115-148.

Rushton, J.R. & C. Ward, 1979, The estimation of groundwater recharge, J. Hydrol., 41, 345-361.

Rutter, A.J., 1975, The hydrological cycle in vegetation. in: J.L. Monteith, Vegetation and the atmosphere, vol 1, Prin ciples. Academic Press, London, 111-154.

Rutter, A.J., Morton, A.J. & P.C. Robins, 1975, A predictive model of rainfall interception in forests. II Generalisation of the model and comparison with observations in some coniferous and hardwood stands. J. Appl. Ecol., 12, 367-380.

Rutter, A.J., Kershaw, K.A., Robins, P.C. & A.J. Morton, 1971, A predictive model of rainfall interception in forests. I Derivation of the model from observations in a plantation of Corsican Pine. Agric. Meteorol., 9, 367-384.

Sauter, 1981, The use of mathematical models in understanding nitrate concentrations of groundwater in the chalk aquifer of East Anglia, U.K.. Unpubl. M.Sc. Thesis, Univ. Birmingham, 97p.

Sauter, M., 1989, Auswertung hydraulischer Feldversuche zur Bestimmung der geohydraulischen Eigenschaften eines Karstgrundwasserleiters. Unpubl. report to VEDEWA, Stgt.

Sauter, M., 1990, Double Porosity Models in Kastified Limestone Aquifers, Proc. Int. Symp. Field Seminar on Hydrogeological Processes in Karst Terranes, 7. - 17.Oct.1990, Antalya, Turkey.

Sauter, M., 1991, Assessment of hydraulic conductivity in a karst aquifer at local and at regional scale. Proc. Third Con ference on Hydrogeology, Ecology, Monitoring and Management of Ground Water in Karst Terranes, Dec. 1991, Nashville.

Sageev, A., 1986, Slug test analysis. Wat. Res. Res., 22, 1323-1333.

Sauveplane, C., 1984, Pumping test analysis in fractured aquifer formations: state of the art and some perspectives. in: J. Rosenshein & G.D. Bennett, Groundwater Hydraulics, Am. Geophys. Union, Water Resourc. Monogr., 9, 171-206.

Scanlon, B.R. & J. Thrailkill, 1987, Chemical similarities among physically distinct spring types in a karst terrain. J. Hydrol., 89, 259-279.

Schädel, K. & I. Stober, 1988, Dispersion als Hinweis auf den Karsttypus. Dt. Gewkdl. Mittl., 32, 107-110.

Schroeder, M., 1989, Interzeptionsmessungen an der Großlysimeteranlage St. Arnold in den Jahren 1984 bis 1987 und die Extrapolation der Meßwerte mit Hilfe eines Rechenmodells. Dt. Gew. Kdl. Mittl., 33, 56-64.

Schroeder, M., 1984, Die Interzeptionsmessungen an der Großlysimeteranlage St. Arnold, Dt. Gew. Kdl. Mittl., 28, 5/6, 164-171.

Seiler, K.-P., Maloszewski, P. & H. Behrens, 1989, Results on hydrodynamic dispersion in the karstified aquifer of the Upper Jura of Franconian Alb, FR Germany. In: Kobus, H. & W. Kinzelbach, Contaminant Transport in Groundwater, Balkema, 83-87.

Shuster, E.T. & W.B. White, 1971, Seasonal fluctuations in the chemistry of limestone springs; A possible means for characterising carbonate aquifers. J. Hydrol., 14, 93-128.

Simpson, E.S., 1988, The discrete state compartment model and its application to flow through karstic aquifers. Karst Hydrogeology and Karst Environment Protection, Proc. of the 21st Congress of the Int. Assoc. o.Hydrogeologists, Guilin, China, 671-676.

Sklash, M.G. & R.N. Farvolden, The role of groundwater in storm runoff. J. Hydrol., 43, 45-65.

Smart, P.L. & H. Friederich, 1986, Water movement and storage in the unsaturated zone of a maturely karstified car bonate aquifer. Mendip Hills, England, Proc. of the Environmental Problems in Karst Terranes and their Solutions Conference, National Water Well Association, Bowling Green, Kentucky.

Smart, P.L. & S.L. Hobbs, 1986, Characterisation of carbonate aquifers: A conceptual base. Proc. of the Environmental Problems in Karst Terranes and their Solutions Conference, National Water Well Association, Bowling Green, Kentucky, 1-4.

Smith, L., Schwartz, F. & C. Mase, 1987, Applications of stochastic methods for the simulation of solute transport in discrete and continuum models of fractured rock systems. Proc. of the Conference on Geostatistical, Sensitivity and Uncertainty Methods for Groundwater Flow and Radionuclide Transport Modelling, S. Francisco, 425-440.

Snow, D.T., 1965, A parallel plate model of fractured permeable media. Ph.D. thesis, Univ. of California, Berkeley, 330p.

Sokollek, V., 1983, Der Einfluss der Bodennutzung auf den Wasserhaushalt kleiner Einzugsgebiete in unteren Mittel gebirgslagen., Ph.D. thesis, Giessen, 296p.

Soulios, G., 1985, Récherches sur l'unité des systèmes aquifères karstiques d`après des examples du karst Hellenique. J. Hydrol., 81, 333-354.

Steele, K.F., Widmann, R.K., Wickliff, D.S. & D.L. Parr, 1985, The effect of rainstorm events on spring water che mistry in a limestone terrain. Proc. AGWSE, Southern Reg. Groundwater Conference, NWWA, San Antonio, Texas, 50-66.

Stichler, W., Moser, H. & M. Schroeder, 1984, Measurements of seepage velocity in a sand lysimeter by means of ^{18}O - content. Proc. Int. Symp. Recent Investigations in the zone of Aeration, Munich, Oct 1984.

Stober, I., 1991, Strömungsvorgänge und Durchlässigkeitsverteilung innerhalb des Weißjura - Aquifers im baden-würt tembergischen Anteil des Molassebeckens. Laichinger Höhlenfreund, 26, 29-42.

Streltsova, T.D., 1988, Well testing in heterogeneous formations. Wiley, N.Y., 412p.

Strayle, G., 1970, Karsthydrologische Untersuchungen auf der Ebinger Alb (Schwäbischer Jura). Jh. geol. Landesamt Baden-Württemberg, 12, 109-209.

de Swaan, A.O., 1976, Analytic solutions for determining naturally fractured reservoir properties by well testing. Soc. Petr. Eng. J., 16, p117.

Teutsch, G., 1989, Groundwater models in karstified terraines - two practical examples from the Swabian Alb, S. Ger many. Proc. of the 4th Conference - Solving Groundwater Problems with Models, Indianapolis, USA, Feb. 7-9 1989, 929-953.

Teutsch, G., 1988, Grundwassermodelle im Karst: Praktische Ansätze am Beispiel zweier Einzugsgebiete im Tiefen und Seichten Malmkarst der Schwäbischen Alb. Ph.D. Thesis, Universität Tübingen, 205p.

Teutsch, G. & M. Sauter, 1991, Groundwater modeling in karst terranes: scale effects, data acquisition and field vali dation. Proc. Third Conference on Hydrogeology, Ecology, Monitoring and Management of Ground Water in Karst Terranes, Dec. 1991, Nashville.

Thiem, G., 1906, Hydrologische Methoden. Leipzig, Gebhardt.

Theis, C.V., 1935, Relation between the lowering of the piezometric surface and the rate and duration of discharge of a well using groundwater storage. Eos, Trans. Am. Geophys. Union, 16, 519-524.

Thompson, D.B., 1987, A microcomputer program for interpreting time-lag permeability tests. Ground Water, 25, 212-218.

Thornthwaite, C.W., & J.R. Mather, 1957, Instructions and tables for computing potential evapotranspiration and the water balance. Publ. Climatol., Drexel Inst. Technol., 10.

Thrailkill, J.T., 1986, Models and methods for shallow conduit-flow carbonate aquifers. Proc. of the Environmental Problems in Karst Terranes and their Solutions Conference, National Water Well Association, Bowling Green, Kentucky, 17-31.

Thrailkill, J.T., S.B. Sullivan & D.R. Gouzie, 1991, Flow parameters in a shallow conduit-flow carbonate aquifer, Inner Bluegrass Karst Region, Kentucky, USA. J. Hydrol.,

Tibbals, C.H., 1990, Hydrology of the Floridan aquifer system in east-central Florida. U.S.G.S. Professional Paper, 1043-E.

Trainer, F.W. & F.A. Watkins, jr., 1974, Use of base-runoff recession curves to determine areal transmissivities in the Upper Potomac river basin. USGS J. Res., 2, 125-131.

Trudggill, S.T., Pickles, A. & K.R.J. Smettem, 1983, Soil water residence time and solute uptake. 2. Dye tracing and preferential flow predictions. J. Hydrol., 62, 279-285.

Uhlig, S., 1959, Wasserhaushaltsbetrachtungen nach Thornthwaite. Z. f. Acker- und Pflanzenbau, 109, Berlin, 384-407.

Villinger, E., 1986, Untersuchungen zur Flußgeschichte von Aare-Donau/Alpenrhein und zur Entwicklung des Malm-Karsts in SW Deutschland, Jh. Geol. Landesamt Baden-Württemberg, 28, 297-362.

Vervier, P., 1990, Hydrochemical characterisation of the water dynamics of a karstic system. J. Hydrol. 121, 103-117

Villinger, E., Hydrogeologisches Gutachten über die weiteren Ergebnisse der Wassererschließung im Gewann Stetten bei Veringenstadt, Lkr. Sigmaringen. Unpubl. report, Geologisches Landesamt Baden-Württemberg, 4763-6/88 SIG.

Villinger, E., 1977, Über Potentialverteilung und Strömungssysteme im Karstwasser der Schwäbischen Alb (Ob. Jura, SW-Deutschland). Geolog. Jahrbuch, C18, 92p.

Villinger, E., 1972, Seichter Karst und Tiefer Karst in der Schwäbischen Alb. Geol. Jb. C2, 153-188.

Warren, J.E. & P.J. Root, 1963, The behaviour of naturally fractured reservoirs, Soc. Petrol. Eng. J., 3, 245-255.

Weiß, E.G., 1987, Porositäten, Permeabilitäten und Verkarstungserscheinungen im mittleren und oberen Malm der Südlichen Frankenalb. Ph.D. Thesis, Universität Erlangen, 240p.

Werner, J., 1978, Quartär, Holozän. in: Erläuterungen zur Geologischen Karte Baden-Wüttemberg, 1:25000, Blatt 7821, Veringenstadt, Landesvermessungsamt Baden-Württemberg, Stuttgart.

White, W.B., 1977, Conceptual Models for Karst Aquifers: Revisited. in: Dilamarter, R.R. & Csallany, C.S. (eds), Hy drologic Problems in Karst Regions, Western Kentucky Univ. Press, Bowling Green, Kentucky, 76-87.

White, W.B., 1988, Geomorphology and hydrology of karst terrains. Oxford University Press, 464p.

Widdowson, M.A., Molz F.J. & J.G. Melville, 1990, An analysis technique for multilevel and partially penetrating slug test data. Ground Water, 28, 937-945.

Williams, P.W., 1985, Subcutaneous hydrology and the development of doline and cockpit karst. Zeit. Geomorph., 29, 463-482.

Williams, P.W., 1983, The role of the subcutaneous zone in karst hydrology. J. o. Hyd., 61, 45-67.

Yilin, C., Hongtao, W. & X. Xinhui, 1988, Dual-media flow models of karst areas and their application in north China. Karst Hydrogeology and Karst Environment Protection, Proc. of the 21st Congress of the Int. Assoc. o.Hydrogeologists, Guilin, China.

Yusun, C. & B. Ji, 1988, The media and movement of karst water. Karst Hydrogeology and Karst Environment Protec tion, Proc. of the 21st Congress of the Int. Assoc. o. Hydrogeologists, Guilin, China, 704.

Zaltsberg, E.A., 1984, Forecast of karst water levels in: A. Burger & L. Dubertret. eds, Hydrogeology of Karstic Ter raines, International Contributions to Hydrogeology, Heise, Hannover, 40-42.

Zeidler, N., 1987, Hydraulisch - hydrochemische Untersuchungen und Modellrechnungen im Malmkarst der Schwäbischen Alb. Unpubl. Report, Geologisches Inst. Universität Tübingen, 74p.

9 Appendices

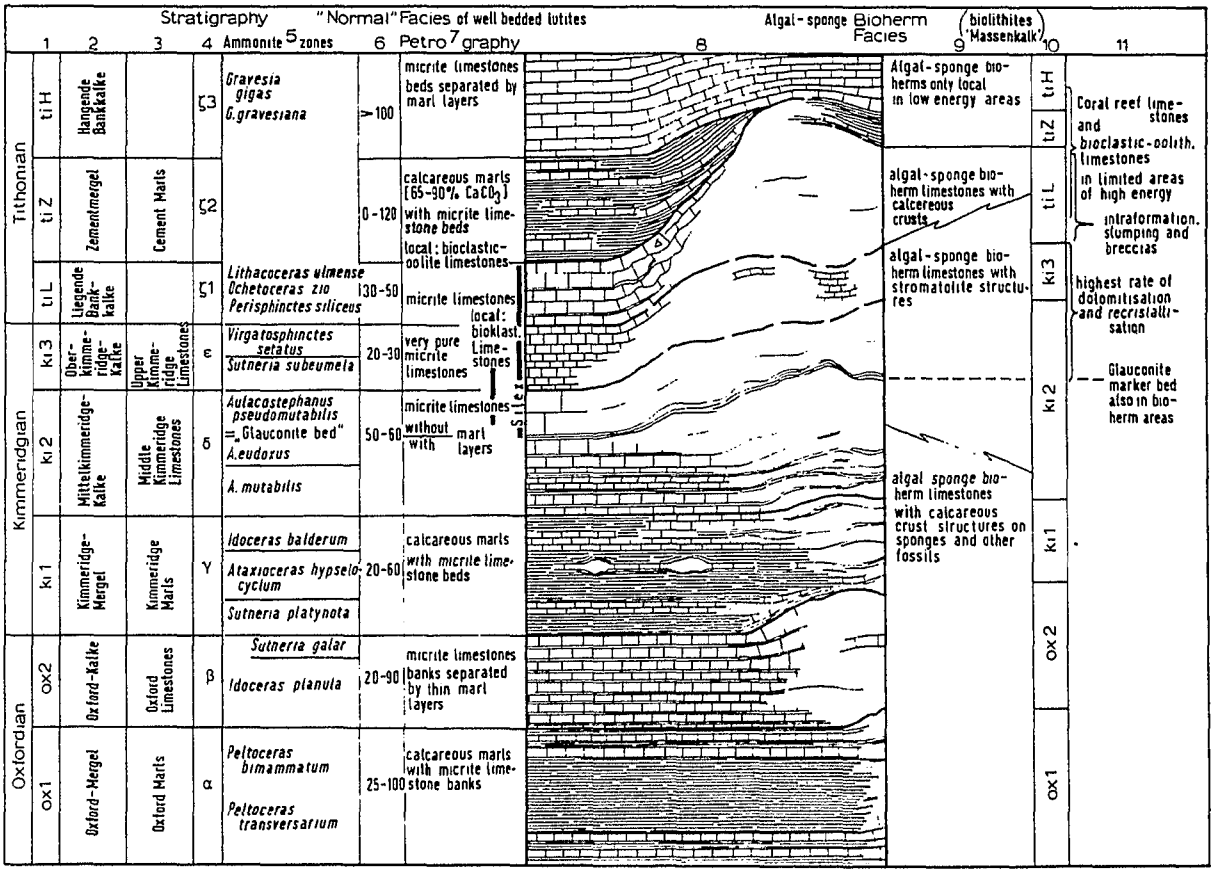

Columns 1, 2, and 10: stratigraphy now used on geological maps and in this paper
column 3: English translation used in this paper
column 4: subdivision by QUENSTEDT, widely used up to now
column 6: thickness of bedded sediments ("normal facies")
column 8: schematic profile, also illustrating the distribution of micritic and bioherm sediments
column 11: remarks

App. 2-1 Stratigraphy and Facies of the Upper Jurassic of the Swabian Alb (Gwinner, 1976)

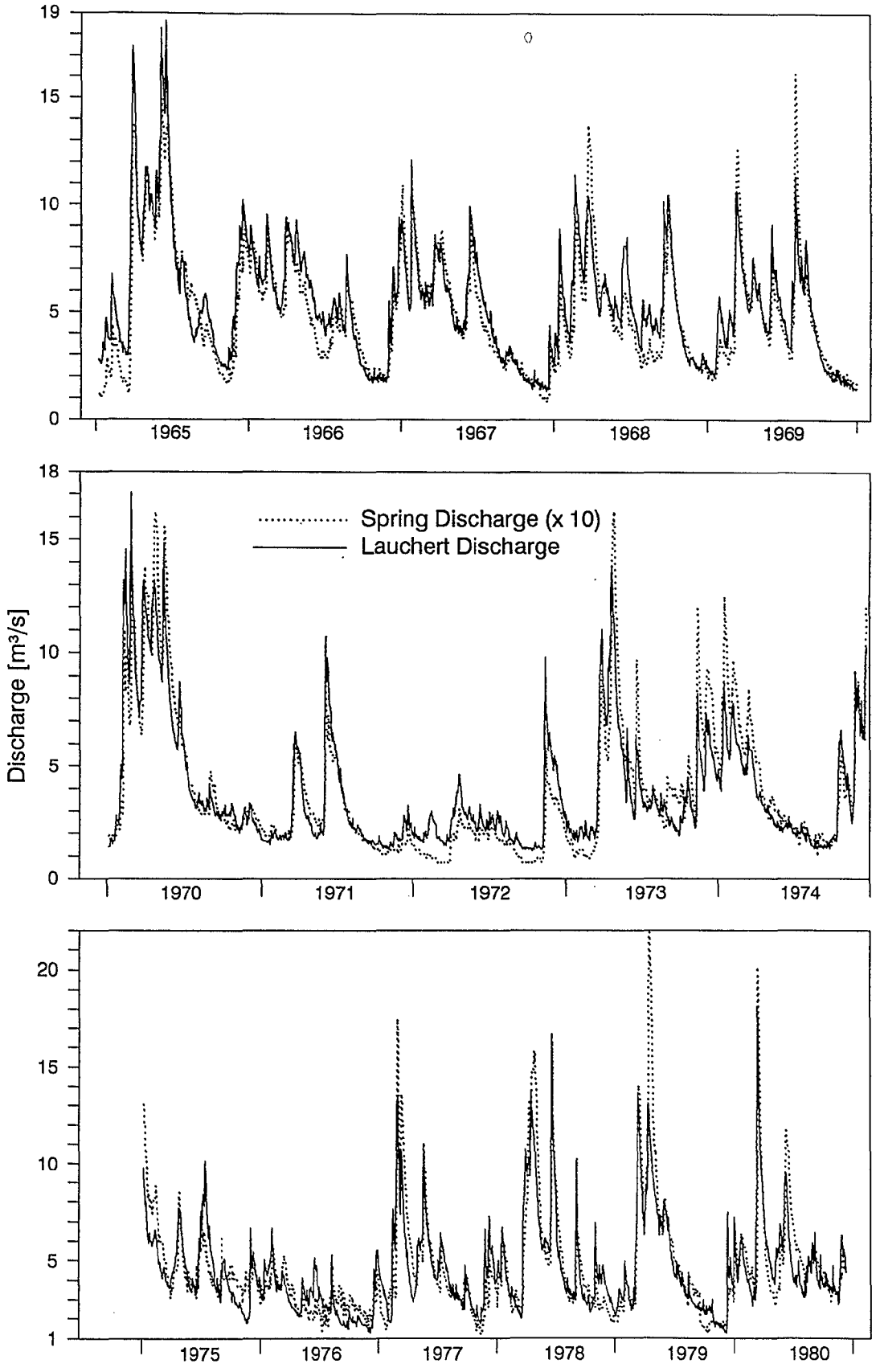

App. 2-2 Comparison between Gallusquelle Spring Discharge and Lauchert River Discharge for the Period 1965 - 1980

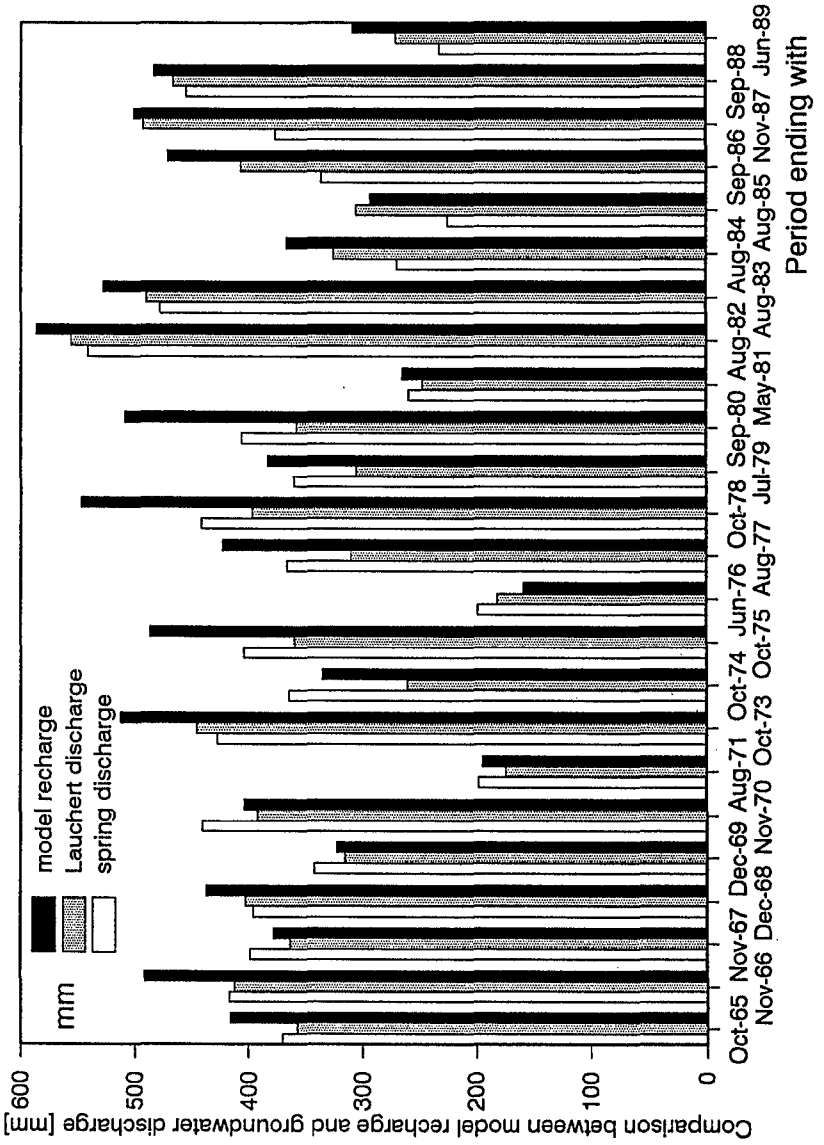

App. 4-1 Comparison between Model Recharge and Groundwater Discharge (Lauchert, Gallusquelle)

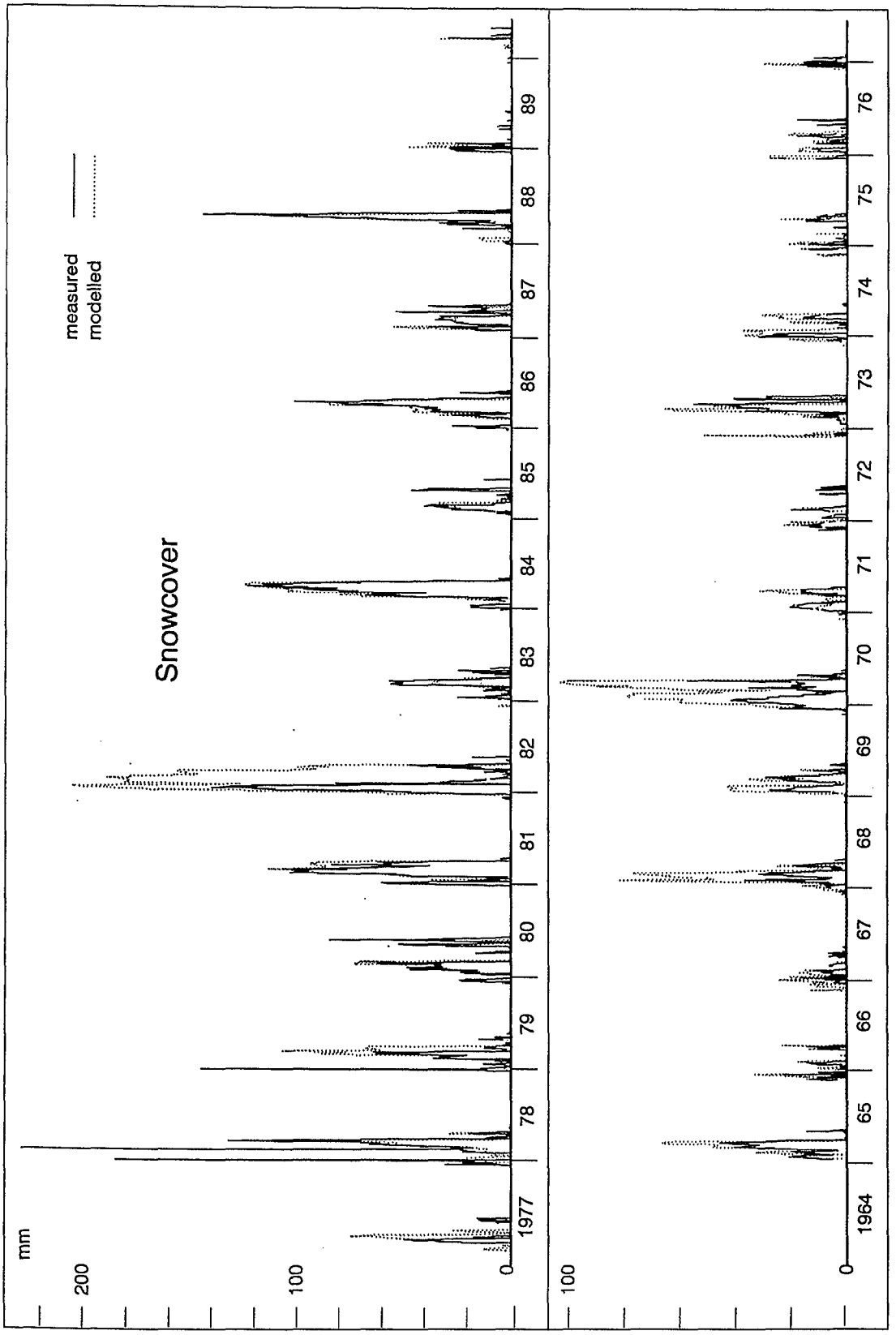

App. 4-2 Comparison between Modelled and Measured Depth of Snow Cover (1965 - 1989)

App. 4-3 (a) Sensitivity Analysis for Recharge Calculation, Annual Values

Sensitivity analysis, 1965-1990, annual values

field capacity				40	60	70	75	80	100	130	75	75	75	75	75	75	75	75	75
interception capacity				4.7	4.7	4.7	4.7	4.7	4.7	4.7	4.7	4	3	2	1	4.7	4.7	4.7	4.7
rapid recharge (wood,agri)				75,6	75,6	75,6	75,6	75,6	75,6	75,6	75,6	75,6	75,6	75,6	75,6	35,6	25,6	15,6	10,6
all in mm		Spring	Lauch.	fieldcapacity variations ----------							Intercept. cap. var. -------					rapid rech. var. -----			
Period		disch.	disch.	st4	st3	st2	st1	st5	st6	st7	st1	st8	st9	st10	st11	st12	st13	st14	st15
Mar-65	Oct-65	370.4	357.3	447.9	429.8	410.7	406.9	404.4	399.7	399.7	406.9	408.0	410.0	414.5	421.6	406.9	410.3	421.7	435.5
Oct-65	Nov-66	417.5	412.7	547.8	515.9	487.7	480.0	470.3	445.5	425.1	480.0	482.2	486.4	492.5	502.9	480.0	480.0	481.7	489.1
Nov-66	Nov-67	398.8	363.4	413.1	392.2	373.4	371.1	359.3	343.7	331.6	371.1	371.8	373.6	376.1	380.5	371.1	371.1	374.2	381.9
Nov-67	Dec-68	395.9	402.9	490.4	458.3	433.5	424.9	420.6	383.3	334.1	424.9	427.5	432.7	440.2	451.1	424.9	424.8	438.0	440.4
Dec-68	Dec-69	342.5	315.7	374.2	350.8	317.3	313.5	308.0	295.1	295.1	313.5	316.5	318.8	323.2	330.3	313.5	316.2	329.6	360.7
Dec-69	Nov-70	440.6	392.7	425.6	420.3	400.2	398.0	393.4	377.2	354.7	398.0	399.6	400.9	402.8	404.3	398.0	398.1	406.7	410.5
Nov-70	Aug-71	198.0	174.4	222.5	204.3	193.1	189.5	184.2	153.5	118.5	189.5	190.2	192.1	193.7	196.8	189.5	189.5	191.5	196.8
Aug-71	Oct-73	427.5	445.3	589.7	540.9	507.3	499.1	479.6	433.3	376.2	499.1	501.0	504.7	508.8	515.7	499.1	499.0	505.7	532.4
Oct-73	Oct-74	363.9	260.2	365.0	346.0	334.2	332.4	328.3	310.8	282.7	332.4	332.8	333.6	334.8	337.0	332.4	332.4	336.6	349.6
Oct-74	Oct-75	403.8	359.3	541.2	508.3	486.6	480.2	472.5	427.7	390.0	480.2	482.0	484.5	488.7	495.6	480.2	480.2	480.8	487.2
Oct-75	Jun-76	198.2	181.4	182.7	170.0	155.8	153.0	149.7	140.0	114.9	153.0	153.6	154.9	156.9	159.3	153.0	153.0	154.3	157.6
Jun-76	Aug-77	366.0	309.5	473.2	439.1	420.1	414.1	406.8	379.0	348.8	414.1	415.5	418.1	421.9	428.0	414.0	418.5	424.2	429.1
Aug-77	Oct-78	441.4	396.6	600.0	568.6	543.7	539.6	531.4	508.2	480.1	539.6	540.5	543.2	545.6	552.9	539.5	541.8	553.7	572.3
Oct-78	Jul-79	360.1	304.4	396.7	384.3	380.4	378.7	373.4	360.6	345.2	378.7	380.3	381.9	384.1	387.9	378.7	378.7	378.8	388.8
Jul-79	Sep-80	405.6	357.2	551.5	522.4	504.7	499.7	491.5	469.4	442.7	499.7	501.9	505.8	510.4	516.2	499.7	500.0	506.5	516.8
Sep-80	May-81	259.3	247.4	285.9	269.7	262.3	260.1	256.6	241.5	218.8	260.1	261.1	262.7	265.2	268.5	260.1	260.1	259.5	264.3
May-81	Aug-82	541.4	556.3	655.9	611.8	584.0	577.1	567.3	535.8	510.8	577.1	578.2	580.3	584.9	595.4	577.1	584.0	592.7	603.0
Aug-82	Aug-83	477.8	489.7	552.2	533.9	523.3	520.0	513.4	502.7	472.8	520.0	521.1	523.3	526.6	532.0	520.0	520.0	520.3	520.0
Aug-83	Aug-84	269.2	325.0	404.7	381.0	364.7	360.1	362.2	327.5	301.8	360.1	361.1	363.1	365.4	370.1	360.1	360.1	371.6	374.6
Aug-84	Aug-85	224.8	304.9	331.6	313.6	287.4	283.5	279.0	261.6	235.7	283.5	285.9	289.4	294.7	301.6	283.5	283.5	284.5	291.3
Aug-85	Sep-86	336.2	406.8	504.2	484.1	465.4	461.8	456.6	439.7	414.9	461.8	463.2	466.1	470.5	477.6	461.8	461.8	477.3	489.7
Sep-86	Nov-87	376.1	492.6	566.9	531.3	496.7	490.5	478.2	459.3	432.6	490.5	493.0	497.2	503.3	510.6	490.5	493.0	506.4	524.3
Nov-87	Sep-88	454.7	466.5	501.2	490.0	477.7	474.7	469.3	448.6	421.8	474.7	476.2	477.6	479.3	483.2	474.7	474.7	474.7	474.7
Sep-88	Jun-89	232.4	270.3	328.7	316.0	304.4	302.4	298.6	284.1	268.6	302.4	304.0	306.8	311.4	317.5	302.4	302.4	302.4	302.4
sum		8702	8592	10753	10183	9715	9611	9455	8928	8317	9611	9647	9708	9796	9937	9611	9633	9773	9993

Sensitivity analysis, 1986-1990, monthly values

field capacity	40	60	70	75	80	100	130	75	75	75	75	75	75	75	75	75
interception capacity	4.7	4.7	4.7	4.7	4.7	4.7	4.7	4.7	4	3	2	1	4.7	4.7	4.7	4.7
rapid recharge (wood,agri)	75,6	75,6	75,6	75,6	75,6	75,6	75,6	75,6	75,6	75,6	75,6	75,6	35,6	25,6	15,6	10,6
all in mm	fieldcapacity variations ----------							Intercept. cap. var. -------					rapid rech. var. -----			
date	st4	st3	st2	st1	st5	st6	st7	st1	st8	st9	st10	st11	st12	st13	st14	st15
Jan-86	85.5	85.5	85.5	85.5	85.5	82.5	63.0	85.5	85.5	85.5	85.5	85.5	85.5	85.5	85.5	85.5
Feb-86	0.0	0.0	0.0	0.0	0.0	0.0	0.0	0.0	0.0	0.0	0.0	0.0	0.0	0.0	0.0	0.0
Mar-86	100.4	99.7	99.7	99.7	99.7	99.7	99.7	99.7	99.9	100.2	100.5	100.8	99.7	99.7	99.7	99.7
Apr-86	118.4	118.0	118.0	118.0	118.0	118.0	118.0	118.0	118.2	118.5	118.8	119.6	118.0	118.0	118.0	118.0
May-86	25.2	26.1	16.6	16.6	16.6	16.6	16.6	16.6	16.6	17.0	19.0	22.5	16.6	16.6	17.2	20.2
Jun-86	50.3	48.6	48.6	47.7	47.4	47.4	47.4	47.7	48.3	49.4	50.4	51.6	47.7	47.7	47.2	46.0
Jul-86	14.5	14.3	14.3	14.3	14.3	14.3	14.3	14.3	14.3	14.3	14.3	14.3	14.3	14.3	26.4	23.3
Aug-86	27.2	27.2	27.9	27.9	27.2	27.2	27.2	27.9	27.9	27.9	27.9	27.9	27.9	27.9	30.2	38.6
Sep-86	18.9	12.8	12.8	12.8	12.8	12.8	12.8	12.8	12.8	12.8	12.8	12.8	12.8	12.8	15.7	21.1
Oct-86	51.7	42.1	37.4	35.5	33.1	23.5	18.6	35.5	35.9	36.6	37.5	38.2	35.5	35.5	34.0	40.0
Nov-86	21.4	20.6	18.3	18.3	16.8	14.2	3.2	18.3	18.5	18.9	19.2	19.7	18.3	18.3	18.2	10.3
Dec-86	69.5	69.2	69.2	69.2	69.2	65.4	54.6	69.2	69.2	69.3	69.4	69.6	69.2	69.2	69.2	69.2
Jan-87	15.8	15.8	15.8	15.8	15.8	15.8	15.8	15.8	15.8	15.8	15.8	15.8	15.8	15.8	15.8	15.8
Feb-87	87.1	86.9	86.9	86.9	86.9	86.9	86.9	86.9	86.9	86.9	86.9	86.9	86.9	86.9	86.9	86.9
Mar-87	35.7	35.2	35.2	35.2	35.2	35.2	35.2	35.2	35.2	35.2	35.2	35.2	35.2	35.2	35.2	35.2
Apr-87	14.0	13.9	13.9	13.9	13.9	13.9	13.9	13.9	14.1	14.3	14.8	15.4	13.9	13.9	13.9	13.9
May-87	53.3	48.0	43.9	42.7	40.6	39.1	39.1	42.7	43.3	44.2	46.4	48.2	42.7	42.7	42.6	42.6
Jun-87	97.0	95.3	94.0	94.0	94.0	94.0	94.0	94.0	94.3	94.8	95.5	97.3	94.0	94.0	94.0	94.0
Jul-87	38.0	44.8	34.0	33.1	30.7	30.4	30.4	33.1	33.4	34.1	34.8	35.5	33.1	33.1	38.0	46.3
Aug-87	22.7	16.9	13.4	13.4	11.7	11.6	11.6	13.4	13.4	13.4	13.4	13.4	13.4	13.4	13.4	15.9
Sep-87	19.1	15.9	14.8	14.8	14.8	14.8	14.8	14.8	14.8	14.8	14.8	14.8	14.8	20.5	26.5	29.5
Oct-87	21.5	12.8	7.7	5.9	5.9	5.9	5.9	5.9	6.0	6.6	7.3	8.2	5.9	5.9	7.2	10.2
Nov-87	66.2	65.8	63.2	62.8	58.9	43.2	16.4	62.8	63.2	63.4	63.4	63.6	62.8	59.4	54.3	49.6
Dec-87	47.0	47.0	47.0	47.0	47.0	47.0	47.0	47.0	47.0	47.0	47.0	47.1	47.0	47.0	47.0	47.0
Jan-88	49.6	49.4	49.4	49.4	49.4	49.4	49.4	49.4	49.4	49.5	49.5	49.7	49.4	49.4	49.4	49.4
Feb-88	32.3	32.6	32.6	32.6	32.6	32.6	32.6	32.6	32.6	32.6	32.6	32.6	32.6	32.6	32.6	32.6
Mar-88	188.5	188.1	188.1	188.1	188.1	188.1	188.1	188.1	188.1	188.1	188.1	188.2	188.1	188.1	188.1	188.1
Apr-88	28.0	27.0	27.0	27.0	27.0	27.0	27.0	27.0	27.3	27.6	28.2	29.0	27.0	27.0	27.0	27.0
May-88	23.9	19.9	16.0	14.2	12.4	11.7	11.7	14.2	15.3	15.9	16.6	18.3	14.2	14.2	14.4	17.4
Jun-88	41.3	39.4	33.0	31.8	30.8	29.0	29.0	31.8	31.9	32.2	32.6	33.5	31.8	31.8	31.7	29.9
Jul-88	8.2	8.4	7.3	7.3	7.3	7.3	7.3	7.3	7.3	7.3	7.3	7.3	7.3	7.3	7.3	7.3
Aug-88	8.8	8.8	12.3	12.3	12.3	8.8	8.8	12.3	12.3	12.3	12.3	12.3	12.3	12.3	12.7	15.7
Sep-88	20.8	16.9	13.4	13.4	12.5	12.5	12.5	13.4	13.4	13.4	13.4	13.4	13.4	13.4	13.4	14.4
Oct-88	51.3	44.0	38.3	36.5	33.1	18.6	15.0	36.5	37.1	38.0	39.7	41.5	36.5	36.5	36.5	35.4
Nov-88	24.3	22.9	21.7	21.7	21.7	21.7	11.3	21.7	21.9	22.4	23.2	24.7	21.7	21.7	21.7	21.7
Dec-88	121.5	121.5	121.5	121.5	121.5	121.5	120.0	121.5	121.5	121.5	121.5	121.5	121.5	121.5	121.5	121.5
Jan-89	7.8	7.8	7.8	7.8	7.8	7.8	7.8	7.8	7.8	7.8	7.9	7.9	7.8	7.8	7.8	7.8
Feb-89	30.3	29.8	29.8	29.8	29.8	29.8	29.8	29.8	29.9	30.0	30.2	30.5	29.8	29.8	29.8	29.8
Mar-89	5.9	5.8	5.8	5.8	5.8	5.8	5.8	5.8	5.8	5.8	5.8	5.8	5.8	5.8	5.8	5.8
Apr-89	79.9	76.5	71.8	71.6	71.2	71.2	71.2	71.6	72.3	73.6	75.4	77.9	71.6	71.6	71.6	71.6
May-89	1.2	1.2	1.2	1.2	1.2	1.2	1.2	1.2	1.2	1.2	1.2	1.2	1.2	1.2	1.2	1.2
Jun-89	8.2	8.2	8.2	8.2	8.2	8.3	8.2	8.2	8.2	8.2	8.2	8.2	8.2	8.2	11.4	14.4
Jul-89	33.4	25.6	22.2	20.4	20.1	20.1	20.1	20.4	20.9	21.7	23.0	24.8	20.4	24.5	30.5	34.4
Aug-89	1.3	1.3	1.3	1.3	1.3	1.3	1.3	1.3	1.3	1.3	1.3	1.3	1.3	1.3	1.3	1.3
Sep-89	0.0	0.0	0.0	0.0	0.0	0.0	0.0	0.0	0.0	0.0	0.0	0.0	0.0	0.0	0.0	0.0
Oct-89	5.9	5.4	5.4	5.4	5.4	5.4	5.4	5.4	5.4	5.4	5.4	5.4	5.4	5.4	5.4	6.8
Nov-89	13.6	4.0	4.0	4.0	4.0	4.0	4.0	4.0	4.0	4.0	4.0	4.0	4.0	4.0	4.0	6.6
Dec-89	65.6	61.9	53.5	51.1	46.9	30.8	12.9	51.1	51.8	53.0	54.3	55.9	51.1	51.1	51.1	51.1
Jan-90	15.2	15.2	15.2	15.2	15.2	15.2	9.0	15.2	15.2	15.2	15.2	15.2	15.2	15.2	15.2	15.2
Feb-90	102.0	101.2	101.0	101.0	101.0	101.0	98.8	101.0	101.3	101.9	102.7	103.9	101.0	101.0	101.0	101.0
Mar-90	3.4	1.0	1.0	1.0	1.0	1.0	1.0	1.0	1.0	1.0	1.0	1.0	1.0	1.0	1.0	1.0
Apr-90	21.3	18.8	13.5	13.5	13.5	13.5	13.5	13.5	14.1	15.1	16.6	19.0	13.5	13.5	13.5	13.5

Sensitivity analysis, April 89, daily values

field capacity	40	60	70	75	80	100	130	75	75	75	75	75	75	75	75	75
interception capacity	4.7	4.7	4.7	4.7	4.7	4.7	4.7	4.7	4	3	2	1	4.7	4.7	4.7	4.7
rapid recharge (wood,agri)	75,6	75,6	75,6	75,6	75,6	75,6	75,6	75,6	75,6	75,6	75,6	75,6	35,6	25,6	15,6	10,6
all in mm	fieldcapacity variations ----------							Intercept. cap. var. -------					rapid rech. var. -----			
date	st4	st3	st2	st1	st5	st6	st7	st1	st8	st9	st10	st11	st12	st13	st14	st15
890401	24.7	22.9	21.4	21.2	21.2	21.2	21.2	21.2	21.8	22.7	23.7	24.7	21.2	21.2	24.5	27.5
890402	10.0	10.0	10.0	10.0	10.0	10.0	10.0	10.0	10.0	10.0	10.0	10.0	10.0	10.0	6.7	4.3
890403	0.1	0.1	0.1	0.1	0.1	0.1	0.1	0.1	0.1	0.1	0.1	0.1	0.1	0.1	0.1	0.0
890404	0.0	0.0	0.0	0.0	0.0	0.0	0.0	0.0	0.0	0.0	0.0	0.0	0.0	0.0	0.0	0.0
890405	0.0	0.0	0.0	0.0	0.0	0.0	0.0	0.0	0.0	0.0	0.0	0.0	0.0	0.0	0.0	0.0
890406	0.0	0.0	0.0	0.0	0.0	0.0	0.0	0.0	0.0	0.0	0.0	0.0	0.0	0.0	0.0	0.0
890407	0.0	0.0	0.0	0.0	0.0	0.0	0.0	0.0	0.0	0.0	0.0	0.0	0.0	0.0	0.0	0.0
890408	0.1	0.1	0.1	0.1	0.1	0.1	0.1	0.1	0.1	0.1	0.1	0.3	0.1	0.1	0.1	0.1
890409	0.0	0.0	0.0	0.0	0.0	0.0	0.0	0.0	0.0	0.0	0.0	0.0	0.0	0.0	0.0	0.0
890410	0.0	0.0	0.0	0.0	0.0	0.0	0.0	0.0	0.0	0.0	0.0	0.0	0.0	0.0	0.0	0.0
890411	0.0	0.0	0.0	0.0	0.0	0.0	0.0	0.0	0.0	0.0	0.0	0.0	0.0	0.0	0.0	0.0
890412	0.0	0.0	0.0	0.0	0.0	0.0	0.0	0.0	0.0	0.0	0.0	0.0	0.0	0.0	0.0	0.0
890413	0.2	0.2	0.2	0.2	0.2	0.2	0.2	0.2	0.2	0.2	0.2	0.9	0.2	0.2	0.2	0.2
890414	7.3	6.1	5.3	5.3	5.3	5.3	5.3	5.3	5.4	5.6	5.9	5.9	5.3	5.3	5.3	4.8
890415	0.0	0.0	0.0	0.0	0.0	0.0	0.0	0.0	0.0	0.0	0.0	0.0	0.0	0.0	0.0	0.0
890416	7.1	7.1	5.9	5.9	5.9	5.9	5.9	5.9	5.9	5.9	5.9	5.9	5.9	5.9	5.9	5.9
890417	15.9	15.9	14.7	14.7	14.3	14.3	14.3	14.7	14.7	14.7	14.7	14.7	14.7	14.7	14.7	14.7
890418	0.0	0.0	0.0	0.0	0.0	0.0	0.0	0.0	0.0	0.0	0.0	0.0	0.0	0.0	0.0	0.0
890419	0.3	0.3	0.3	0.3	0.3	0.3	0.3	0.3	0.3	0.3	0.3	0.3	0.3	0.3	0.3	0.3
890420	1.5	1.5	1.5	1.5	1.5	1.5	1.5	1.5	1.5	1.5	1.5	1.5	1.5	1.5	1.5	1.5
890421	8.4	8.4	8.4	8.4	8.4	8.4	8.4	8.4	8.4	8.4	8.4	8.4	8.4	8.4	8.4	8.4
890422	2.9	2.9	2.9	2.9	2.9	2.9	2.9	2.9	2.9	2.9	2.9	2.9	2.9	2.9	2.9	2.9
890423	0.0	0.0	0.0	0.0	0.0	0.0	0.0	0.0	0.0	0.0	0.0	0.0	0.0	0.0	0.0	0.0
890424	0.0	0.0	0.0	0.0	0.0	0.0	0.0	0.0	0.0	0.0	0.0	0.0	0.0	0.0	0.0	0.0
890425	0.0	0.0	0.0	0.0	0.0	0.0	0.0	0.0	0.0	0.0	0.0	0.0	0.0	0.0	0.0	0.0
890426	0.0	0.0	0.0	0.0	0.0	0.0	0.0	0.0	0.0	0.0	0.0	0.0	0.0	0.0	0.0	0.0
890427	0.0	0.0	0.0	0.0	0.0	0.0	0.0	0.0	0.0	0.0	0.0	0.0	0.0	0.0	0.0	0.0
890428	1.4	1.0	1.0	1.0	1.0	1.0	1.0	1.0	1.0	1.2	1.7	2.3	1.0	1.0	1.0	1.0
890429	0.0	0.0	0.0	0.0	0.0	0.0	0.0	0.0	0.0	0.0	0.0	0.0	0.0	0.0	0.0	0.0
890430	0.0	0.0	0.0	0.0	0.0	0.0	0.0	0.0	0.0	0.0	0.0	0.0	0.0	0.0	0.0	0.0

Sensitivity analysis, June 1988, daily values

field capacity	40	60	70	75	80	100	130	75	75	75	75	75	75	75	75	75
interception capacity	4.7	4.7	4.7	4.7	4.7	4.7	4.7	4.7	4	3	2	1	4.7	4.7	4.7	4.7
rapid recharge (wood,agri)	75,6	75,6	75,6	75,6	75,6	75,6	75,6	75,6	75,6	75,6	75,6	75,6	35,6	25,6	15,6	10,6
all in mm	fieldcapacity variations ----------							Intercept. cap. var. -------					rapid rech. var. -----			
date	st4	st3	st2	st1	st5	st6	st7	st1	st8	st9	st10	st11	st12	st13	st14	st15
880601	0.0	0.0	0.0	0.0	0.0	0.0	0.0	0.0	0.0	0.0	0.0	0.0	0.0	0.0	0.0	0.0
880602	0.0	0.0	0.0	0.0	0.0	0.0	0.0	0.0	0.0	0.0	0.0	0.0	0.0	0.0	0.0	0.0
880603	2.4	2.4	2.4	2.4	2.4	2.4	2.4	2.4	2.4	2.4	2.4	2.4	2.4	2.4	2.4	2.4
880604	0.7	0.7	0.7	0.7	0.7	0.7	0.7	0.7	0.7	0.7	0.7	0.7	0.7	0.7	0.7	0.7
880605	2.8	1.9	1.6	1.6	1.6	1.6	1.6	1.6	1.6	1.6	1.6	1.6	1.6	1.6	1.6	1.6
880606	18.4	17.6	13.1	11.9	11.1	9.3	9.3	11.9	12.0	12.2	12.5	13.1	11.9	11.9	11.8	10.4
880607	0.0	0.0	0.0	0.0	0.0	0.0	0.0	0.0	0.0	0.0	0.0	0.0	0.0	0.0	0.0	0.0
880608	0.5	0.5	0.0	0.0	0.0	0.0	0.0	0.0	0.0	0.0	0.0	0.0	0.0	0.0	0.0	0.0
880609	0.0	0.0	0.0	0.0	0.0	0.0	0.0	0.0	0.0	0.0	0.0	0.0	0.0	0.0	0.0	0.0
880610	0.0	0.0	0.0	0.0	0.0	0.0	0.0	0.0	0.0	0.0	0.0	0.0	0.0	0.0	0.0	0.0
880611	8.3	8.1	7.0	7.0	6.9	6.9	6.9	7.0	7.0	7.1	7.2	7.5	7.0	7.0	7.0	7.0
880612	7.1	7.1	7.1	7.1	7.0	7.0	7.0	7.1	7.1	7.1	7.1	7.1	7.1	7.1	7.1	7.1
880613	0.6	0.6	0.6	0.6	0.6	0.6	0.6	0.6	0.6	0.6	0.6	0.6	0.6	0.6	0.6	0.6
880614	0.0	0.0	0.0	0.0	0.0	0.0	0.0	0.0	0.0	0.0	0.0	0.0	0.0	0.0	0.0	0.0
880615	0.0	0.0	0.0	0.0	0.0	0.0	0.0	0.0	0.0	0.0	0.0	0.0	0.0	0.0	0.0	0.0
880616	0.5	0.5	0.5	0.5	0.5	0.5	0.5	0.5	0.5	0.5	0.5	0.5	0.5	0.5	0.5	0.5
880617	0.0	0.0	0.0	0.0	0.0	0.0	0.0	0.0	0.0	0.0	0.0	0.0	0.0	0.0	0.0	0.0
880618	0.0	0.0	0.0	0.0	0.0	0.0	0.0	0.0	0.0	0.0	0.0	0.0	0.0	0.0	0.0	0.0
880619	0.0	0.0	0.0	0.0	0.0	0.0	0.0	0.0	0.0	0.0	0.0	0.0	0.0	0.0	0.0	0.0
880620	0.0	0.0	0.0	0.0	0.0	0.0	0.0	0.0	0.0	0.0	0.0	0.0	0.0	0.0	0.0	0.0
880621	0.0	0.0	0.0	0.0	0.0	0.0	0.0	0.0	0.0	0.0	0.0	0.0	0.0	0.0	0.0	0.0
880622	0.0	0.0	0.0	0.0	0.0	0.0	0.0	0.0	0.0	0.0	0.0	0.0	0.0	0.0	0.0	0.0
880623	0.0	0.0	0.0	0.0	0.0	0.0	0.0	0.0	0.0	0.0	0.0	0.0	0.0	0.0	0.0	0.0
880624	0.0	0.0	0.0	0.0	0.0	0.0	0.0	0.0	0.0	0.0	0.0	0.0	0.0	0.0	0.0	0.0
880625	0.0	0.0	0.0	0.0	0.0	0.0	0.0	0.0	0.0	0.0	0.0	0.0	0.0	0.0	0.0	0.0
880626	0.0	0.0	0.0	0.0	0.0	0.0	0.0	0.0	0.0	0.0	0.0	0.0	0.0	0.0	0.0	0.0
880627	0.0	0.0	0.0	0.0	0.0	0.0	0.0	0.0	0.0	0.0	0.0	0.0	0.0	0.0	0.0	0.0
880628	0.0	0.0	0.0	0.0	0.0	0.0	0.0	0.0	0.0	0.0	0.0	0.0	0.0	0.0	0.0	0.0
880629	0.0	0.0	0.0	0.0	0.0	0.0	0.0	0.0	0.0	0.0	0.0	0.0	0.0	0.0	0.0	0.0
880630	0.0	0.0	0.0	0.0	0.0	0.0	0.0	0.0	0.0	0.0	0.0	0.0	0.0	0.0	0.0	0.0

Sensitivity analysis, January 1988, daily values

field capacity	40	60	70	75	80	100	130	75	75	75	75	75	75	75	75	75
interception capacity	4.7	4.7	4.7	4.7	4.7	4.7	4.7	4.7	4	3	2	1	4.7	4.7	4.7	4.7
rapid recharge (wood,agri)	75,6	75,6	75,6	75,6	75,6	75,6	75,6	75,6	75,6	75,6	75,6	75,6	35,6	25,6	15,6	10,6
all in mm	fieldcapacity variations ----------							Intercept. cap. var. -------					rapid rech. var. -----			
date	st4	st3	st2	st1	st5	st6	st7	st1	st8	st9	st10	st11	st12	st13	st14	st15
880101	0.0	0.0	0.0	0.0	0.0	0.0	0.0	0.0	0.0	0.0	0.0	0.0	0.0	0.0	0.0	0.0
880102	1.6	1.5	1.5	1.5	1.5	1.5	1.5	1.5	1.5	1.6	1.6	1.8	1.5	1.5	1.5	1.5
880103	0.8	0.8	0.8	0.8	0.8	0.8	0.8	0.8	0.8	0.8	0.8	0.8	0.8	0.8	0.8	0.8
880104	16.6	16.6	16.6	16.6	16.6	16.6	16.6	16.6	16.6	16.6	16.6	16.6	16.6	16.6	16.6	16.6
880105	0.0	0.0	0.0	0.0	0.0	0.0	0.0	0.0	0.0	0.0	0.0	0.0	0.0	0.0	0.0	0.0
880106	0.3	0.3	0.3	0.3	0.3	0.3	0.3	0.3	0.3	0.3	0.3	0.3	0.3	0.3	0.3	0.3
880107	0.0	0.0	0.0	0.0	0.0	0.0	0.0	0.0	0.0	0.0	0.0	0.0	0.0	0.0	0.0	0.0
880108	0.0	0.0	0.0	0.0	0.0	0.0	0.0	0.0	0.0	0.0	0.0	0.0	0.0	0.0	0.0	0.0
880109	0.0	0.0	0.0	0.0	0.0	0.0	0.0	0.0	0.0	0.0	0.0	0.0	0.0	0.0	0.0	0.0
880110	0.0	0.0	0.0	0.0	0.0	0.0	0.0	0.0	0.0	0.0	0.0	0.0	0.0	0.0	0.0	0.0
880111	0.0	0.0	0.0	0.0	0.0	0.0	0.0	0.0	0.0	0.0	0.0	0.0	0.0	0.0	0.0	0.0
880112	0.0	0.0	0.0	0.0	0.0	0.0	0.0	0.0	0.0	0.0	0.0	0.0	0.0	0.0	0.0	0.0
880113	0.0	0.0	0.0	0.0	0.0	0.0	0.0	0.0	0.0	0.0	0.0	0.0	0.0	0.0	0.0	0.0
880114	0.0	0.0	0.0	0.0	0.0	0.0	0.0	0.0	0.0	0.0	0.0	0.0	0.0	0.0	0.0	0.0
880115	0.0	0.0	0.0	0.0	0.0	0.0	0.0	0.0	0.0	0.0	0.0	0.0	0.0	0.0	0.0	0.0
880116	1.5	0.6	0.6	0.6	0.6	0.6	0.6	0.6	0.6	0.6	0.6	0.6	0.6	0.6	0.6	0.6
880117	0.7	1.5	1.5	1.5	1.5	1.5	1.5	1.5	1.5	1.5	1.5	1.5	1.5	1.5	1.5	1.5
880118	0.0	0.0	0.0	0.0	0.0	0.0	0.0	0.0	0.0	0.0	0.0	0.0	0.0	0.0	0.0	0.0
880119	0.0	0.0	0.0	0.0	0.0	0.0	0.0	0.0	0.0	0.0	0.0	0.0	0.0	0.0	0.0	0.0
880120	0.0	0.0	0.0	0.0	0.0	0.0	0.0	0.0	0.0	0.0	0.0	0.0	0.0	0.0	0.0	0.0
880121	0.0	0.0	0.0	0.0	0.0	0.0	0.0	0.0	0.0	0.0	0.0	0.0	0.0	0.0	0.0	0.0
880122	0.0	0.0	0.0	0.0	0.0	0.0	0.0	0.0	0.0	0.0	0.0	0.0	0.0	0.0	0.0	0.0
880123	0.0	0.0	0.0	0.0	0.0	0.0	0.0	0.0	0.0	0.0	0.0	0.0	0.0	0.0	0.0	0.0
880124	16.0	16.0	16.0	16.0	16.0	16.0	16.0	16.0	16.0	16.0	16.0	16.0	16.0	16.0	16.0	16.0
880125	4.2	4.2	4.2	4.2	4.2	4.2	4.2	4.2	4.2	4.2	4.2	4.2	4.2	4.2	4.2	4.2
880126	4.6	4.6	4.6	4.6	4.6	4.6	4.6	4.6	4.6	4.6	4.6	4.6	4.6	4.6	4.6	4.6
880127	0.0	0.0	0.0	0.0	0.0	0.0	0.0	0.0	0.0	0.0	0.0	0.0	0.0	0.0	0.0	0.0
880128	1.0	1.0	1.0	1.0	1.0	1.0	1.0	1.0	1.0	1.0	1.0	1.0	1.0	1.0	1.0	1.0
880129	0.6	0.6	0.6	0.6	0.6	0.6	0.6	0.6	0.6	0.6	0.6	0.6	0.6	0.6	0.6	0.6
880130	1.7	1.7	1.7	1.7	1.7	1.7	1.7	1.7	1.7	1.7	1.7	1.7	1.7	1.7	1.7	1.7
880131	0.0	0.0	0.0	0.0	0.0	0.0	0.0	0.0	0.0	0.0	0.0	0.0	0.0	0.0	0.0	0.0

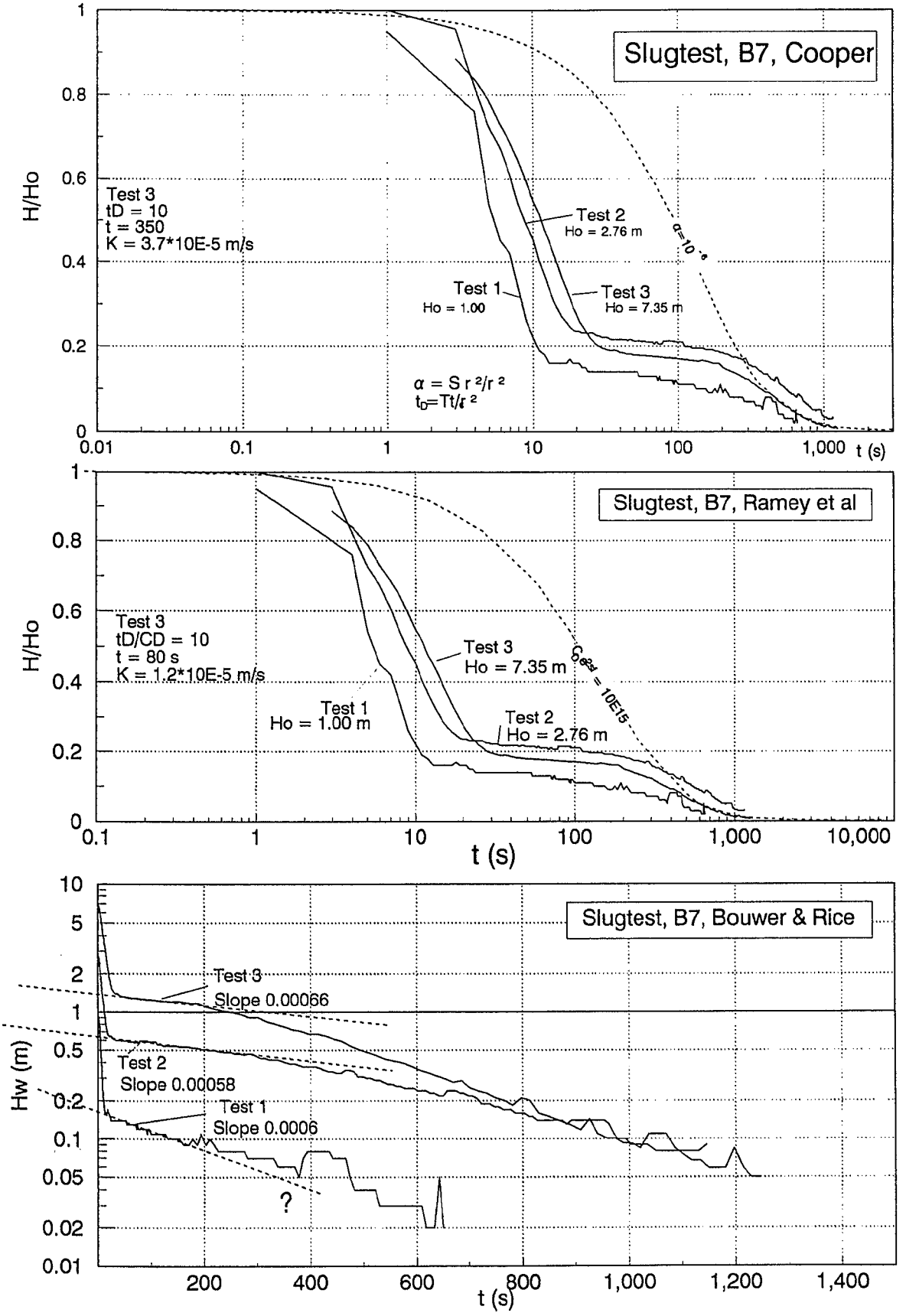

App. 4-4 (a) Slugtest Evaluation, using Type Curve Matching Procedures for Single Porosity Homogeneous Media (B7)

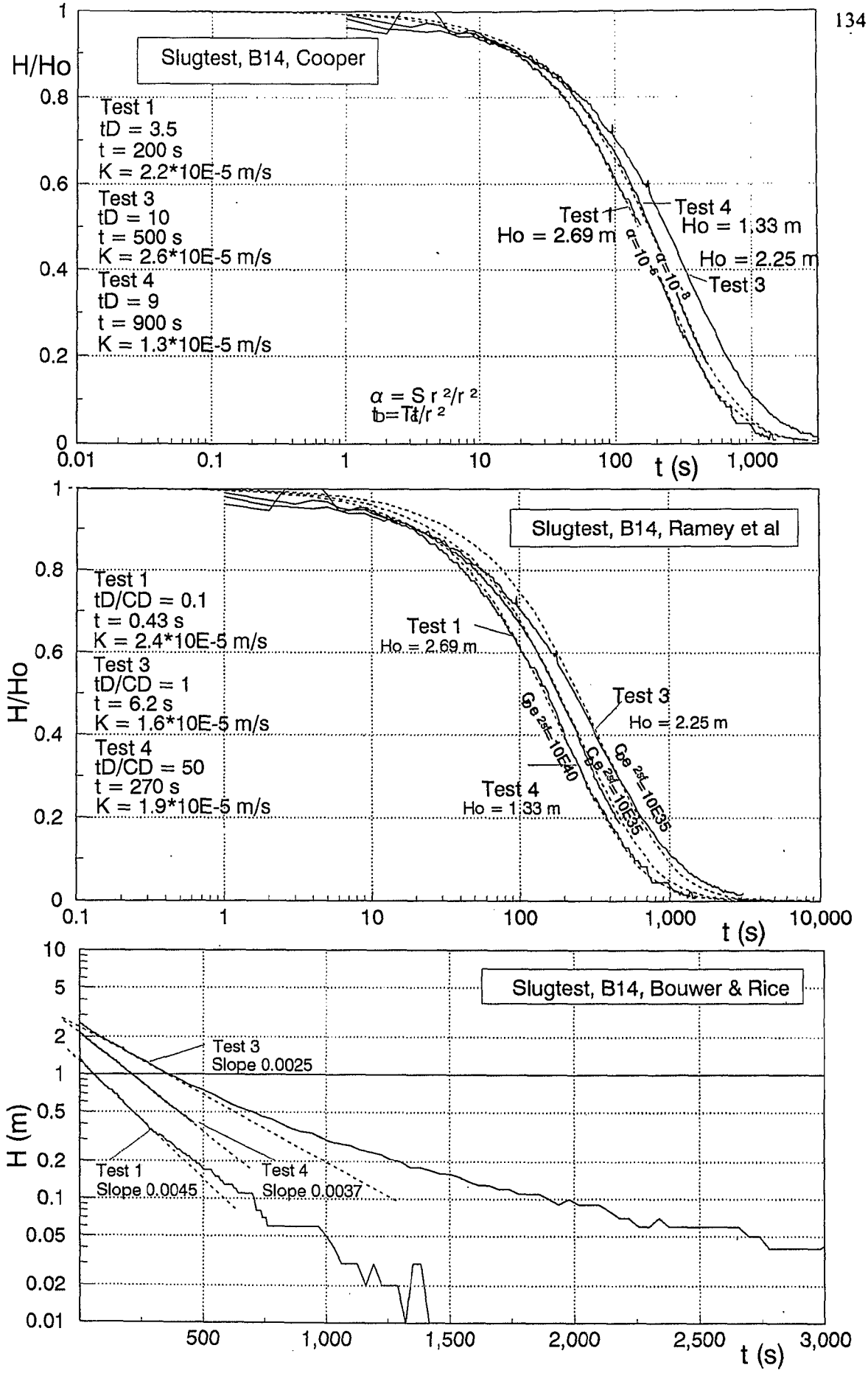

App. 4-4 (b) Slugtest Evaluation using Type Curve Matching Procedures for Single Porosity Homogeneous Media (B14)

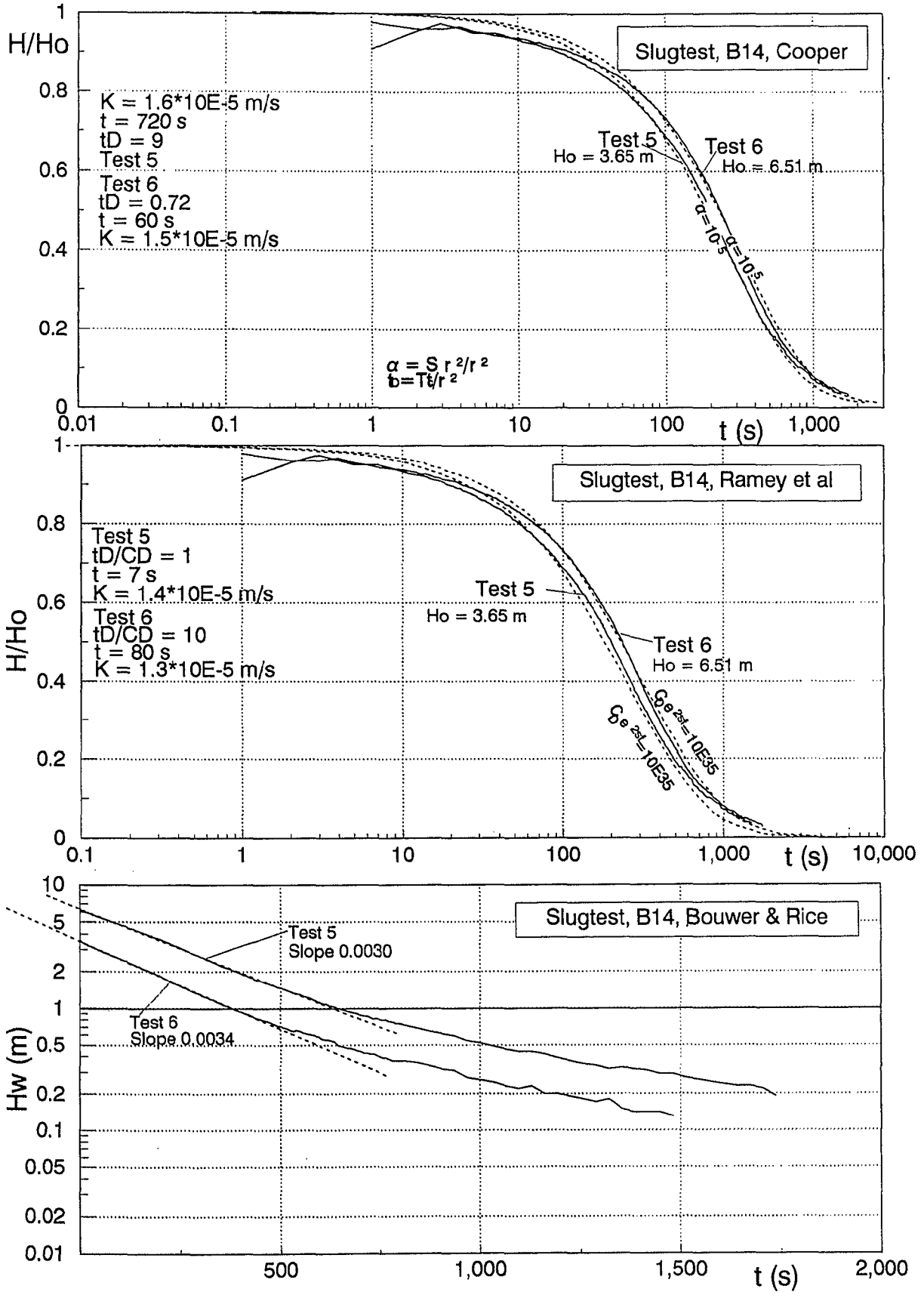

App. 4-4 (c) Slugtest Evaluation using Type Curve-Matching Procedures for Single Porosity Homogeneous Media (B14)

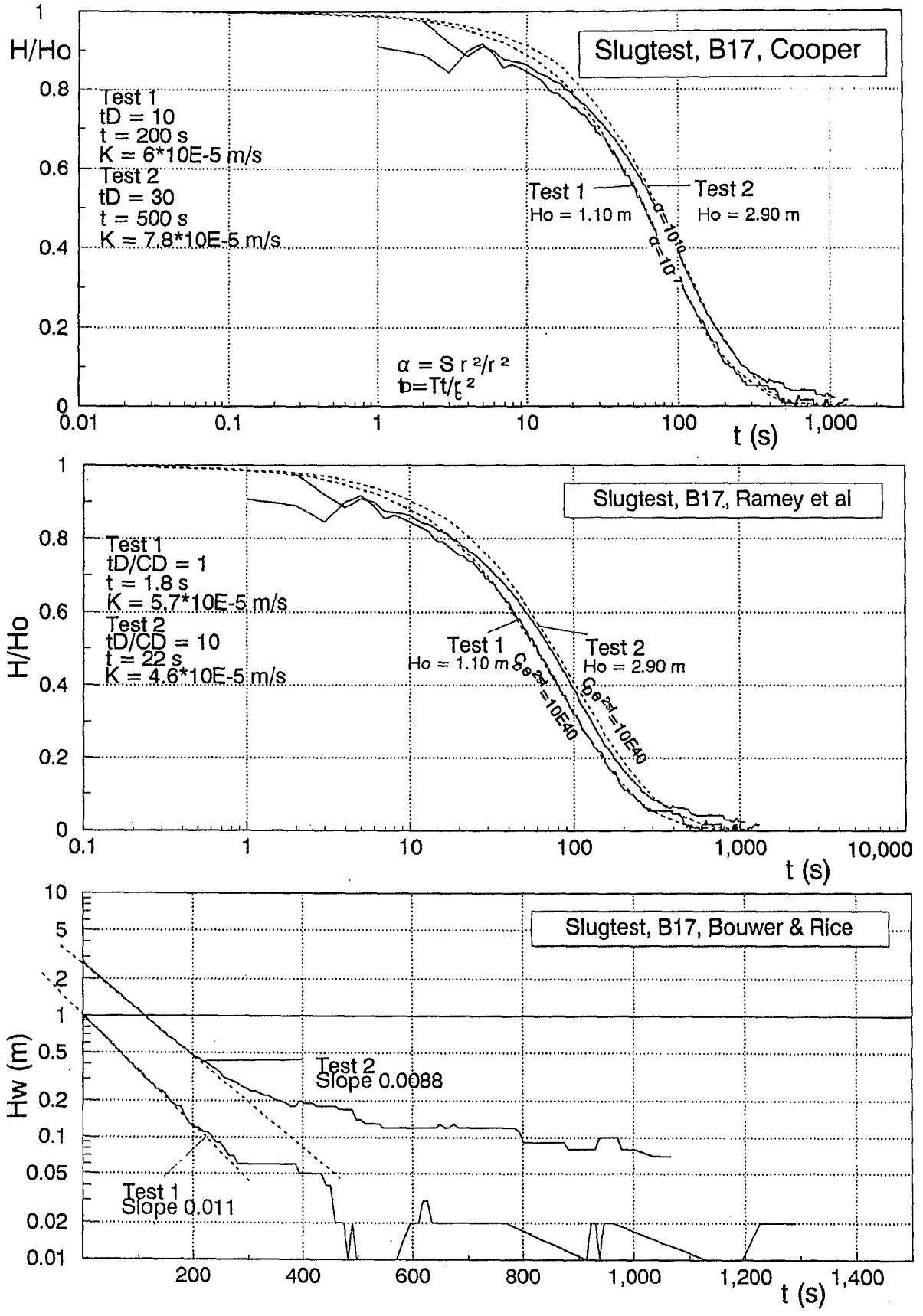

App. 4-4 (d) Slugtest Evaluation using Type Curve Matching Procedures for Single Porosity Homogeneous Media (B17)

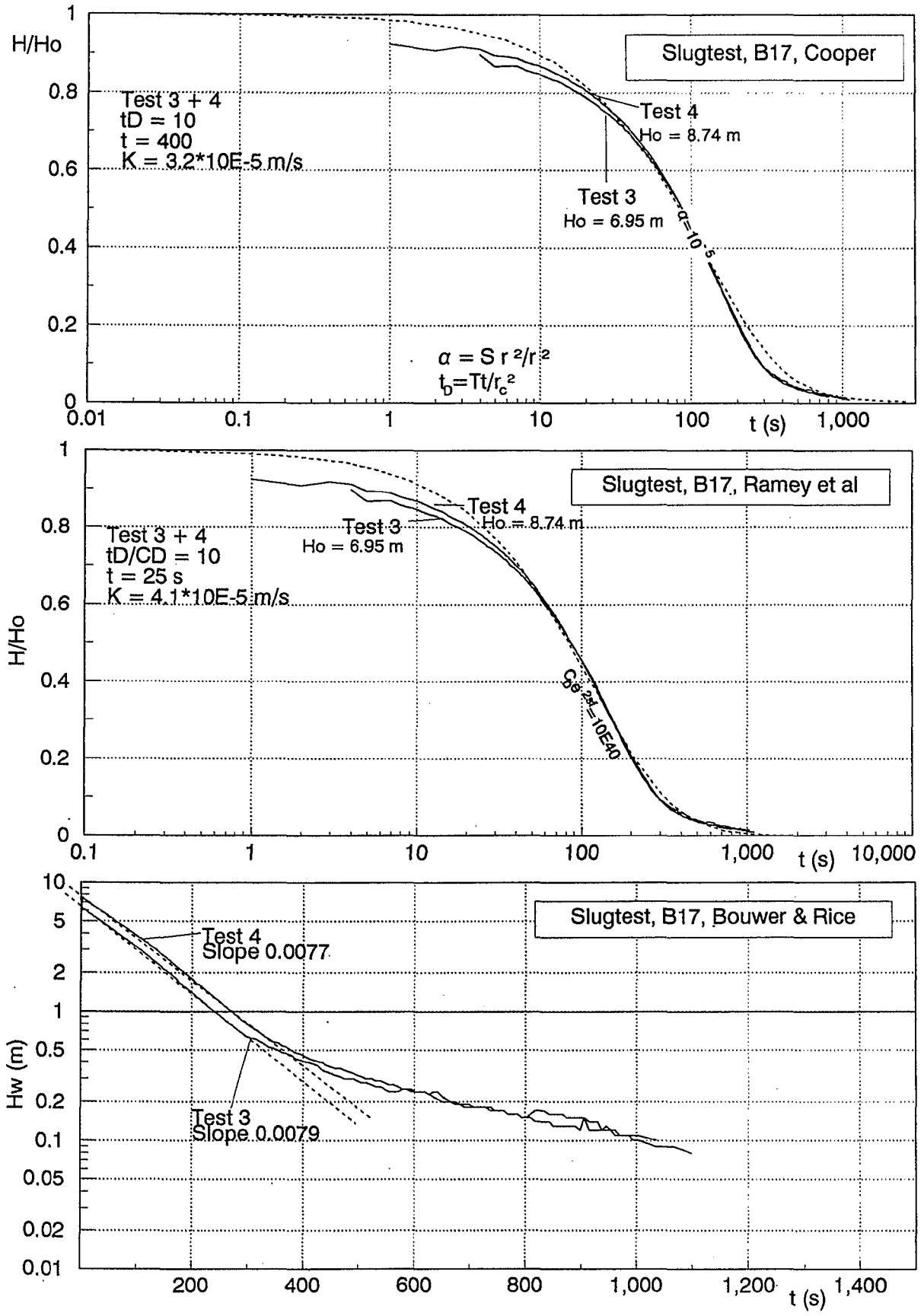

App. 4-4 (e) Slugtest Evaluation using Type Curve Matching Procedures for Single Porosity Homogeneous Media (B17)

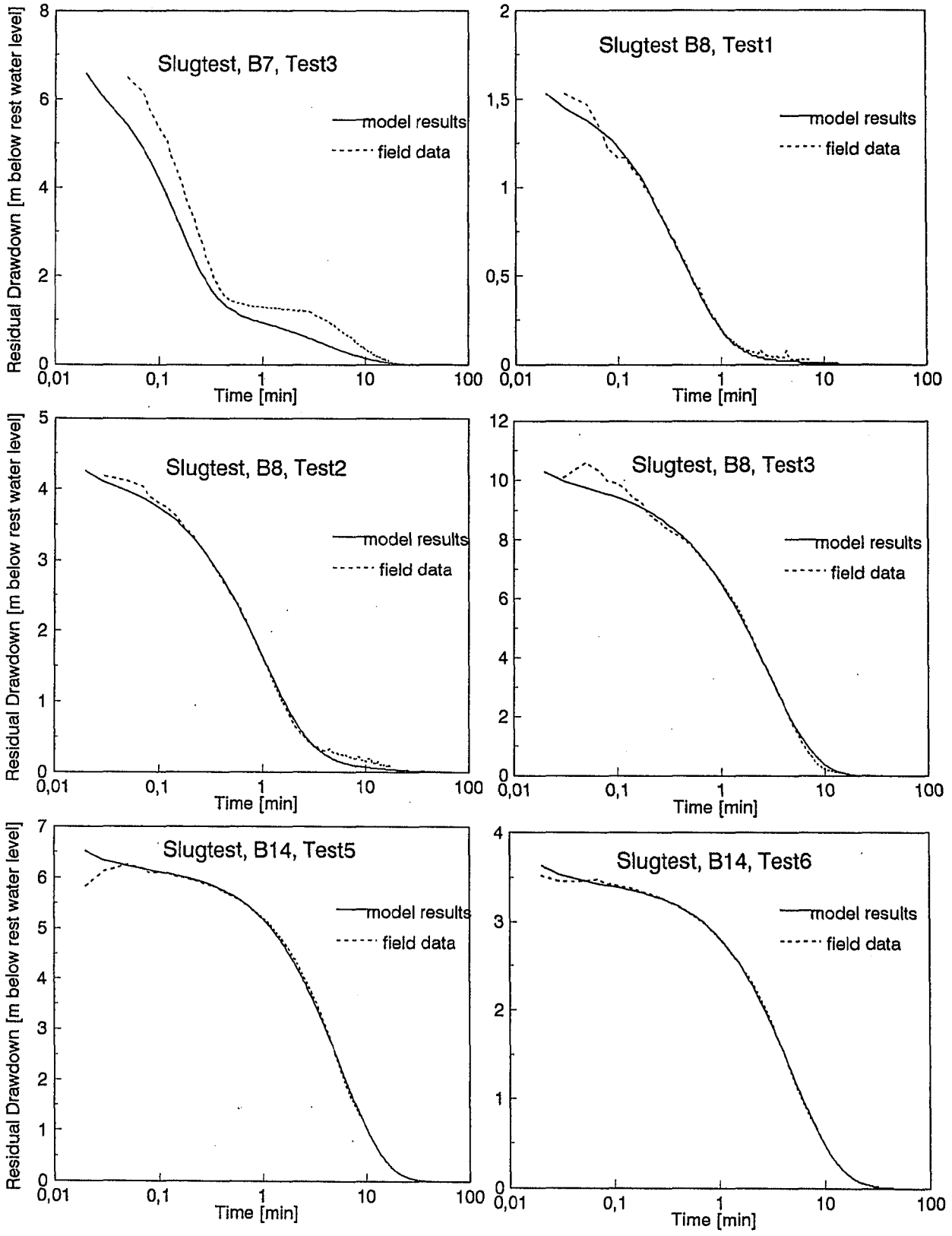

App. 4-5 (a) Slug Test Evaluation - Comparison between Field Data and Model Results

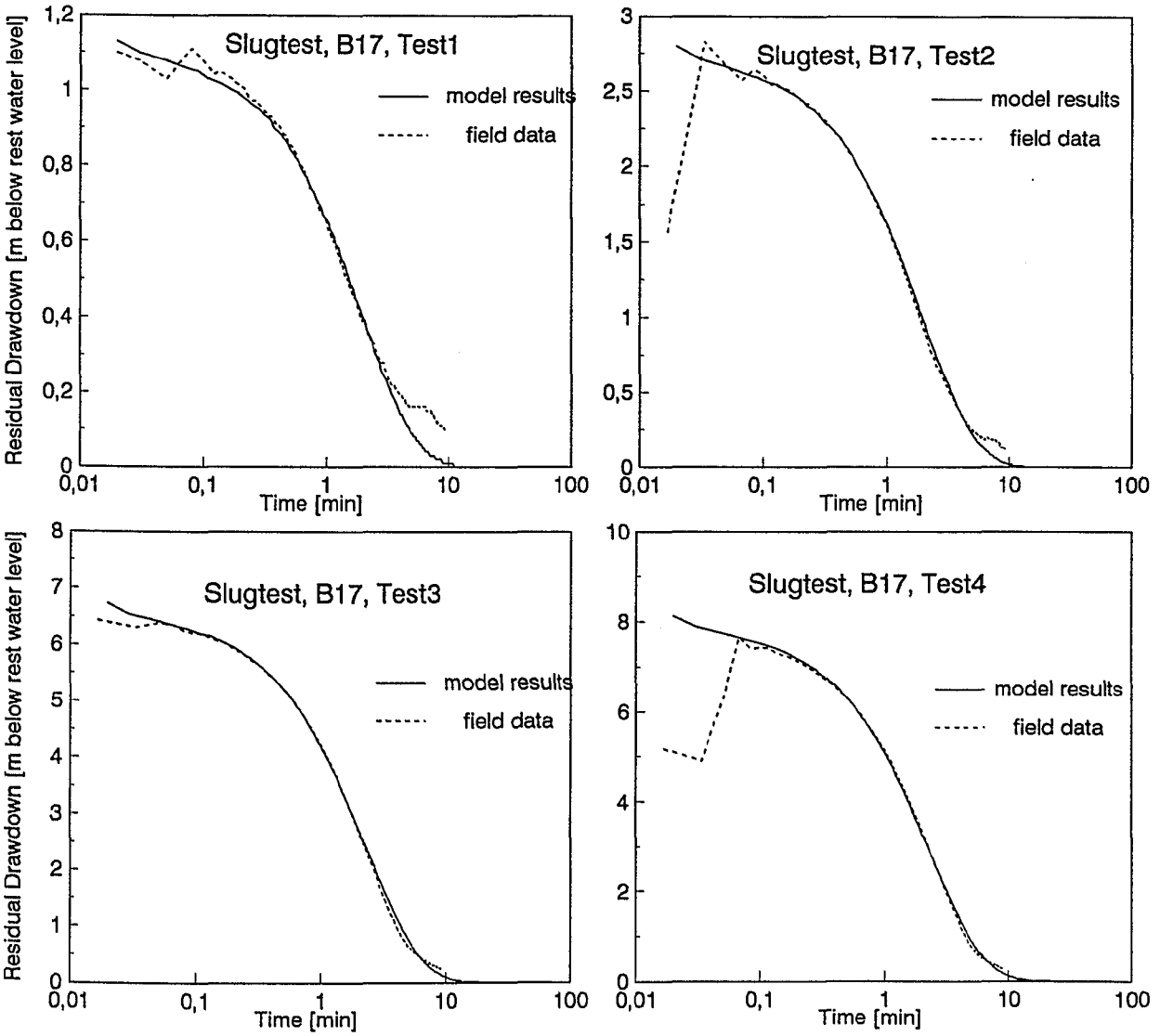

App. 4-5 (b) Slug Test Evaluation - Comparison between Field Data and Model Results

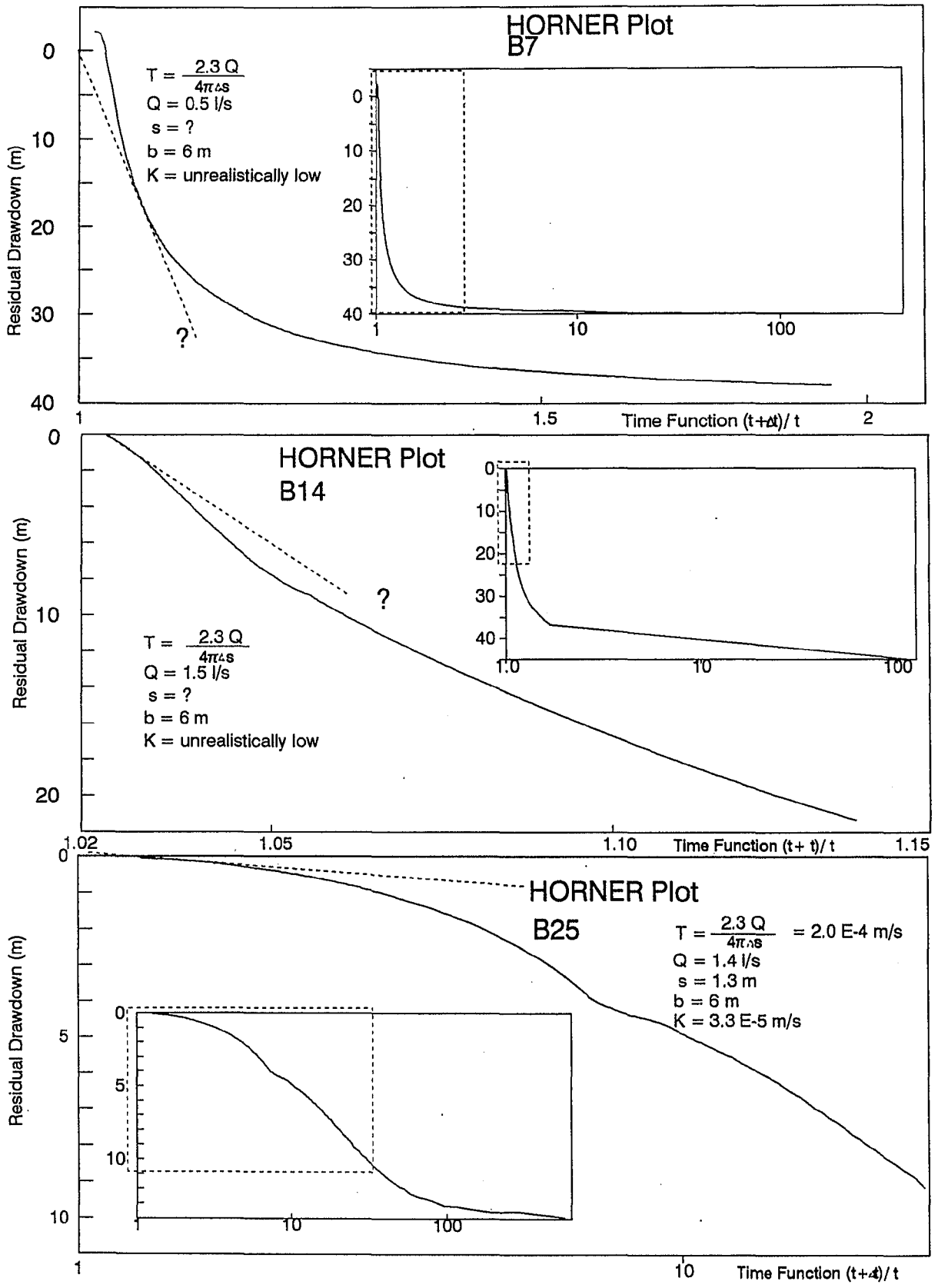

App. 4-6 HORNER Plot Evaluation of Injection Test Data (B7, B14, B25)

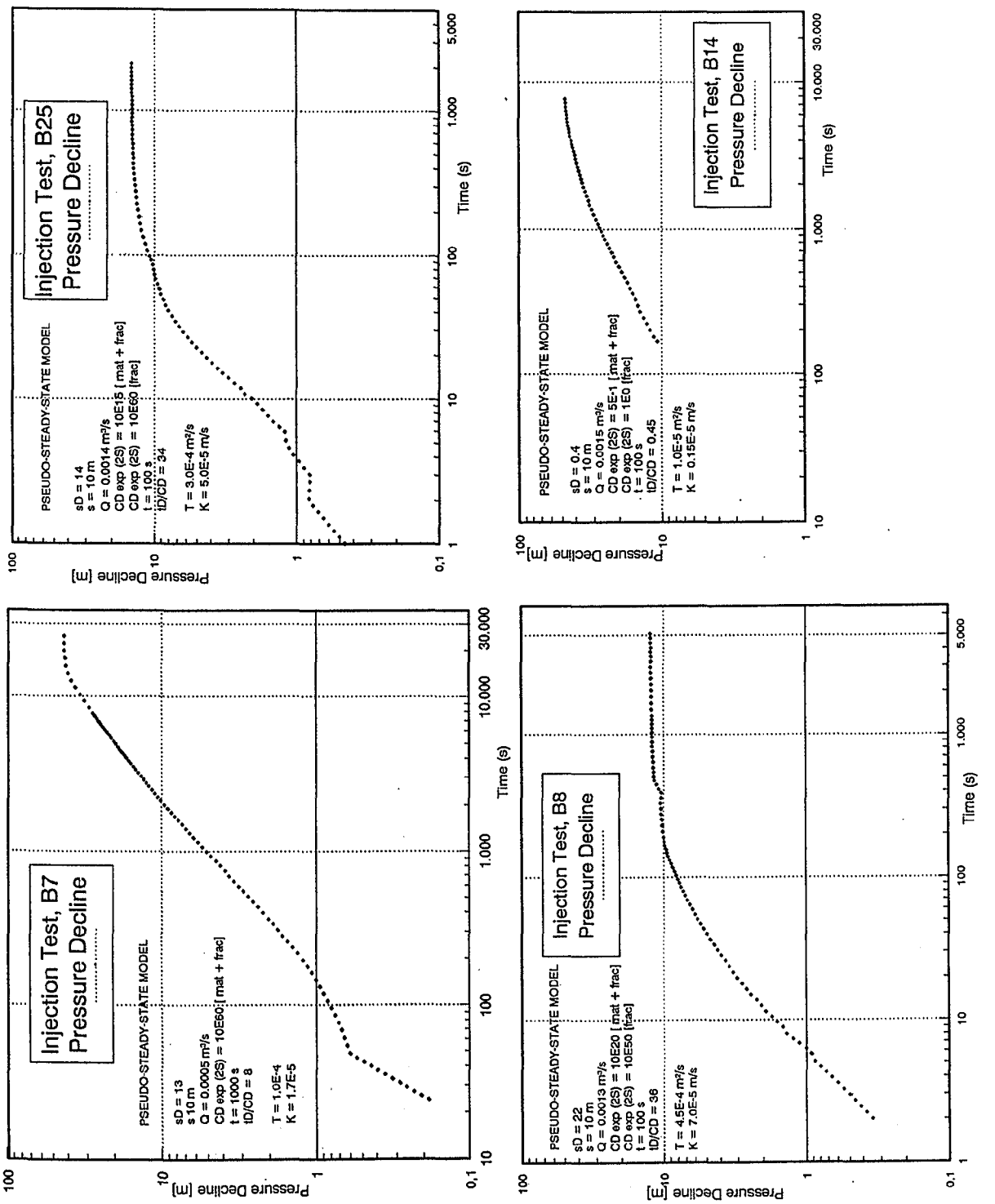

App. 4-7 Log-Log Plots of Injection Test Data, Evaluated Using Bourdet and Gringarten (1980), B7, B8, B14, B25

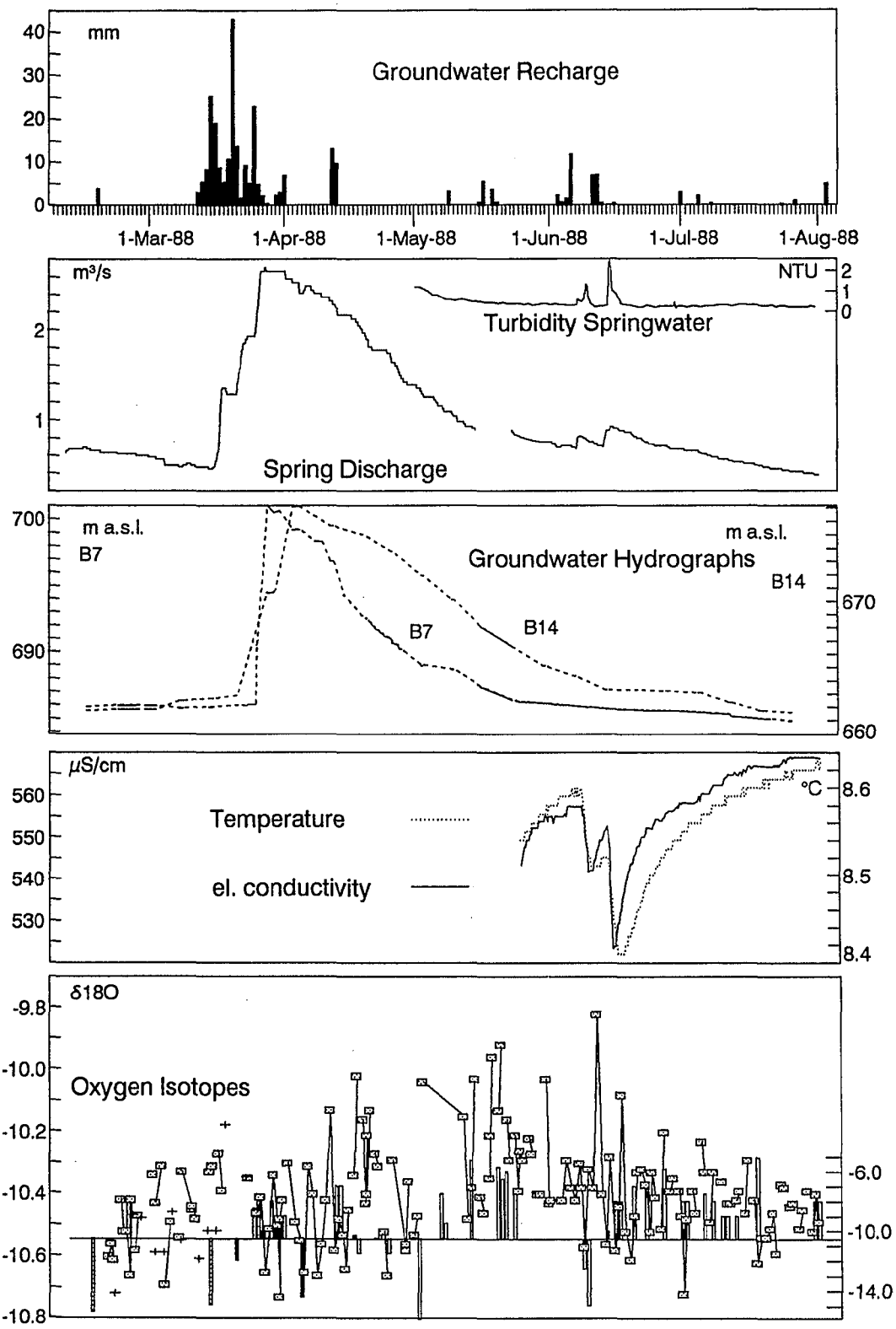

App. 4-8 (a) Time Series of Hydraulic and Physico-Chemical Parameters in the Gallusquelle Karst Aquifer (Mar 1988)

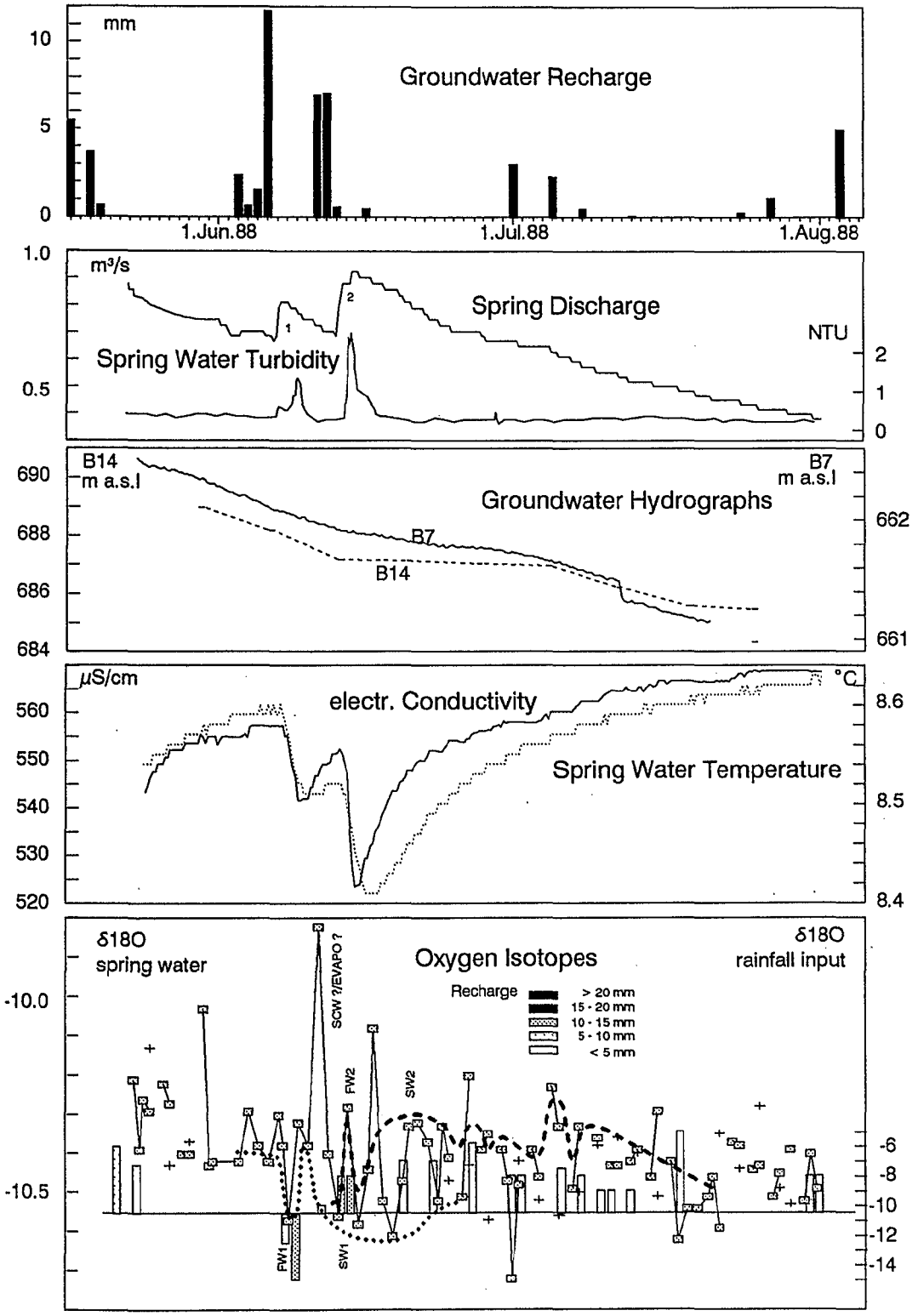

App. 4-8 (b) Time Series of Hydraulic and Physico-Chemical Parameters in the Gallusquelle Karst Aquifer (Jun 1988)

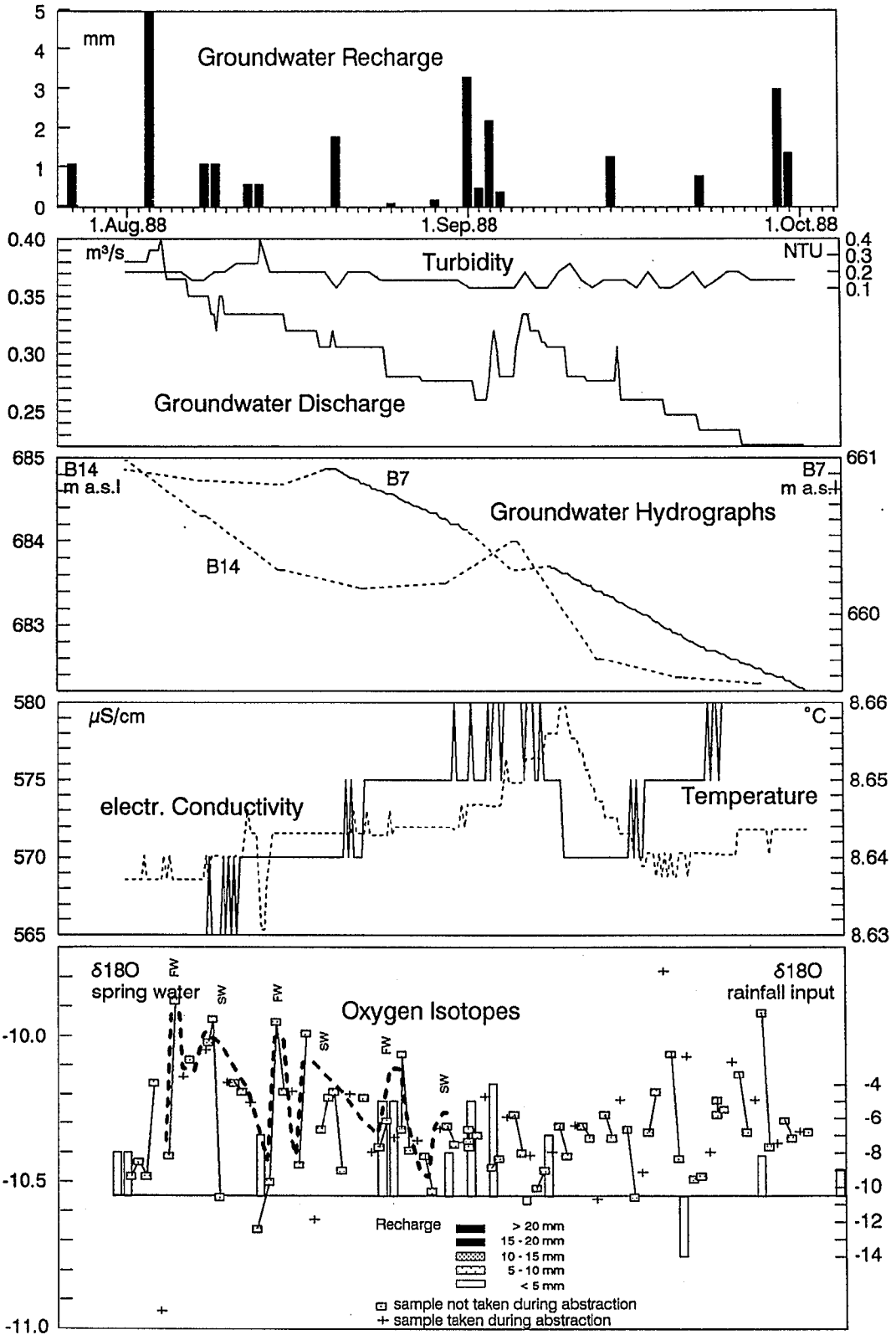

App. 4-8 (c) Time Series of Hydraulic and Physico-Chemical Parameters in the Gallusquelle Karst Aquifer (Aug 1988)

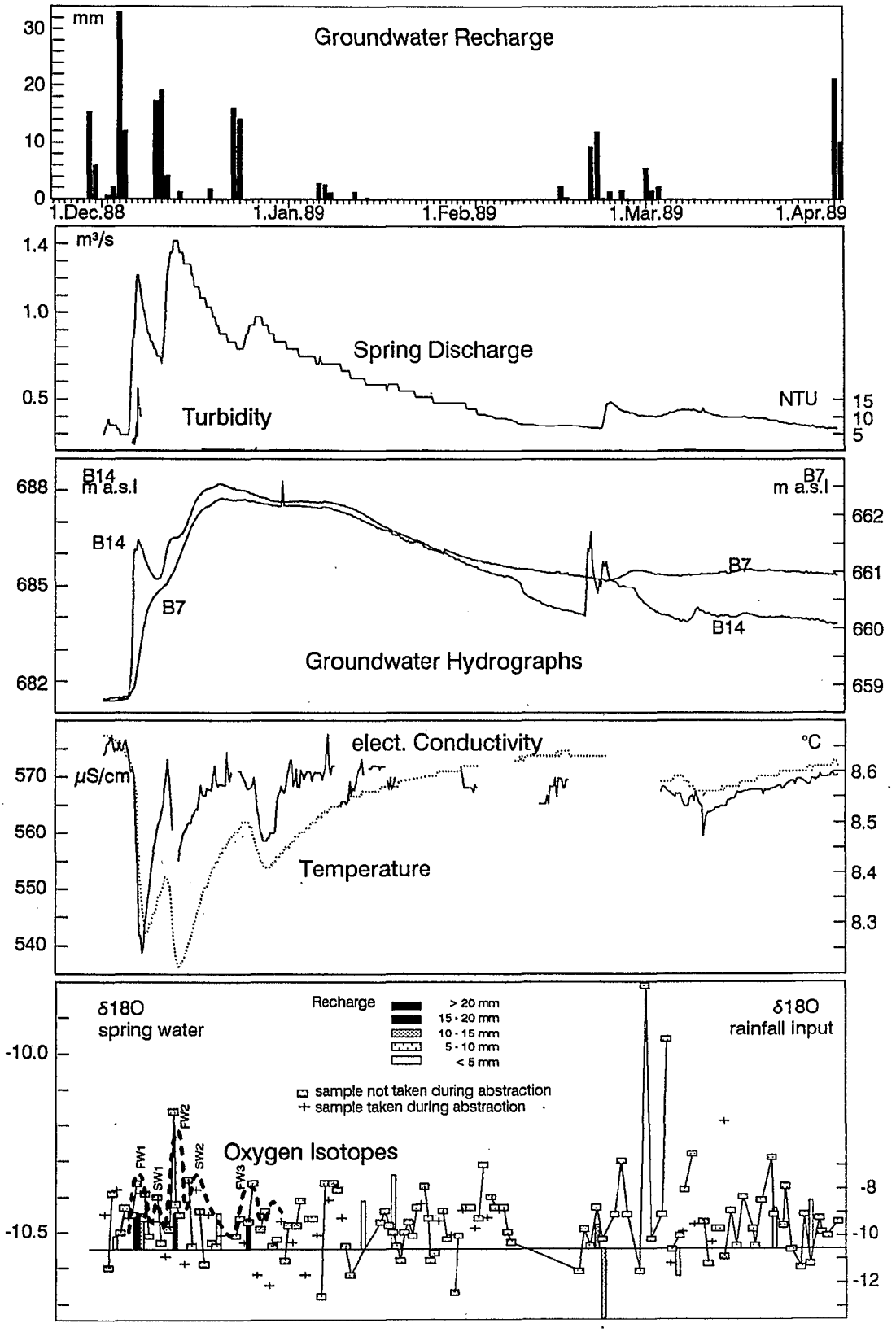

App. 4-8 (d) Time Series of Hydraulic and Physico-Chemical Parameters in the Gallusquelle Karst Aquifer (Dec 1988)

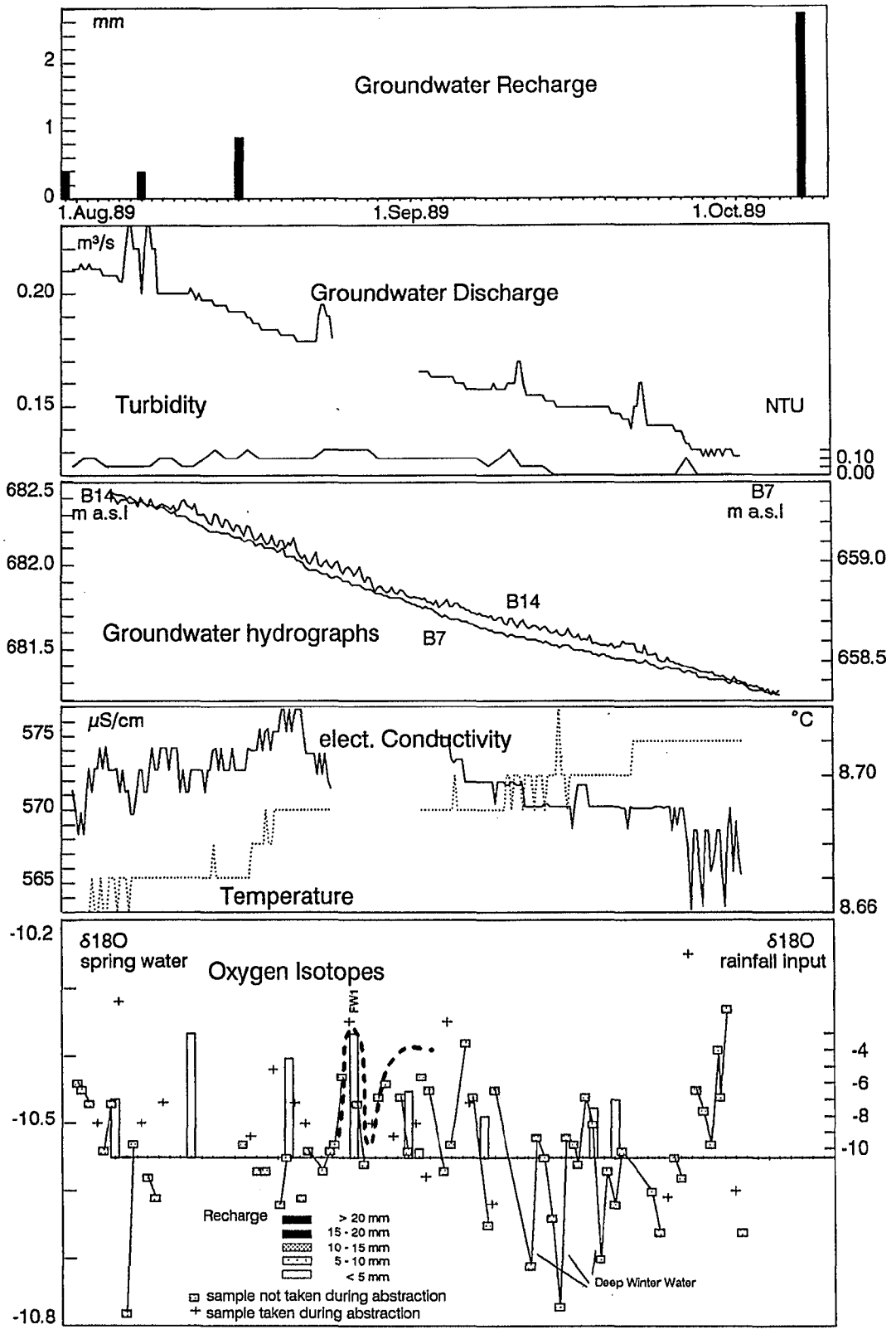

App. 4-8 (e) Time Series of Hydraulic and Physico-Chemical Parameters in the Gallusquelle Karst Aquifer (Aug 1989)

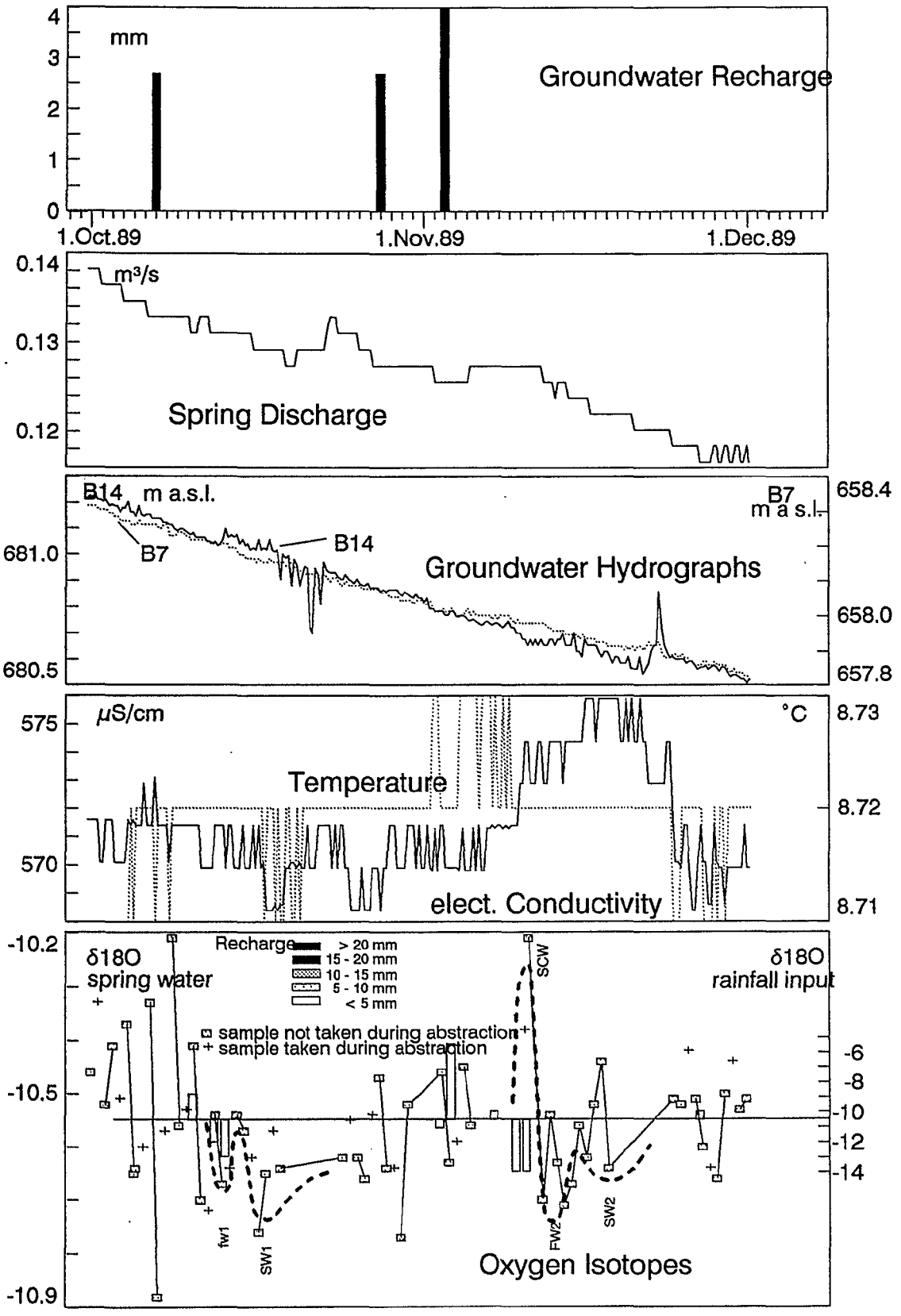

App. 4-8 (f) Time Series of Hydraulic and Physico-Chemical Parameters in the Gallusquelle Karst Aquifer (Oct 1989)

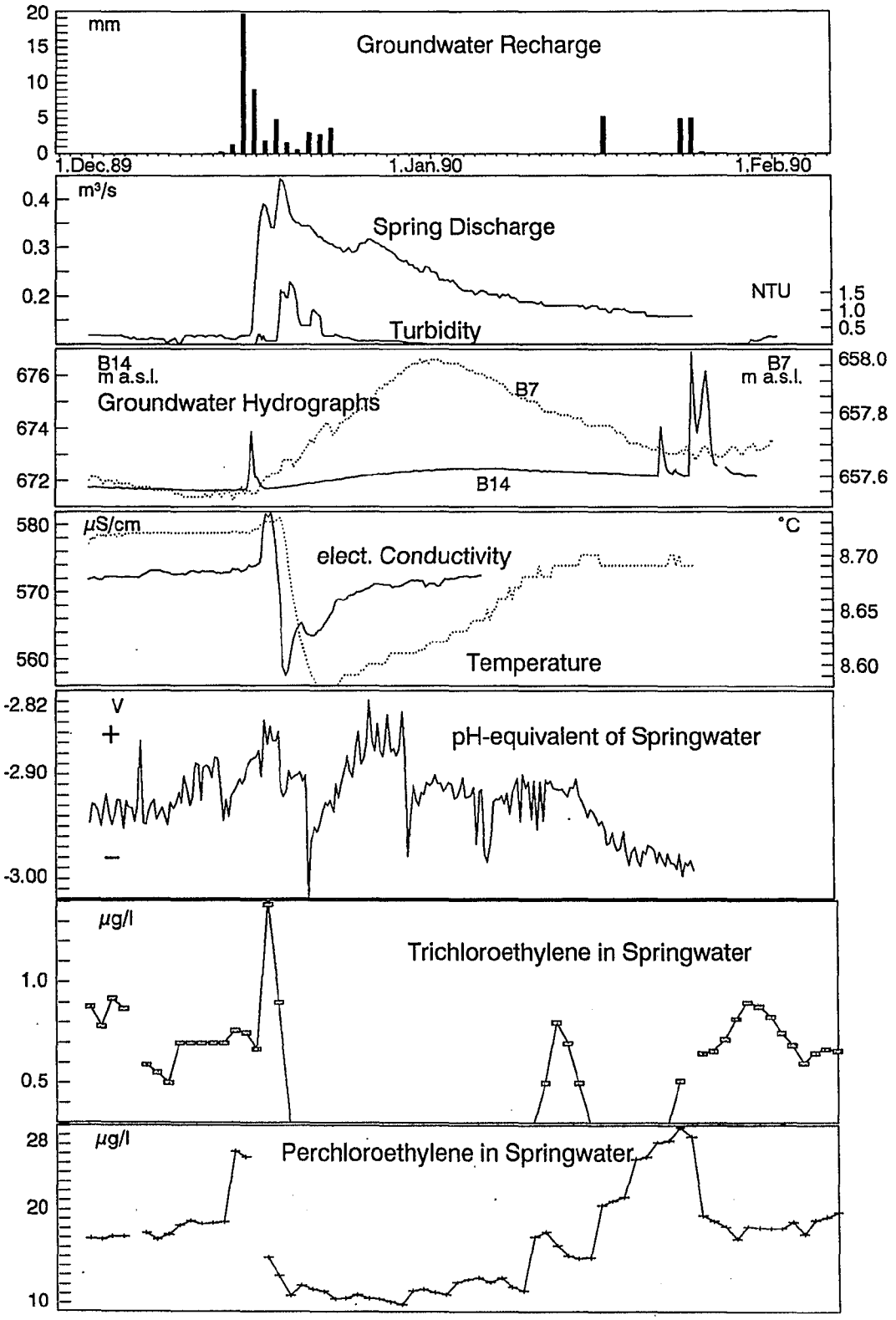

App. 4-8 (g) Time Series of Hydraulic and Physico-Chemical Parameters in the Gallusquelle Karst Aquifer (Dec 1989)

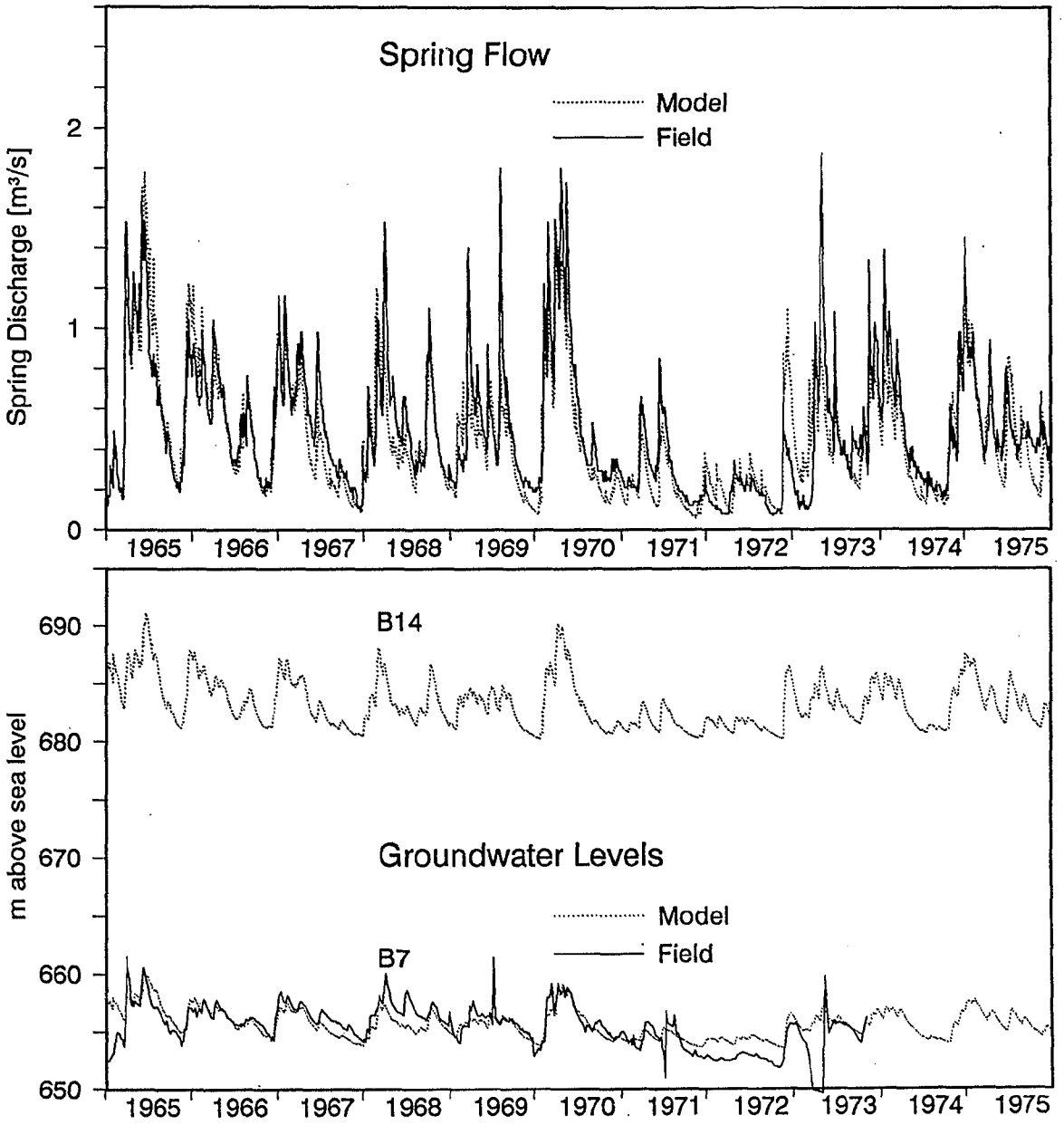

App. 5-1 Flow Modeling - Comparison between Model Results and Field Data (Flow, Groundwater Levels, 1965-1975)

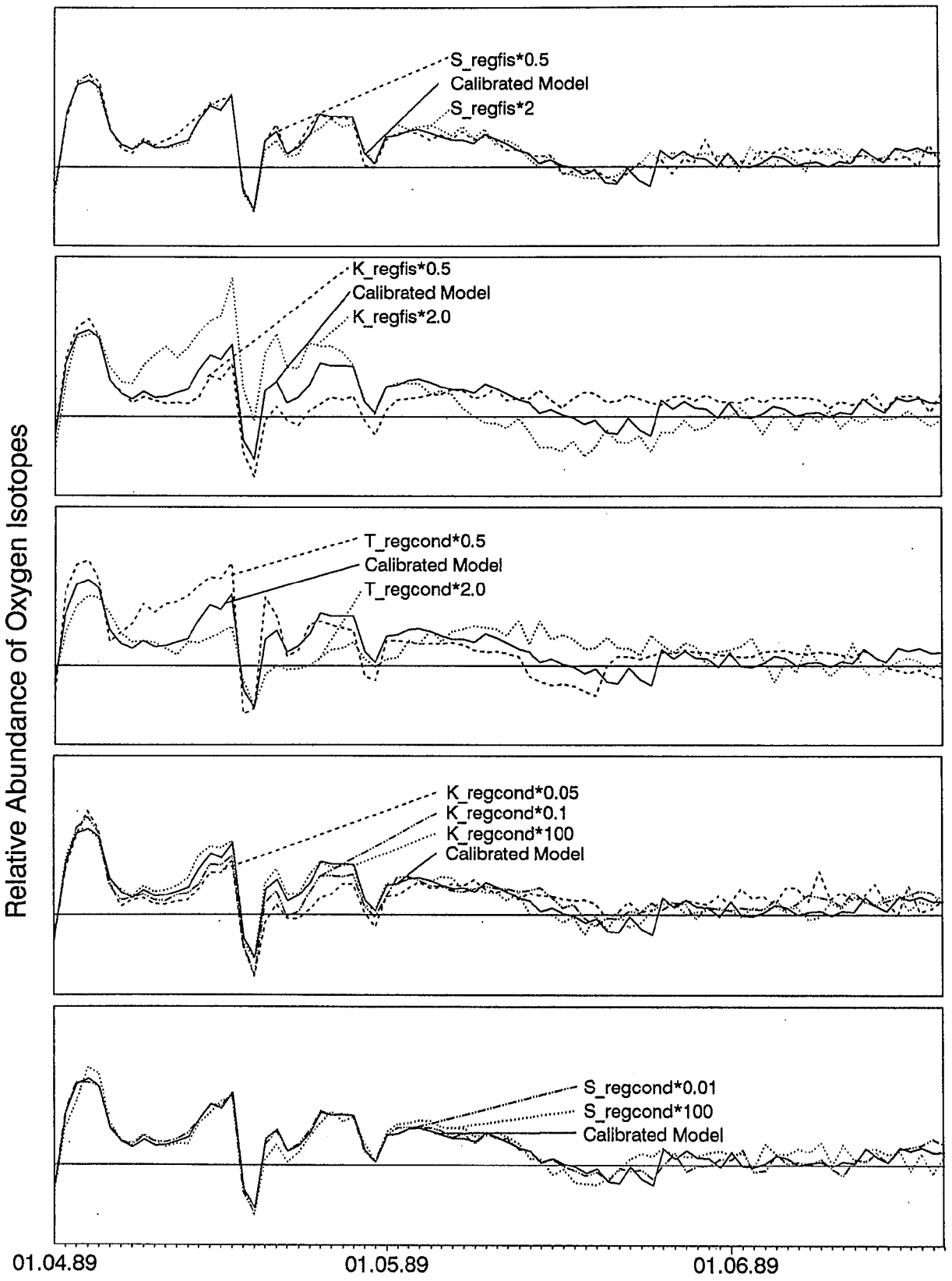

App. 6-1 Sensitivity Analysis for the Variation in Concentration of Areal Tracer with Changing Hydraulic Parameters

In der Reihe C der Tübinger Geowissenschaftlichen Abhandlungen erschienen bisher folgende Hefte:

Nr. 1: Grathwohl, P. (1989): Verteilung unpolarer organischer Verbindungen in der wasserungesättigten Bodenzone am Beispiel der leichtflüchtigen aliphatischen Chlorkohlenwasserstoffe. 102 S.

Nr. 2: Eisele, G. (1989): Labor- und Felduntersuchungen zur Ausbreitung und Verteilung leichtflüchtiger chlorierter Kohlenwasserstoffe (LCKW) im Übergangsbereich wasserungesättigte/wassergesättigte Zone. 84 S.

Nr. 3: Ehmann, M. (1989): Auswirkungen atmogener Stoffeinträge auf Boden- und Grundwässer sowie Stoffbilanzierungen in drei bewaldeten Einzugsgebieten im Oberen Buntsandstein (Nordschwarzwald). 134 S.

Nr. 4: Irouschek, T. (1990): Hydrogeologie und Stoffumsatz im Buntsandstein des Nordschwarzwaldes. 144 S.

Nr. 5: Sanns, M. (1990): Experimentelle Untersuchungen zum Ausbreitungsverhalten von leichtflüchtigen Chlorkohlenwasserstoffen (LCKW) in der wassergesättigten Zone. 122 S.

Nr. 6: Seeger, T. (1990): Fluß- und Stofffrachtseparation in Buntsandstein des Nordschwarzwaldes. 154 S.

Nr. 7: Einsele, G. & Pfeffer, K.-H. (1990): Untersuchungen über die Auswirkungen des Reaktorunfalls von Tschernobyl auf Böden, Klärschlamm und Sickerwasser im Raum von Oberschwaben und Tübingen. 151 S.

Nr. 8: Douveas, N.-G. (1990): Verwitterungstiefe und Untergrundabdichtung beim Talsperrenbau in dem verkarsteten Nord-Pindos-Flysch (Projekt Pigai-Aoos, NW-Griechenland). 165 S.

Nr. 9: Schlöser, H. (1991): Quantifizierung der Silikatverwitterung in karbonatfreien Deckschichten des Mittleren Buntsandsteins im Nordschwarzwald. 93 S.

Nr. 10: Köhler, W.-R. (1991): Beschaffenheit ausgewählter, nicht direkt anthropogen beeinflußter oberflächennaher und tiefer Grundwasservorkommen in Baden Württemberg. 144 S.

Nr. 11: Bundschuh, J. (1991): Der Aquifer als thermodynamisch offenes System. Untersuchungen zum Wärmetransport in oberflächennahen Grundwasserleitern unter besonderer Berücksichtigung von Quellwassertemperaturen (Modellversuche und Geländebeispiele). 100 S.

Nr. 12: Herbert, M. (1992): Sorptions- und Desorptionsverhalten von ausgewählten polyzyklischen Kohlenwasserstoffen (PAK) im Grundwasserbereich. 111 S.